

Max Planck Institute
for
Dynamics and Self-Organization

RESEARCH REPORT



2016



DIRECTORS

Prof. Dr. Stephan Herminghaus (Managing Director)
Prof. Dr. Eberhard Bodenschatz
Prof. Dr. Theo Geisel

SCIENTIFIC ADVISORY BOARD

Prof. Dr. David K. Campbell, Boston University, Boston (USA)
Prof. Dr. Bruno Eckhardt, Philipps-Universität, Marburg (Germany)
Prof. Dr. Leon M. Glass, McGill University, Montreal (Canada)
Prof. Dr. Elizabeth Guazzelli, Aix-Marseille Université, Marseille (France)
Prof. Dr. Andreas Herz, LMU, Munich (Germany)
Prof. Dr. Alain Karma, Northeastern University, Boston (USA)
Prof. Dr. Charles Meneveau, Johns Hopkins University, Baltimore (USA)
Prof. Dr. Elisha Moses, Weizmann Institute of Science, Rehovot (Israel)
Prof. Dr. David Quéré, ESPCI, Paris (France)
Prof. Dr. Haim Sompolinsky, The Hebrew University, Jerusalem (Israel)
Prof. Dr. Cécile Sykes, Institut Curie, Paris (France)

No matter how well we understand how a single droplet of water is formed in the laboratory, we cannot predict how countless droplets form clouds that substantially affect the Earth's climate. And although we can accurately characterize a single neuron's impulse, we do not yet understand how billions of them form a single thought. In such systems, animate or inanimate, processes of self-organization are at work: Many interacting parts organize themselves independently, without external control, into a complex whole. At our institute we explore the mechanisms underlying these processes in order to gain a detailed understanding of complex systems. Also the major challenges of the 21st century, from climate change and economic crises to problems in energy supply and transport, are closely linked to these scientific questions. Without a deep understanding of dynamics and self-organization in complex and highly networked systems we cannot face these challenges. With our basic research not only do we want to deepen our understanding of nature, but also want to contribute to a sustainable existence on this planet.

CONTENTS

- 1 Departments 7
 - 1.1 Department of Nonlinear Dynamics 8
 - 1.2 Department Dynamics of Complex Fluids 12
 - 1.3 Department of Fluid Dynamics, Pattern Formation and Bio-complexity 16
- 2 Research Groups 23
 - 2.1 Max Planck Research Group: Biological Physics and Morphogenesis 24
 - 2.2 Research Group: Biomedical Physics 26
 - 2.3 Max Planck Research Group: Neural Dynamics and Behavior 28
 - 2.4 Max Planck Research Group: Network Dynamics 29
 - 2.5 Max Planck Research Group: Theory of Turbulent Flows 32
 - 2.6 Research Group Theoretical Neurophysics 34
 - 2.7 Max Planck Emeritus Group Molecular Interactions 36
 - 2.8 External Scientific Member: Biomedical NMR Research 38
 - 2.9 External Scientific Member: Physics of Fluids 39

Research

- 3 Large Scale Research Initiatives 45
 - 3.1 European high-performance infrastructures in turbulence 46
 - 3.2 Max Planck synthetic biology initiative: from microcompartments to cilia-driven motility 47
 - 3.3 Bernstein Center for Computational Neuroscience (BCCN) Goettingen 49
- 4 Frontiers Far from Equilibrium – Statistical Physics of Strongly Driven Systems 51
 - 4.1 Turbulent thermal convection: Experiment 52
 - 4.2 Turbulent thermal convection: Theory 54
 - 4.3 Cloud microphysics measurements on the Zugspitze 56
 - 4.4 Statistics of turbulence 57
 - 4.5 Tracking particles to decipher the mystery of turbulence 59
 - 4.6 An analytical model for intermittency in turbulence 61
 - 4.7 Turbulent flows: How local is ‘non-local’? 63
 - 4.8 Nonequilibrium transitions in granular matter 64
 - 4.9 A ‘potential’ for non-equilibrium states? 65

- 4.10 Stochastic processes with random resetting 66
- 4.11 Dynamics and pattern formation in nonequilibrium, entropically driven systems 67
- 5 Transport in Complex Media 69
 - 5.1 Defects, flow, and transport in liquid crystals 70
 - 5.2 Hydrodynamics near Contact Lines 73
 - 5.3 A wetting transition in Hilbert space 74
 - 5.4 First passage time distributions of particles in Gaussian velocity fields 76
 - 5.5 Random focusing of tsunami waves 77
 - 5.6 Flux distribution in porous media 81
 - 5.7 Fluid invasion in porous media: solving a long standing conundrum 82
 - 5.8 Watching paint dry 84
 - 5.9 The role of dimensional confinement and hydrodynamics in microswimmer dynamics 85
 - 5.10 Biofluid dynamics from physics to medicine 87
 - 5.11 Microswimmers in complex geometries I: Microalgae swimming in Confinement 88
 - 5.12 Microswimmers in complex geometries II: Artificial droplet swimmers 89
 - 5.13 Microswimmers in complex geometries III: Taxis and Biofilm 90
- 6 Disorder in Space and Time 91
 - 6.1 Processing of randomly sampled data 92
 - 6.2 Friction with your neighbors? Think locally! 93
 - 6.3 Branched flow in anisotropic media 94
 - 6.4 Space-time correlations of wall turbulence 96
 - 6.5 Characterizing multi-scale interaction in turbulence 98
 - 6.6 Anomalous dynamics in disordered systems 100
 - 6.7 Heterogeneity in models of infectious diseases 102
 - 6.8 Morphogenesis control by mechanical stresses 104
 - 6.9 Stochastic terminal dynamics in Epithelial cell intercalation 105
 - 6.10 Towards a theory of efficient stimulus encoding at auditory synapses 106
 - 6.11 Feature-based and machine-learning analyses of neural data 107
 - 6.12 Inferring dynamical states under spatial subsampling 109
 - 6.13 Field biology as a data analysis challenge 110
- 7 Patterns and Instabilities 111
 - 7.1 Curvotaxis and pattern formation in the actin cortex of motile cells 113
 - 7.2 Mechanics and dynamics of biological adhesion 114
 - 7.3 The combinatorics underlying simplex equations, and “polygon equations” 115
 - 7.4 Spatiotemporal complexity of electroconvection patterns in nematics 116
 - 7.5 Evolving crack networks: from craquelure to crocodiles 117

- 7.6 Patterns and parameter inference of populations of *Dictyostelium discoideum* 118
 - 7.7 Pseudo obstacles: a novel concept for rotor initiation in excitable media 119
 - 7.8 Flow-driven waves in *Dictyostelium discoideum* 120
 - 7.9 Electrotaxis: The migration of amoeba cells in an electric field 121
 - 7.10 Gas-particle interaction: instabilities in protoplanetary disks 122
 - 7.11 Genetic assimilation of visual cortical architecture 123
 - 7.12 A synthetic neurobiology approach to orientation selectivity 124
 - 7.13 Precision measurement and dynamical switching of visual cortical architecture 125
 - 7.14 Music: A Dynamical Systems Perspective 126
 - 7.15 Control of Spatial-temporal Complexity of the Heart 127
 - 7.16 Modelling and Data Analysis in Biomedical Physics 131
 - 7.17 Oscillatory actin instabilities and motility statistics of amoeboid cells 134
- 8 Networks 135
- 8.1 Pruning to increase particle spread in transport networks 136
 - 8.2 The form and function of biological flow networks 137
 - 8.3 The encoding bandwidth of the cortical gateway 139
 - 8.4 Neuronal sodium channels: surface density and kinetics 140
 - 8.5 Nano-physiology of the action potential generator 141
 - 8.6 Modelling the role of neural oscillations in information routing 142
 - 8.7 Attractor basins of stable state sequences in balanced circuits of spiking neurons 143
 - 8.8 Selective processing in neuronal circuits 144
 - 8.9 Information processing in neural networks 146
 - 8.10 Dynamics and self-organization in brain networks 147
 - 8.11 Connectomics through dynamics: Revealing synaptic connectivity from spikes 149
 - 8.12 *EcoBus* – flexible public mobility 150
 - 8.13 Characterization and Reconstruction of Complex Networked Systems 152
 - 8.14 Model-free inference of networks from dynamics 153
 - 8.15 Dynamically smart power grids: Collective stability, economy and control 154
 - 8.16 Signal propagation and integration in adapting tubular networks 155
 - 8.17 Biodiversity and extinction 157

Infrastructure

Public Relations, Equal Opportunities, and Support for Young Scientists



Eberhard Bodenschatz (in front), Karen Alim, Marc Timme, Michael Wilczek (front row, from left to right), Theo Geisel, Fred Wolf, Stephan Herminghaus, Stefan Luther (standing, from left to right).
Göttingen, November 2015

DEPARTMENTS



CONTENTS

- 1.1 Department of Nonlinear Dynamics 8
 - 1.2 Department Dynamics of Complex Fluids 12
 - 1.3 Department of Fluid Dynamics, Pattern Formation and Bio-complexity 16
-

1.1 DEPARTMENT OF NONLINEAR DYNAMICS



Prof. Dr. Theo Geisel studied physics at the Universities of Frankfurt and Regensburg, where he received his doctorate in 1975. After postdoctoral research at the MPI for Solid State Research in Stuttgart and the Xerox Palo Alto Research Center, he was appointed Heisenberg Fellow in 1983. He was Professor of Theoretical Physics at the Universities of Würzburg (1988-1989) and Frankfurt (1989-1996), where he headed the Sonderforschungsbereich (SFB) for Nonlinear Dynamics of the DFG. In 1996 he was appointed Director at the MPI for Flow Research (now MPI for Dynamics and Self-Organization), he also teaches as a full professor in the Faculty of Physics of the University of Göttingen and is a member of the Academy of Sciences and Humanities, Göttingen. A recipient of the Leibniz Prize and other awards, he initiated the Bernstein Center for Computational Neuroscience (BCCN) Göttingen and headed it for 9 years. His research is driven by the fascination of complex dynamics emerging in nonlinear systems as diverse as neuronal networks, nanostructures, and the population dynamics of infectious diseases.

Dynamical phenomena are abundant in nature, many of them are easy to dissect for a human observer, while others have challenged theoreticians for decades. Simple mathematical models that give rise to chaotic behaviour have long been studied as paradigms for complex systems and have provided us with new tools, but many of them have had little direct application to physical reality. A quarter century ago our group began focusing on applications to real physical systems. In particular, we have studied chaos and quantum chaos in mesoscopic systems such as semiconductor nanostructures and the dynamics of biological neural networks. Today looking at our contributions in this volume, it is amazing to see how far this approach can reach - much farther than I initially expected - e.g., in uncovering brain function.

In neuroscience, in particular, many important problems and questions are related to dynamics and self-organization. How do the neurons in our brain cooperate when we perceive an object or perform a task? What is the role of different dynamical states, e.g. critical avalanches, for brain function? How do cortical networks quickly switch between different states, e.g. for context-dependent information routing? While computer simulations of even very large neuronal networks are becoming fashionable, they are of only limited use for answering such questions in depth.

On the other hand rigorous mathematical analyses of the dynamics of neural networks cannot rely on mainstream recipes but pose formidable mathematical challenges. Neural systems exhibit several features that elude standard mathematical treatment: the units of the network communicate or interact only at discrete times and not continuously as in many-body theory in physics; there are significant interaction delays that make the systems formally infinite-dimensional; and complex connectivities give rise to novel multioperator problems - enough "reasons d'être" for a group of theoreticians. Meeting such challenges has often been facilitated by cross-fertilization within the wide scope of problems addressed in our department, from diverse stochastic processes in complex environments to wave phenomena in random and complex media such as the random focussing of tsunamis or the localization of Bose-Einstein condensates in optical lattices. Our recent research achievements demonstrate that abstraction and mathematical rigor do not impede but in fact deepen our understanding of complex systems.

The Department of Nonlinear Dynamics was created by the Max Planck Society in 1996 to start a scientific reorientation of the former MPI for Flow Research towards modern nonlinear dynamics. We have initiated and host the federally (BMBF) funded Bernstein Center for Computational Neuroscience Göttingen, in which we cooperate with experimental neuroscience labs. Our group is closely linked also to the Faculty of Physics, where Theo Geisel teaches as a full professor. It is financed to a large extent by the Max Planck Society and to a smaller extent by the University of Göttingen through its Institute for Nonlinear Dynamics and plays a bridging role between the Faculty of Physics and the MPIDS.



Dr. Demian Battaglia studied physics at the University of Turin and received his PhD in 2005 at the International School for Advanced Studies (SISSA, Trieste), doing research at the interface between statistical mechanics and theoretical computer science. From 2006 to 2008 he was postdoctoral researcher at the Laboratory of Neurophysics and Physiology (University Paris Descartes). In 2009 he joined the group of Theo Geisel as a Postdoc at the MPI for Dynamics and Self-organization. Since May 2010, he has been principal investigator of the Bernstein Center for Computational Neuroscience Göttingen where he was appointed *Bernstein Fellow* in 2013. He accepted a position as Marie Curie Fellow at Aix-Marseille University, where he became CNRS research scientist in 2015. He continues on a part-time appointment at the MPIDS and as PI of the Bernstein Center.



Dr. Stephan Eule studied physics at the Westfaelische-Wilhelms University in Muenster where he received his PhD in 2008. In 2009 he joined the Department of Nonlinear Dynamics at the Max Planck Institute for Dynamics and Self-Organization working on problems in stochastic population dynamics and fluctuating physical and biological systems with a focus on the description of anomalous diffusion processes. In 2015 he worked as a visiting scientist in the lab of Johan Paulsson at Harvard Medical School.



Dr. Ragnar Fleischmann studied physics at the Johann-Wolfgang-Goethe University in Frankfurt am Main and received his PhD in 1997. His thesis was awarded the Otto-Hahn-Medal of the Max-Planck-Society. From 1997 to 1999 he was postdoctoral researcher in the group of Theo Geisel at the Max-Planck-Institut für Strömungsforschung and from 1999 to 2000 in the group of Eric Heller at Harvard University. Since 2000 he has worked as a scientific staff member in the Department for Nonlinear Dynamics. His research focuses on the theory of mesoscopic systems and wave propagation in complex and random media.



Dr. Denny Fliegner studied physics at the University of Heidelberg and received his doctoral degree in theoretical particle physics in 1997. From 1997 to 2000 he was postdoctoral researcher at Karlsruhe University working on parallel computer algebra and symbolic manipulation in high energy physics. He joined the group of Theo Geisel at the Max Planck Institute for Dynamics and Self-Organization as an IT and HPC coordinator in 2000. Since 2007 he is the leading IT manager for high performance computing of the entire MPIDS.



Dr. Markus Helmer studied physics at the Universität Ulm and Lunds Universitet (Sweden). In 2011 he began his PhD-studies at the Max Planck Institute for Dynamics and Self-Organization and the Bernstein Center for Computational Neuroscience focusing on the dynamics of a local microcircuit. After receiving his PhD he became a postdoctoral researcher at the MPIDS in October 2015 before moving on to postdoctoral studies at Yale University in June 2016. He is interested in using data-constrained models to study how cognition could emerge from the structure and dynamics of the neuronal substrate.



Dr. Anna Levina studied mathematics at the St. Petersburg State University (Russia) and received her doctorate in mathematics from the University of Göttingen in 2008. Her thesis was carried out in the group of Theo Geisel at the Max Planck Institute for Dynamics and Self-Organization and was awarded the Otto-Hahn-Medal of the Max Planck Society. In 2011 she started working part-time again on self-organized criticality in neuronal networks as a postdoctoral fellow at the MPIDS and the Bernstein Center for Computational Neuroscience Göttingen. In June 2015 she left the department to become an IST-fellow at the Institute of Science and Technology, Austria.



Dr. Jakob Metzger studied physics at Imperial College in London and the University of Freiburg. He received his doctorate from the University of Göttingen in 2010, working in the group of Theo Geisel at the Max Planck Institute for Dynamics and Self-Organization. He was awarded the Otto-Hahn-Medal for his work on particle and wave flows in random media. He also applies methods from nonlinear dynamics and stochastic processes to the study of population genetics and fate determination in stem cells. He left the department in May 2015 to work on early development of human stem cells as a postdoc at Rockefeller University.



Dr. Viola Priesemann studied physics at the Technical University Darmstadt and the Universidade Nova de Lisboa (Portugal). She started her PhD as a joint theoretical and experimental project between the Ecole Normale Supérieure (France) and Caltech (USA). She then moved with her supervisor Gilles Laurent from Caltech to the Max Planck Institute for Brain Research in Frankfurt, where she defended in 2013. As a PostDoc, she continued her research with Theo Geisel at the MPI for Dynamics and Self-Organization in Göttingen. In 2014, she became Bernstein Fellow and group leader, and in 2015 she successfully applied for a Max Planck Research Group, which will start in 2016. Combining her expertise in theoretical and experimental neuroscience, she studies information processing in neural networks, addressing the question how networks provide the functional architecture for our cognitive abilities.



Dr. Annette Witt studied mathematics at the Humboldt-University Berlin and received her doctorate in theoretical physics from the University of Potsdam in 1996. Her thesis was awarded the Otto-Hahn-Medal of the Max Planck Society. Annette worked as postdoctoral researcher at various physical and geoscientific institutes in Potsdam, Florence (Italy) and London (U.K.). In 2007, she joined the Department of Nonlinear Dynamics at the MPIDS where she develops tools for characterizing recordings of complex systems and as a PI of the Bernstein Center for Computational Neuroscience Göttingen applied them to neuroscience problems. In 2015 she has joined the research group of Biomedical Physics of the MPIDS where she continues working in data analysis.

Technical and Administrative Staff



Yorck-Fabian Beensen studied physics at the Georg-August-University Göttingen and the University of Aarhus (Denmark). In 1997 he received his diploma from the faculty of geophysics for a work in the field of seismological data analysis which earned him the Berliner-Ungewitter-Prize. He joined the department of Nonlinear Dynamics in 2000 as an IT administrator. In 2001 he was elected as a member of the institute's staff council and has been the head of the council for the last three terms.



Barbara Guichemer has been working as an IT assistant of the Department of Nonlinear Dynamics and the HPC group since February 2007. Since January 2016 she is responsible for IT project management and IT controlling activities in both the HPC group and the central IT service group.



Viktoryia Novak has been working as a foreign language assistant of the department since March 2011. Beyond office management tasks she is responsible for the organization of conferences and visits of international guests as well as for supporting Prof. Fred Wolf in administrative issues and the management of external funds. **Ayse Bolik** is a *European Business Assistant* certified in English and French and has been administrative assistant to Prof. Theo Geisel and the Bernstein Center for Computational Neuroscience since 2010. **Regina Wunderlich** is a *General Business Administrator* and has been administrative assistant to Prof. Theo Geisel and Prof. Eberhard Bodenschatz at the Institute of Nonlinear Dynamics of the Georg-August-University Göttingen since June 2001 and at the Bernstein Center for Computational Neuroscience since 2005.

1.2 DEPARTMENT DYNAMICS OF COMPLEX FLUIDS



Prof. Dr. Stephan Herminghaus received a PhD in physics from the University of Mainz in 1989. After a postdoctoral stay at the IBM Research Center in San Jose (California, USA), he became a research associate at the University of Konstanz in 1991, where he received his habilitation in 1994. In 1996 he became head of an independent Max-Planck Research Group at the MPI for Colloids and Interfaces in Berlin. In 1998, he received calls on full professorships at the Universities of Fribourg (Switzerland) and Ulm, and decided for heading the department of Applied Physics in Ulm. Since 2003 he has been Director at the MPIDS, and since 2005 holds an additional appointment as an adjunct professor at the University of Göttingen. He was appointed as Professeur Invité at the Université Paris VI for the winter term 2006/7 and at the Université Paris Sud for the summer term 2013.

A complex fluid consists of (a large number of) similar mobile entities which are complex enough by themselves to preclude a straightforward prediction of the collective behaviour of the whole. Our research aims at understanding phenomena of self-organization, such as pattern formation and self-assembly, in complex fluids. We hope to identify suitable model systems which yield insight into overarching principles of self-organization in systems as diverse as granular flows, pattern formation in geological settings, aggregation of planetesimals in primordial clouds, swarming in bacterial colonies or in plancton, or patterns in traffic flow. One challenging question is: are there general common 'principles' behind the various instance of symmetry breaking, structure formation, and emergence in open systems? Either finding such principles or proving their non-existence would be equally rewarding. Aside from spontaneous symmetry breaking mechanisms, an important branch of study with great application potential are systems with quenched disorder, such as wetting of random structures. We employ a wide scope of methods, including analytical statistical theory, advanced simulation tools, and cutting edge experimental techniques.

On the fundamental side, granular materials (both dry and wet) have proved to be versatile model systems for studying collective behavior in systems violating detailed balance on the microscopic level. Their particular charm lies in their position at the border of complex interfaces, soft matter, and systems far from thermal equilibrium, thereby connecting fields of expertise of different subgroups of the department. This becomes particularly obvious in our projects investigating the pore-scale physics of oil recovery (funded by BP Inc.), which combines granular physics and wetting with quenched disorder. On the complex side, biological matter and bio-systems are the most intricate systems we are studying, but we try to concentrate on those which are still simple enough to be described by physical and physico-chemical principles. By combination with our expertise in granular systems, a naturally emerging focus of our research is on life in complex geometries. A project with particularly close connection to everyday life concerns public transportation, where we try to establish a demand-driven system in Southern Lower Saxony, on the basis of first-principles statistical physics and state-of-the-art numerical simulations.

During the last two years there have been substantial fluctuations in our personnel. Martin Brinkmann, Matthias Schröter and Jürgen Vollmer left the institute, but are still associated in research projects. Corinna Maaß has joined our department as a new group leader in 2014, while Oliver Bäumchen and Marco Mazza could considerably extend their groups and establish a coherent research profile.



Dr. Oliver Bäumchen studied physics and mathematics at Saarland University (Germany) and graduated in physics in 2006. In 2010 he received his PhD in soft matter physics from Saarland University. He worked as a lecturer at the University of Applied Sciences (Saarbrücken) from 2007 to 2008. In 2011 he was awarded a DFG research fellowship and joined the McMaster University, Canada, as a PostDoc. Since August 2013 he has been a group leader at our institute. Aside from instabilities of complex liquids, he is interested in biological systems at interfaces. In 2015 he was awarded a 'Joliot Chair' and joined the ESPCI Paris as a visiting faculty.



Dr. Christian Bahr studied chemistry at the TU Berlin and received his PhD in 1988. Research stays and postdoctoral work took place at the Raman Research Institute (Bangalore, India) and the Laboratoire de Physique des Solides of the Université Paris-Sud (Orsay, France). After his habilitation for physical chemistry at the TU Berlin in 1992, he moved to the University Marburg as a holder of a Heisenberg-Fellowship in 1996. From 2001 he worked as a software developer in industrial projects before he joined our institute in 2004. Research topics comprise experimental studies of soft matter, mainly thermotropic liquid crystals.



Dr. Lucas Goehring studied physics at the University of British Columbia (B.Sc. 2002) and the University of Toronto (M.Sc. 2003, Ph.D. 2008). He has since continued to study geophysical pattern formation, for example in fossil biofilms or permafrost soils, through experimentally accessible analogues. Between 2008 and 2011 he was elected a research fellow of Wolfson College at the University of Cambridge, where he investigated the cracking behavior of colloidal materials. He joined our institute in 2011 and is currently studying pattern formation in geophysical systems, the solidification of colloidal systems, and the ordering of crack networks. In 2015 he habilitated in Physics at the Georg August University of Göttingen



Dr. Kristian Hantke studied physics at the University of Manchester (B.Sc. 2000) and at the Philipps-University Marburg (Diploma 2002). In 2005 he received his PhD from the University of Marburg. After studying the optical injection of spin currents during a post-doctoral stay at the University of Marburg he joined the group of Prof. S. Herminghaus at our institute as a scientific staff member in 2007. Being the lab coordinator for the laser and microscopy setups, his work centers around the application of new experimental techniques based on nonlinear vibrational imaging and multi-photon laser scanning microscopy.



Dr. Corinna Maaß studied Physics at the University of Konstanz, Germany. She was a fellow with the International Research Training Group "Soft Condensed Matter Physics of Model Systems" and received her PhD in 2009 from the University of Konstanz for research on levitated granular gases. From 2010-2013 Corinna worked as a postdoc in DNA nanotechnology at New York University, USA, from 2010-2011 as a fellow of the German Academic Exchange Service. She joined our institute in 2014 as leader of the working group 'Active Soft Matter'. Her current research focuses on droplet swimmers in complex geometries as well as collective interactions in large scale swimmer systems under variable dimensional confinement.



Dr. Marco G. Mazza received his Master's degree in physics in 2001 from the University of Catania (Italy), followed by a research grant. In 2005 he joined the Boston University as a teaching and research assistant. In 2009 he received his PhD with the thesis "Thermodynamics and dynamics of supercooled water" under supervision of H. Eugene Stanley. Between 2009 and 2012 he worked as a postdoc and lecturer at TU Berlin in the group of Martin Schoen. Since 2012 he has been working as a group leader at the MPIDS on the nonequilibrium physics of granular, soft, and biological matter.

Associated Scientists



Dr. Martin Brinkmann studied physics and mathematics at the FU Berlin and received his Diploma in Physics 1998. After an internship at the Dornier Labs (Immenstaad, Germany) in 1999 he joined the MPI of Colloids and Interfaces (Potsdam, Germany). In 2003 he received his PhD from the University of Potsdam and performed a PostDoc stay at the Interdisciplinary Research Institute in Lille (France). From 2005 to 2012 he has been group leader in our institute. Since then he holds a senior scientist position at Saarland University and is still associated with the MPIDS by the GeoMorph project funded by BP and the SFB 937. He explored wetting of regular and random geometries by simulations and modelings.



Dr. Matthias Schröter studied philosophy and physics at the Universities of Frankfurt and Kassel. He obtained his PhD in 2003 from the University of Magdeburg while working in the group of Ingo Rehberg on pattern formation in electrodeposition. During his postdoctoral stay with Harry Swinney at the Center for Nonlinear Dynamics at the University of Austin he studied the statics and dynamics of granular media. In May 2008 he joined the Department of Dynamics of Complex Fluids as a group leader; since May 2015 he holds a senior scientist position at the university of Erlangen. Main research topics are the statistical mechanics of static granular media and X-ray tomography of complex materials.



Prof. Dr. Ralf Seemann studied physics at the University of Konstanz where he received his Diploma in 1997. The diploma work was carried out at the MPI of Colloids and Interfaces in Berlin-Adlershof. He received his PhD in 2001 from the University of Ulm. In 2003 he received the Science Award of Ulm followed by a PostDoc stay at the University of California in Santa Barbara. Since 2003 he was a group leader at the MPIDS, Göttingen and in 2007 he was appointed as professor at the Saarland University. Among other topics he is concerned with wetting of topographic substrates, wet granular media, and discrete microfluidics. He is still associated with the MPIDS in the framework of the GeoMorph project funded by BP.



apl. Prof. Dr. Jürgen Vollmer studied physics in Bielefeld and Utrecht. In 1994 he received his doctorate at the University Basel (Switzerland). After pursuing postdoctoral studies in Essen, Brussels and Mainz, he joined the Philipps University Marburg. Since April 2007 he has been a group leader at our institute. He holds an appointment as an Associate ("außerplanmäßiger") Professor at the Faculty of Physics of the University Göttingen, and he is a faculty member of the Göttingen Graduate School for Neurosciences, Biophysics, and Molecular Biosciences. In 2013 he became an Associate Editor of *Frontiers in Interdisciplinary Physics*.

Technical Staff



Monika Teuteberg and Dr. Guido Schriever support the head of the department. Monika Teuteberg runs the office as secretary and takes care of administration issues at Faßberg and at Bunsenstraße. Guido Schriever's tasks as the scientific assistant imply among other things scientific reporting and organization of visits and events.



Sibylle Nägle and Thomas Eggers take care of the information technology. Sibylle Nägle focuses on the webpage of the department as well as image creation and processing, while Thomas Eggers supports the desktop computers of the scientists, the computer clusters, the DCF network and the email accounts.



Diana Strüver and Markus Benderoth are responsible for our chemical and biological laboratories. This includes along side the daily operation all safety issues.



Christian Jacob and Wolf Keiderling belong to the service group of the department. Wolf Keiderling operates the mechanical workshop and Christian Jacob works in the electronics workshop.

1.3 DEPARTMENT OF FLUID DYNAMICS, PATTERN FORMATION AND BIOCOMPLEXITY



Prof. Dr. Dr. h.c. Eberhard Bodenschatz received his PhD in theoretical physics from U. Bayreuth in 1989. From 1989 to 1992 he was a post-doctoral associate in experimental physics at UCSB. From 1992 until 2005 he was Professor of Physics at Cornell. In 2003 he became a Director at the MPIDS. Since 2005 he is Adj. Professor at Cornell and since 2007 Professor of Physics at U. Göttingen. From 2012 to 2014 he was Vice-Chair and currently is Chair of the Chemistry, Physics and Technology Section of the Max Planck Society. He is an Alfred P. Sloan Research Fellow, Cottrell Scholar, Fellow of the American Physical Society, Institute of Physics, and the European Mechanics Society. He is Stanley Corrsin Award recipient of the APS and received a Honorary Doctorate from the Ecole Normal Superior de Lyon. He was Editor in Chief of NJP from 2003 - 2015, is on the editorial board of Ann. Rev. Cond. Mat. Phys. and of EPJH. He is a member of the Göttingen Research Council, Vice Speaker of the German Centre for Cardiovascular Research in Göttingen, founding member of the Heart Research Center Göttingen, and coordinator of the European High Performance Infrastructure in Turbulence.

Dynamics and self-organization occurs in many-body systems that are out of energetic equilibrium. If we want to understand the world around us, we must rely on simplifying descriptions that capture the fundamental physical principles. Thus we need to identify *complex systems* that include all necessary parameters, boundary conditions and initial conditions. These together with a rigorous mathematical description, must allow for a quantitative understanding. The understanding and controlling of complex systems poses a major challenge both to physics and mathematics, since the equations are usually coupled, nonlinear, and nonlocal. Nonetheless, though very different in detail, the fundamentals of complex systems can be described by unifying concepts.

Our aim is the search for and the understanding of those concepts in the physics of *fluid- and biomechanics*. In our approach we rely on methods from non-equilibrium statistical mechanics and nonlinear systems theory. Currently we are investigating turbulence in thermal convection; fundamentals of turbulence; inertial and tracer particle transport in fully developed turbulence with implications for fundamental theories, but also for practical issues like turbulent mixing, particle aggregation and cloud micro-physics; the spatio-temporal dynamics in reaction diffusion systems; biofluid mechanics of the heart and brain; and the intra-cellular and self-organizing processes leading to eukaryotic cell motility, chemotaxis, electrotaxis, curvotaxis, and tissue development. We are also partner in the Max Planck Synthetic Biology Initiative, where we focus on micro-fluidic technology and synthetic cilia based motility. The laboratory provides a microscopy facility, a cell biology laboratory, and shares with the other groups a class 1000 clean room for micro-fabrication. It established the Göttingen Turbulence Facility, which consists of a set of experimental systems and a compressed gas facility to achieve ultra-high turbulence levels. The latter is part of the European Infrastructure Network EuHIT, which is coordinated by the department. For investigations of cloud micro-physics we have an outpost at the Environmental Research Station Schneefernerhaus on the Zugspitze at 2650m, where we are also part of the Virtual Alpine Observatory. In 2012, with Stefan Herminghaus we have founded the Focus on Complex Fluid Dynamics.

Our research has been and will continue to be truly interdisciplinary from engineering, material science, physics, geophysics, and applied mathematics, to chemistry, biology, and medicine. We connect seamlessly to the other departments and research groups and are a member of the International Collaboration for Turbulence Research and the German Centre for Cardiovascular Research (DZHK). We collaborate with groups at the MPI for Biophysical Chemistry, the Physics Department, and the Medical Center at the University of Göttingen. In addition, we are embedded in a network of national and international collaborations.



Dr. Albert Bae received his PhD in physics from Cornell University in 2011. His research topic involved the use of microfluidic techniques to provide well controlled environments to investigating the life cycle of *Dictyostelium discoideum*. He continued this work as a postdoctoral researcher at the University of California in San Diego. In 2015, he joined the institute as the leading scientist of the MaxSynBio microfluidics facility.



Prof. Dr. Carsten Beta studied Chemistry in Tübingen, Karlsruhe, and Paris. In 2001, he joined the the Fritz Haber Institute (Prof. G. Ertl) and graduated from the Free University Berlin in 2004. After working as a postdoctoral researcher at Cornell and UCSD, he became a senior scientist at the institute in 2005. In 2007 he was appointed Prof. of Biological Physics at U. Potsdam and stayed associated with the institute. His research focuses on biophysics (cell motility, chemotaxis, actin dynamics, single cell manipulation techniques) and on pattern formation in reaction-diffusion systems.



Prof. Dr. Gregory Bewley received his bachelor's degree from the Mechanical and Aerospace Engineering department (MAE) at Cornell University in 2000. In 2006, he graduated from Yale University for his seminal experimental work on quantum turbulence. He continued this work at the University of Maryland before joining the institute in 2007. Since 2015 he is also a Visiting Assistant Professor in MAE at Cornell University. His work focuses on turbulence, both its intrinsic properties and its role in various environmental settings.



Dr. Christoph Blum studied mathematics and physics at TU at Clausthal and at U. Münster. He received his diplomas (Physics & Mathematics) working on the modeling the convection of fluid above porous media together with Prof. Dr. Rudolf Friedrich and Prof. Dr. Mario Ohlberger. In 2011, he joined the institute as a doctoral student and graduated in 2015. His thesis work includes the experimental investigation of the geometry dependent cell motility and the intracellular dynamics of the actin cortex of *Dictyostelium discoideum*. He is continuing his research as a postdoctoral scientist.



Dr. Azam Gholami studied physics at Sharif University (Iran) where she received her bachelor in 1999. After her master in physics from the Institute for Advanced Studies in Basic Sciences (Zanjan, Iran) in 2001, she continued her study in theoretical physics at the LMU, München and graduated in 2007. In 2008, she joined the institute to work on actin-based motility and flow-driven waves in *Dictyostelium discoideum*. Since 2012, she is a senior researcher. She is coordinating the MaxSynBio project and works on artificial cilia and cilia-driven motility.



Dr. Isabella Guido began her study in electrical engineering at the University of Bologna, Italy. In 2006 she joined the Fraunhofer IBMT in Potsdam and in 2010 received her doctorate in physical engineering from the TU Berlin. From 2010-12 she was postdoctoral researcher at Peking University (China) and from 2012-13 at U. Glasgow developing microsystems for single cells manipulation and characterizing cellular mechanical properties. In June 2013 she joined the institute as a postdoctoral researcher working on cell electrotaxis. Since August 2014 she is a senior researcher within the synthetic biology initiative *MaxSynBio* working on constituting artificial cilia.



Dr. Hsin-Fang Hsu received her master from National Taiwan University in 2010 investigating the mechanism of DNA repair. She joined the institute as a PhD student in 2011. She received her PhD from the Georg-August University Göttingen in 2015 for her work on the oscillatory instabilities of intracellular actin networks. Currently she is a postdoctoral researcher investigating the mechanism of different regulators of the actin network.



Dr. habil. Alexei Krekhov received his PhD in theoretical physics from the Perm State University (Russia) in 1990 studying defects in liquid crystals. During his Humboldt Research Fellowship at U. Bayreuth from 1994-96 he studied pattern formation in liquid crystals. Starting 1999 he was a researcher at U. Bayreuth working on pattern formation in complex fluids and soft matter theory. In 2010 he received the habilitation in theoretical physics from U. Bayreuth. He joined the institute in October 2013. His current research interests include nonlinear dynamics in excitable media, two phase convection and modeling of cell motility.



Dr. John Lawson studied aeronautical engineering at the University of Cambridge and received his Masters degree in 2011. He later completed his PhD there in 2015, where he showed how the statistics of fine-scale turbulence are shaped by the forces generated by self-organized, small-scale motions. This experimental study was made possible by the high-resolution volumetric measurement technique he developed. In September 2015 he joined the institute as a postdoctoral researcher, where his research is focused on the Lagrangian properties of high Reynolds number turbulence.



Dr. Jan Moláček studied mathematics at the University of Cambridge (UK), where he received his BA and MA degrees. In 2013 he received his PhD in applied mathematics from the Massachusetts Institute of Technology (Cambridge, USA) for his experimental and theoretical investigations of droplets bouncing and walking on a vibrating liquid bath. He joined the institute in September 2013 as a postdoctoral researcher and is now a senior scientist. He is mainly involved in experimental investigations of warm and mixed-phase clouds at the research station Schneefernerhaus (UFS) near Zugspitze.



Dr. habil. Holger Nobach received his doctorate in electrical engineering from the University of Rostock in 1997. During his postdoctoral research at Dantec Dynamics in Copenhagen (Denmark) and at the Technical University of Darmstadt, he developed measurement techniques for flow investigations. Since 2005 he has been a senior scientist at the institute with a research visit at Cornell University (NY, USA). In 2007, he received the habilitation in mechanical engineering from the Technical University of Darmstadt. He works on the experimental investigation of turbulent flows and thermal convection and is editor for ISRN Signal Processing.



Prof. Dr. Alain Pumir studied Physics at the ENS in Paris, France. After finishing his studies, he became CNRS junior researcher (1983). He was visiting Scientist at Cornell (1984-1987 and 1990-1991). Back to Paris, he received his Habilitation in 1987. In 1992, he became CNRS Research Director at the Institut Non Linéaire in Nice, France, and joined in 2008 the Laboratoire de Physique at ENS de Lyon. His work is devoted to theoretical and numerical studies in fluid mechanics and biophysics. His collaboration with the institute started in 2008 and has solidified in 2014 with the support of a Humboldt Forschungspreis (2013).



PD Dr. Olga Shishkina studied mathematics at the Lomonosov Moscow State University (LMSU) until 1987. In 1990 she received her doctorate in scientific computing from the Moscow University for Telecommunication & Informatics. After being a senior lecturer at the Rybinsk Aviation Technological Academy until 1994, she worked as a researcher at the LMSU until 2002 and at the DLR Göttingen until 2014. In 2009 she habilitated in fluid mechanics at the TU Ilmenau and in 2014 also in mathematics at U. Göttingen. In 2014 she became Heisenberg fellow and joined the institute where she leads an independent group.



Dr. Michael Sinhuber studied physics at U. Münster. He received his diploma working on turbulent Rayleigh-Bénard convection with the late Prof. Rudolf Friedrich. In 2011, he joined the institute as a doctoral student and graduated in 2015. His thesis work included experimental studies on high Reynolds-number decaying turbulence and the investigation of scaling properties of turbulent flows. Since June 2015, he is a postdoctoral scientist investigating grid geometry effects on decaying turbulence.



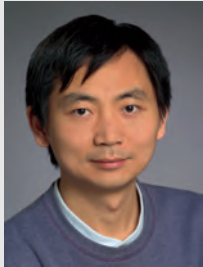
Dr. Marco Tarantola received his diploma at the Würzburg U. in 2005 - focusing on biotechnology - and his PhD in 2010 at the physical chemistry of the Mainz U. for the study of dynamics of epithelial monolayers. In 2010, he became coordinator of the CRC 937. He then joined the institute as a postdoctoral scientist until 2012 to work on *D. discoideum* (D.d.) actin oscillations, before leaving for a stay at the UC San Diego until 2013, where he focused on adhesion and cell polarization of D.d.. Since 2014, he is a senior scientist and currently studies quantitative biology of D.d. and cardiac fibrosis and comparable synthetic model systems.



Dr. Yong Wang studied mechanical engineering and applied mathematics at Xi'an Jiaotong University (China) and, in 2010, received his PhD degree in engineering thermal physics for his development of a lattice Boltzmann method as applied to thermo acoustics and PIV measurements for oscillatory flows. From 2011-15 he was a postdoctoral researcher at UC Irvine (USA), and investigated the turbulent flow in human upper airway with DNS. He then joined the institute as a research scientist in March 2015. His research interests are in biofluidics with patient specific geometry, such as blood flow in beating heart and CSF flow in the ventricles of the brain.



Dr. Stephan Weiß received his diploma in physics from U. Bayreuth in 2005 and a PhD in experimental physics from U. Göttingen in 2009. He worked as a postdoc at the UC Santa Barbara (DFG-Fellowship) on turbulent thermal convection and at U. Michigan about spirals in oscillating chemical reactions. In August 2015 he joined the institute as a senior researcher, where he leads the experimental research on thermal convection.



Prof. Dr. Haitao Xu received his PhD from Cornell in 2003. From 2003 to 2006, he was a post-doctoral researcher at the Laboratory of Atomic and Solid State Physics, Cornell. In August 2006, he joined the institute as a senior scientist. Since 2015, he is a full professor in the Center for Combustion Energy, Tsinghua University, China and stays associated with the institute. His main research interest is the fundamental properties of fluid turbulence and the interactions between turbulence and additives, such as particles or flexible long-chain polymers.



Dr. Vladimir S. Zykov studied physics at the Institute of Physics and Technology (Moscow, Russia). He graduated in 1973, received PhD in 1979, was habilitated in 1990 and occupied the position of leading scientific researcher at the Institute of Control Sciences (Moscow, Russia). In 1992 he joined the group of Prof. Mueller first at the MPI of Molecular Physiology and since 1996 at the Magdeburg University. Since 2001 he was a research scientist at the TU Berlin and in 2010 joined the institute. His research interests include pattern formation processes in nonlinear reaction-diffusion media and control methods of self-organization.



Sabrina Volkmar is responsible for the administration of travel expenses and supports the EuHIT project since 2011.

Angela Meister is a certified foreign language correspondent in English, French, and Italian and has been employed as Administrative Assistant to the Director since May 2005.



Andreas Renner has been employed as a technician in the service area with specialization on electrics since January 2007.

Dr. Artur Kubitzek supports scientists in preparing their experimental set-ups. He is involved in the design, construction and development of scientific facilities as well as management of the service team.

Marcel Meyer received his apprenticeship at the institute and since 2012 works as a mechanic for the GTF.

Andreas Kopp works since 2009 at the institute and he is responsible for the organization of the experimental hall.



Ortwin Kurre is responsible for education in electronics at the institute and supports the team in all matters of electronics.

Gerhard Nolte is responsible for the IT infrastructure and user support of the department since 2005. He joined the institute in 1993.

Dipl. Biologist Maren Stella Müller has been a biological technical assistant at the institute since April 2013. She is responsible for cultivation and genotyping cell lines of *Dictyostelium discoideum*.

Ugur Mavu is a trainee in the electronics shop.

RESEARCH GROUPS

2

CONTENTS

- 2.1 Max Planck Research Group: Biological Physics and Morphogenesis 24
 - 2.2 Research Group: Biomedical Physics 26
 - 2.3 Max Planck Research Group: Neural Dynamics and Behavior 28
 - 2.4 Max Planck Research Group: Network Dynamics 29
 - 2.5 Max Planck Research Group: Theory of Turbulent Flows 32
 - 2.6 Research Group Theoretical Neurophysics 34
 - 2.7 Max Planck Emeritus Group Molecular Interactions 36
 - 2.8 External Scientific Member: Biomedical NMR Research 38
 - 2.9 External Scientific Member: Physics of Fluids 39
-

2.1 MAX PLANCK RESEARCH GROUP: BIOLOGICAL PHYSICS AND MORPHOGENESIS



Dr. Karen Alim studied physics in Karlsruhe, Manchester and Munich. She obtained an MSc in Theoretical Physics in 2004 working with Alan J. Bray from Manchester University, U.K., followed by a Diplom (MSc) in Physics and Biophysics at the LMU Munich. During her PhD with Erwin Frey at the LMU in Munich she investigated the form of biological materials like DNA or actin and patterning mechanism during leaf development. As a grad fellow at the KITP in Santa Barbara, United States, she investigated the mechanics of plant growth. After her doctoral degree in 2010 she joined Michael P. Brenner's group at Harvard University where she focused on the adaptation dynamics of the network-like forager *Physarum polycephalum*. In 2015 she started as an independent group leader at the Max Planck Institute for Dynamics and Self-Organization. Karen is recipient of the John Birks Award of Manchester University and held an appointment as lecturer in Applied Mathematics at Harvard University.

How can an organism grow to form a desired structure and pattern? Understanding the morphogenesis of an organism, the collective self-organization of cells that gives rise to a functional structure is at the heart of decoding life. Unveiling the mechanism nature uses to control the dynamics of development also generates new concepts for bioengineering and synthetic implementations of biological processes. We aim to identify the rules of development by studying the physical principles underlying the formation and adaptation of biological organisms. We combine insights from biological signals with knowledge of physical processes to discover how physical forces induce, transmit and respond to biological signals and thus control development and shape morphology.

We currently focus on two model systems. First, we study the role of mechanical forces in tissues during plant development. Plant tissues are a prime example to study the role of mechanical forces in regulating morphogenesis since plant cell growth is the mechanical yielding of cell walls in response to osmotic pressure. Investigating the dynamics of organ growth we want to answer how stresses build up and interact with cell growth, cell divisions and biological signals to give rise to robust and reproducible organ shape. Second, we investigate the function of fluid mechanics for transport and signal transfer in shaping network growth dynamics primarily in the network-forming slime molds *Physarum polycephalum* and in fungi and the animal vertebrate system. These networks have in common that they continuously grow and adapt their morphology in response to stimuli. Investigating the dynamics of fluid flow and the associated transport of signals throughout these networks we want to unveil the mechanism controlling signal transfer and integration into network morphology. As physical forces are universal, findings are expected to be of general importance for the organization of tissues and the structure of tubular networks, paving the way for bio-mimetic applications in engineering and medicine.

Prior to the start of the group in October 2015 we successfully joined the second term of the Collaborative Research Center 937 on Collective Behavior of Soft and Biological Matter with a project on plant tissue dynamics. In our effort to decode signal transfer in *Physarum polycephalum* we succeeded experimentally to trace the propagation of signals within the networks and are currently marrying the experimental finding with a theoretical model of signal propagation. The first building block to identify the rules of self-organized morphological adaptation of tubular networks.



Dr. Natalie Andrew studied Physics and Cognitive Science at the University of Birmingham, UK. She completed her PhD studying cell motility and pseudopod formation patterns in the social amoeba *Dictyostelium discoideum* in 2006. In 2007 she moved to Harvard Medical School's Systems Biology department to investigate calcium signalling dynamics in mammalian cells using microfluidics. In 2013 she joined the department of Organismic and Evolutionary Biology at Harvard University and began research on fluid flow dynamics and foraging behaviour in the true slime mold *Physarum polycephalum*. She joined the group in February 2016.



Dr. Jean-Daniel Julien received his Master's degree in physics at the École Normale Supérieure de Lyon (ENS Lyon, France) in 2012. As a PhD student, he worked on the mechanics and growth of plants morphogenesis, using computational approaches, in the Physics laboratory and the Plants Reproduction and Development laboratory of the ENS Lyon. In 2015 he was a graduate fellow in the Kavli Institute for Theoretical Physics (Santa Barbara, United-States). His domains of interest are continuum mechanics, non-linear physics, statistical mechanics, and scientific programming. He joined the group in January 2016.

2.2 RESEARCH GROUP: BIOMEDICAL PHYSICS



Hon.-Prof. Dr. Stefan Luther studied Physics at the Georg-August-Universität Göttingen, where he received his doctoral degree in 2000. Postdoctoral research on non-ideal turbulence (University of Twente, 2001-2004) and cardiac dynamics (Cornell University, 2004-2007).

Since 2007, he is head of the independent Research Group Biomedical Physics (tenured 2012) at MPI DS and since 2008 Honorarprofessor at the Georg-August-Universität Göttingen. He received the Medical Technology Innovation Award 2008 and the GO-Bio Award 2012. He is faculty member at the Institute for Nonlinear Dynamics, the Georg-August University School of Science (GAUSS), founding member of the Heart Research Center Göttingen, and member of the DZHK e.V.

Self-organized complex spatial-temporal dynamics underlie physiological and pathological states in excitable biological systems. This holds true in particular for life-threatening cardiac arrhythmias, a major cause for morbidity and mortality world-wide. The term dynamical disease was coined for arrhythmias, suggesting that they can be best understood from the dynamical systems perspective, integrating multi-disciplinary research on all relevant spatial and temporal scales. We are driven by the vision that the systematic integration and evaluation of dynamics on all levels from sub-cellular, cellular, tissue, and organ to the in vivo organism is key to the understanding of complex biological systems and will open – on a long-term perspective – new paths for translating fundamental scientific discoveries into practical applications that may improve human health. Our translational research group focuses on the following objectives: physiological modeling of cardiac dynamics and electro-mechanical instabilities, multivariate analysis, classification and prediction of biosignals, and control of arrhythmias by novel approaches. These aims will be achieved by a data driven, integrative strategy that combines high-resolution imaging techniques with state of the art numerical modeling through innovative state and parameter estimation and model evaluation methods. Based on this approach, we have successfully developed a novel method for low-energy termination of electrical turbulence in the heart. In collaboration with our research partners, we demonstrated that low-energy anti-fibrillation pacing (LEAP) reduces the energy by 80-90%, compared to conventional, state of the art defibrillation methods. Towards clinical application, we aim at disease specific optimization of LEAP in pre-clinical large animal models of myocardial infarction and heart failure. Our group continues to strive for excellence in research and training of young scientists and contributes to the curriculum of Biophysics and Physics of Complex Systems of the Faculty of Physics at the Georg-August-Universität Göttingen. The Biomedical Physics Group is supported through the Gründungsoffensive Biotechnologie 2012 (German Ministry for Education and Research) and participates in several large-scale cross-disciplinary collaborative initiatives including the German Center for Cardiovascular Research (DZHK e.V.), the EU Marie Skłodowska-Curie Innovative Training Network BE-OPTICAL, and the collaborative research centers SFB 937 and SFB 1002.



apl. Prof. Dr. Ulrich Parlitz studied physics at the Georg-August-Universität Göttingen, where he received his PhD in 1987. After five years at the Inst. for Appl. Physics of the TU Darmstadt he returned to Göttingen in 1994 where he was habilitated in 1997 and appointed apl. Prof. of Physics in 2001. He was a visiting scientist at the Santa Fe Institute (1992), the UC Berkeley (1992), and the UC San Diego (2002, 2003). His research interests include nonlinear dynamics, data analysis and cardiac dynamics. In 2010 he joined the Research Group Biomedical Physics. He is faculty member at the Institute for Nonlinear Dynamics, GAUSS, PI at the BCCN, and member of the DZHK e.V.



Dr. Edda Boccia studied biomedical engineering at the University Campus Bio-Medico of Rome, where she received her PhD in March 2014. Her PhD research interests focused on biomedical image analysis, mathematical modeling, and simulations of non-linear biological systems. In particular, she focused on heart dynamics and on the development of novel methodologies for the design of bone conduction cochlear prosthesis. In June 2014 she joined the Research Group Biomedical Physics. Her current research interests include cardiac dynamics, 3D FEM models reconstruction, simulations, mathematical modeling and biomedical image analysis.



Dr. Jan Christoph studied physics at the Georg-August-Universität Göttingen, where he received his Diploma degree in February 2011 and his doctoral degree in October 2014. His thesis focused on multi-modality imaging and inverse imaging problems of cardiac dynamics. He works as a postdoctoral associate in the Research Group Biomedical Physics at the MPI DS. His research interests include cardiac dynamics, tissue electrophysiology and mechanics, mapping and imaging techniques, multi-modality fluorescence imaging, echocardiography as well as tissue engineering and morphogenesis.



Dr. Daniel Hornung studied physics at the Georg-August-Universität Göttingen (2001-2008). After graduation he worked as a research assistant in the Research Group Biomedical Physics at the MPI DS, where he received his PhD in November 2014. At his current position as a postdoctoral research associate in the Research Group Biomedical Physics, he focuses on the interaction between structure and dynamics in excitable media and state transitions in oscillatory systems.



Prof. Dr. Valentin Krinski studied physics at the Institute of Physics and Technology, Moscow, where he received his PhD in 1964. After 12 years at the Institute of Biological Physics in Puschino, he was appointed Head of the Autowave Laboratory in 1976, Prof. of Biological Physics at the Institute of Physics and Technology, Moscow in 1980. Since 1993, he was Directeur de Recherche, CNRS, INLN, Nice, France. His research interests include rotating vortices in biological excitable tissues and novel approaches for the termination of life-threatening chaos in the heart. In 2007 he joined the Research Group Biomedical Physics.



Dr. Claudia Richter studied biology at the University of Rostock, with focus on animal physiology and forensic biology (2000-2005). After graduation she worked as research associate at the department of forensic genetics at the Institute of Legal Medicine in Rostock. She received her PhD in February 2011 and since March 2011 works as a postdoctoral associate in the Research Group Biomedical Physics at the MPI DS. Her research interests include cardiac dynamics, biophysics and molecular biology, biomaterials, and tissue engineering.

2.3 MAX PLANCK RESEARCH GROUP: NEURAL DYNAMICS AND BEHAVIOR



Viola Priesemann studied physics in Darmstadt and Lisbon. For her PhD, she switched to neuroscience, combining theoretical work at the Ecole Normale Supérieure (Paris, France) with experiments at Caltech (Pasadena, USA), and subsequently at the MPI for Brain Research (Frankfurt, D).

After a brief postdoc at the MPI-DS (Göttingen), she became Bernstein Fellow and started establishing her group on neural dynamics and information processing. In 2015, she was offered a free-floater Max Planck Research Group, which provides funding for an independent research group.

Viola Priesemann is faculty member in the Göttingen Graduate School for Neurosciences, Chair of the Computational Neuroscience Social of the Society for Neuroscience (2015), reviewer for the European Commission, and Fellow of the Schiemann Kolleg.

How do neural networks provide the basis for reliable, yet flexible information processing *in vivo*, and how does the functional network architecture impact our performance? We address this question in the context of critical phenomena, because criticality maximizes information processing capacity in models. Most interestingly, already small deviations from criticality, due to small changes in network parameters, can have large impact on computational properties and network dynamics. We hypothesize that the brain makes use of this extraordinary sensitivity, using it as a tuning mechanism to adjust its functional properties to task requirements.

Our research on information processing and collective dynamics of brain networks requires combining approaches from physics, biology and medicine: Specifically, we draw on statistical physics, information theory, network dynamics, neurophysiology, and neuropathology. Combining these approaches, we address the following objectives: (a) When comparing theory and experiment, it is crucial to correctly quantify information processing and collective dynamics from brain recordings. These, however, are either limited to sampling just a few hundred among the billions of neurons (spatial subsampling), or to measuring a coarse version of neural activity (local field potential, EEG, BOLD). Our most recent result is the derivation of a measure that allows us for the first time to quantify the distance to the critical point under subsampling. Using this measure, we (b) want to identify the relation between information processing and dynamical state. Here we could demonstrate recently that the processing capacity *diverges* at the critical point not only in models, but also in experiments. This clearly demonstrated the sensitivity of processing in neural networks to small changes around criticality. The key questions are thus (c) whether and how this relation is harnessed by the brain to adapt processing to task specific needs, whether we can identify the underlying network-physiological mechanisms, and whether we can understand the neuropathological implications of misregulations. We address this body of questions in close collaboration with experimentalists from Bonn, Beer Sheva, Cambridge and Göttingen. Such diverse collaborations allow us to identify the fundamental principles of network function and pathology across scales, from single neurons *in vitro* to spiking networks in humans. (d) Finally, we want to characterize human behavior in live musical performances as a marker of neural information processing. The dynamics of music is expected to mirror neural network dynamics and the musical information content is expected to be a signature of processing in the brain.

With our research, we tackle one of the most fascinating questions in science: How is it possible that the network of neurons in our head can make us think, feel and reason? Our work addresses central aspects of this question by identifying fundamental principles of function-driven network organization.

2.4 MAX PLANCK RESEARCH GROUP: NETWORK DYNAMICS

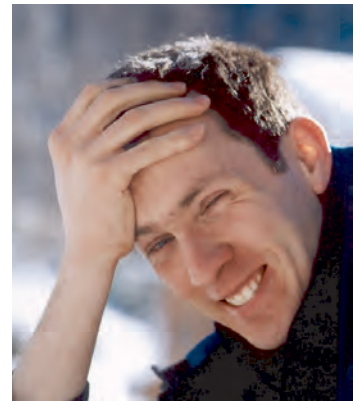
Networks are everywhere. And most of them are dynamic. From biochemical reactions in the cells of our bodies to the neuronal circuits in our brains that make us behave; from social ties forming networks of our friendships to the power grids that provide huge amounts of electric energy; all of these systems form networks of units that interact to yield complex, emergent forms of functions – and all are crucial to our everyday life.

Fundamental research on the dynamics of networks thus is an intrinsically transdisciplinary endeavor and as such not represented by traditional subjects focused on by institutes and departments at most universities and research institutions. A researcher starting to work on what is on its way to become “Network Science” in the future thus needs to read text books and articles on graph theory and stochastics, nonlinear dynamics, statistical physics, computation, and algorithms, as well as the specific subject she is aiming to investigate, e.g. in biology, physics or engineering.

In the Network Dynamics team, we are working towards a unifying understanding of the fundamentals underlying the dynamics of large, nonlinear interconnected systems. We theoretically study topical questions arising from a broad range of phenomena in physics, in neurobiology, in evolution, and in the engineering of self-organizing “intelligent” systems.

Moreover, a substantial part of our work is investigating emergent mathematical objects and developing mathematical and computational tools necessary to understand the novel phenomena arising in network dynamical systems.

These seemingly disjoint research topics are strongly overlapping as they are joined by two types of links: The first set of links is methodological, resulting from developing mathematical and computational tools of nonlinear dynamics and statistical physics of networked systems. The second set of links exists on a systems level; most of our work focuses on the theory of collective dynamics of nonequilibrium, nonstationary, excitable or oscillatory networks (and their constituents).



Marc Timme (Prof. Dr. rer. nat, MA) studied physics and mathematics in Würzburg, Stony Brook (New York, USA) and Göttingen. He received a Masters’ degree in physics in 1998 (Stony Brook) and a doctorate in theoretical physics in 2002 (Göttingen). After a Postdoc at the MPI for Flow Research from 2003, he was a Research Scholar at the Center of Applied Mathematics, Cornell University (USA), in 2005 and 2006. In December 2006 he became the head of the research group *Network Dynamics* of the Max Planck Society and in 2009, Adjunct Professor at the University of Göttingen. He is part of the steering committees of the International Max Planck Research School (IMPRS) Physics of Biological and Complex Systems as well as the Program for Theoretical and Computational Neuroscience and faculty member at the Georg August University School of Science (GAUSS).

Current topical research of our *Network Dynamics* team include:

- **Model-free Inference of Network Topology from Dynamics.** Given the collective nonlinear dynamics of the units of a network, can we find its interaction topology without any detailed dynamic model? We affirmatively answer this question for a large class of network dynamical systems in Chp. 8.14 and Chp. 8.11.
- **Collective Nonlinear Dynamics of Modern Power Grids.** We started a novel research direction with a 2012 publication on decentralized network dynamics in the presence of renewable energy sources. It was highlighted in *Physics* and marked as Editorial Suggestion in *Physical Review Letters*. In 2013/2014 we further initiated a major BMBF-funded research collaboration with five theoretically working research institutions and five additional application partners from academia and industry. Please see Chp. 8.15.
- **Selective Processing in Neural Systems.** How can a neuronal network respond to one but not to another stimulus if both are statistically the same? How can one steer the propagation of collective signals in neural circuits by non-specific global signals? Combining insights from neurobiology and nonlinear dynamics, we work towards clarifying such questions in neuroscience, see Chp. 8.8.
- **Nonstandard Phase Transitions.** After our theoretical explanation of classes of percolation transitions that have properties of both continuous and discontinuous phase transitions (*Nature Physics*, 2011), we are currently working towards experimentally identifying such nonstandard transitions in physical systems of fluid aggregates. We also work on predicting transitions to extreme events.
- **High-Dimensional Data from Social and Biological Networks.** Interestingly, data on social and on biological networked systems come with a number of similar obstacles for data analysis, including extremely high dimensionality, largely incomplete data sets, and many hidden, unobservable units. We are working out theoretical tools to overcome limitations in analysis of such data, often following unconventional paths, for instance bundling data orthogonal to accepted classes, on purpose ignoring details that commonly were thought key, or skipping data to learn more. See Chp. 6.13 for examples.
- **EcoBus - Flexible Public Mobility by "Intelligent" Networking.** Together with the Department of Complex Fluids, we proposed a flexible public mobility system integrating the flexibility of taxis with the sharability of buses. Please see Chp. 8.12 for details.



Dr. Sarah Hallerberg did her PhD project on time series analysis and predictability of extreme events in stochastic processes under the supervision of Prof. Dr. H. Kantz at the MPIPKS in Dresden. In 2007 she was also a visiting scientist at the Centre for the Analysis of Time Series at the London School of Economics, working on the predictability of forecast errors in meteorological ensemble forecasts. In 2008 she received her PhD in theoretical physics and started to work as a temporary Lecturer at the Department for Applied Mathematics at the University of Cantabria. There she also became interested in scaling properties of perturbations in spatio-temporal chaotic systems. In 2011 she joined the MPIDS to work on the analysis of whale vocalizations, perturbations in high dimensional chaotic systems and several other data analysis projects.



Dr. Wen-Chuang Chou received the B.S. degree in civil engineering from National Taiwan University, Taiwan in 2003 and the M.S. degree in electrical engineering from National Dong Hwa University, Taiwan in 2005. After receiving another M.S. degree in electrical engineering from Polytechnic Institute of New York University, USA in 2009, he spent six months working on the visual working memory in the Department of Neuroscience, Baylor College of Medicine, USA. In October 2009, he joined the Network Dynamics group, where his research in sensory coding focuses on the neural modeling of collective olfactory functions. He received the Ph.D. degree in Physics from the University of Göttingen in 2014 and continues working on the same theoretical topic in neuroscience.



Dr. Nora Molkenthin studied Physics at the Freie Universität Berlin, Manchester University (UK) and the University of Cambridge, where she received her Master of Advanced Study in 2009. After research at Uppsala University (Sweden), she received her PhD at the Potsdam Institute of Climate Impact Research and the Humbolt University Berlin in 2014 with a thesis on the relationship of flow dynamics and climate network topology. In parallel, she was member of the graduate school Visibility and Visualization at Postdam University. She joined the Network Dynamics Group in December 2014. Her research interests focus on conceptual modelling of complex disordered systems.



Dr. Jose Casadiego received his Licentiate (equivalent to German Diplom) in Physics at the University of Carabobo (Venezuela) after studies from 2004 to 2009. After a research project at the Center of Medical and Biotechnological Research (CIMBUC) in Carabobo in 2010, he came to Göttingen to do a PhD on neuroscience. He joined the Network Dynamics group in 2011 and finished his PhD thesis on inverse problems on network dynamics in 2015. His work mainly focuses on the development of model-free approaches for inferring network structures from their dynamics.

2.5 MAX PLANCK RESEARCH GROUP: THEORY OF TURBULENT FLOWS



Dr. Michael Wilczek studied physics at the Westfälische Wilhelms-University Münster from which he received his Diploma in 2007 and his doctorate in 2011 in Theoretical Physics under supervision of Prof. Rudolf Friedrich. After a stay at the Kavli Institute for Theoretical Physics at Santa Barbara (USA), he continued to work as a postdoctoral fellow at the Institute of Theoretical Physics at the University of Münster. In 2013 he joined the group of Prof. Charles Men-
eveau at the Department of Mechanical Engineering at Johns Hopkins University, Baltimore (USA) as postdoctoral fellow funded by the DFG. After a short stay in the group of Prof. Rainer Grauer at the Ruhr-University of Bochum, he joined the MPIDS as an independent research group leader in 2015. Since summer 2015 he is building his group dedicated to fundamental aspects of turbulent flows.

Fully developed turbulence is a paradigm of a dissipative system with many, strongly interacting degrees of freedom. It is the generic state of fluid motion, and our atmosphere and the oceans represent two prominent examples from nature in which turbulence plays a key role. It also is of central importance for many engineering applications ranging from mixing and combustion to wind energy conversion.

Due to the broad impact on different branches of science, turbulence research has become an increasingly interdisciplinary research field, yet many fundamental questions remain open. The central challenge lies in deriving a statistical description of turbulence based on first principles. This is impeded by its inherent non-Gaussianity and the breaking of statistical self-similarity, both of which are related to small-scale coherent structures and the occurrence of extreme events. Therefore turbulence constitutes a prototypical problem of non-equilibrium statistical mechanics and, in fact, is sometimes considered as the last grand challenge of classical physics.

From the viewpoint of fundamental research, we are witnessing an exciting era in which the latest experiments and state-of-the-art numerical simulations can access overlapping Reynolds numbers ranges. This allows to draw a picture of turbulent flows at an unprecedented level of detail. In view of the rapid development of experimental and numerical techniques since the start of this century the time is right to focus on novel theoretical concepts.

The goal of our team, which was established in summer 2015, is to develop these concepts through a simulation-assisted theoretical approach. We employ state-of-the-art parallel direct numerical simulations to explore turbulent flows with focus on multi-scale interactions and small-scale structures. We also study their impact on mixing and Lagrangian transport. We thereby seek to identify relevant dynamical and topological features, which serve as inspiration for the development of analytical theories. While we draw our main motivation from the investigation of turbulent flows, many of the theoretical and numerical techniques are relevant in a much broader context and help to advance, for instance, the field of non-equilibrium statistical mechanics.

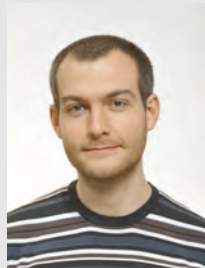
With the knowledge gained, we furthermore strive to address problems from neighboring fields such as geophysics and atmospheric sciences. Turbulent convection, the dynamo problem and the investigation of atmospheric boundary layers with application to wind energy research constitute just a few examples. Our group participates in various national and international collaborations such as the NSF-supported WINDINSPIRE collaboration dedicated to wind energy research.



Dr. Cristian C. Lalescu studied physics at the University of Craiova (UCv), from which he received his diploma in 2006. He then spent a year at the Free University of Brussels (ULB), through the SOCRATES/ERASMUS exchange program. In 2007 he started a joint doctorate program, under the supervision of Prof. Daniele Carati from ULB and Prof. Bucur D. Grecu from UCv, working mostly in Brussels. After having defended his thesis in 2011, he joined the group of Prof. Gregory L. Eyink in the Department of Applied Mathematics and Statistics of the Johns Hopkins University in Baltimore, USA, as a postdoctoral fellow. In the summer of 2015 he moved to the MPIDS to work in the Wilczek group. He is primarily interested in dynamical system theory, turbulence and the related mathematics and computer science.

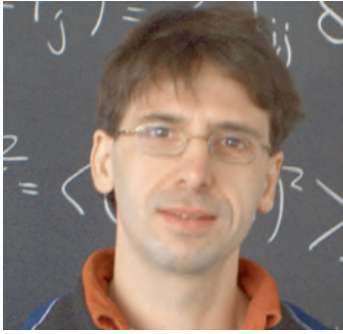


Dr. Laura J. Lukassen studied Computational Engineering at the Technische Universität Darmstadt. She was member of the Graduate School of Excellence Computational Engineering at TU Darmstadt and received her doctorate in Mechanical Engineering from TU Darmstadt in April 2015 supervised by Prof. Martin Oberlack and Prof. Dieter Bothe. During her doctoral studies she spent the fall term of 2012 as a Visiting Graduate Student at the Johns Hopkins University in Baltimore, USA, in the group of Prof. Andrea Prosperetti working on the numerical simulation of particle flows. Her doctoral research was focused on the stochastic description of non-Brownian particles. Since June 2015 she is working in the field of statistics of turbulence with a focus on intermittency and space-time correlations in the group of Dr. Michael Wilczek at the MPIDS.



Dr. Dimitar G. Vlaykov finished his undergraduate degree in mathematics at the University of Cambridge in 2006. He was selected for the first class of the Astromundus Masters course in astrophysics, which he completed in 2012 with a thesis on the 'Observable consequence of open inflation' at the University of Göttingen under the supervision of Dr. Thorsten Battefeld. His doctorate studies were completed at the same university under the supervision of PD Wolfram Schmidt in 2015 with a thesis titled 'Sub-grid scale modelling of compressible magnetohydrodynamic turbulence: derivation and a priori analysis'. Currently, his work is centered around non-locality and small-scale structure of incompressible hydrodynamical turbulence within the group of Dr. Michael Wilczek.

2.6 RESEARCH GROUP THEORETICAL NEUROPHYSICS



Prof. Dr. Fred Wolf studied physics and neuroscience at the University of Frankfurt, where he received his doctorate in theoretical physics in 1999.

After postdoctoral research at the Interdisciplinary Center for Neural Computation of the Hebrew University of Jerusalem (Israel), he became a research associate at the MPI für Strömungsforschung in 2001. Since 2001 he spent various periods as a visiting scientist and program director at the KITP (Santa Barbara, USA). In 2004 he became head of the research group Theoretical Neurophysics at the MPIDS. He is a founding member of the Bernstein Center for Computational Neuroscience in Göttingen and faculty of several Physics and Neuroscience PhD programs at the University of Göttingen.

Since 2011-2015 he served as Section Coordinator for Computational Neuroscience of the German Neuroscience Society. Since 2013 he is Chairperson of the Bernstein Center of Computational Neuroscience in Göttingen and since 2015 Co-Chairperson of Göttingen University's research focus area Physics-to-Medicine. In 2014 he was elected Fellow of the American Physical Society and became a member of the review committee for research grants of the Human Frontier Science Program.

The brains of humans and animals arguably are among the most complex systems in nature. Understanding their operation crucially depends on the ability to analyze the cooperative dynamics of spatially distributed multi-component systems: Even the most elementary sensory stimulus engages large ensembles of interacting nerve cells distributed throughout the brain. The processing power of biological neuronal circuits exactly results from their collective dynamics. In addition, complex nervous systems utilize processes of dynamical self-organization to generate and maintain their processing architecture. The amount of information in a mammalian genome is by far insufficient to specify the wiring of biological neuronal networks in microscopic detail. Functionally useful processing architectures are thus dynamically generated by self-organization on the level of neuronal circuits. Finally, even an individual nerve cell is a complex dynamical system. Virtually all single neuron computations critically depend on the dynamical interaction of a multitude of subcellular components such as ion channels and other interacting biological nano-structures. It is due to this ubiquity of collective behaviors that neuroscience provides a rich source of attractive research questions for the theoretical physics of complex systems.

The Research Group Theoretical Neurophysics examines neurobiological and biophysical phenomena that provide challenging problems for the development of mathematical theory and can be approached in precise quantitative experiments. Our work extends from the formulation and development of novel mathematical approaches tailored to the specifics of neuronal systems dynamics, over the development of analysis methods for turning biological experimental observations into theoretically informative quantitative data, to the development of experimental paradigms optimally designed to provide insight into cooperative and dynamical aspects of neuronal function. To achieve a close interaction of theory and experiment, many projects are pursued in collaboration with experimental biological research groups around the world. Three problems are at the core of our research agenda: (1) The self-organization of neuronal circuits in the visual cortex. In this system our analyses demonstrate that biological neural networks follow apparently universal quantitative laws which require the development of adequate mathematical theories of neuronal self-organization. (2) The dynamics of large networks of pulse-coupled neurons and its impact on the representation of sensory information. Here the ergodic theory of network dynamical systems promises to provide a natural language that links details of the network dynamics to information preservation, decay and flux. (3) The biophysical nature and dynamics of high-bandwidth action potential encoding. Here we are integrating concepts from non-equilibrium statistical physics with the biophysics of membranes and ion channels. The identification of dynamically realistic models of single neuron operations is essential for understanding collective computations in the brain.



Dr. Andreas Neef received his Diploma in physics in 2000 from the University of Jena, Germany. He joined the MRC Laboratory of Molecular Biology, Cambridge (UK) as a visiting scientist to work on retinal neurons and then worked on his PhD at the Research Centre Jülich, Germany, where he received his doctorate from Cologne University in 2004. After being a postdoctoral researcher at the Institute for Biological Information Processing I in Jülich (2004) and at the Bernstein Center for Computational Neuroscience, Göttingen he became a Bernstein Fellow associated with the Department of Fluid Dynamics, Pattern Formation, and Nanobiocomplexity in 2006. Since 2013 he heads the research group Biophysics of Neuronal Computation at the Bernstein Center for Computational Neuroscience.



Dr. Guillaume Lajoie studied mathematics at the University of Ottawa (Canada) and applied mathematics at the University of Washington (USA) where he received a PhD in Applied Mathematics in 2013. In 2010 he worked as a visiting scholar at the Instituto de Mathematica Pura e Aplicada in Rio de Janeiro (Brazil). His research focuses on the development and application of dynamical systems techniques to understand information processing in networks of spiking neurons. He worked at the MPIDS and the Bernstein Center for Computational Neuroscience Göttingen as a Bernstein Fellow from 2012 to 2014 and then accepted a position at the University of Washington (Seattle, USA).



Dr. Juan Daniel Flórez Weidinger studied physics at Los Andes University (Bogota, Colombia) and attended the International Max Planck Research School for Neuroscience master courses. He obtained his PhD in 2013 at the Max Planck Institute for Dynamics and Self Organization studying the dynamics of self-organizing disordered visual cortical architectures. Since then, he is a postdoctoral fellow at the Max Planck institute for Dynamics and Self Organization where he uses a combination of theoretical physics and data analysis methods to understand the evolutionary origins and dynamics of orientation domains in the visual cortex.



Dr. Maximilian Puelma Touzel studied physics at the University of Toronto (Canada) and has been a member of the Max Planck Institute for Dynamics and Self Organization since 2011. He obtained his PhD in 2015 in the International Max Planck Research School for the Physics of Biological and Complex Systems for theoretical work on the stability of network dynamics with intrinsic degrees of freedom. Since November 2015, he is a postdoctoral researcher within the Laboratoire de physique theorique at the Physics Department of the Ecole Normale Supérieure in Paris, France.



Dr. Yvonne Reimann studied biology at the University of Göttingen and finished her PhD at the Max Planck Institute for Biophysical Chemistry in Göttingen in 2008 for work on cell fate determination during cortical development. From 2008 to 2009 she was a Postdoc in the Department Molecular Cell Biology at the Max Planck Institute for Biophysical Chemistry. She did postgraduate studies in science management at the German University of Administrative Sciences Speyer from 2009 to 2010. From 2010 to 2012 she worked as scientific coordinator at the Leibniz Research Laboratories for Biotechnology and Artificial Organs at Hannover Medical School before changing to the Research Department of University of Göttingen. Since December 2012, she is the administrative coordinator of the Bernstein Center for Computational Neuroscience Göttingen and Bernstein Focus Neurotechnology Göttingen.

2.7 MAX PLANCK EMERITUS GROUP MOLECULAR INTERACTIONS



Prof. Dr. Dr. h.c. mult. J. Peter Toennies studied physics and chemistry at Brown University, Providence, USA where he received his Ph.D. in 1957. He came to Germany in 1957 where he was a postdoc and "Assistent" 1957-1965 in Wolfgang Paul's Physics Institute in Bonn. After his habilitation (1965) he was a Dozent until becoming director at the MPI Strömungsforschung in Göttingen (1969-2002). Since 1971 he is Associate Professor at the University of Göttingen and Adjunct Professor at the University of Bonn.

Together with the late Hans Pauly (1928 - 2004) we came to Göttingen in 1969 from the University of Bonn to establish the new research direction of molecular beam investigations of elementary collision processes between molecules at the newly reorganized Max-Planck-Institut für Strömungsforschung. In the following years the Institute became one of the leading international centers for experimental and theoretical research in determining the laws governing the dynamics of molecular collisions as well as the van der Waals forces between atoms and molecules. These forces are of fundamental importance for understanding both the static and dynamic properties of gases, liquids and solids as well as their phase transitions. Our research led to the development of a new model for the van der Waals interaction, the Tang-Toennies potential, which is now widely used for accurate simulations in place of the well-known Lennard-Jones potential

In the course of these studies our group observed in the late 1970's that helium free jet gas expansions behaved in a remarkable way. Instead of the usual velocity distributions with $\delta v/v \equiv 10\%$, the helium atom beams had very sharp velocity distributions and were nearly monoenergetic with $\Delta v/v \leq 1\%$. This unexpected observation was found to be related to the extremely weak interatomic forces between He atoms, with the consequence that their collision cross section, at the ultra-low ambient temperatures ($T < 1\text{K}$ in the expanding gas) rises to 259.000, more than 4 orders of magnitude larger than the cross section at room temperature. These nearly monoenergetic helium atom beams have found widespread application. In expansions with small concentrations of molecules the excess of helium atoms serves to cool the molecules down to temperature of several degrees K. This became a great boon for molecular spectroscopy since at these temperatures the hot bands that otherwise obscure the molecular spectra are eliminated.

Our group later exploited the helium atom beams for exploring the structures and vibrations at the surfaces of solid crystals. In complete analogy to neutrons, which are routinely used to study the structures and phonon dispersion curves inside solids, helium atoms are the ideal scattering probe method for investigating the structures and dispersion curves of phonons at solid surfaces, which are not accessible with neutrons. The study of over 200 different surfaces by helium atom scattering (HAS) and the complimentary method of inelastic electron scattering (EELS) have led to a much more profound knowledge of interatomic forces at surfaces and how atoms and molecules interact with metal surfaces, which is of basic importance for understanding catalysis. In the following years we became even more fascinated by this unusual element helium, which is the only substance which exhibits superfluidity, a collective quantum phenomena similar to superconductivity. In its superfluid state below 2.2 K liquid helium flows without friction, just as the electrons in a superconductor flow without resistance. Thus it was natural to ask if small clusters and droplets of helium might also ex-

hibit superfluidity. Our finding that atoms and molecules were trapped in the droplet's interior opened up the possibility of employing their spectroscopy to interrogate the physical properties of helium droplets. Surprisingly the sharp spectral features of the embedded molecules indicated that the molecules rotate freely as if they were in a vacuum and not at all strongly hindered as expected for an ordinary liquid. Subsequent experiments revealed that this remarkable behavior was related to the superfluidity of these droplets and has since been accepted as the first microscopic finite size manifestation of superfluidity.

Helium nanodroplets are now being used in more than 25 laboratories worldwide as a uniquely cold ($0.15 - 0.37K$) and gentle matrix for high resolution molecular spectroscopic investigations of atoms, molecules, and "tailor made" clusters, their chemical reactions, and their response to photo-excitation. Our group used this technique to provide the first evidence that para-hydrogen molecules which, like He atoms are spinless bosons, can also exhibit microscopic superfluidity. Our most recent experiments were directed at exploring the nature of small pure clusters ($N \leq 100$) of helium and hydrogen molecules. To this end we developed an apparatus to study the matter-wave diffraction of cluster beams from nanostructured transmission gratings. These experiments led to the first evidence for the existence of the dimer and the precise measurement of its size and of the van der Waals interactions of a number of atoms and molecules with solid surfaces. Unexpected magic numbers were found in larger clusters ($N \leq 50$), which have led to the first insight into the elementary excitations of these nano-sized superfluids.

At present we are collaborating with several groups in three main areas of research: (1) With the theory group of Giorgio Benedek at the University of Milan we are preparing a monograph entitled "Surface Phonons". This monograph will provide a survey of the present understanding of surface phonons and the related theory for the interaction of atoms with surfaces; (2) We have recently completed the analysis of experimental data relating to the flow of solid helium through a 100 micron capillary. The analysis indicates that the flow is non-classical in that it does not follow the Hagen-Poiseuille law. Rather it exhibits an unexpected large velocity which is independent of the pressure gradient. This phenomenon is attributed to a type of Bose-Einstein Condensation of a solid with high concentration of vacancies. (3) In collaboration with a Master student we are currently investigating a new model for the van der Waals potentials of the alkali atoms Na, K, Rb, and Cs in the weakly bound lowest triplet state. These potentials are of great current interest for understanding the collisions in laser trapped ultra-cold gases and their Bose-Einstein Condensation.

2.8 EXTERNAL SCIENTIFIC MEMBER: BIOMEDICAL NMR RESEARCH



Prof. Dr. Jens Frahm is Director of the Biomedizinische NMR Forschungs GmbH at the Max Planck Institute for Biophysical Chemistry in Göttingen (Germany). He studied physics at the Georg-August-Universität in Göttingen and received a diploma degree in 1974 and a PhD in physical chemistry in 1977. In 1982 he founded a Biomedical NMR group at the Max Planck Institute for Biophysical Chemistry which since 1993 operates as a non-profit research company fully financed by its MRI patents. Frahm is a recipient of the European Magnetic Resonance Award, the Gold Medal of the International Society for Magnetic Resonance in Medicine, the Karl Heinz Beckurts-Award, the State Award of Lower Saxony for Science, the Research Award of the Sobek Foundation for Multiple Sclerosis, and the Science Award of the Foundation for German Science. He is an ordinary member of the Göttingen Academy of Science and Humanities.

Our research is devoted to the further development and application of magnetic resonance imaging (MRI) and localized magnetic resonance spectroscopy for noninvasive studies of animals and humans. Current projects range from advanced methods that monitor the dynamics of myocardial functions and blood flow in real time to neurofeedback training in humans by functional brain mapping. The use of genetically modified animals allows us to link molecular and genetic information to MRI-accessible functions at the system level.

Our recent breakthrough towards real-time MRI is based on the use of non-Cartesian spatial encoding, pronounced data undersampling, and image reconstruction by regularized nonlinear inversion. Pertinent techniques bear the potential to alter the future of (clinical) MRI. They allow for movie recordings of speech production, turbulent flow or the beating heart – without synchronization to the ECG and during free breathing. The computational demand is met by a parallelized algorithm and multiple graphical processing units which could be fully integrated into the software framework of a commercial MRI system.

A second area of research focuses on studies of the functional organization of the human brain and its axonal connectivity. Diffusion MRI provides information about the orientational dependence of the anisotropic water mobility in brain tissue and may be exploited for three-dimensional reconstructions of nerve fiber tracts. In order to overcome limitations of the standard echo-planar imaging technique we developed a single-shot stimulated-echo MRI sequence which is now further extended by radial undersampling and nonlinear inverse reconstruction. Functional brain mapping deals with the neural encoding of sensorimotor functions. Our results for fine-scale finger somatotopy in humans indicate consistent intra-digit topographic maps for the little but not the index finger within the primary somatosensory cortex. Neurofeedback training of brain activity is a potential treatment option for psychiatric diseases offering access to arbitrary structures. Our aim is to investigate the role of fMRI-based neurofeedback in the anterior mid-cingulate cortex which relates to higher-order cognitive processes.

Animal MRI research addresses the pathophysiologic mechanisms underlying human brain disorders. The development of MRI techniques for transgenic mice allows for structural, metabolic, and functional assessments of the mouse brain at high spatial resolution. An observation of utmost importance is the high but reversible elevation of brain lactate in response to volatile anesthetics. The metabolite responses to various neuromodulators indicate a stimulation of adrenergic pathways as well as an inhibition of the respiratory chain. Corresponding findings in conditional Cox10 mutant mice, in which oligodendrocytes suffer from impaired oxidative energy metabolism, suggest the use of lactate as brain energy source, so that oligodendrocytes survive by enhanced nonoxidative glucose consumption which in turn secures the maintenance of myelin as well as long-term axonal integrity.

2.9 EXTERNAL SCIENTIFIC MEMBER: PHYSICS OF FLUIDS

Scientific profile and characteristics of work

Lohse's Physics of Fluids (PoF) group presently works on a variety of aspects in the fundamentals of fluid mechanics. The subjects include turbulence and multiphase flow, micro- and nanofluidics, granular matter, and biomedical flow. Both experimental, theoretical, and numerical methods are used. We closely collaborate with several companies, among them Océ and ASML. On the experimental side the key expertise of the group lies in high-speed imaging. Further information, including an updated list of publications, is available under <http://pof.tnw.utwente.nl/>

The main characteristics of Lohse's work is the direct interaction of experiment, theory, and numerics, all done in the PoF group. He is not method-driven, but problem-driven, and often had to acquire the required methods or knowledge from some neighboring fields to solve some particular research questions he had been obsessed with. This led to various fruitful interactions and collaborations with neighboring disciplines, such as engineering, mathematics, chemistry, acoustics, medicine, biology, or even computer science. As will be seen from the list below, various of his subjects have an "application perspective". Lohse and his coworkers also understand to visually present the scientific questions they are addressing and their results. This led to ten winning video entries to the Gallery of Fluid Motion from the American Physical Society, Division of Fluid Dynamics, and various television reports and newspaper articles on their work. It also makes Lohse's science very visual for laymen, with a positive effect on the outreach of science in general.

Overview on present main research subjects

Turbulence

Rayleigh-Bénard (RB) flow, the flow in a box heated from below and cooled from above, and Taylor-Couette (TC) flow, the flow between two coaxial, independently rotating cylinders, are the two paradigmatic systems of physics of fluids. They are the drosophilas of the field and various new concepts in fluid dynamics have been tested with these systems. In the last few years, in joint work between Göttingen and Twente, we succeeded to realise the transition from the so-called classical turbulence to the so-called ultimate turbulence for RB turbulence and TC turbulence, thanks to the Göttingen U-Boot facility and the Twente turbulent TC facility (T³C), with which we can achieve and precisely measure an unprecedented degree of turbulence. In the ultimate state, not only the bulk of the flow is turbulent, but also the boundary layers, which for weaker driving (in the classical regime) is mainly of laminar type. The transition from one regime to the other is



Prof. Dr. Detlef Lohse studied Physics in Kiel and Bonn, finishing with a Diploma thesis on the theory of meson-meson interaction in 1989. He then did his PhD with Prof. Siegfried Grossmann on the theory of turbulence in Marburg/Germany, graduating in 1992. As a postdoc in Chicago (with Prof. Leo Kadanoff) and later in Marburg (habilitation 1997) he worked on single bubble sonoluminescence. In 1998 he got appointed as Chair of Physics of Fluids at the University of Twente, where he still is. Lohse is elected Member of the German Academy of Science (Leopoldina, 2002), the Royal Dutch Academy of Science (KNAW, 2005), and Member of the Max Planck Society. He also is Fellow of the American Physical Society, Division of Fluid Dynamics (2002), and of the Institute of Physics (IoP, 2004). He received various prizes such as the Spinoza Prize (2005), the Simon Stevin Prize (2009), an ERC-Advanced Grant (2010), the Physica Prize (2011), the George K. Batchelor Prize for Fluid Dynamics (2012), and the AkzoNobel Prize (2012). He also got knighted by the Dutch Queen as 'Ridder in de Orde van de Nederlandse Leeuw' (2010). Lohse is Associate Editor of Journal of Fluid Mechanics, Annual Review of Fluid Mechanics, and several other journals.

so important because it dramatically changes the heat or momentum transfer properties of the system. E.g., if one used the heat transfer scaling laws of the classical regime for heat transfer estimates for large temperature differences as they occur in geophysical and astrophysical situations, one would easily be off by a factor of 10 and more! So it is crucial to understand the nature of the transition and the properties of the ultimate state of turbulence.

Next to the experiments on TC flow, we perform highly parallelized (10^5 cores) direct numerical simulations (DNS) on both TC and RB flow, and also on double diffusion convection and other related systems, also focusing on the understanding of the flow. We also look at drag reduction in these systems by adding bubbles and particles.

Multiphase flow and free surface flow

The largest setup in the PoF lab is a 8m high turbulent water channel in which bubbly turbulence or turbulence with particles is studied, accompanied by numerical work. We developed new experimental techniques to follow thousands of bubbles and particles both in time and in three-dimensional space, allowing for a better understanding of the turbulent multiphase flow organization and the dynamics of particle and bubble clusters in these flows. Recently we started to focus on multiphase flow with phase transitions.

Our research on the impact of objects on free liquid surfaces aims at revealing the mechanism of the resulting observed jet formation, combining experiments, theory, and numerical simulations. This process is very relevant for the gas exchange between the atmosphere and the ocean. Vice versa, we also study the impact of drops on solid surfaces, including superheated ones, focusing on heat exchange, splash formation, and droplet spreading.

Inkjet printing and droplet impact

On this subject the PoF group very closely collaborates with Océ Technologies. Together they revealed the disturbing role of bubbles entrained into piezoacoustic ink channels and offered solutions to resolve this problem. They also found the origin of the bubble entrainment, namely capillarity driven flow on the nozzle plate, and developed models for the droplet formation and impact of droplets on substances. Lohse's work on inkjet printing is both fundamental and applied at the same time. The present work in the PoF group includes inkjet printing of suspensions and nanoparticles (in the context of printing of solar cells and OLEDs (organic light emitting diodes)), inkjet printing of living cells, and droplet solidification. We also work on tin droplet jetting and impact in the context of extreme ultraviolet (EUV) lithography, together with ASML.

Wetting phenomena and droplet evaporation

We work on wetting phenomena on smooth, chemically, or geometrically structured surfaces and in particular on surface nanodroplets

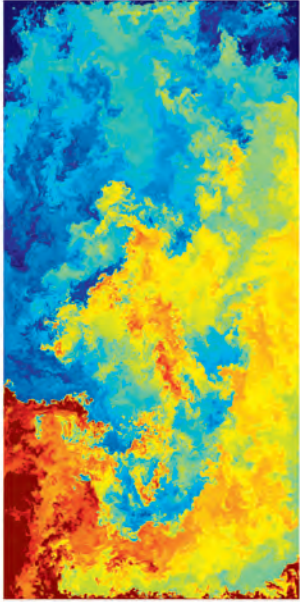


Figure 2.2: Snapshot of an numerical simulation of Rayleigh-Bénard flow at a Rayleigh number of $Ra = 1 \cdot 10^{12}$ and a Prandtl number of $Pr = 0.7$.

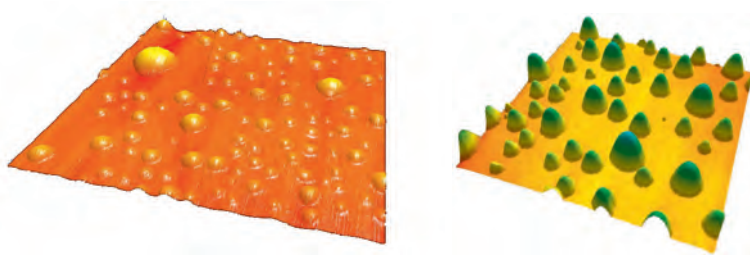


Figure 2.3: (a) AFM image of nanobubbles produced by the solvent exchange method on HOPG. The imaged area is $4 \times 4 \mu\text{m}^2$. (b) AFM image of nanodroplets produced by the solvent exchange method on hydrophobized silicon. The imaged area is $30 \times 30 \mu\text{m}^2$, and the color code is from 0 to 800 nm. Taken from Lohse, Zhang, *Rev. Mod. Phys.* **87**, 981 (2015).

and nanodroplets, whose counterintuitive stability we could account for. We try to better understand the nucleation and growth or the dissolution of nanobubbles and nanodroplets, either in another liquid or in a gas (then called condensation/evaporation). We firmly believe that major progress can be achieved at the interface between surface chemistry and fluid dynamics, by combining the methods from these two fields, both on the experimental, numerical, and theoretical side. This also holds for catalysis and electrolysis, where emerging nanobubbles at the surface often cause a major problem.

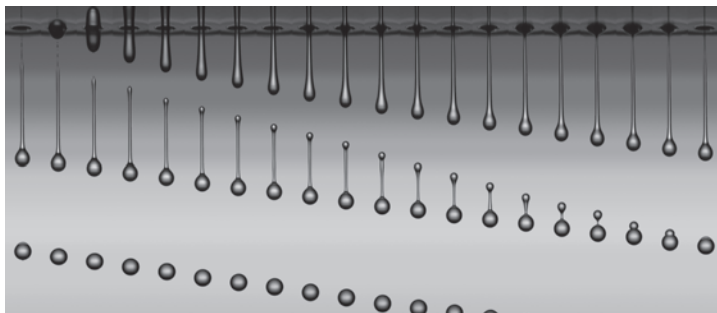


Figure 2.4: Liquid droplet formation in piezoacoustic inkjet printing generation visualized by an ultra-high-speed stroboscopic technique. Figure taken from A. van der Bos et al., *Phys. Rev. Applied* **1**, 014004 (2014)

Ultra-high-speed imaging and cavitation

The PoF group developed the world's fastest camera, the so-called Brandaris 128, allowing for 125 digital images with a frame rate of 25 million frames per second, thus enabling visualization at time scales down to 40 nanoseconds. We also pushed forward other ultra-high-speed imaging and visualization techniques, opening a totally new world of ultra-fast processes in various subfields of fluid dynamics. In particular, we have used these techniques for ultrasound diagnostics and local gene and drug delivery to cells. We also look at various cavitation phenomena, such as cavitation of vapor bubbles in microcapillaries. These events can induce a supersonic liquid jet, which has great potential for needle-free injections in the medical context.

PART I

RESEARCH

LARGE SCALE RESEARCH INITIATIVES

3

CONTENTS

- 3.1 European high-performance infrastructures in turbulence 46
 - 3.2 Max Planck synthetic biology initiative: from microcompartments to cilia-driven motility 47
 - 3.3 Bernstein Center for Computational Neuroscience (BCCN) Goettingen 49
-



3.1 EUROPEAN HIGH-PERFORMANCE INFRASTRUCTURES IN TURBULENCE

Coordinators E. Bodenschatz, H. Nobach

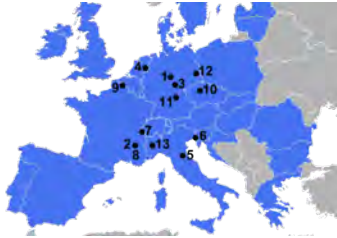


Figure 3.1: The EuHIT facilities

1. Göttingen Turbulence Facility
2. Grenoble Helium Infrastructures
3. Barrel of Ilmenau
4. Twente Turbulence Facilities
5. Center of International Cooperation in Long Pipe Experiments
6. High Rayleigh Number Cryogenic Facility
7. CERN Cryogenic Turbulence Facility
8. CORIOLIS Rotating Platform
9. LML Boundary Layer Wind Tunnel
10. Czech Cryogenic Turbulence Facility
11. Refractive Index Matched Tunnel
12. Cottbus Turbulence Experiment Facilities
13. Turin Rotating Platform

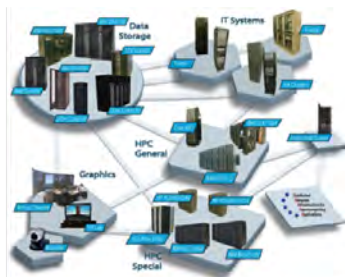


Figure 3.2: Digital Library of Turbulence Data

Advances in key economical and societal issues facing Europe like ground-, air-, and sea-transport, energy generation and delivery, processing in chemical industries, marine biosphere management, climate change impact, atmospheric and marine pollution prediction, and carbon capture and storage processes are obstructed by the lack of understanding of turbulence. The reason lies in the fact that turbulent flows underlie all macroscopic natural and technological flows as soon as mass transport is large. In the past 10 years Europe has surpassed all other nations in research output and development of national infrastructures.

Within the Seventh Framework Programme FP7-Infrastructures-2012-1 the European Commission supports the project European High-Performance Infrastructures in Turbulence (EuHIT, Grant Agreement Number 312778), an access programme of infrastructures for studying turbulence phenomena and applications. It is coordinated by Eberhard Bodenschatz.

EuHIT integrates cutting-edge European facilities for turbulence research across national boundaries. The goal of EuHIT is to significantly advance the competitive edge of European turbulence research with special focus on providing the knowledge for technological innovation and for addressing grand societal challenges. Current members of EuHIT include 25 research institutes and 2 industrial partners from 10 European countries. EuHIT is based on 14 national turbulence research infrastructures, which — together with the knowledge developed upon them — are interconnected by a Networking Program and Joint Research Activities.

EuHIT provides a network linking research activities and training programs at the infrastructures. It gives free access for researchers from academia and industry to the infrastructures and to the knowledge-base of turbulence data. In addition, EuHIT promises to offer assistance in questions of data analysis and measurement technology. EuHIT develops new techniques, algorithms, and next generation instruments through Joint Research Activities to maintain the EuHIT infrastructures at the leading edge and it implements new tools and procedures to foster easy and open access to data and techniques developed from EuHIT, including the transfer of knowledge from academia to industries.

EuHIT implements the European Turbulence Database (TurBase), an easily accessible knowledge-base infrastructure for high quality turbulence data. It provides easy access to experimental and numerical data, as well as data derived from theoretical models. It efficiently curates, preserves and provides access to the data and metadata collected or produced by EuHIT.

[1] <http://www.euhit.org>
 [2] MPI-DS@euhit.org

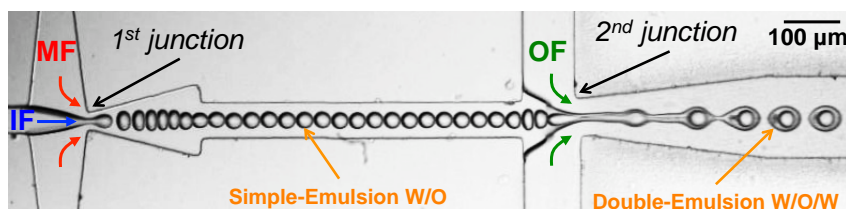
3.2 MAX PLANCK SYNTHETIC BIOLOGY INITIATIVE: FROM MICROCOMPARTMENTS TO CILIA-DRIVEN MOTILITY

A. Bae, O. Bäumchen, A. Gholami, I. Guido, J. Petit, M. Tarantola,
E. Bodenschatz, S. Herminghaus
L. Thomi, F. Wurm, K. Landfester (MPIP, Mainz), I. Polenz, J.-C. Baret
(Bordeaux), R. Faubel, G. Eichele (MPIBPC, Göttingen)

Synthetic biology aims at creating biological-like function by assembling bio-inspired building blocks. The bottom-up approach of *MaxSynBio* has as ultimate goal the realization of a minimal artificial cell. In order for these synthetic systems to be functional, they have to be capable of biochemical processes that are essential for a living cell, e.g. a metabolism or a motility. In nature the functional units are typically localized and linked to membrane-bound components. Thus, the cell membrane is of paramount importance for the cell functionality and cellular life in general.

One of the key challenges in this field is the fabrication of synthetic micro-compartments that provide the possibility of encapsulating other components with high efficiency as well as membrane functionalization. Vesicles appear as ideal candidates and can either be formed from the self-assembly of phospholipid molecules (liposomes) and also amphiphilic block-copolymers (polymersomes). The design of polymersomes strongly benefits from the vast experience in polymer synthesis. Their properties such as the membrane thickness, molecular composition and mobility can be tailored by tuning the polymeric building blocks, e.g. their chemical composition and molecular weight.

Within the *MaxSynBio* initiative, we develop PDMS-based microfluidic chips for the fabrication of liposomes and polymersomes based on a double-emulsion approach (see Fig. 3.3) [1]. A flow-focusing configuration results in the formation of stable water/oil/water double emulsions (see Fig. 3.4). The middle (oil) phase contains the dissolved polymer molecules which are self-assembling while the oil is removed in a solvent-extraction process. The resulting polymersomes exhibit an excellent monodispersity; their size can be precisely controlled by adjusting the flow rates of the fluid phases (see Fig. 3.5). Under non-specific storage conditions the vesicles are stable for several months.



In custom-made PBD-*b*-PEO polymersomes, the membrane molecules may exhibit an end-group functionalization with an alkyne and/or an acrylate group, as evidenced by the reaction of specific fluorescent

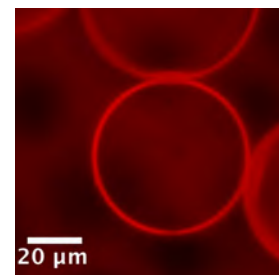


Figure 3.3: Poly(butadiene)-*b*-poly(ethylene oxide) polymersomes fabricated on a microfluidic platform.

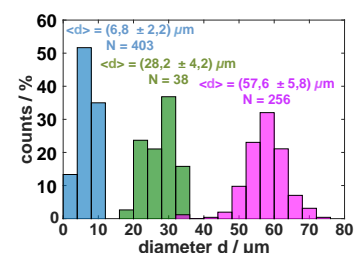


Figure 3.4: Size distribution of the polymersomes resulting from different combinations (different colours) of flow rates of the fluid phases.

Figure 3.5: Microfluidic realisation of double emulsions: A first junction creates a single emulsion from an aqueous inner (IF) and an oily middle fluid (MF), sheared by an aqueous outer fluid (OF) at a second junction.

dyes. Such functionalized block-copolymer molecules enable further modifications, such as e.g. the linkage of certain biomolecules.



Figure 3.6: Encapsulation of isolated cilia inside droplets generated in a microfluidic setup.

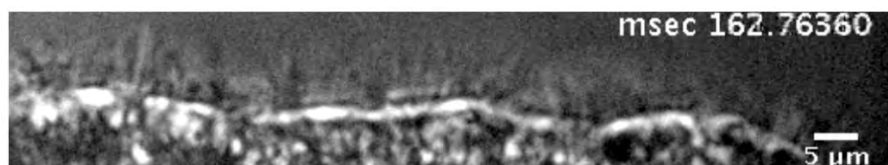


Figure 3.7: The ventricular system of the mouse brain is filled with cerebrospinal fluid (CSF) and is surrounded by brain tissue. The luminal surface of the ventricular system is covered with ependymal cells. Ependymal cells have rod-shaped protrusions called cilia. Cilia exert a lash-like movement to induce a directional flow of CSF along the ependyma [2].

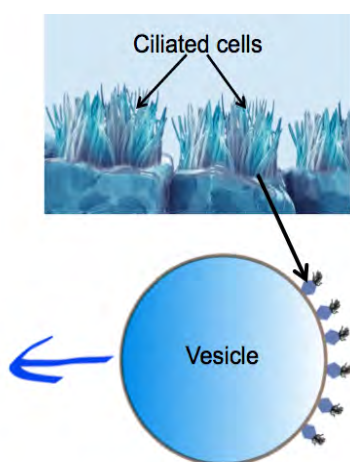


Figure 3.8: Schematic representation of natural cilia (top) and of a synthetic ciliated system (bottom).

Monodisperse polymersomes and liposomes can be used as compartments for encapsulation of active microtubule structures such as cilia [3], or for developing ciliated systems capable of swimming. Many small organisms and cells swim in a viscous environment using the active motion of cilia and flagella. These hair-like appendages can undergo periodic motion and use hydrodynamic friction to induce cellular self-propulsion. We have successfully isolated cilia from the ventricular system of the mouse brain by means of a calcium shock technique [4] (see Fig. 3.7). The membrane of the isolated cilia can be permeabilized to add ATP which is a chemical fuel for dynein and kinesin molecular motors. These motors generate internal forces and thus induce periodic waving or beating patterns of motion. By encapsulating these beating cilia in polymersomes we intend to create mixing flows inside the compartment and thus beating diffusion [5]. Furthermore, by using a few essential components such as microtubules and motor proteins, we intend to develop simple biological beating structures that resemble cellular cilia [6]. We can use them for developing ciliated systems able to propel themselves forward or to move a fluid across a fixed surface. For this task we perform (i) the polymerization of microtubules, (ii) a successful binding of these structures to a surface and (iii) the inclusion of motor proteins for spontaneous oscillations. As a proof of concept, a bead coated with streptavidin is chosen as the body for the microtubule binding. Biotinylated microtubule seeds act as anchor system for binding the cilia-like structures to the bead surface reproducing a ciliated system. For the optimization of this binding procedure, we aim to use Microtubule Associate Proteins (MAPs) mixtures. These proteins contain a microtubule-binding domain that attaches to the external lateral surface of microtubules. After a successful development of a ciliated polymersome we intend to characterize the dynamics of these developed microtubule structures that mimic cellular cilia.

- [1] D. van Swaay and A. deMello, *Lab Chip* **13**, 752 (2013).
- [2] R. Faubel, C. Westendorf, E. Bodenschatz, G. Eichele, *preprint* (2015).
- [3] T. Sanchez et. al., *Nature* **49** 431 (2012).
- [4] W. Bönigk et. al., *J. Neurosci.* **19** 5332 (1999).
- [5] C. Felix et. al., *Science* **345** 1135 (2014)
- [6] T. Sanchez et. al., *Science* **333** 456 (2011)

3.3 BERNSTEIN CENTER FOR COMPUTATIONAL NEUROSCIENCE (BCCN) GOETTINGEN

Coordinator F. Wolf



Complex system theories for neuroscience. The central research objective of BCCN Goettingen is to understand the cooperative dynamics of neuronal systems on different hierarchical levels of nervous system organization, from cellular function, through sensory systems, to cognition and behavioral control by addressing four fundamental questions: How do supramolecular complexes and interacting intracellular structures contribute to adaptive single neuron computation? How does the collective dynamics of biological neural networks drive processes of adaptive coding and learning? How do dynamical interactions within sets of brain areas mediate the flexible use of neuronal processing resources and strategies? How can the interaction between neuronal motor control and high-dimensional movement kinematics generate smooth, precise, and effective movements? To answer these questions, dynamical systems approaches and complex system theories are used to elucidate how biological instantiations of cooperative dynamics lead to adaptive information processing.

Bernstein Fellow program. The Bernstein Fellow program provides early independence for advanced postdoctoral researchers who want to develop their own internationally competitive research agenda or who want to independently collaborate with PIs and laboratories at the MPIDS and the BCCN Goettingen.

Educating a new generation of scientists. With the objective to train a new generation of scientists who are familiar with both, the most advanced theoretical and mathematical concepts as well as the biology of nervous systems, BCCN Goettingen has set up a PhD program in Theoretical and Computational Neuroscience (PTCN). It was one of the first programs in the Goettingen Graduate School for Neurosciences, Biophysics, and Molecular Biosciences. In PTCN, students are jointly advised by a committee of three faculty members that can be chosen from all involved disciplines to match the background, scientific interests and the research project of the student.

Integrating research groups across the Goettingen Campus. BCCN Goettingen integrates research groups at the Georg-August University of Goettingen, Max Planck Institute for biophysical Chemistry (incl. BiomedNMR), Max Planck Institute for experimental Medicine, Max Planck Institute for Dynamics and Self-Organization, German Primate Center, and Otto-Bock HealthCare. The interdisciplinary research center is embedded in the Goettingen Campus providing access to an impressive collection of resources, facilities, infrastructure, and support services. BCCN Goettingen is one of the core structural elements of the growing National Bernstein Network for Computational Neuroscience, funded by the Federal Ministry of Education and Research, Germany. Network Partners are mutually connected by the exchange of data, analysis methods, computer models, and theoretical approaches. Teaching and training of young researchers and integrating the discipline

'Computational Neuroscience' into University education by establishing interdisciplinary training programs constitutes a central element of the Bernstein Network.

New initiatives. The top-level research at BCCN and strong interactions with partners at Goettingen Campus provide a breeding ground for new collaborative research initiatives. Collaborative Research Centers (CRC) funded by the German Research Foundation like the CRC 889, as well as the Leibniz Science Campus Primate Cognition are only two examples for successful initiatives spawned by BCCN research. Funded by the Volkswagen Foundation, BCCN partners are presently involved in three new joint initiatives that will be developed further as collaborative research clusters: 1) Physics to Medicine, 2) Functional Principles of Living Matter: Life at the Nanoscale, and 3) Primate Cognition: From Information Integration to Decision-Making.

FRONTIERS FAR FROM EQUILIBRIUM – STATISTICAL PHYSICS OF STRONGLY DRIVEN SYSTEMS

4

Most systems of relevance in nature are far from thermal equilibrium, due to some internal or external drive. Since our textbook knowledge can so far only treat situations close to equilibrium, there is a long standing need for improving our conceptual tools. In this chapter, we focus on a subset of systems which are of particular relevance, such as turbulence, which governs oceans, clouds and climate, and granular gases, which are paradigmatic for systems breaching detailed balance on a microscopic level, and together with turbulence are essential in cosmic structure formation. Turbulence is studied both theoretically and experimentally in a number of facilities and with different methods. Our studies of driven granular gases proceed mainly *in silico*, and lead us to very fundamental questions about the deeper structures of non-equilibrium physics. The latter then branch out into various aspects of living *vs.* non-living systems.

CONTENTS

- 4.1 Turbulent thermal convection: Experiment 52
 - 4.2 Turbulent thermal convection: Theory 54
 - 4.3 Cloud microphysics measurements on the Zugspitze 56
 - 4.4 Statistics of turbulence 57
 - 4.5 Tracking particles to decipher the mystery of turbulence 59
 - 4.6 An analytical model for intermittency in turbulence 61
 - 4.7 Turbulent flows: How local is 'non-local'? 63
 - 4.8 Nonequilibrium transitions in granular matter 64
 - 4.9 A 'potential' for non-equilibrium states? 65
 - 4.10 Stochastic processes with random resetting 66
 - 4.11 Dynamics and pattern formation in nonequilibrium, entropically driven systems 67
-

4.1 TURBULENT THERMAL CONVECTION: EXPERIMENT

S. Weiss, X. He (Harbin Inst. of Technology, China), D. van Gils (Univ. of Twente, The Netherlands), G. Ahlers, E. Bodenschatz, P. Prabhakaran, H. Nobach, O. Shishkina, A. Schröder (DLR, Göttingen)

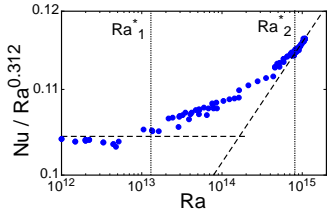


Figure 4.1: The heat transport Nu , compensated by $Ra^{0.312}$, is plotted against the non-dimensional temperature difference Ra . At $Ra \leq Ra_1^*$, the system is in the classical state with an effective exponent $\gamma_{eff} \approx 0.312$. After a transition range $Ra_1^* < Ra < Ra_2^*$ the effective exponent is $\gamma_{eff} \approx 0.38$, consistent with theoretical predictions for the ultimate state [2].

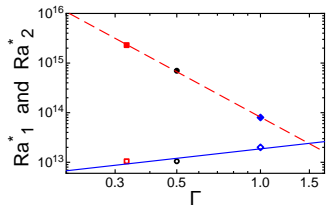


Figure 4.2: The lower (Ra_1^* , open symbols) and upper (Ra_2^* , solid symbols) bound of the transition region as a function of Γ . The transition range becomes smaller with increasing aspect ratio.

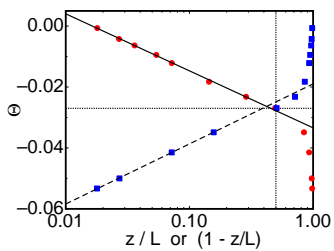


Figure 4.3: The dimensionless temperature $\Theta = (T(z) - T_m) / \Delta T$ as a function of vertical distance z/L or $1 - z/L$ from the plates on a logarithmic scale for $Ra = 9.9 \times 10^{14}$. Red circles: $\Theta(z/L)$. Blue squares: $\Theta(1 - z/L)$.

Rayleigh-Bénard convection (RBC), where a fluid is confined by a warm plate from below and a cold one from above, served for many years as a model for buoyancy-driven convection which occurs for instance in astrophysical and geophysical systems as well as in industrial processes. It was investigated extensively both experimentally and numerically [1]. Much of the research focused on the quantitative relation between the thermal driving (the Rayleigh number Ra) and the convective heat transport (the Nusselt number Nu) as well as the induced flow velocity (the Reynolds number Re).

While for Ra up to $\approx 10^{12}$ (the so-called *classical* regime) power-law relations for $Nu(Ra)$ and $Re(Ra)$ were measured and theoretically explained, for larger Ra such as those occurring in geo- and astro-physical systems the relationships have not yet been fully elucidated. Kraichnan [2] predicted that the thermal and viscous boundary layers close to the top and bottom plate, which are laminar in the classical regime, become turbulent at a critical $Ra = Ra^*$. As a result, the power laws describing Nu and Re are predicted to have larger exponents. The heat flux is no longer determined by the boundary layers, but by the convective flow in the bulk. Measuring and understanding the properties of this so-called *ultimate regime* is essential for the extrapolation of laboratory measurements to geo- and astro-physical systems.

With the unique high-pressure facility known as the “U-Boot” of Göttingen at the MPIDS we recently reached very large Ra up to 4×10^{15} and made measurements that compared well with predictions and (at modest Ra) with simulations. We used sulfur hexafluoride (SF_6) at pressures up to 19 bar confined in cylindrical cells of diameter $D = 1.12$ m and various heights up to $L = 3.3$ m. The Prandtl number in these experiments was $Pr \approx 0.8$, similar to that of the atmosphere.

We observed a change of the local exponent γ_{eff} for $Nu \propto Ra^{\gamma_{eff}}$ from $\gamma_{eff} \approx 0.31$ for $Ra < Ra_1^*$ (for $\Gamma = 0.50$) to $\gamma_{eff} = 0.38$ for $Ra > Ra_2^*$ (fig. 4.1) [3]. The lower and upper values Ra_1^* and Ra_2^* define a transition range where γ_{eff} increases continuously with increasing Ra . The exponent for $Ra \geq Ra_2^*$ agrees well with the predicted exponent for the ultimate-state scaling [2, 4], and the predicted value of Ra^* [5] falls within the observed transition range, i.e. $Ra_1^* < Ra^* < Ra_2^*$.

Experiments with different aspect ratios $\Gamma = D/L$ reveal a Γ dependence of the transition range (fig. 4.2). While Ra_1^* increases slightly, Ra_2^* decreases strongly with increasing Γ and thus the width of the transition region becomes smaller. Extrapolation of the data suggests a crossing of $Ra_1^*(\Gamma)$ and $Ra_2^*(\Gamma)$ near $\Gamma \approx 1.4$, suggesting that there will be no range and instead a unique Ra^* for larger Γ .

We also determined an effective Reynolds number Re_{eff} , based on the mean velocity U and the rms fluctuation velocity \bar{V} ($V_{eff} =$

$\sqrt{U^2 + V^2}$), from local temperature measurements using the elliptical approximation of He and Zhang [6, 7]. The exponent ζ of the power law $Re_{eff} \propto Ra^\zeta$ also changed in the transition range. While in the classical regime $\zeta \simeq 0.43$ was consistent with predictions [5], for $Ra > Ra_2^*$ we measured $\zeta = 0.50$, as predicted for the ultimate state [4]. In the transition range the Re_{eff} values yielded estimates of the boundary-layer shear Reynolds-numbers ranging from about 200 to 400, consistent with the expected transition to turbulent BLs in shear flows.

An important discovery coming from local temperature measurements was the observation of logarithmic temperature profiles in the bulk [8], both in the classical and the ultimate state (fig. 4.3). We were able to show that there is a close analogy between these log profiles and the ‘‘Law of the Wall’’ of turbulent shear flow when it is assumed that the plumes emanating from the plates in RBC play the same role as the coherent eddies in shear flow [9]. The parameters of the log profiles were different in the classical and the ultimate state [9].

Convection in geo- and astro-physical systems often is influenced by rotation. Thus, recently we built a rotating table capable of carrying a load of 3000 kg and rotating at up to 3 rad/s, and placed the $L = 2.24$ m cell ($\Gamma = 0.50$) onto it (fig. 4.4). We are especially interested in the turbulent geostrophic regime where local Coriolis forces are balanced by local pressure gradients. This regime is very difficult to access in laboratory experiments or numerical simulations, and yet important for the understanding of *e.g.*, Earth’s atmosphere and currents in the oceans. We will be able to reach this regime with our high-pressure convection facility, and expect to test existing theoretical predictions. Preliminary experiments at lower pressure using air have been completed. For Ra up to 2×10^{11} they agree well with numerical simulations and experimental measurements of other groups. Measurements at larger Ra (where there are no other results) are about to begin.

In a separate project we studied turbulent moist convection in a two-phase binary mixture of SF_6 and He for Ra up to 10^8 in a rectangular cell with $\Gamma = 3.0$. The cell was filled such that liquid SF_6 was located at its bottom with a gaseous He/ SF_6 mixture above it. Due to the applied temperature gradient, SF_6 constantly evaporated from the liquid into the gas phase, where it condensed into microscopic droplets. The resulting SF_6 clouds were driven by the underlying turbulent flow. With this experiment we try to better understand cloud formation, in particular the nucleation and growth of liquid droplets as well as the interaction between the droplets and the turbulent flow.

- [1] G. Ahlers, S. Grossmann, D. Lohse, *Rev. Mod. Phys.* **81**, 503 (2009)
- [2] R. H. Kraichnan, *Phys. Fluids* **5**, 1374 (1962)
- [3] X. He, et al., *Phys. Rev. Lett.* **108**, 024502 (2012)
- [4] S. Grossmann and D. Lohse, *Phys. Fluids* **23**, 045108 (2011)
- [5] S. Grossmann and D. Lohse, *Phys. Rev. E* **66**, 016305 (2002)
- [6] G.-W. He and J.-B. Zhang, *Phys. Rev. E* **73**, 055303 (2006)
- [7] X. He, et al., *New J. Phys.* **17**, 063028 (2015)
- [8] G. Ahlers, E. Bodenschatz, et al., *Phys. Rev. Lett.* **109**, 114501 (2012)
- [9] G. Ahlers, E. Bodenschatz and X. He, *J. Fluid Mech.* **758**, 436 (2014)

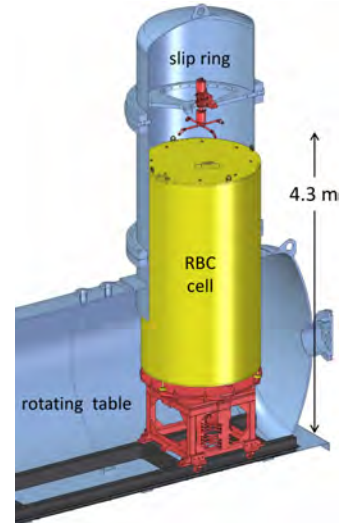


Figure 4.4: Schematic of the rotating turbulent convection setup. The $\Gamma = 0.50$ cell (yellow) stands on a rotating table (red) inside the U-Boot (blue), which is filled with SF_6 at 19 bar. Two slip rings and a water feed through provide electrical connections as well as temperature-regulated water from the stationary into the rotating frame.

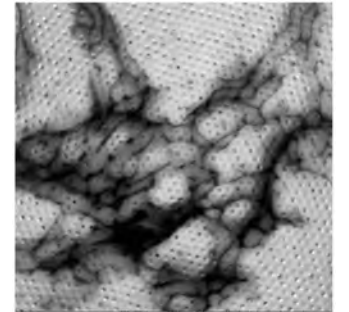


Figure 4.5: Condensation of SF_6 in a turbulent thermal convection of an He- SF_6 mixture.

We acknowledge the support from the DFG Collaborative Research Center (SFB) 963 ‘‘Astrophysical Flow Instabilities and Turbulence’’, project A06 ‘‘Transition in rotating turbulent Rayleigh-Bénard convection’’.

AstroFiT
Astrophysical Flow Instabilities and Turbulence

4.2 TURBULENT THERMAL CONVECTION: THEORY

O. Shishkina

E. Bodenschatz, E. S. C. Ching (The Chinese Univ. of Hong Kong), S. Grossmann (Philipps-Univ. Marburg), S. Horn (Imperial College, London, UK), D. Lohse (Univ. of Twente, Enschede, The Netherlands, and MPIDS), S. Wagner (Audi AG, Ingolstadt), S. Weiss

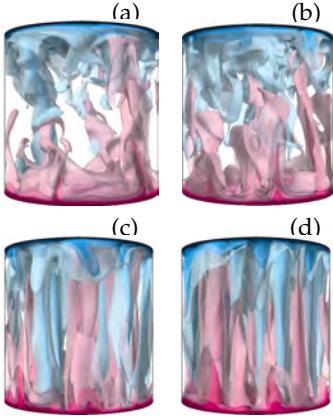


Figure 4.6: Isotherms (pink = warm, blue = cold) in rotational RBC in water for $Ra = 10^8$. Inversed Rossby number $1/Ro$ (rotation rate) increases as (a) 0.7, (b) 1.4, (c) 7.1, (d) 14.1. Adopted from [7].

Turbulent thermal convection is ubiquitous in nature; its investigation is needed for better understanding of geophysical and astrophysical flows and for technological improvements in industrial applications. Classical examples are turbulent Rayleigh–Bénard convection (RBC, Fig. 4.6) [1] and vertical convection (VC) [2], where a fluid layer is confined between a heated plate and a cooled plate, which are located, respectively, horizontally or vertically. In inclined convection (IC) the layer is tilted with respect to the gravity direction, and thus, not only buoyancy, but also shear drives the flow in this case. In so-called horizontal convection (HC, Fig. 4.7) [3] heat is exchanged exclusively through a single, top or bottom, surface of a fluid layer. The latter flow configurations are especially relevant in ocean convection, as heat is supplied to and removed from the ocean predominantly through its upper surface, where the ocean contacts the atmosphere.

We investigate turbulent RBC both, experimentally and numerically, including RBC enhanced by rotation (Fig. 4.6) and by the roughness of the heated/cooled plates (Fig. 4.10). The other types of turbulent thermal convection – VC, IC and HC – are studied so far numerically, and are the subject of future challenging experimental studies at MPIDS. Our theoretical investigations are aimed on better understanding of turbulent thermal convection in the above flow configurations and on the development of models to predict main mean flow characteristics such as mean momentum and heat transport, measured, respectively, by Reynolds (Re) and Nusselt (Nu) numbers, and their scalings with the control parameters of the corresponding convection system, namely, Rayleigh (Ra), Prandtl (Pr) and Rossby (Ro) numbers and geometrical aspect ratios of the convection cell.

Boundary layer (BL) structures in turbulent thermal convection.

Viscous and thermal BLs play a critical role in the heat transfer. The classical BL Prandtl–Blasius–Pohlhausen (PBP) theory cannot describe well the BLs in turbulent RBC as its inherent features like pressure gradients within the BLs, fluctuations and buoyancy, are assumed to be negligible in that approach. Therefore we advanced the BL theory

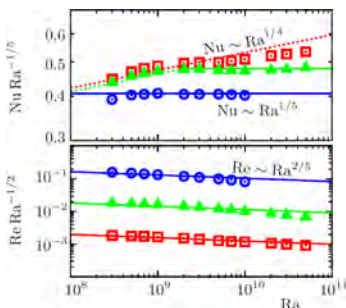


Figure 4.8: Ra -dependences of Nu and Re for $Pr = 0.1$ (\odot), $Pr = 1$ (\blacktriangle) and $Pr = 10$ (\square). Shishkina et al. (2015).

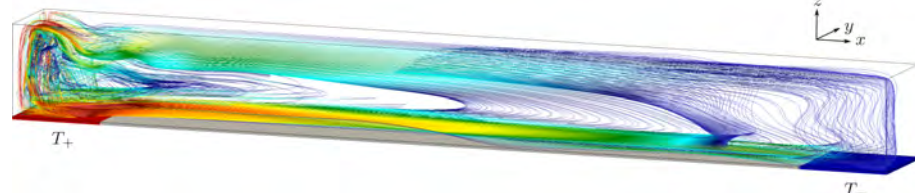


Figure 4.7: Scheme of a HC setup together with the streamlines for $Ra = 10^{10}$ and $Pr = 1$, as obtained in the simulations. $1/10$ of the bottom is heated (left, $T = T_+$, red), while the other $1/10$ of the bottom is cooled (right, $T = T_- < T_+$, blue). The top and side walls and the rest of the bottom are adiabatic. Shishkina et al. (2015), submitted.

for turbulent RBC by its extension to the case of a non-vanishing pressure gradient within the BLs, when a large-scale circulation (LSC) approaches the heating/cooling plates not parallel to them [4, 5].

Further, we studied the effect of fluctuations within the BLs [6] by considering the turbulent thermal diffusivity κ_t there. We derived that in the vicinity of the plates κ_t is a cubic function on the vertical coordinate z , and only later, for larger z , where the velocity and temperature profiles start to follow a log-law, κ_t is almost linear on z . The new developed BL equations were solved analytically for the case of infinitely large Pr and $Pr \sim 1$ (see Fig. 4.9) and an excellent agreement with the Direct Numerical Simulations (DNS) was demonstrated [6].

Rotational RBC (Fig. 4.6). We conduct DNS for various Ra , Ro and Pr , taking into account the temperature dependences of the fluid properties. The aim of the study is to investigate rotating RBC in the regime of geostrophic turbulence which is considered as most relevant for the description of geo- and astrophysical phenomena. It translates to very high Ra and low Ro , i.e. turbulence in the presence of strong rotational constraints. Further, in [8] we proposed a new method to identify the flow regimes, which is based on an analysis of the balance of the poloidal energy and toroidal energy. This method has the advantage, that it captures all known transitions and is robust.

The effect of wall roughness in thermal convection. Surface roughness is known to have a large impact on the global heat transfer. Therefore we study numerically the effect of the roughness introduced by a set of distinct obstacles attached to the heating and cooling plates, for different Ra , Pr and configurations of the cell geometry (see Fig. 4.10) [9, 10]. In [10] we suggested a simple parameter-free model, which captures well the mean heat flux enhancement due to regular wall roughness, the height of which is larger or comparable with the thickness of the thermal BL in the case of smooth plates. The model predictions were shown to be in good agreement with the DNS data.

Scalings in turbulent thermal convection. The scalings of Re and Nu with Ra depend strongly on the imposed boundary conditions in particular convection systems. We investigate the scalings in VC, IC and HC (see Fig. 4.8) and develop theoretical models for heat and momentum transport scalings, based on ideas by Grossmann and Lohse [11], applied to these flows.

We acknowledge the support of our studies by the German Research Foundation (DFG) and the Leibniz Rechenzentrum (LRZ).

- [1] G. Ahlers, S. Grossmann, and D. Lohse, *Rev. Mod. Phys.* **35**, 58 (2009)
- [2] C. S. Ng, A. Ooi, D. Lohse, and D. Chung, *J. Fluid Mech.* **764**, 349 (2015)
- [3] H. T. Rossby, *Deep Sea Res.* **12**, 9 (1965)
- [4] O. Shishkina, S. Horn, S. Wagner, *J. Fluid Mech.* **730**, 442 (2013)
- [5] O. Shishkina, S. Wagner, S. Horn, *Phys. Rev. E* **89**, 033014 (2014)
- [6] O. Shishkina, S. Horn, S. Wagner, E. S. C. Ching, *PRL* **114**, 114302 (2015)
- [7] S. Horn, O. Shishkina, *Phys. Fluids* **26**, 055111 (2014)
- [8] S. Horn, O. Shishkina, *J. Fluid Mech.* **762**, 232–255 (2015)
- [9] S. Wagner, O. Shishkina, *Phys. Fluids* **25**, 085110 (2013)
- [10] S. Wagner, O. Shishkina, *J. Fluid Mech.* **763**, 109 (2015)
- [11] S. Grossmann, D. Lohse, *J. Fluid Mech.* **27**, 407 (2000)

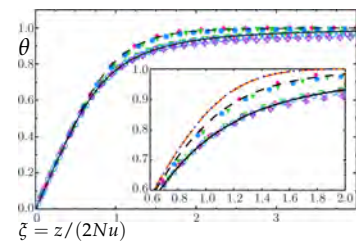


Figure 4.9: Temperature profiles in RBC for $Pr = 4.38$ (open symbols) and 2547.9 (filled). Excellent agreement between our theory (—) and DNS for $Ra = 10^{10}$ (\oplus), 10^9 (\circ), 10^8 (∇) and 10^7 (\diamond). Inset: expanded view with PBP predictions (orange). Adopted from [6].

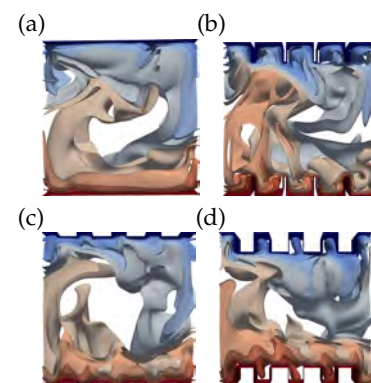


Figure 4.10: Isotherms (red = warm, blue = cold) in RBC cells with rough walls for $Ra = 10^7$ and $Pr = 0.786$. Adopted from [10].

DFG Deutsche Forschungsgemeinschaft

project SH405/3
project SH405/4
project SH405/5



AstroFiT
Astrophysical Flow Instabilities and Turbulence

lrz Leibniz-Rechenzentrum
der Bayerischen Akademie der Wissenschaften

4.3 CLOUD MICROPHYSICS MEASUREMENTS ON THE ZUGSPITZE

E. Bodenschatz, J. Moláček, H. Xu

S. Risius (DLR Göttingen), H. Xi (Shenzhen, China), S. Malinowski (U. Warsaw, Poland), R. A. Shaw (Michigan Tech. U., USA), H. Siebert (IfT Leipzig, Germany), Z. Warhaft (Cornell, USA)



Figure 4.11: Research station Schneefernerhaus. Our experiments are conducted on the cylindrical tower's rooftop to minimize influence of the mountain on the flow.

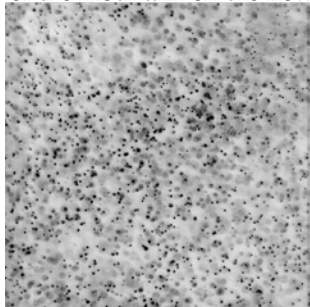


Figure 4.12: Still image of cloud droplets, typically about $20\mu\text{m}$ in diameter, from a video taken by our high-speed camera.

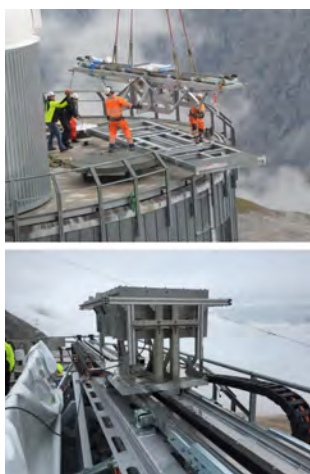


Figure 4.13: Transport (top) and testing (bottom) of the "seesaw" at the UFS.

Clouds present one of the most readily observable ways in which turbulence manifests itself, and arguably one of the most important. From precipitation patterns to the global energy balance, clouds play a crucial role in sustaining conditions necessary for life as we know it. However, there remain fundamental aspects of their dynamics that we do not sufficiently understand [1], due to the inherent difficulty of capturing the full range of scales integral to clouds both numerically and in laboratory settings.

For the initiation of rain in a warm cloud, it is necessary that the suspended droplets grow beyond a certain size, a process that happens much faster in reality than in the best current models. It has been suggested that the enhancement of cloud drop collisions and coalescence by turbulence may be the cause of this discrepancy, an explanation we are uniquely fit to test using our Lagrangian particle tracking (LPT) techniques. To complement our novel laboratory experiments [2, 3], we are also increasingly involved in field measurements at the environmental research station Schneefernerhaus (UFS).

The station (Fig. 4.11), situated at an altitude of 2650m near Germany's highest point, was chosen for its predictable wind direction and high likelihood of being in clouds during summer months. First experiments using a set of sonic anemometers have shown [4, 5] that under typical conditions the turbulence properties measured at UFS are similar to those in free clouds and exhibit Taylor-microscale Reynolds numbers up to 10^4 . Using a static LPT system we have obtained the first data on cloud droplet dynamics at smallest scales [6] (Fig. 4.12).

In order to obtain the best statistics, it is desirable to match the velocity of the LPT system and the cloud particles as closely as possible. To this end, we have built an apparatus, nicknamed "seesaw" (Fig. 4.13), capable of transporting a payload of 350kg at speeds of up to 7m/s over a 5m distance. After being transported to UFS in late 2014 and tested under the harsh local conditions, it is expected to start proper operation in the summer of 2016. Starting with extensive investigations of droplet velocity, acceleration and spatial distribution statistics, the seesaw will make feasible several hitherto unrealized probes into Lagrangian aspects of atmospheric turbulence, thanks to the great flexibility of its design.

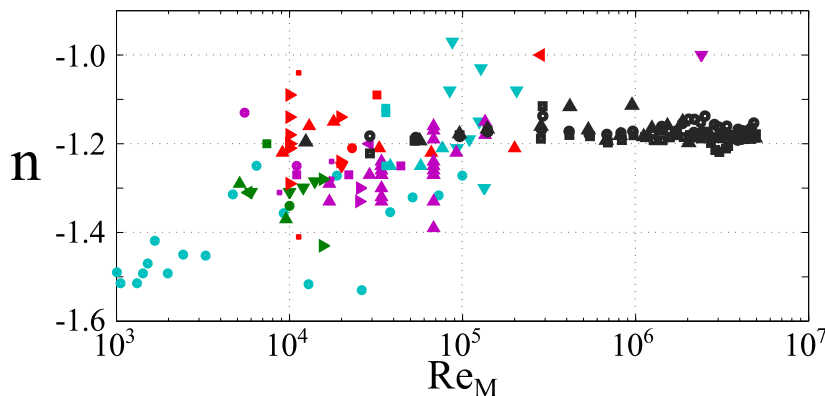
- [1] B. J. Devenish, P. Bartello, *et al.*, Q. J. R. Meteorol. Soc., **138**, 1401 (2012)
- [2] G. P. Bewley, E.-W. Saw, E. Bodenschatz, *New J Phys.*, **15**, 083051 (2013)
- [3] E.-W. Saw, G. P. Bewley, *et al.*, *Phys. Fluids*, **26**, 111702 (2014)
- [4] S. Risius, H. Xu, F. DiLorenzo, *et al.*, *Atmos. Meas. Tech.*, **8**, 3209 (2015)
- [5] H. Siebert, R. A. Shaw, *et al.*, *Atmos. Meas. Tech.*, **8**, 3219-3228 (2015)
- [6] J. Moláček, H. Xu, E. Bodenschatz, *et al.*, in preparation

4.4 STATISTICS OF TURBULENCE

M. Sinhuber, G. Bewley, E. Bodenschatz
M. Hultmark, A. Smits (Princeton, USA)
M. Vallikivi (GE Global Research)

Flows in nature tend to be strongly violent and often possess high Reynolds numbers $Re = UL/\nu$. At these high Reynolds numbers, turbulence is thought to exhibit special features such as an inertial range and universal statistical properties. Of great interest is the question of how the Reynolds number influences the statistical properties of the flow; this question cannot be answered from measurements made in high-Reynolds-number atmospheric turbulence, for example. Wind tunnels are an excellent tool to produce homogenous, isotropic turbulence under well-controlled conditions yet are usually limited to low Reynolds numbers. In the Variable Density Turbulence Tunnel (VDTT), we have overcome the limitations of low Reynolds numbers by using pressurized sulfur hexafluoride as a working gas, so that we produced extremely high Taylor-Reynolds numbers of R_λ up to 1600 with a passive grid, yielding higher Reynolds numbers and a wider range of them than any previous comparable experiment [1]. The measurements are conducted using state-of-the-art nano-fabricated hot wires (NSTAPS), developed at Princeton University to resolve all relevant scales in the flow [2].

Turbulence dissipates kinetic energy; in the absence of energy input to the system, turbulent motion eventually comes to rest. However, the answer to the question of how fast this process happens and whether it depends on the Reynolds number is not known precisely. Classical theories by Kolmogorov [3] and Saffman [4] predict a Reynolds-number-independent power-law decay of the kinetic energy, while there are also arguments for an approach to a so-called self-similar decay at high Reynolds numbers [5]. The VDTT makes it possible to adjust the Reynolds number independent of any other flow parameter such as the mean speed or the geometrical boundary conditions, and so to isolate the influence of the Reynolds number on the decay.



In an extensive study over a wide range of Reynolds numbers, we found that the grid turbulence produced in the VDTT is completely compatible with Saffman's prediction independent of the Reynolds

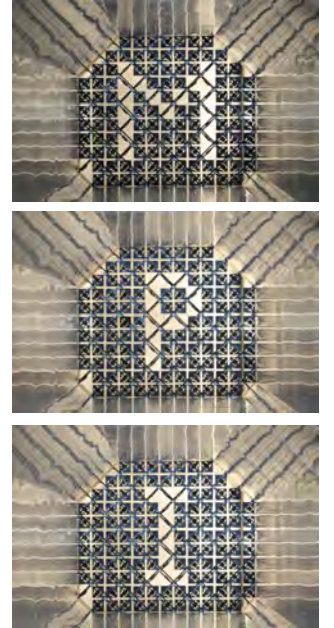


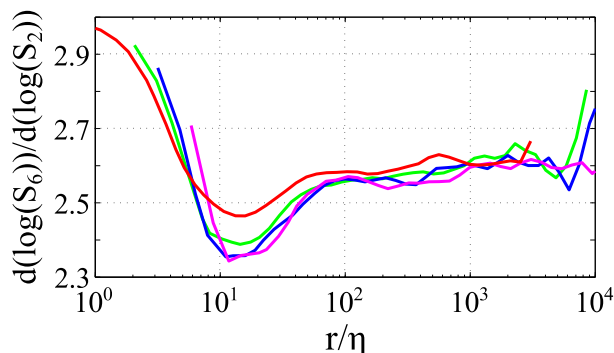
Figure 4.14: Snapshots of the active grid looking upstream into a wind tunnel. The grid is composed of 127 paddles. Each paddle has its own motor and controller and can move independently of the other paddles. This makes it possible to imprint different structures into the flow through the grid.

Figure 4.15: The decay exponents measured in the VDTT (black symbols) and published experimental data from previous experiments (colored symbols). With our data, an approach towards a self-similar decay at high Reynolds numbers can be ruled out as the generic high Reynolds-number limit [6].

number. In addition, there seems to be no approach toward a self-similar decay at high Reynolds numbers whatsoever [6]. With the use of passive grids of different geometries and especially the active grid we are able to thoroughly study the connection of the large scale structure of the turbulent flow to its statistical quantities.

Apart from its capabilities to change the Reynolds number over wide ranges, the VDTT is also well-suited to measure extremely long time series. We exploited this feature to measure times series as long as 4 days, corresponding to 10^{10} samples of the turbulent fluctuating velocity, to uncover fine details of the inertial-range statistics. Classical theories predict an approach with increasing Reynolds number to power-law scaling of the structure functions of velocity increments in the inertial range with Reynolds-number independent exponents [7]. As scaling properties are difficult to identify directly in experimental datasets, one usually applies a technique called Extended Self-Similarity (ESS), finding scaling between structure functions of different order [8]. With the long time series from the VDTT, we uncovered that ideal scaling is absent even in the sense of ESS and that significant dissipative effects influence the statistical properties of turbulent flows even in the inertial range.

Figure 4.16: Deviation from power-law scaling visualized by ESS, where power laws would appear as horizontal lines. Shown are measurements at $R_\lambda = 300$ (red), $R_\lambda = 600$ (green), $R_\lambda = 900$ (blue) and $R_\lambda = 1300$ (purple). Dissipative effects deeply penetrate the inertial range.



In coming months, the VDTT will be advanced into a fully functional Lagrangian measurement system, including a particle seeding mechanism, high speed cameras moving with the mean flow, a powerful lighting unit and an active grid producing customizable flows. With this improved facility, we will be able to address the many unsolved questions on particle behavior in turbulent flows.

- [1] E. Bodenschatz, G. P. Bewley, H. Nobach, M. Sinhuber and H. Xu, *Rev. Sci. Instrum.* **85**, 093908 (2014)
- [2] Bailey, S. C. C., Kunkel, G. J., Hultmark, M., Vallikivi, M., Hill, M., Meyer, J. P., Tsay, K. A., Arnold, C. B. and Smits, A. J., *J. Fluid Mech.* **663**, 160-179 (2010)
- [3] Kolmogorov, A. N., *Dokl. Akad. Nauk SSSR* **31**, 538-541 (1941)
- [4] Saffman, P. G. *Phys. Fluids* **10**, 1349 (1967)
- [5] George, W. K. *Phys. Fluids A* **4**, 1492-1509 (1990)
- [6] M. Sinhuber, E. Bodenschatz and G. P. Bewley, *Phys. Rev. Lett.* **114**, 034501 (2015)
- [7] Kolmogorov, A. N., *J. Fluid Mech.* **13**, 82-85 (1962)
- [8] Benzi, R., Ciliberto, S., Tripicciono, R., Baudet, C., Massaioli and Succi, S., *Phys. Rev. E* **48**, R29-R32 (1993)

4.5 TRACKING PARTICLES TO DECIPHER THE MYSTERY OF TURBULENCE

E. Bodenschatz, J. Jucha, J. Molacek, H.Xu, A. Pumir (ENS-Lyon, FR)
 G. Boffetta (U. Turino, IT), G. Falkovich (WIS, IL),
 R. Grauer (U. Bochum, DE)

Turbulent flows are characterized by a finite dissipation of energy, even though the dissipative process, due to viscosity or friction, seems to be *a-priori* very weak (the Reynolds number is large). The presence of a finite dissipation in the flow is the source of a deep irreversibility in turbulence. From a fundamental point of view, it makes turbulence a system very far from equilibrium, for which the application of ideas developed in the context of statistical mechanics close to equilibrium fails to produce meaningful results.

How does the irreversibility of the flow affect the motion of small particles? The underlying fundamental problem is to understand the statistical properties of the motion of a particle carried by a turbulent flow. This ostensibly simple question has been so far incompletely addressed for lack of reliable data. The experimental data from MPIDS revealed a remarkable manifestation of irreversibility in the motion of individual particles in 3 dimensional (3D) turbulent flows. Namely, it was discovered that the rate of growth of kinetic energy of particles is much smaller than the rate of energy decay [1]. This observation allows us to distinguish the arrow of time, since changing $t \rightarrow -t$ (observing the motion of particles backwards in time, as playing a movie backward) would lead to the opposite conclusion. One of the consequences of this experimental observation is that the average of the third power of p , the total power of the forces acting on the fluid particle, $\langle p^3 \rangle$ is *negative*. In addition, by combining numerical and experimental results, a remarkably simple power-law dependence was found: $\langle p^3 \rangle \approx -\epsilon^3 R_\lambda^2$, where ϵ is the dissipation of kinetic energy in the fluid, and R_λ is the Reynolds number, indicating the intensity of turbulence. This remarkable dependence of $\langle p^3 \rangle$ is also valid in flows in 2 spatial dimension (2D), where the physics is completely different. This observation has raised several questions.

First, among the various forces arising in a moving fluid, such as pressure gradient and viscous stresses, which one is responsible for the asymmetry in the statistical properties of the power p acting on a tracer particle? The answer turns out to be quite surprising [2]. On the one hand, in both 2D and 3D it has been unambiguously established that the variances of the fluctuations of power are completely dominated by the pressure-gradient terms. On the other hand, in 3 dimensional flows, the third moment of the power due to the pressure forces is much smaller than the third moment of p , and is even slightly *positive*. This intriguing observation is in fact a manifestation of a very unexpected property of the pressure forces: in a turbulent flow in 3D, the pressure forces tend to *accelerate* the fastest particles in the flow, while in 2D, this effect is absent – the pressure forces redistribute energy equally among fluid particles, regardless of their velocity (see Figure 4.17). This

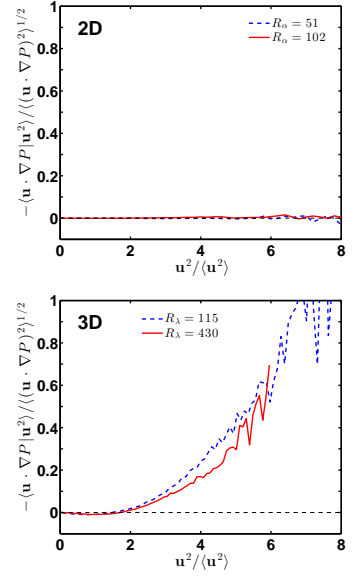


Figure 4.17: The role of pressure in redistributing kinetic energy among fluid particles points to the dramatic difference between 2D and 3D turbulence. (a) The average of the work by pressure forces conditioned on the kinetic energy of the fluid particle, $\langle -\mathbf{u} \cdot \nabla P | u^2 \rangle$, in 2D turbulence at two Reynolds numbers. The average of $-\mathbf{u} \cdot \nabla P$, conditioned on u^2 is extremely small, and consistent with being 0, implying that, on average, pressure does not redistribute energy among particles in 2D flows. (b) The same conditional average for 3D turbulence at two Reynolds numbers. Contrary to the 2D case, the conditional mean of the pressure term is negative for particles with small u^2 , and becomes strongly positive for larger values of u^2 , which implies that, on average, the pressure term in 3D turbulence takes energy from *slow* particles and gives to *fast* particles. This leads to a run-away effect and may result in singular structures in a turbulent fluid.

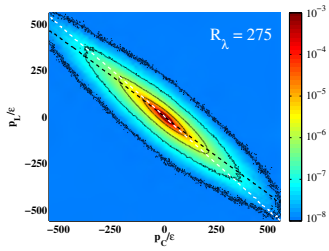


Figure 4.18:

The joint probability density function (PDF) between p_C/ϵ (horizontal) and p_L/ϵ (vertical) in a numerically simulated 3D turbulent flow at $R_\lambda = 275$, color-coded in a logarithmic scale. Equal-probability contours, separated by factors of 10, are shown. The black dashed line shows the conditional average $\langle p_L | p_C \rangle / \epsilon$, which is approximately $-0.86 \times p_C / \epsilon$. The white dashed line shows $\langle p_C | p_L \rangle / \epsilon$, which is approximately $-p_L / \epsilon$. This and other statistics show that p_C slightly dominates p_L .

is suggestive of a potentially important role of the pressure forces in the development of incipient singular structures in 3D turbulent flows.

Second, while it is clear that the generation of small-scale structures by a turbulent flow should lead to time irreversibility, it remains uncertain whether the mechanisms leading to generation of motion at fine scales in the fluid also causes the observed irreversibility of the tracer particle motion. In other words, is small-scale generation related to the asymmetry in the gain and losses of energy along trajectories? Using a combination of theoretical and numerical arguments, we showed that in 3-dimensional turbulent flows, the third moment $\langle p^3 \rangle$ is related to the vorticity stretching, i.e. the generation of small-scales in the flow [3]. In particular, the negative sign of $\langle p^3 \rangle$ is a direct consequence of the positive vortex stretching. Our argument [3] is based on decomposing the change of energy $p = p_C + p_L$, where the convective part p_C accounts for the change of energy along particle trajectory, and the local part p_L is due to the time dependence of the flow. We found numerically that p_C and p_L nearly cancel each other, resulting in p much smaller than p_C or p_L in magnitudes. Moreover, p_C slightly dominates p_L and determines the sign of the moments of p (see Figure 4.18). Interestingly, the fluctuations of p_C can be exactly computed, and shown to relate to vortex stretching. This theoretical property is an important first step in establishing the relation between the motion of individual particles and other known flow properties, in particular those related to small-scale generation.

Manifestations of the fundamental irreversibility of the turbulent flow can also be found by studying the relative motion of two or more particles [4]. Specifically, it can be shown directly from the Navier-Stokes equations, and verified by using the experimental data from MPIDS, that particles separate faster backwards than forwards in time. This effect is rigorously established at short times, and persists at longer times.

This line of research, summarized in a short review article [5], opens up new promising perspectives, not only for the physics of turbulence, but also for the general area of statistical mechanics very far from equilibrium. In this respect, we stress that the dimensionless quantity $-\langle p^3 \rangle / \epsilon^3$ can be considered as an enticing measure of irreversibility, which increases with the Reynolds number. In this sense, our work provides a way to quantify irreversibility in a complex system, which may be of much broader significance in the study of systems far from equilibrium.

- [1] H. Xu, A. Pumir, G. Falkovich, E. Bodenschatz, et al., PNAS, **111**:7558-7563 (2014).
- [2] A. Pumir, H. Xu, G. Boffetta, G. Falkovich and E. Bodenschatz, Phys. Rev. X **4**:041006 (2014).
- [3] A. Pumir, H. Xu, R. Grauer and E. Bodenschatz, under review.
- [4] J. Jucha, H. Xu, A. Pumir and E. Bodenschatz. Phys. Rev. Lett. **113**:054501 (2014).
- [5] H. Xu, A. Pumir and E. Bodenschatz, Science China – Phys. Mech. & Astron., **59**:614702 (2016).

4.6 AN ANALYTICAL MODEL FOR INTERMITTENCY IN TURBULENCE

L.J. Lukassen, M. Wilczek

Turbulent flows can be described by the Navier-Stokes equations. Small perturbations in the initial conditions lead to completely differently evolving structures in the flow. Consequently, turbulence constitutes a complex system which needs to be described statistically.

The production, transfer and dissipation of energy in turbulence can be described via a cascade process over a wide range of scales. According to the so-called K41 theory [6], the statistics in the intermediate range, referred to as inertial range, depend solely on the average dissipation rate. Most importantly, the scaling of the structure functions as predicted by K41 leads to self-similar statistics of velocity increments in the inertial range, cf. [4, 9]. Experiments as presented in [1] revealed that the Kolmogorov scaling approximates only low-order structure functions well, cf. [9]. As a result, the probability density function (PDF) for velocity increments changes from a Gaussian to a non-Gaussian distribution with decreasing length scale. This effect, known as intermittency, poses a challenge in the statistical theory of turbulence. As one of its consequences, extreme events at small and intermediate scales occur with significantly increased probability in comparison to a Gaussian field. A refinement of K41 from 1962 introduced a log-normally fluctuating local dissipation instead of the mean dissipation to account for intermittency [7, 8, 9]. The K62 phenomenology, however, displays some severe mathematical shortcomings in capturing the statistics at very high orders. This deficiency is resolved within the multifractal phenomenology which envisions turbulent velocity fields as composed of fractal sets with varying local scaling exponents [4].

In this project, we focus on fully developed homogeneous isotropic turbulence. We address the challenge of formulating a mathematical framework that mimics the behavior of turbulence but maintains analytical tractability. Unlike previous approaches our framework is based on an ensemble of Gaussian velocity *fields*. Each ensemble member differs in certain properties (e.g. characteristic length- or time scales) drawn from a model distribution. While this approach is fairly general, we will restrict ourselves in the following to one-dimensional fields with varying energy dissipation as a proof of concept. In this sense, our framework is a field-theoretic generalization of models like K62 and PDF models such as the one introduced by Castaing et al. [2]. Mathematically, our approach is based on the characteristic functional $\varphi[\alpha] = \langle \exp(i \int dx \alpha(x) u(x)) \rangle$, which captures the statistics of the velocity field $u(x)$ comprehensively. Taking into account the distribution of the dissipation, $P(\epsilon)$, the characteristic functional of the ensemble takes the form $\varphi[\alpha] = \int d\epsilon P(\epsilon) \varphi_\epsilon^G[\alpha]$ with φ_ϵ^G denoting the Gaussian characteristic functional. Moments, multipoint-PDFs etc. can be obtained from this expression by simple projection.

For the numerical evaluation of the ensemble, a Fourier series representation is used to generate Gaussian fields with a prescribed

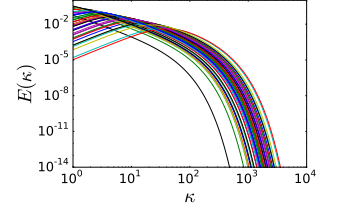


Figure 4.19: Representative energy spectra $E(\kappa)$ for different realizations of the dissipation, with κ as the wavenumber. Higher dissipations correspond to a higher cut-off wavenumber. All figures are created with [5].

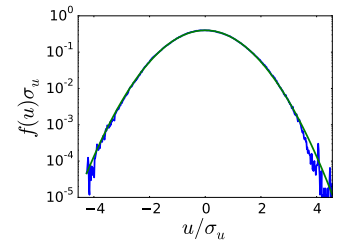


Figure 4.20: Standardized PDF for velocity u (blue) compared to a standardized Gaussian PDF (green).

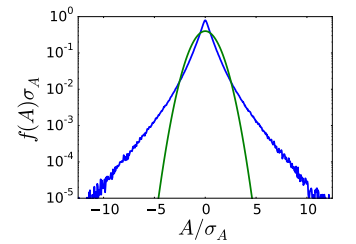


Figure 4.21: Standardized PDF for $A = \partial_x u$ (blue), compared to a standardized Gaussian distribution (green).

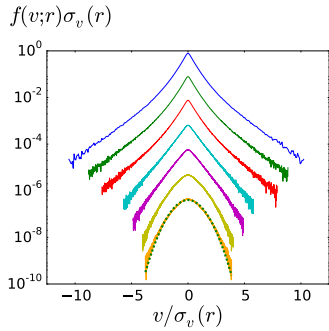


Figure 4.22: Standardized distribution for the velocity increment v . For increasing increment step sizes: $\{0.13, 0.54, 1.07, 4.02, 8.04, 32.15, 64.29\} \eta_{(\epsilon)}$ (from blue to orange) the increment distribution becomes Gaussian. The orange curve is compared to a standardized Gaussian distribution (thick dashed green). The curves are shifted vertically for clarity.

spectrum. We use a model for the energy spectrum as given in [9]. The dissipation of the respective ensemble members is chosen according to a log-normal distribution. Exemplary energy spectra for different realizations are presented in Fig. 4.19. For the following presentation, the turbulent kinetic energy is kept fixed across the ensemble members. The integral length scale L and the Kolmogorov length scale η , characterizing the large and the small characteristic scales of the field, respectively, differ due to the varying dissipation. As a result, each ensemble member obtains its own “local Reynolds number”.

The PDF of the ensemble-averaged velocity field follows an approximately Gaussian distribution, cf. Fig. 4.20. Furthermore, the spatial gradient of the velocity field $A(x) = \partial_x u(x)$ has a highly non-Gaussian PDF as demonstrated in Fig. 4.21, which also can be shown analytically. Most importantly, the statistics of the velocity increments, $v(x, r) = u(x + r) - u(x)$, show the transition from a Gaussian to a non-Gaussian distribution in Fig. 4.22, thus, intermittency. The increment size is given in terms of the Kolmogorov length scale based on the ensemble-averaged dissipation $\eta_{(\epsilon)}$. Figure 4.22 shows that the transition is continuously evolving from the inertial to the dissipative range. The blue PDF corresponding to the smallest increment size tends to the gradient PDF given in Fig. 4.21. These numerical evaluations illustrate that our approach is conceptually capable of capturing intermittency.

As a next step, the ensemble will be analyzed in more detail. In particular, we will consider distributions other than the log-normal one. In addition to a varying dissipation, we will explore alternative mechanisms to generate intermittency in our ensemble. We furthermore plan to include the skewness phenomenon currently missing in our description. It will be interesting to set this novel approach into the context of existing ones such as the multifractal model presented in [3]. Besides the above described Eulerian description, this approach will also be applied to the Lagrangian turbulence. The closure, investigated numerically and experimentally in [10], will be obtained analytically by computing the joint statistics of the Lagrangian acceleration and the temporal velocity increment from the characteristic functional.

- [1] Anselmet, F.; Gagne, Y.; Hopfinger, E.; Antonia, R. *J. Fluid Mech.* **140** (1984) 63
- [2] Castaing, B.; Gagne, Y.; Hopfinger, E. *J. Physica D* **46** (1990) 177
- [3] Chevillard, L.; Castaing, B.; Arneodo, A.; Lévêque, E.; Pinton, J.-F.; Roux, S. G. C. *R. Phys.* **13** (2012) 899
- [4] Frisch, U. *Turbulence: The Legacy of A. N. Kolmogorov*, Cambridge University Press (1995)
- [5] Hunter, J. D. *Comput. Sci. Eng.* **9** 3 (2007) 90
- [6] Kolmogorov, A. N. In: “Dokl. Akad. Nauk SSSR”, volume 30 (1941) 299 (Reprinted translation by V. Levin in Proc. R. Soc. Lond. A **434** (1991) 9)
- [7] Kolmogorov, A. N. *J. Fluid Mech.* **13** (1962) 82
- [8] Oboukhov, A. *J. Fluid Mech.* **13** (1962) 77
- [9] Pope, S. *Turbulent Flows*, Cambridge University Press (2000)
- [10] Wilczek, M.; Xu, H.; Ouellette, N. T.; Friedrich, R.; Bodenschatz, E. *New J. Phys.* **15** (2013) 055015

4.7 TURBULENT FLOWS: HOW LOCAL IS 'NON-LOCAL'?

D. G. Vlaykov, M. Wilczek

The complexity of turbulence flows arises from two basic properties – non-linearity and non-locality. Non-linearity facilitates the quasi-universal presence of long-lived structures – vortex tubes and strain sheets, at most turbulent scales (see Fig. 4.23). Non-locality, the formal dependence of even the short-term evolution of a fluid element on the state of the entire system, complicates the dynamics even further. In hydrodynamics the governing Navier-Stokes equations (NSE) encode the latter effect through the kinematic pressure gradient term. Thus we focus our investigation on its properties.

In incompressible hydrodynamics the NSE lead to a Poisson equation for the pressure. For an infinite or periodic domain \mathcal{D} it has a general solution of the form

$$p(\mathbf{x}, t) = \int_{\mathcal{D}} \frac{1}{4\pi|\mathbf{x} - \mathbf{x}'|} \left(\text{Tr}(S^2(\mathbf{x}', t)) - \frac{1}{2}\omega^2(\mathbf{x}', t) \right) d\mathbf{x}'.$$

This formulation demonstrates the explicit connection of the pressure to the different turbulent structures. As shown in Fig. 4.23, the enstrophy $\omega^2/2$ represents the vortex strength, while $\text{Tr}(S^2)$ encodes the magnitude of straining, shearing structures. Recent investigations [4] indicate in fact that the pressure is governed by turbulent structures. The property of non-locality is evident in this formulation as well – the pressure at a point is determined by an integral over the entire domain. The decaying kernel $|\mathbf{x} - \mathbf{x}'|^{-1}$ provides a counterpoint and raises a question. Is there a neighborhood which contains the majority of the contributions to the pressure and how may it be characterized?

To pursue this question we propose to distinguish between local and background pressure contributions (similarly to [1]) to glean the overall non-locality effect. Simultaneously, we shall consider the link between the small-scale structure topology and the destructive interference between vortices and strain sheets. As Fig. 4.24 demonstrates, due to cancellation the tight bundles of structures with opposite signs have much stronger impact in their immediate neighborhood than at large distances. Naturally, this will lead to the investigation of the distribution of these structures and in particular the importance of rare extreme events as compared to average values.

Eventually, this investigation may give rise to improved low - dimensional models (e.g. [2, 3]) which faithfully represent the key turbulent dynamics but reduce its complexity.

- [1] P. E. Hamlington, J. Schumacher, W. J. A. Dahm, *Phys. Rev. E*, **77**, 026303 (2008)
- [2] C. Meneveau, *Annu. Rev. Fluid Mech.* **43**, 219 (2011)
- [3] M. Wilczek, C. Meneveau, *J. Fluid Mech.* **76**, 191-225 (2014)
- [4] J. M. Lawson, J. R. Dawson, *J. Fluid Mech.* **780**, 60-98 (2015)

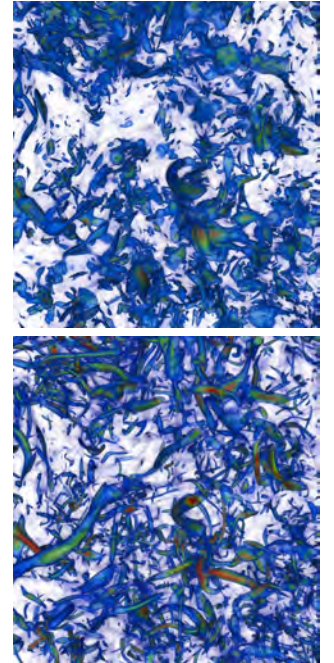


Figure 4.23: Iso-surfaces of the trace of the rate-of-strain magnitude $\text{Tr}(S^2)$ (top) and enstrophy $\omega^2/2$ (bottom) for a simulation of incompressible fully-developed homogeneous and isotropic turbulence in a periodic box. Amplitude increases from blue to red.

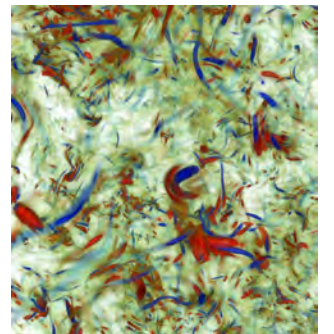


Figure 4.24: Iso-surfaces of $\text{Tr}(S^2) - \omega^2/2$ for the simulation described above, demonstrating the distribution of destructive interference between rate-of-strain and enstrophy. The blue shades represent large negative values, the red shades – positive ones; low amplitudes are shown in green shades.

4.8 NONEQUILIBRIUM TRANSITIONS IN GRANULAR MATTER

M. G. Mazza

R. M. Bowley (U. of Nottingham), J. P. D. Clewett, S. Herminghaus, M. Hummel, M. R. Swift (U. of Nottingham), J. Wade (U. of Nottingham)

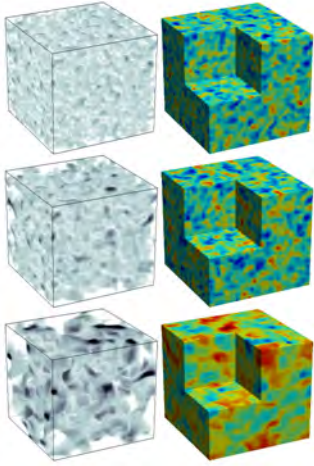


Figure 4.25: Evolution of a 3D granular gas with a coefficient of restitution $\varepsilon = 0.9$. From top to bottom snapshots of the density (left column) and temperature (right column) fields at increasing times.

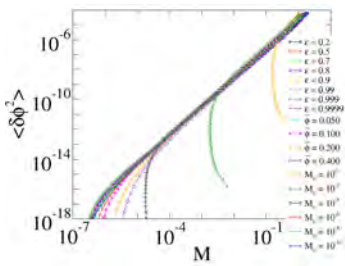


Figure 4.26: Universal scaling of the density fluctuations in terms of the system's average Mach number M .

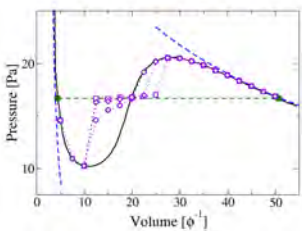


Figure 4.27: Solid line: calculations in a small cell. As the system size increases (open symbols) the pressures converges to the large cell (solid circles). Gray, dashed lines: low (left) and high (right) temperature asymptotes.

Geophysical processes, the solar corona, the asteroid belt between Mars and Jupiter, planetary rings, protoplanetary disks, and the formation of cosmological structures are systems where granular clustering processes are at play. Even a small degree of dissipation in the kinetics of granular particles produces spatial correlations and structures in a dilute, homogeneous gas. Hydrodynamic treatments suggest that a shear instability initiates this transition. However, what exactly initiates this process is not known.

We solve the compressible Navier–Stokes equations for the density, momentum, and temperature of granular matter in three dimensions by performing direct numerical simulations (DNS) of the hydrodynamic equations. This gives access to hydrodynamic fields at each point of space and time. DNS allows therefore to directly observe fluctuations and structure formation on scales inaccessible to molecular dynamics simulations (see Fig. 4.25). We find [1] from DNS and analytical calculations that the density fluctuations follow a universal quadratic dependence on the system's Mach number $\mathcal{M} \equiv \sqrt{\langle v^2 \rangle / \langle T \rangle}$, which is a dimensionless order parameter of the granular dynamics, where the angle brackets indicate spatial averages. The granular gas develops visible clusters when \mathcal{M} is of order unity, that is the threshold of supersonic flow. Regardless of the system parameters or the initial state, the density fluctuations converge onto the locus $\langle \delta \rho^2 \rangle(\mathcal{M}) = c\mathcal{M}^2$, where c is a constant. This locus plays the role of an “attractor” for the evolution of the granular gas. Once the initial conditions are “forgotten”, all systems investigated show universal behavior, as visible from the collapse of all curves in Fig. 4.26 over several decades.

Granular systems also offer nontrivial transitions in the steady state. A common way to balance the energy loss is provided by shaking the walls of the system's container. We combine experiments and molecular dynamics (MD) simulations of a vibrated system and study the nonequilibrium liquid-gas granular transition. Upon changing driving amplitude and filling fraction a granular system spontaneously separates into a dilute, gas-like region, and into a dense, liquid-like region. We find [2] that the densities of the dilute and the dense phase follow a lever rule and obey an equation of state. A Maxwell equal-areas construction (see Fig. 4.27) predicts the coexisting pressure and binodal densities remarkably well, even though the system is far from thermal equilibrium. This construction can be linked to the minimization of mechanical work associated with density fluctuations without invoking any concept related to equilibrium-like free energies.

[1] M. Hummel, J. P. D. Clewett and M. G. Mazza, under review (2015).

[2] J. P. D. Clewett, J. Wade, R. M. Bowley, S. Herminghaus, M. R. Swift and M. G. Mazza, under review (2015)

4.9 A 'POTENTIAL' FOR NON-EQUILIBRIUM STATES?

S. Herminghaus, M. G. Mazza
J. Clewett, M. Swift (Nottingham)

We have just seen (section 4.8) that the non-equilibrium steady state (NESS) of an agitated granular gas may exhibit a two-phase region, similar to regular, equilibrium fluids. The agreement of the coexisting densities with the Maxwell construction (cf. Fig. 4.27) suggests to search for a functional \mathcal{V} which is minimized by the NESS, analogous to the free energy of equilibrium thermodynamics.

If each NESS is characterized by its density profile, $\rho(x)$ (cf. Fig. 4.28), the space of all NESS is the (real) Hilbert space, in which the dynamics of the system creates a trajectory between 'states' $\rho_i(x)$. This can be described by a master equation (ME) for the probabilities P_i of finding the system at state i , $\partial_t P_i = \sum_j P_j a_{ji} - P_i a_{ij}$, which (in the case of infinitely many states) can be written as a Fokker-Planck equation, $\partial_t P\{\rho\} = -\nabla(j_D + j_K)$ by virtue of the Kramers-Moyal expansion. $P\{\rho\}$ is then the probability density in Hilbert space, $j_D = -\mathcal{D}\nabla P\{\rho\}$ the diffusion current, and $j_K = P\{\rho\}\mathcal{K}$ is the drift current, with drift field \mathcal{K} and diffusivity \mathcal{D} .

The profile which is most frequently encountered corresponds to $\nabla P\{\rho\} = 0$, at which $j_D = 0$. In Fig. 4.29, where the contour lines of P are sketched in grey, the maximum is at the black dot. In a system far from equilibrium detailed balance (DB) is breached, such that $j_D + j_K \neq 0$ and hence $j_K \neq 0$ (red arrows in Fig. 4.29). In fact, we observe these orbits as strong oscillatory fluctuations in agitated granular gases (cf. Fig. 4.30).

Now assume the system tends to the minimum of some functional $\mathcal{V}\{\rho\}$, such that $\partial_t \rho \propto \delta\mathcal{V}$. Then since $\mathcal{K} = \partial_t \rho$ and $j_K = P\mathcal{K} \neq 0$, this minimum is *not* at the maximum of P . One may anticipate, however, that if we reparametrize the space of states such as to consider closed orbits instead of points in Hilbert space, in analogy to the Poincaré map (cf. Fig. 4.29), we might recover a motion which is closer to random diffusion, and thereby DB. In fact, going back to the ME, it can be shown that characterizing the system through the set of all possible cycles in state space (instead of the states themselves), one obtains a transformed ME for which DB holds [1]. Hence in cycle space there is indeed a potential $\mathcal{U}\{\rho\}$ the minimum of which corresponds to the (strongly fluctuating) NESS of the system.

However, the transform to cycle space (and back), and hence $\mathcal{V} \rightarrow \mathcal{U}$, involves the inversion of a matrix with n rows, where n is the number of possible cycles in a system with m states. Not only is m very large (if not infinite), but n grows factorially with m , such that the existence of \mathcal{U} does not help to find the NESS: a full solution of the dynamics is, in general for non-equilibrium systems, much easier than finding \mathcal{U} .

[1] B. Altaner, S. Grosskinsky, S. Herminghaus, L. Katthän, M. Timme, J. Vollmer, Phys. Rev. E **85**, 041133 (2012)

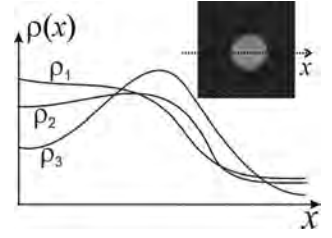


Figure 4.28: Schematic representation of states, i , of the system by their corresponding profiles, $\rho_i(x)$, where x , in general, is a vector. Inset: photograph of a 'bubble' of low density in a dense granular phase.

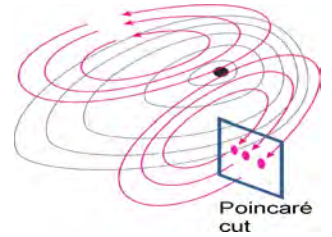


Figure 4.29: Contours (grey) of the probability density $P\{\rho\}$. The black circle indicates the maximum of P , i.e., the most probable state. The red arrows indicate the (source-free) drift current, which in absence of DB does not vanish at the maximum of P . A Poincaré-type map of the 'orbits' in state space can transform the current away, yielding a system with DB.

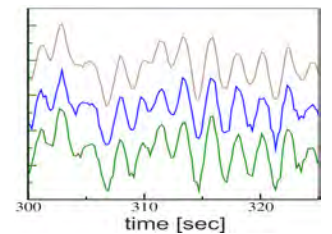


Figure 4.30: Fluctuations of interface position (grey), filling fraction of the dense phase (blue), and pressure (green) in a phase-separating driven granular gas.

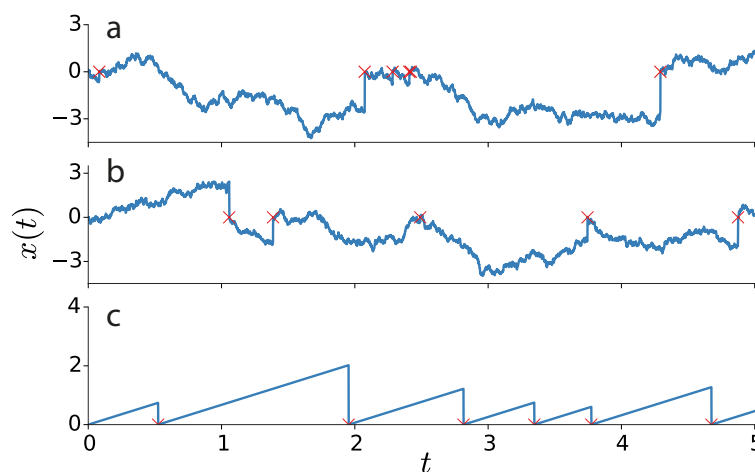
4.10 STOCHASTIC PROCESSES WITH RANDOM RESETTING

S. Eule, J.J. Metzger (Rockefeller)
S. Reuveni (Harvard)

Suppose that you are working on a difficult problem. While trying to find a solution, you may get the impression that you are stuck or got on the wrong track. A natural strategy in such a situation is to reset from time to time and start over. This behavior can be modeled by a stochastic exploration process, which is interrupted by a random resetting to the initial condition. Over the last years a special case of such processes, a diffusion process interrupted at constant rate by reset events, has attracted considerable attention, because it represents a particularly simple and analytically approachable example of a non-equilibrium steady state (NESS). The investigation of processes with random resetting is also one of natural interest to the study of first passage times, e.g. in the catalysis time of chemical reactions, in kinetic proofreading, and in areas where search optimality is crucial.

We analyze stochastic processes whose reset events are governed by arbitrary waiting time distributions $\psi(\tau)$. This allows for the investigation of a broader class of much more realistic processes, such as multistep dissociation reactions and the inclusion of a reset probability that depends on the time elapsed since the last reset event, respectively. Sample traces of the processes under investigation are displayed in Fig. 4.31. We find that both, the NESS as well as the search efficiency, are

Figure 4.31: Examples of different processes $x(t)$ with random resetting (marked with red crosses). All cases share the same mean duration between resets, $\langle\tau\rangle = 1$, but their distributions differ. (a) Diffusion with intermittent resetting. A resetting event is more likely to occur when another one has happened recently. (b) Diffusion with resetting times that are comparatively regular. (c) Deterministic, linear motion between resetting events.



sensitive to the full waiting time distribution and not only determined by the characteristic mean waiting time $\langle\tau\rangle$ and show that the relaxation towards the NESS is non-trivial [1]. Furthermore, we investigate the consequence of non-exponential unbinding (resetting) and completion time distributions in the classical theory of kinetic proofreading. Our work gives rise to the exciting possibility of engineering a dissociation rate dependent chemical filter [2].

[1] S. Eule and J. J. Metzger, (*under revision*) (2015).

[2] S. Eule and S. Reuveni, (*in preparation*) (2015).

4.11 DYNAMICS AND PATTERN FORMATION IN NONEQUILIBRIUM, ENTROPICALLY DRIVEN SYSTEMS

M. G. Mazza, S. Herminghaus
H. Hornischer

What are the underlying principles of intelligent behavior? For that we first ask: How did complex organism with the potential of higher intelligence arise out of a process of evolution? One basic principle of evolution is survival, that is, organisms distance themselves from situations threatening their physical health. This requires the ability of processing information about the environment. For any configuration of environmental variables there must be a configuration of internal variables (e.g. genetic expressions, metabolization rates) that maximizes the fitness of an organism [1]. The internal states provide information about the environment. Thus, there is a maximum fitness at any given amount of information.

This information about the system needs to be interpreted and used for predicting its future development in order to identify threats and act accordingly, moving away from situations limiting the space of possible future options. By not only taking instantaneous maximization of options into account (such as a chemotactic bacterium following the gradient of a nutrient) but instead considering longer future evolutions of the system, more complex situations can be assessed. The amount or diversity of possible future evolutions of a system can be quantified.

In 2013, Wissner-Gross and Freer [2] proposed a connection between intelligent behavior and the maximization of a general definition of entropy, which is based on a dynamical version of the Boltzmann-Shannon entropy. That is, instead of considering the probability of macrostates, the causal entropy is based on the probability of a finite path in phase space. This fundamental model can be applied to various fields and problems, such as game theory where it was possible to create a skilled artificial player in the game of Go using the principle of maximizing the amount of possible future moves.

Following [2], we define the causal entropy S_c on the set of possible future paths of finite duration τ through the phase space of the system,

$$S_c(\mathbf{X}, \tau) = -k_B \int \Pr(\mathcal{X}_\tau | \mathbf{x}(0)) \ln [\Pr(\mathcal{X}_\tau | \mathbf{x}(0))] \mathcal{D}\mathcal{X}_\tau. \quad (4.1)$$

We maximize S_c by applying the causal entropic force [3]

$$\mathbf{F}_c(\mathbf{X}_0, \tau) = T_c \nabla_{\mathbf{X}} S_c(\mathbf{X}, \tau) |_{\mathbf{x}_0}. \quad (4.2)$$

We call ‘agents’ the particles subject to the force in Eq. 4.2. We study systems with constraints of different nature, and with different numbers of agents.

We first test the system in a bottleneck problem. Many physical problems can be cast as evolutions through bottlenecks, for example in the protein folding process a global minimum in a very complex

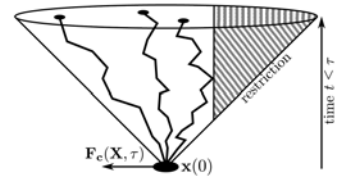


Figure 4.32: Light-cone representing the possible states a system can reach within a time horizon τ . Three future trajectories of the system are shown, all starting from the same initial state of the system $x(0)$, its position in phase space at time $t = 0$.

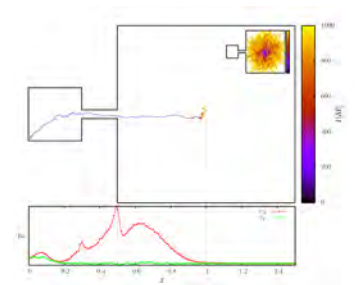


Figure 4.33: Trajectory of a single agent confined in a geometrical bottleneck. The color code represents the time; the lower panel shows the average velocity profile.

and rugged potential energy landscape must be found. For simplicity we choose a geometrical bottleneck. We find [3] that a single agent is capable to overcome the potential barrier represented by the bottleneck and find the center of the larger box (the most favorable location).

Entropic forces are common in polymeric systems. We can interpret a *single* entropically driven agent as the center of mass of a polymer and thus compare its dynamics with experiments. In 2002 Turner, Cabodi and Craighead [4] examined the dynamics of DNA molecules confined by nanopillars, but in proximity to an entropically more favorable area. They observe that strands of DNA are strongly pulled into the area free of nanopillars as soon as an end of the DNA strand reaches into it. We simulate the same system (see Fig. 4.34) and find [3] the same relationship between the time to reach an entropically favorable area and the distance from it.

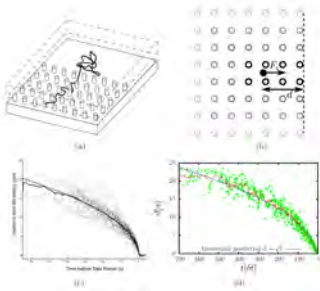


Figure 4.34: Dependence of the time employed to reach an entropically favorable area on the distance from it. Panels (a) and (c) show the experiment with DNA of Ref. [4]; panels (b) and (d) our simulations.

Finally, we explore the problem of decision making and *collective* organization through the approach of the causal entropy. Note that enumeration of ‘states’ is now qualitatively different from the polymer case. We find [3] that a system of many agents subject to Eq. 4.2 develops stable spatial patterns. Figure 4.35 shows some typical examples for various systems. No specific dynamic rule is assumed of these

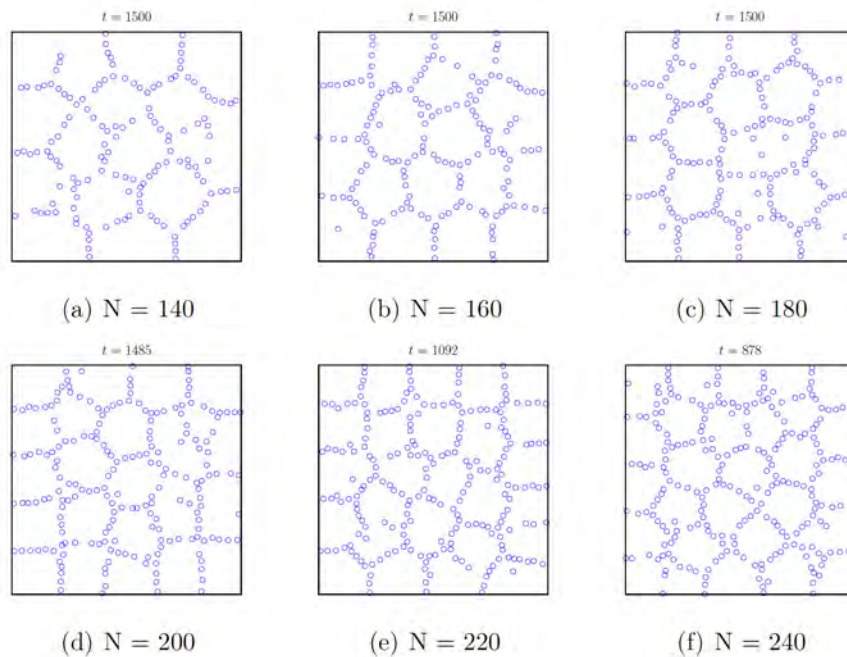


Figure 4.35: Steady state of a 2D system of entropically driven agents for parameters $S = 1.0$, F_M , $\frac{T_c}{T_r} = 4$, $T_r = 0.015$.

systems. Instead, each agent maximizes the entropy of *future* dynamical trajectories. As our results show, this leads to distinct patterns of organization.

- [1] S. F. Taylor, N. Tishby and W. Bialek, Arxiv:0712.4382 (2007).
- [2] A. D. Wissner-Gross and C. E. Freer, Phys. Rev. Lett. **110** 168702, (2013).
- [3] H. Hornischer, S. Herminghaus and M. G. Mazza, in preparation (2015).
- [4] S. W. P. Turner, M. Cabodi, and H. G. Craighead, Phys. Rev. Lett. **88** 128103, (2002).

TRANSPORT IN COMPLEX MEDIA

5

Complex media consist of a mix of different phases of matter. From the broad length scales feeding into the dynamics within a complex medium intricate dynamics of transport emerge. What essential details control the emergent behaviour? How can we control the dynamics? In this chapter we study carefully chosen simplified systems to address these questions. Systems of choice range from granular micro models to rugged surfaces like ocean floor and sandblasted copper to active fluids composed of microswimmers or driven by the heart muscle. We control transport along defect lines in liquid crystals and predict transport dynamics in random velocity fields

CONTENTS

- 5.1 Defects, flow, and transport in liquid crystals 70
 - 5.2 Hydrodynamics near Contact Lines 73
 - 5.3 A wetting transition in Hilbert space 74
 - 5.4 First passage time distributions of particles in Gaussian velocity fields 76
 - 5.5 Random focusing of tsunami waves 77
 - 5.6 Flux distribution in porous media 81
 - 5.7 Fluid invasion in porous media: solving a long standing conundrum 82
 - 5.8 Watching paint dry 84
 - 5.9 The role of dimensional confinement and hydrodynamics in microswimmer dynamics 85
 - 5.10 Biofluid dynamics from physics to medicine 87
 - 5.11 Microswimmers in complex geometries I: Microalgae swimming in Confinement 88
 - 5.12 Microswimmers in complex geometries II: Artificial droplet swimmers 89
 - 5.13 Microswimmers in complex geometries III: Taxis and Biofilm 90
-

5.1 DEFECTS, FLOW, AND TRANSPORT IN LIQUID CRYSTALS

Ch. Bahr, M. G. Mazza, C. C. Maass, S. Herminghaus,
H. Agha, K.-W. Lee, C. Krüger, V. S. R. Jampani,
T. Stieger (Technical University Berlin), S. Püschel-Schlotthauer (TU
Berlin), M. Melle (TU Berlin), M. Schoen (TU Berlin), Y. Sasaki
(Hokkaido University), H. Orihara (Hokkaido University)

In microfluidic channels with hybrid anchoring conditions (perpendicular on three side walls, parallel on the fourth wall) nematic liquid crystals can spontaneously form a line defect (disclination) that may be

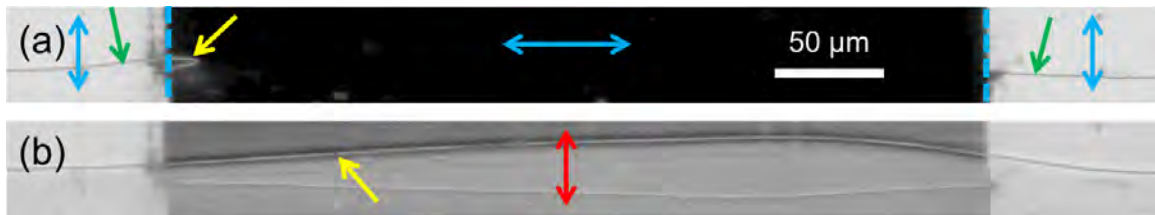


Figure 5.1: Connecting and disconnecting disclination lines in microfluidic channels. (a) Absence of electric field. Because of the director orientation on the parallel-anchoring wall (indicated by blue arrows), disclination lines (green arrows) are present only at the left and right edge of the shown micrographs but not in the central section (between the two dashed lines). The nematic liquid crystal is flowing from left to right and the left disclination extends with a small half-loop (yellow arrow) into the “forbidden” zone. (b) A low-frequency AC electric field is applied perpendicular to the channel axis (red arrow). The director field is reconfigured in a way that the left disclination extends as a half-loop across the central region and finally connects to the right disclination. The left and right parts of the channel are now connected by a continuous disclination (yellow arrow). If the field is removed, the configuration shown in (a) is re-established.

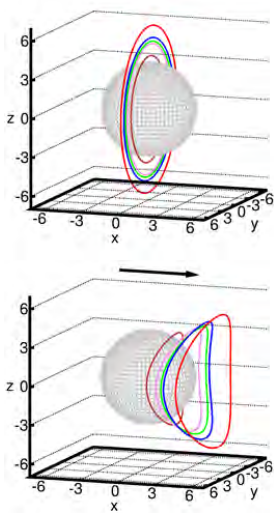


Figure 5.2: Disclination lines produced by a colloid immersed in a nematic liquid crystal at zero flow (top) and convected downstream by a flow along x (bottom). As the lines are convected we observe also a deformation of their shape. These results are the first molecular dynamics simulations to correctly reproduce the experimental results of Khullar *et al.* [7].

used as a soft rail for the transport of colloids or droplets [1, 2]. In order to gain enhanced control on the soft rails, we have developed a method to connect and disconnect disclination lines using the interplay between anchoring, flow, and electric field. We showed that the application of an electric field establishes a continuous disclination that spans across a channel region in which a disclination usually does not exist (because of different anchoring conditions), demonstrating an interruptible (and reconnectable) soft rail for colloidal transport (Fig. 5.1).

We explored theoretically the effect of flow on liquid crystal defect structures. We employed molecular dynamics simulations, based on the anisotropic Hess-Su model potential, to study the effect of flow on disclinations and other topological defects near colloidal particles in a nematic matrix [3, 4]. As shown in Fig. 5.2, we found that disclinations are convected downstream along the flow direction, in accordance with experimental observations, but contradicting earlier theoretical predictions [5]. We elucidated the underlying processes at play and resolved a controversy between theory and experiments.

In a second study we extended the stochastic rotation dynamics (SRD) model to anisotropic liquids [6]. The anisotropy is introduced by including a simplified Ericksen-Leslie formulation of nematic hydrodynamics. We first designed a two-dimensional implementation (Fig. 5.3) and tested our model by simulating the dynamics of defect annihilation and the effect of shear flow. We found that the annihilation

of the $+\frac{1}{2}$ and $-\frac{1}{2}$ defects follows a scaling law predicted theoretically. Recently, we succeeded in designing a three-dimensional implementation of our approach and started to study the flow of nematic liquid crystals in microfluidic environments, e. g., the behavior of disclination lines in microfluidic channels (see Fig. 5.1). Furthermore, we developed a theoretical procedure that bridges the gap between molecular scale information and effective, mesoscopic descriptions. By combining Monte Carlo simulations, a local Landau–de Gennes theory, classical density functional theory, and finite-size scaling theory we provide the first, consistent theoretical derivation of the aggregation angle of colloids with planar anchoring immersed in a nematic liquid crystal [8]. Experimentally, this angle is observed to amount $\approx 30^\circ$. As shown in Fig. 5.4, our model indeed predicts the potential to be attractive in this region.

The interplay between topological defects and flow influences also the behavior of liquid-crystal microswimmers, which consist of droplets of mesogenic compounds immersed in aqueous surfactant solutions (see also Chapter 5.9). The droplets undergo a dissolution process (micellar solubilization) during which they show self-propelled motion, induced by a self-sustained Marangoni flow at the droplet surface [9]. As shown in Fig. 5.5 (top), the shape of the trajectories of the self-propelling droplets strongly depends on the state of the droplets: nematic droplets show an intriguing spiralling pattern while isotropic droplets show comparably straight trajectories. The nematic swimmers can be made isotropic either by the admixture of a non-mesogenic oil, or simply by heating them above the nematic – isotropic transition temperature (35°C for the compound used in our experiments), offering a unique possibility to tune the swimming behavior. Detailed inspection of the self-propelling nematic droplets between crossed polarizers reveals two important features: First, the “hedgehog” point defect, which would be located in the center for a resting droplet, is moved by the internal convection of a self-propelling droplet towards the droplet surface. Second, the position of the defect near the surface is not on the polar axis which is defined by the convective flow pattern (and which coincides with the direction of motion), but is deflected away from the axis (see drawing in Fig. 5.5 bottom). It appears that a position of the defect near the stagnation point at the droplet apex is not stable against fluctuations: any deflection will at first grow by increasing surface flows towards the equator until this is countered by the flow in the droplet volume which tends to align the director along the polar axis. This spontaneous symmetry breaking is very probably at the origin of the spiralling trajectories of the nematic droplets. We observe that the deflection of the defect increases with increasing droplet velocity (Fig. 5.5 bottom) and increasing droplet size, thus confirming the qualitative scenario outlined above. To derive quantitative predictions, we plan numerical modelling of the nematic director field in the presence of the observed flow patterns.

As shown in Fig. 5.4, defect structures in nematic liquid crystals are at the origin of strong, attractive interactions between colloidal particles, leading to the formation of self-assembled structures, such

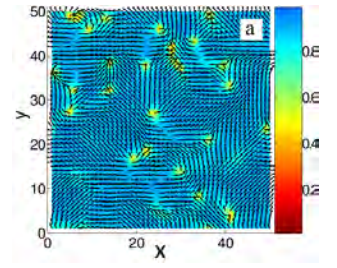


Figure 5.3: Snapshot of the SRD model of a two-dimensional nematic director field. Black dashes indicate the local director orientation and the color the nematic order parameter.

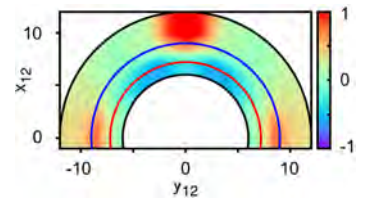


Figure 5.4: Effective potential (blue: attractive, red: repulsive) between two colloids with distance $\mathbf{r}_{12} = (x_{12}, y_{12}, 0)$ immersed in a nematic liquid crystal.

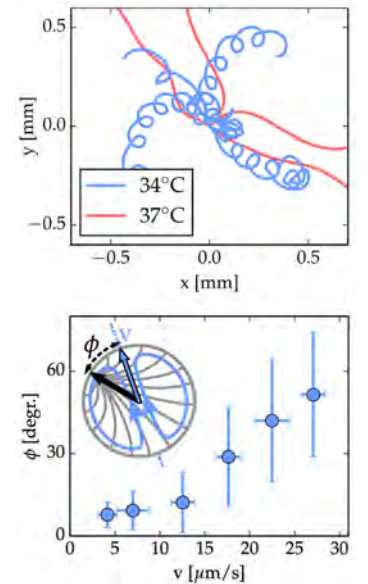


Figure 5.5: Top: Trajectories of self-propelling droplets in the nematic (34°C) and isotropic state (37°C). Bottom: Angle ϕ between defect position and polar axis of a self-propelling nematic droplet as function of the droplet velocity v .

as chains or two-dimensional crystals, of colloids in a nematic matrix [10]. We studied the motion of such colloidal particles and chains in electro-hydrodynamic convection (EHC) rolls which can be induced in some nematic compounds by an external electric field. Colloids in a nematic matrix and the surrounding director field can have a quadrupolar or dipolar symmetry [10]. Whereas quadrupolar colloids simply circulate within a convection roll, dipolar colloids show a directed roll-to-roll hopping because they experience, in addition to the drag of the convection rolls, an extra electrophoretic force [11]. Chains of dipolar colloids show an intriguing caterpillar-like motion (Fig. 5.6 left) through the EHC rolls and we demonstrated the use of such chains as traction engines for the transport of micro-cargo [12, 13] (Fig. 5.6 right).

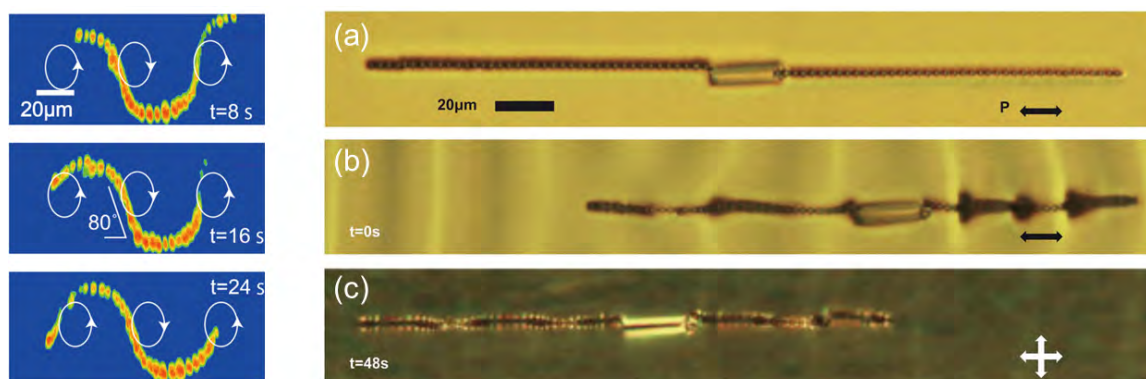


Figure 5.6: Left: Confocal fluorescence micrographs (sideview) showing a colloidal chain moving through electrohydrodynamic convection rolls in a nematic liquid crystal. Right: Micrographs (topview) of an ensemble of two colloidal chains attached to a $20\mu\text{m}$ long glass rod, demonstrating the application as micro traction engines. (a) At rest (zero electric field). (b,c) Electric-field-induced convection rolls move the ensemble from right to left (while an isolated glass rod would not be transported by the convection rolls).

- [1] A. Sengupta, Ch. Bahr, S. Herminghaus, *Soft Matter* **9**, 7251 (2013)
- [2] A. Sengupta, S. Herminghaus, Ch. Bahr, *Liq. Cryst. Rev.* **2**, 73 (2014)
- [3] T. Stieger, M. Schoen, M. G. Mazza, *J. Chem. Phys.* **140**, 054905 (2014)
- [4] T. Stieger, S. Püschel-Schlotthauer, M. Schoen, M. G. Mazza, *Mol. Phys.*, Advance Article, DOI: 10.1080/00268976.2015.1096973 (2015)
- [5] T. Gettelfinger, J. A. Moreno-Razo, G. M. Koenig, Jr., J. P. Hernandez-Ortiz, N. L. Abbott, J. J. de Pablo, *Soft Matter* **6**, 896 (2010)
- [6] K.-W. Lee, M. G. Mazza, *J. Chem. Phys.* **142**, 164110 (2015)
- [7] S. Khullar, C. Zhou, J. J. Feng, *Phys. Rev. Lett.* **99**, 237802 (2007)
- [8] S. Püschel-Schlotthauer, T. Stieger, M. Melle, M. G. Mazza, M. Schoen, *Soft Matter*, Advance Article, DOI: 10.1039/C5SM01860A
- [9] S. Herminghaus, C. C. Maass, C. Krüger, S. Thutupalli, L. Goehring, Ch. Bahr, *Soft Matter* **10**, 7008 (2014)
- [10] I. Musevic, M. Skarabot, U. Tkalec, M. Ravnik, S. Zumer, *Science* **313**, 954 (2006)
- [11] I. Lazo, O. D. Lavrentovich, *Phil. Trans. R. Soc. A* **371**, 20120255 (2013)
- [12] Y. Sasaki, Y. Takikawa, V. S. R. Jampani, H. Hoshikawa, T. Seto, Ch. Bahr, S. Herminghaus, Y. Hidaka, H. Orihara, *Soft Matter* **10**, 8813 (2014)
- [13] Y. Sasaki, H. Hoshikawa, T. Seto, F. Kobayashi, V. S. R. Jampani, S. Herminghaus, Ch. Bahr, H. Orihara, *Langmuir* **31**, 3815 (2015)

5.2 HYDRODYNAMICS NEAR CONTACT LINES

M. Rivetti, O. Bäumchen

T. Salez, M. Benzaquen, E. Raphaël (ESPCI, Paris)

'Not even Herakles could sink a solid.' With these Hellenic terms, Huh and Scriven in the early 1970s already graphically pointed out a paradox of classical hydrodynamics that is still unresolved to this day [1]. The three-phase contact line of a liquid on a solid represents a flow singularity and, thus, the classical concepts for flow in a liquid wedge predict a logarithmic divergence of the viscous dissipation, meaning that an infinite force would be required to move a contact line. In order to relieve the singularity and resolve this paradox, microscopic effects, e.g. hydrodynamic slip at the solid/liquid interface or the existence of a precursor film ahead the contact line, have been invoked.

We designed capillary levelling experiments involving thin liquid films and intentionally incorporated contact lines [2]. 'Capillary levelling' refers to the relaxation of surface perturbations of a liquid towards an equilibrium configuration as a result of Laplace pressure gradients [3]. Capillary flow is resisted by viscous dissipation within the film, predominantly in the proximity of the contact line. The initial geometry of the experiments is a two-dimensional rectangular nanostripe (see Fig. 5.7), featuring high curvature gradients and a non-equilibrium contact angle. Both conditions are successively relaxed and two distinct regimes are found in atomic force microscopy (AFM) measurements of the liquid surface: The first regime is associated with a stationary contact line position and capillary levelling. The onset of a retraction of the contact line precisely defines the dewetting regime.

While the contact line position remains stationary, the nanostripe provides self-similar profiles (see Fig. 5.8) that can be directly matched with numerical solutions of the thin film equation [3]. Nanometric contact angle measurements reveal a characteristic $-1/4$ power-law evolution of the contact angle as a function of time. For different film thicknesses, molecular weights and temperatures, all experiments can be collapsed onto one single master curve by introducing a dimensionless time (see Fig. 5.9). The onset of contact line motion is precisely linked to a universal critical contact angle and dimensionless time at which the liquid film starts to dewet the substrate.

The universality of the onset of contact line motion strongly suggest that the evident features are generic and intrinsically linked to microscopic properties and intermolecular forces. Thus, this system represents a perfect candidate to access and explore the link between the dynamics of mesoscopic liquid morphologies, nanoscale wetting features and molecular phenomena governing the contact line physics.

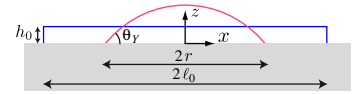


Figure 5.7: Sketch of the initial (rectangular) and equilibrium (cylindrical) geometry [2].

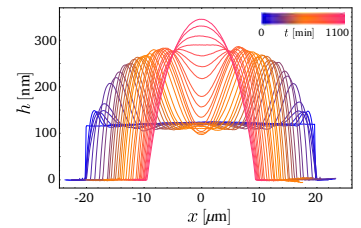


Figure 5.8: Series of AFM height profiles characterizing the spatiotemporal evolution of the liquid stripe [2].

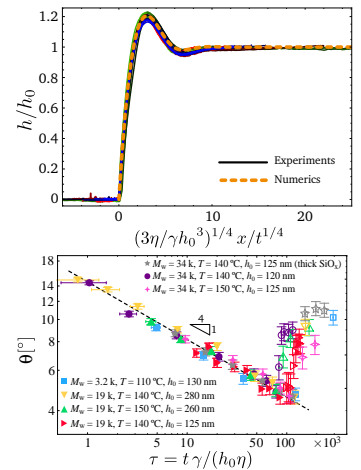


Figure 5.9: Upper: Self-similar profiles and numerical solution of the thin film equation. Lower: Contact angle versus dimensionless time τ . The data collapses on a master curve before dewetting starts [2].

- [1] C. Huh and L. Scriven, *J. Coll. Int. Sci.* **35**, 85 (1971).
- [2] M. Rivetti, T. Salez, M. Benzaquen, E. Raphaël, and O. Bäumchen, *Soft Matter* **11**, 9221 (2015).
- [3] J.D. McGraw, T. Salez, O. Bäumchen, E. Raphaël, and K. Dalnoki-Veress, *Phys. Rev. Lett.* **109**, 128303 (2012).

5.3 A WETTING TRANSITION IN HILBERT SPACE

S. Herminghaus, R. Dufour

M. Brinkmann (Saarbrücken), C. Semperebon ()

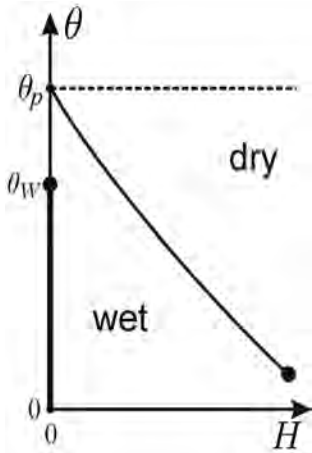


Figure 5.10: The phase diagram describing filling transitions (solid curve) of a liquid with contact angle θ on a randomly rough surface. The dashed line corresponds to a Gaussian random roughness.

Studies of wetting on random roughness has so far been restricted to either simple geometric shapes (e.g., straight grooves with simple cross section, or similar), or to Gaussian roughness models. We showed before [1] that the phase diagram of filling transitions on randomly rough surfaces can be computed analytically if averages of the slope, $\sigma(z)$, encountered along the contour lines at height z , are used to describe the rough surface. System conditions are defined by the microscopic contact angle, θ , and the curvature of the free liquid surface, H (distance from saturated vapor pressure). The result is sketched in Fig. 5.10, where the solid curve (ending in a critical point) indicates the loci of discontinuous jumps at which the troughs of the roughness are filled with liquid. Aside from its simplicity and analytical tractability, one of the striking features of this theory is that it predicts *no such transition line* if the roughness is precisely Gaussian. This is a startling finding, as Gaussian random surfaces are ubiquitously used for modelling rough substrates. It is therefore of substantial importance to know whether this prediction holds, or is just an artifact owing to the approximations used in the theory.

We have therefore performed tests on both natural and various model random surfaces. Filling transitions we detected on a number of different roughness topographies by numerically calculating the free liquid interface profile for variable H , by means of the freely available code SURFACE EVOLVER [2]. The result for a simple muffin tin topography is shown in Fig. 5.11. While the solid curve represents the theoretical prediction, the open squares indicate the filling transitions found numerically. The agreement is very satisfactory.

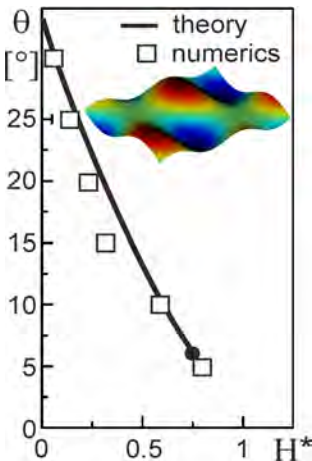


Figure 5.11: Phase diagram obtained for a muffin tin topography as depicted in the inset. Periodic boundary conditions were applied in both x and y direction in order to obtain stable simulations. Note that the critical end point predicted by the theory is very close to the lowest lying jump identified numerically.

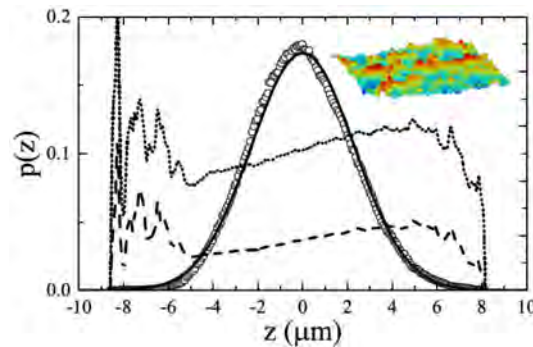


Figure 5.12: Characteristics of a sandblasted copper surface (inset). Open circles: height distribution, $p(z)$. Solid curve: Gaussian fit to $p(z)$. Dotted: $\langle\sigma\rangle(z)$. Dashed: $\langle\sigma^2\rangle(z)$.

We prepared a natural roughness topography by sand blasting a flat piece of copper. The topography was recorded by standard optical surface profilometry and Fourier filtered in order to ensure periodic boundary conditions in real space, and used for numerical studies. The height distribution of the resulting topography is shown in Fig. 5.12 (open circles). This deviates only slightly from the Gaussian fit (solid

curve). For comparison, a (close to) Gaussian model roughness, $g(x, y)$, was generated numerically by adding a large number of Fourier modes with amplitudes $a_{\mathbf{k}} = 1/\sqrt{1 + \mathbf{k}^2}$ (where \mathbf{k} are the wave vectors) and random phases. The set of \mathbf{k} was chosen such that g fulfils periodic boundary conditions in both x and y .

For a number of different values of the contact angle, θ , we have calculated the amount of adsorbed liquid as a function of H . Although $p(z)$ is very similar for both topographies (Fig. 5.12), the shape of the adsorption curves differs strongly. While they are purely monotonous for the Gaussian topography (Fig. 5.13, top panel), they exhibit a back-bending in case of the sandblasted surface (Fig. 5.13, bottom panel).

In order to study the effect of a deviation from Gaussian statistics, $g(x, y)$ was distorted according to $\tilde{g} = g + \varepsilon g^2$, resulting in the height distributions shown in Fig. 5.14a. Figs. 5.14b through 5.14d show the predicted transition lines (solid curves) along with the filling transitions found numerically (grey circles). The latter are indeed near the transition lines. Furthermore, both the transition line and the filling transitions vanish as the Gaussian topography is approached (5.14b). Hence Gaussian topographies constitute a sub-manifold in Hilbert space along which there is no filling transition. This may be viewed as a ‘wetting transition in Hilbert space’.

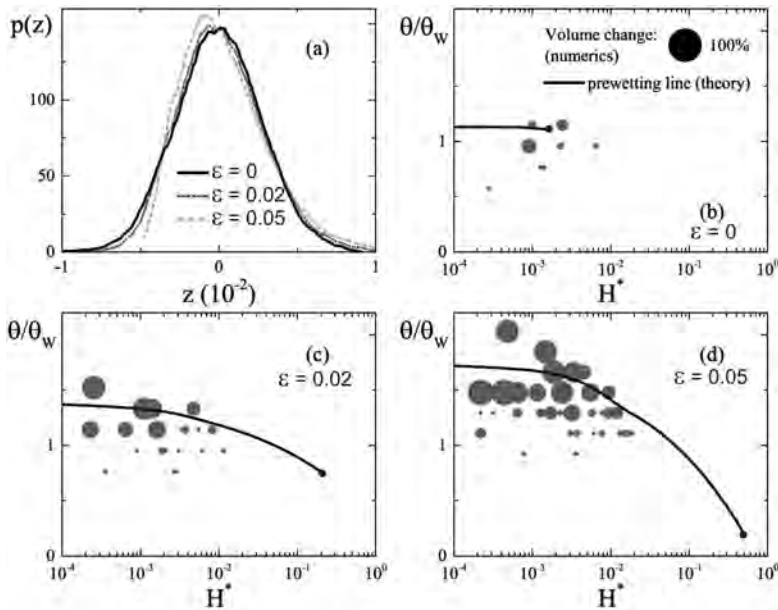


Figure 5.14: (a): height distributions for different values of the distortion parameter ε . Note that even $\varepsilon = 0$ does not yield a perfect Gaussian due to the requirement of periodicity. (b) through (d): filling transition line (solid) and jumps (filling transitions) in the adsorbed amount of liquid identified numerically (grey circles; size of circle corresponds to height of jump) for different values of ε .

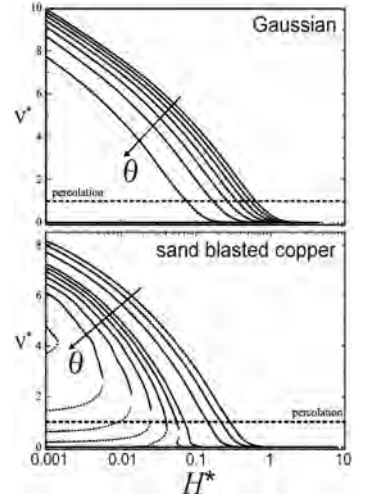


Figure 5.13: Adsorption curves on Gaussian roughness (top) and on a sandblasted copper surface (bottom). The contact angle is used as a parameter (slanted arrows).

- [1] S. Herminghaus, Phys. Rev. Lett. **109**, 236102 (2012)
- [2] K. Brakke, Philos. Trans. R. Soc. London A **354**, 2143 (1996).
- [3] R. Dufour, C. Sempregon, S. Herminghaus, Phys. Rev. E, under review.

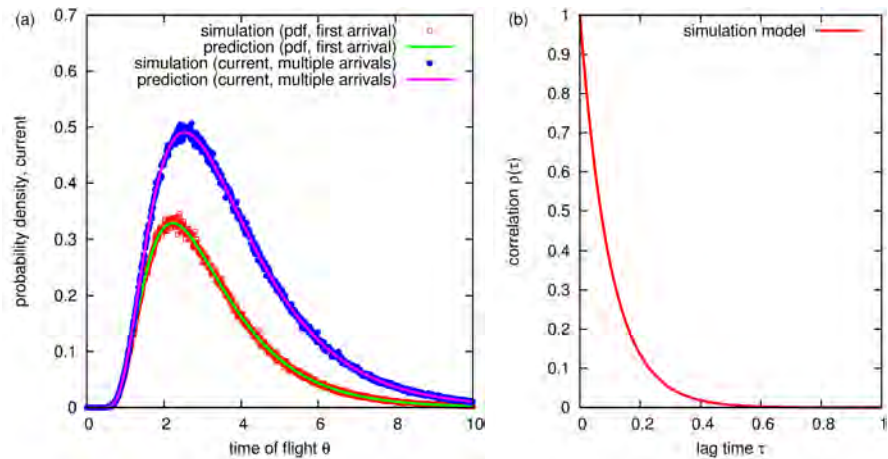
5.4 FIRST PASSAGE TIME DISTRIBUTIONS OF PARTICLES IN GAUSSIAN VELOCITY FIELDS

S. Eule, H. Nobach

First passage properties underlie a wide range of random processes, such as the triggering of chemical reactions or the extinction of a population. While the first passage problem of an over-damped Brownian particle is a classical problem of stochastic analysis, little is known about the first passage properties of particles, where inertia cannot be neglected. We investigate the first passage problem of particles immersed in a random velocity field that is characterized by a given distribution and decaying velocity correlation function and focus on the simplest case of a Gaussian velocity field. This model provides a simple showcase to study first passage problems of turbulent diffusions on intermediate scales, where large and small scales exchange energy and material — a problem highly relevant for technical applications due to the efficient mixing properties of turbulent flows.

As a first step, we study the first-passage time distribution and absolute current of particles in a one-dimensional setup with a mean velocity $\langle v \rangle$ and Lagrangian velocity correlation function $\rho(\tau) = \langle v(t)v(t+\tau) \rangle / \langle v^2(t) \rangle$ [1]. The particles are released at time zero from the origin and the time θ is measured until the particles reach a certain distance x from the origin. In random flows multiple passages are possible that give rise to an absolute current of particles through x that is always larger than the first-passage distribution at x . In Fig. 5.15 our analytical predictions for the first-passage time distribution and the absolute current of arrivals is plotted, which are compared to numerical simulations of the process. Since our theory imposes no restrictions on the particular form of $\rho(\tau)$ arbitrary Lagrangian correlation functions can be processed.

Figure 5.15: (a) Probability distributions of the first passage time and the absolute current at a distance x . Numerical simulation against analytical prediction, (b) Lagrangian correlation function used for the prediction and used in the numerical simulation (for $\langle v(t) \rangle = 1$, $\langle v^2(t) \rangle = 4$, $x = 3$, and an exponential correlation function $\rho(\tau)$ with an integral timescale of 0.1).



[1] H. Nobach and S. Eule, *First Passage Time Distributions and Absolute Currents of Particles in Gaussian Velocity Fields (in preparation)*

5.5 RANDOM FOCUSING OF TSUNAMI WAVES

H. Degueldre, T. Geisel, R. Fleischmann
J. J. Metzger (Rockefeller Univ., NY)

Tsunamis are probably among the deadliest, frequently recurring natural disasters. Typically, submarine earthquakes and landslides excite these extremely long wavelength gravity waves that travel the oceans with speeds of several hundred km/h. Due to the unpredictable nature of the earthquakes that cause them, long term forecasts of tsunamis seem to be far out of reach. However, despite their speed, due to the large distances they might travel over the ocean, there can be hours between their excitation and the time when they hit the shore. Following the devastating tsunami catastrophes in recent times, great efforts are made to use this time for tsunami warning systems. A prerequisite, however, is a thorough scientific understanding not only of the excitation of tsunamis but also of their propagation in the ocean.

An important aspect is that tsunamis exhibit surprisingly strong height fluctuations: run-up measurements and detailed simulations of past tsunami events have shown pronounced fluctuations in the crest height of tsunamis (see Fig. 5.16). While in-detail numerical modeling of the wave propagation in the measured depth-profile of the ocean floor captures many aspects of these fluctuations, only detailed studies of the focusing mechanisms that cause them, will allow one to scrutinize and improve the assumptions made in these models. It has been known, e.g, that the presence of large underwater islands [1] or the shape of the tsunami source [2] can affect the waves heights. We have recently shown that the consecutive effect of even tiny fluctuations in the profile of the ocean floor (the *bathymetry*) can cause unexpectedly strong fluctuations in the wave height of tsunamis with maxima several times higher than the average wave height [3]. This has severe implications for tsunami predictions, as will be discussed below.

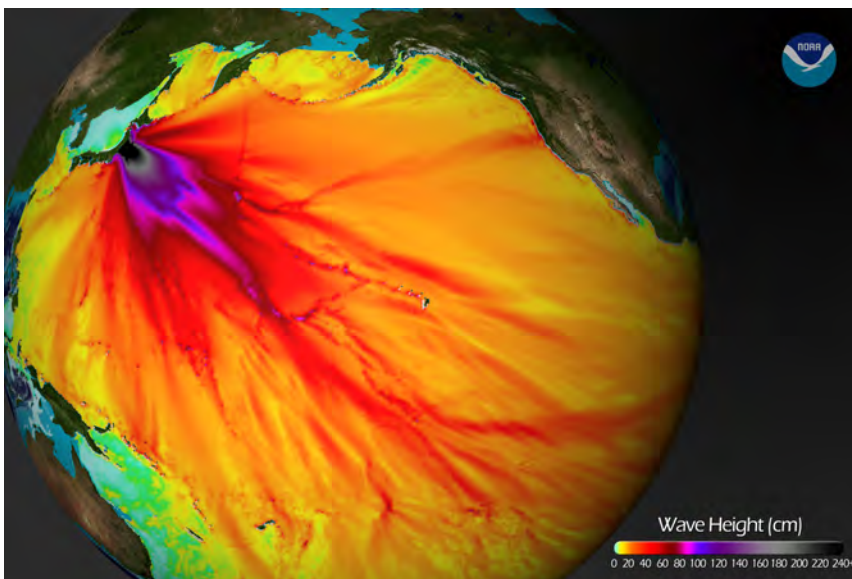
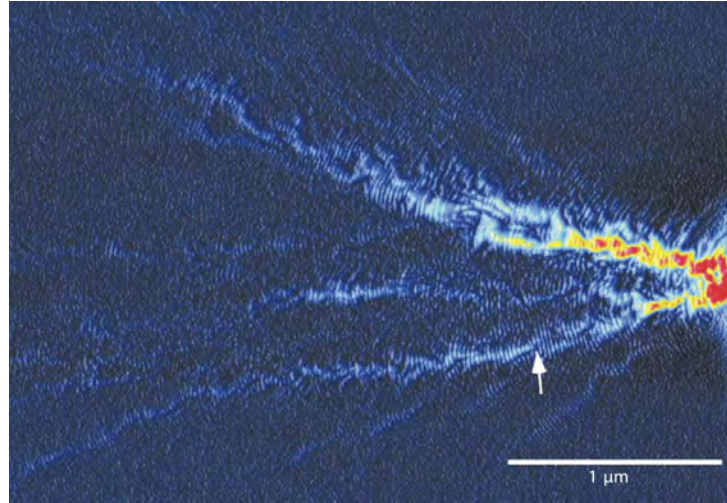


Figure 5.16: Reconstruction of the tsunami on the 11th of March 2011 in the Pacific Ocean by the US National Oceanic and Atmospheric Administration (NOAA) [nctr.pmel.noaa.gov]. The colors code the maximum wave height, which shows a strong filamentation of the wave flow.

Figure 5.17: Measurement of the electron flow emitted from a narrow, nano-scaled opening, a *quantum point contact*, into the two dimensional electron gas of a semiconductor heterostructure [4]. The flow shows pronounced branches (on length scales much shorter than the mean free path of approximately $7\mu\text{m}$), caused by consecutive scattering by the very weak disorder potential generated by impurities. (Taken from [4].)



Electron waves that are scattered by weak impurities in semiconductor crystals show a pronounced *branching of the flow* (see Fig. 5.17), which is closely connected to the occurrence of random caustics [5, 6]. Recently, we contributed substantially [6, 7, 8, 9, 10] to the theoretical and experimental understanding of this very general mechanism leading to the formation of rogue waves. Visually Fig. 5.17 exhibits strong similarities to the filamentation of the tsunami wave shown above. This therefore raised the question, whether tsunamis on length scales of thousands of kilometers are subject to the same focusing mechanisms as electrons on the micrometer scale and which impact this might have for their predictability. Tsunami waves are *shallow water waves* because their wavelength – ranging from ten to several hundreds of kilometers – is much larger than the ocean depths. While propagating over the deep ocean, tsunamis are very well described by the *linear* shallow water wave equations because their amplitude is on the order of a meter whereas the ocean depth is several kilometres. However, the structure of these equations and their ray approximation are quite different from the Schrödinger-equation and its semi-classics, so that the existing statistical theory of branched flows could not simply be used to analyse tsunami waves scattered by small structures in the bathymetry.

First, we demonstrate that tsunamis are indeed affected even by very weak fluctuations in the profile of the ocean floor. We used the GEBCO database [www.gebco.net] and chose a region of the Indian Ocean (see Fig. 5.18) where the bathymetry fluctuations $\beta(x, y)$ have a standard deviation $\sqrt{\langle\beta^2\rangle}$ of less than 7% of the average ocean depth. In this bathymetry we simulated a tsunami excited by a well localized source in the south-western corner. The time integrated wave intensity (i.e. the square of the wave amplitude), which is a good measure of the wave energy, is shown in Fig. 5.18 and exhibits clear branching patterns. In a second step, we theoretically and numerically studied the focusing of tsunami waves and their corresponding rays in random bathymetries. We found that the strongest focusing occurs at distances d_f that scale with the characteristic quantities of the disordered bathymetry

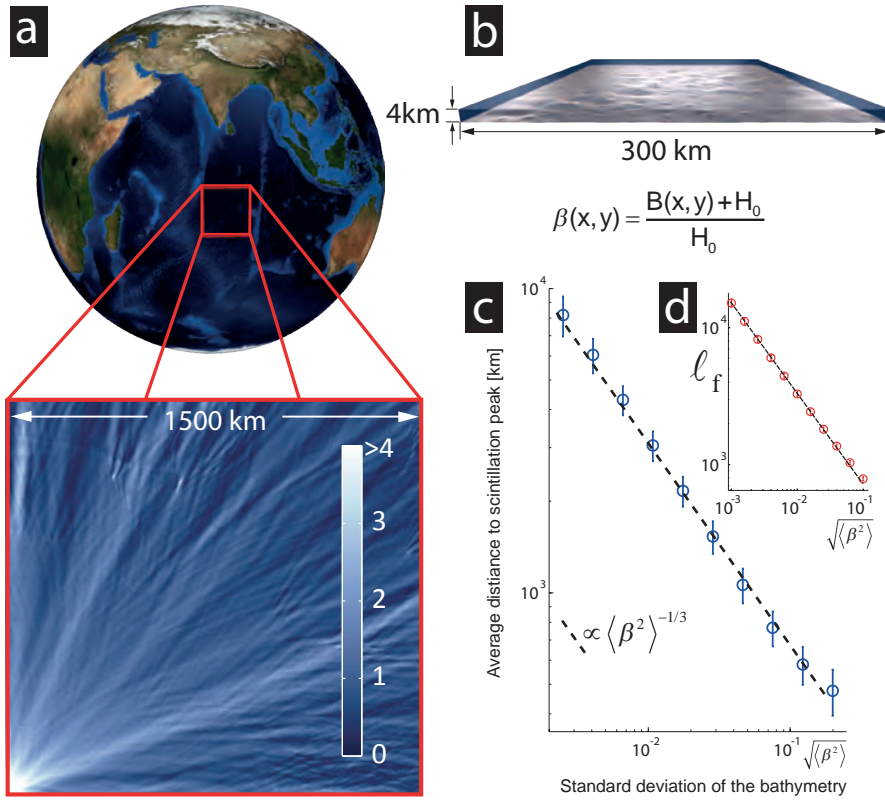


Figure 5.18: (a) Simulated tsunami event showing pronounced branching in the bathymetry of Indian Ocean taken from the GEBCO database. An island-free region was chosen in which the bathymetry $\beta(x,y)$ only fluctuates with a standard deviation of approx. 6.9% of the average ocean depth $H_0 \approx 4km$, illustrated in panel (b). (c+d) Statistical analysis of the focusing of tsunami waves in computer generated bathymetries, showing the average distance to the strongest fluctuations of the waves (c) and the mean distance to the first caustic (d) calculated in the ray approximation. [Adapted from [3], where details of the simulations can be found.]

according to

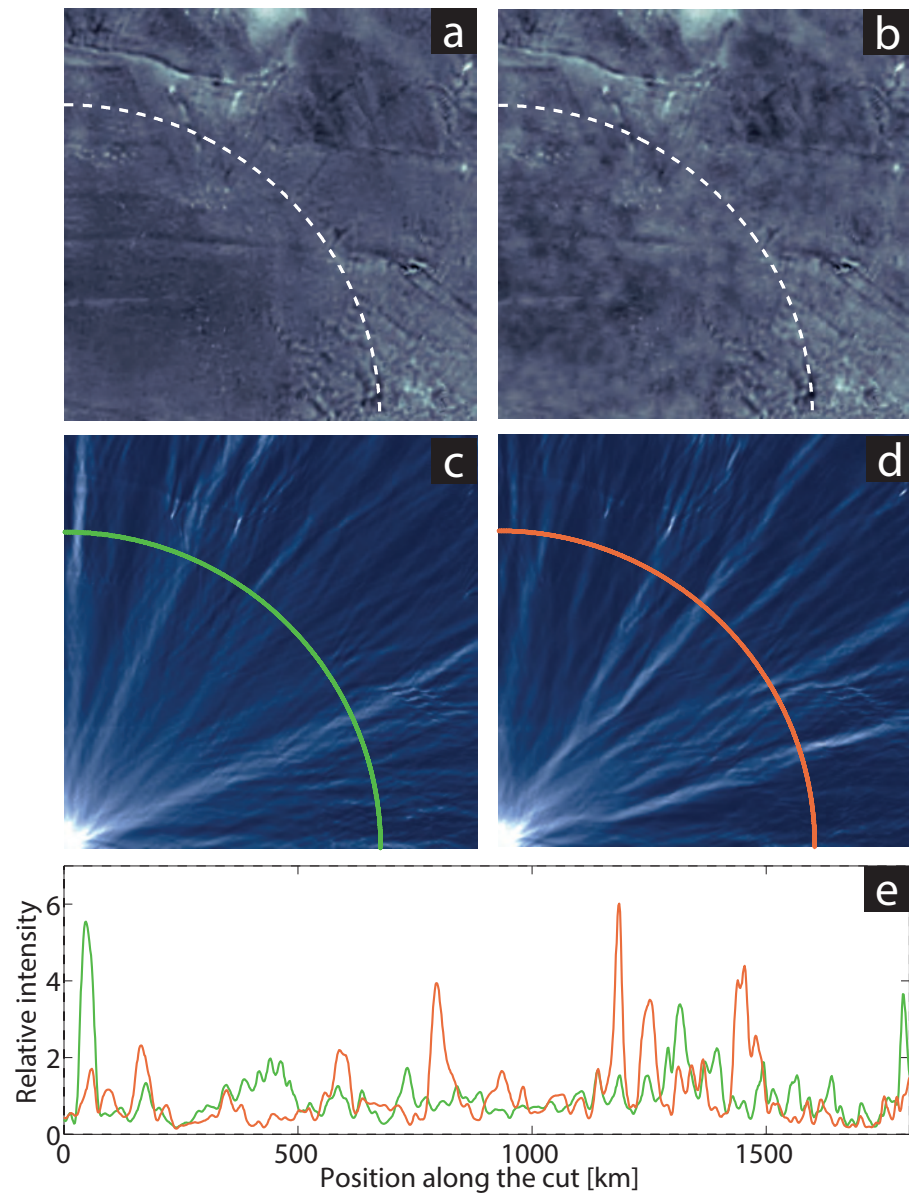
$$d_f \propto \ell_c \langle \beta^2 \rangle^{-1/3}, \quad (5.1)$$

where ℓ_c is the correlation length of the fluctuations. This scaling behaviour is in excellent agreement with the numerics as shown in Fig. 5.18 for waves (c) and rays (d).

From Fig. 5.18c we can read off that already fluctuations as small as 4% standard deviation lead to focussing of the tsunami waves in a distance of approximately 1000km from the source. Such variations are smaller than the uncertainties in the available bathymetry data but might be highly relevant for actual predictions. We tested this by adding random fluctuations of this strength to the measured bathymetry data from Fig. 5.18. An example is shown in Fig. 5.19: Panel (a) and (c) show the original bathymetry data and simulation result from Fig. 5.18 in comparison to the bathymetry (b) and integrated intensity (d) of the the simulation with added fluctuations. Panels (c) and (d) show that the focusing directions are indeed strongly affected by the additional disorder. Cuts through the intensity along the green and red arc, reveal this even more clearly (panel e): pronounced peaks can be seen at completely unrelated positions.

Our work shows that the understanding of the branched flow of tsunamis is crucial for reliable wave height predictions. It is imperative to analyse in detail not only the magnitude of the uncertainties in the bathymetry data but their spatial correlations as well, and to systematically study the effect of additional random, correlated height fluctuations on the predicted wave heights.

Figure 5.19: **(a)+(c)** The same bathymetry region and the branched intensity of the simulated tsunami wave shown in Fig. 5.18. **(b)+(d)** Adding a small additional disorder well below the uncertainties in the measured bathymetry (see text) strongly changes the branching pattern. **(e)** This can be most clearly seen in the cuts along the green in red curve in panels (c) and (d). The wave intensity shows peaks up to 6 times the average at completely unrelated positions.



- [1] M. V. Berry. *Proc. R. Soc. A* **463**:3055 (2007).
- [2] U. Kanoglu et al. *Proc. R. Soc. A* **469**:20130015 (2013).
- [3] H. Degueldre, J.J. Metzger, T. Geisel, and R. Fleischmann, *Nature Physics*, AOP doi:10.1038/nphys3557 (2015).
- [4] M. A. Topinka, B. J. LeRoy, R. M. Westervelt, S. E. J. Shaw, R. Fleischmann, E. J. Heller, K. D. Maranowski, and A. C. Gossard. *Nature* **410**, 183 (2001).
- [5] L. Kaplan. *Phys. Rev. Lett.* **89**, 184103 (2002).
- [6] J. J. Metzger, R. Fleischmann, and T. Geisel. *Phys. Rev. Lett.* **105**, 020601 (2010).
- [7] D. Maryenko et al., *Phys. Rev. B* **85**, 195329 (2012).
- [8] S. Barkhofen et al., *Phys. Rev. Lett.* **111**, 183902 (2013).
- [9] J. J. Metzger, R. Fleischmann, and T. Geisel, *Phys. Rev. Lett.* **111**, 013901 (2013).
- [10] J. J. Metzger, R. Fleischmann, and T. Geisel, *Phys. Rev. Lett.* **112**, 203903 (2014).
- [11] D.T. Sandwell, S.T. Gille, and W.H.F. Smith, *Geoscience Professional Services*, Bethesda, MD (2002), www.igpp.ucsd.edu/bathymetry_workshop

5.6 FLUX DISTRIBUTION IN POROUS MEDIA

K. Alim

M. P. Brenner, S. Parsa, D. A. Weitz, (Harvard, USA)

Fluid flow through a porous medium is an important problem for many technological applications ranging from oil recovery to chemical reactors. Although the flow characteristics on scales much larger than a pore size are well understood, there has been significant controversy about the flow distributions on the scale of individual pores. Observed flow velocity distributions range from Gaussian, to lognormal, to exponential. What causes a specific distribution to occur in a given situation?

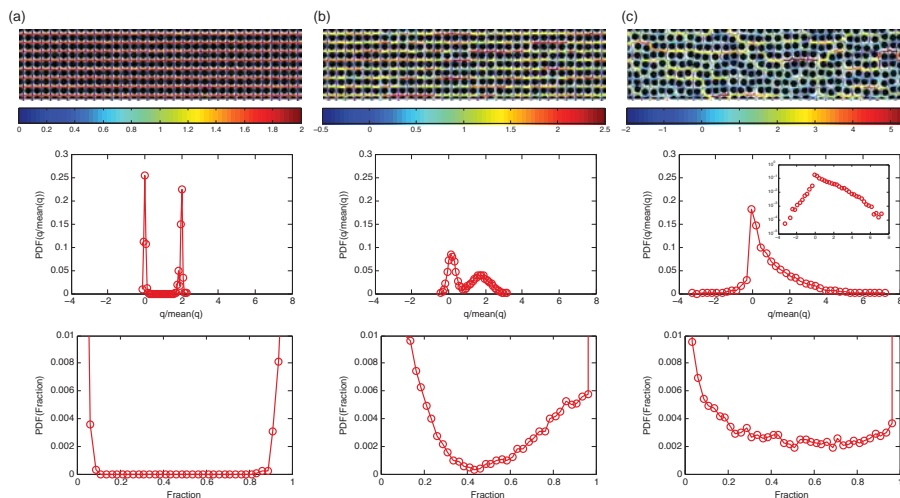


Figure 5.20: Snap shot of flux pattern (*first row*), flux distribution (*second row*) and the distribution of the fraction of propagated fluxes (*third row*) for three different packings of increasing disorder in disk position of 0.1% (a), 1% (b), and 5% (c) disk radius. With the increase in disorder the two delta-like flux distributions in the regular packing, spread out into Gaussians of unequal weight and eventually built up an exponential distribution.

We introduce a model that explains why different flow distributions occur in different situations [1]. The essential ingredient of our model is the local correlations between adjacent pores; these determine the distribution of fractions of fluid flux propagated from one pore to others downstream. We show that when there is sufficient disorder at the pore scale, these fluxes are partitioned randomly. Analytical arguments based on the so called q model, originally proposed to describe force propagation in bead packs [2, 3], then imply that the flow distribution is exponential. We verify these conclusions using numerical simulations of a two dimensional model porous medium, formed of circular discs ordered on a lattice with increasing disorder. The simulations quantitatively reproduce flow distributions from experiments of a two dimensional porous medium, and clearly show a transition of delta-function shaped distributions to Gaussian distribution to an exponential distribution of fluxes with increasing disorder in the ordering of the circular discs, see Fig. 5.20. We thus present a general approach readily applicable to three dimensional porous media.

- [1] K. Alim, S. Parsa, D. A. Weitz, M. P. Brenner, under review
- [2] C.-h. Liu, S. R. Nagel, D. A. Schecter, S. N. Coppersmith, S. Majumdar, O. Narayan, T. A. Witten, *Science* **269**, 513 (1995)
- [3] S. N. Coppersmith, C.-h. Liu, S. Majumdar, O. Narayan, T. A. Witten, *Phys. Rev. E* **53**, 4673 (1996)

5.7 FLUID INVASION IN POROUS MEDIA: SOLVING A LONG STANDING CONUNDRUM

R. Seemann, H. Scholl, K. Singh, S. Herminghaus,
M. Brinkmann (Saarbrücken)

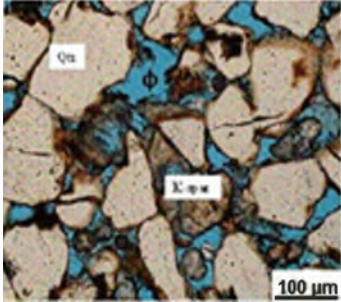


Figure 5.21: Optical microscopy of a thin ($30\ \mu\text{m}$) slice of sandstone, which represents an important class of oil reservoir formations.

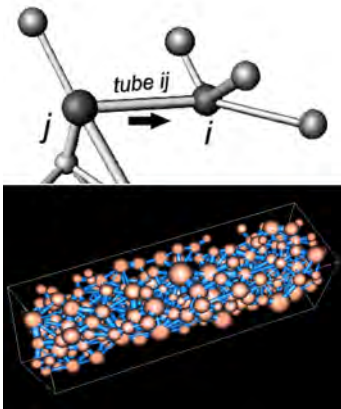


Figure 5.22: *Top*: pores and throats represented as spheres and tubes, respectively. *Bottom*: the porous medium as a pore-throat network.

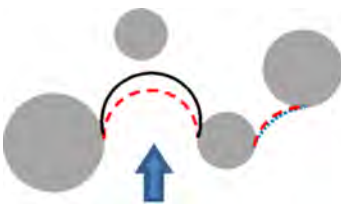


Figure 5.24: A liquid front (solid line) invading a 2D model porous medium consisting of circular disks (grey).

Despite its enormous importance and a substantial body of previous research, there is as yet no conclusive understanding of fluid invasion into porous media such as paper, soil, sandstone (Fig. 5.21), or any granular material. This is due to the enormously complex interplay of different mechanisms possibly involved, like pinning, percolation, or the possible emergence of ‘viscous fingers’, which cover a wide range of length scales.

It has been commonly observed (Fig. 5.23) that if the invading phase wets the medium well (small contact angle θ), the liquid front stays rather compact. If it does not wet well (large θ), the front becomes extremely rough, leaving a large fraction of the defending phase (e.g., crude oil) in the porous medium. Attempts to model this behaviour have commonly represented the porous material by a network of pores and throats (or tubes), as sketched in Fig. 5.22. Despite their complexity, these models were found to have very limited predictive power.

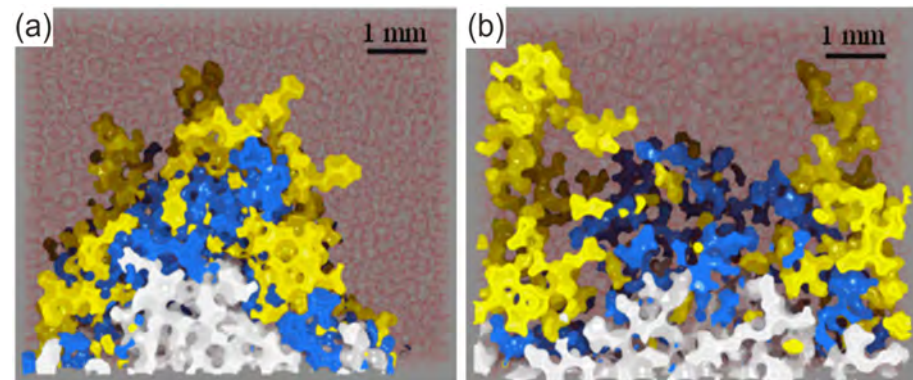


Figure 5.23: X-ray micro-tomography images of an aqueous phase entering a porous medium consisting of a pile of spheres from below, thereby expelling part of the oil filling the interstitial space. *Left*: basalt spheres, $\theta \approx 70^\circ$. *Right*: glass spheres, $\theta \approx 125^\circ$. Different colors correspond to different time steps [3].

For two-dimensional (2D) random arrangements of circular disks, a candidate mechanism has been proposed earlier [1]. If an advancing liquid front experiences a decreasing Laplace pressure before it reaches the opposite pore wall, a burst, or Haines jump [2] (HJ), occurs (Fig. 5.24). Computer simulations [1] had shown that this mediates the breakup of a smooth front into a ramified structure. Since this process becomes more probable at larger contact angles, it gives rise to a (rather sharp) transition from a smooth front at small θ to a rough front at large θ . However, it was not clear how relevant this rather crude model is for the much more complex 3D situation, where computer simulations would be considerably more demanding.

It turns out, however, that the 3D system is much more accessible than the 2D case. The latter is complicated by the fact that there is (in

general) no permeable material in 2D, and extra degrees of randomness had to be added to avoid spurious artefacts [1]. In the most commonly used model porous medium in 3D, a random pile of spheres, tetrahedral arrangements of spheres (Fig. 5.25a) are particularly prevalent, and can be considered as standard pores.

In this case, it is straightforward (Fig. 5.25) to calculate for which θ a liquid bulge entering the pore will see a decreasing Laplace pressure before it reaches the opposite pore wall, or before two invading bulges coalesce (which has the same effect on the front morphology) [1]. Taking the corresponding statistical weights (owing to the different possible orientations of the pore with respect to the invading front) into account, the probability of a HJ to occur can be calculated as a function of θ (Fig. 5.27a). This can even be done analytically when the tetrahedral pore is not perfect, i.e., when not all of the four spheres are in mutual contact. The corresponding distribution of relative angles

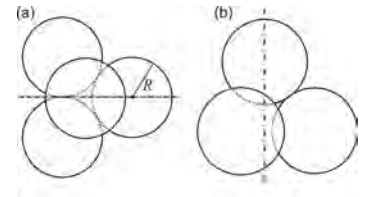


Figure 5.25: The geometry of an ‘ideal’ (tetrahedral) pore consisting of four spheres in mutual contact.

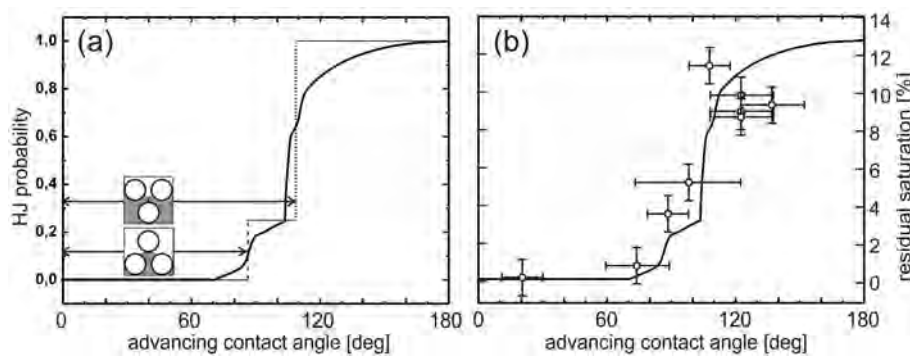


Figure 5.27: *Left*: the probability for HJ to occur, calculated analytically. The stepwise increase is obtained for an ‘ideal’ pore (four spheres in mutual contact). The two steps correspond to the two possible modes (single bulge intruding or more bulges intruding, see sketches). Including the non-ideal character of the pile (Fig. 5.26) leads to the solid curve. *Right*: The solid curve of the left panel, scaled according to the percolation threshold of the defending phase (Fig. 5.28), along with our tomography data for the residual saturation of the defending phase (open circles).

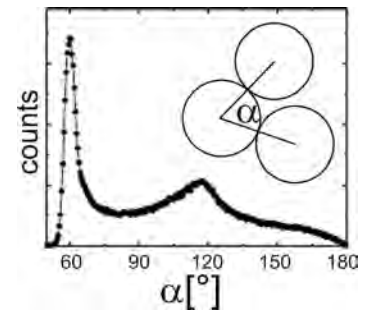


Figure 5.26: The distribution of relative angles (see inset) in a random close pile of spheres, as obtained by x-ray tomography.

for a random close pile can be obtained by x-ray microtomography (Fig. 5.26). If this is taken into account, the probability of HJ as a function of θ is obtained as shown by the solid curve in Fig. 5.27a.

The defending phase will be expelled until it undergoes inverse percolation (Fig. 5.28). From our studies of wet granular material, we know that this occurs at about 13 % of the pore volume. Using this for scaling the vertical axis of Fig. 5.27a, we can present our data of the residual saturation with defending liquid and the probability of HJ in one diagram. This is shown in Fig. 5.27b, demonstrating quantitative agreement, without a single fitting parameter. Since the Laplace pressure is constant (by definition) along any of the tubular throats used in pore-throat network models, we see now why these fail: they have a built-in blind spot which precisely eclipses the relevant mechanism.

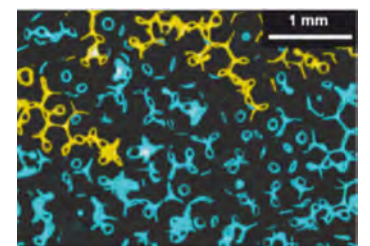


Figure 5.28: X-ray tomography showing the morphology of the defending liquid after expulsion. Clusters disjoint from the outlet are rendered in blue. The morphology is frozen-in close to the percolation threshold.

- [1] Cieplak, M. O. Robbins, Phys. Rev. Lett. **60** (1988) 2042.
- [2] W. B. Haines. J. Agricult. Sci. **20** (1930) 97.
- [3] K. Singh *et al.*, manuscript in preparation.

5.8 WATCHING PAINT DRY

L. Goehring, J. Li, P.-C. Kiatkirakajorn

B. Cabane (ESPCI), R. Botet (Paris-Sud), F. Arzner (Rennes)

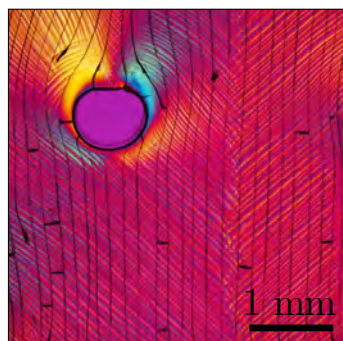


Figure 5.29: Shear-bands (diagonal lines) appear when charged colloidal dispersions (such as latex paint) are dried.

They can be controlled or eliminated by adjusting the inter-particle interactions of the drying dispersions [1].

Their birefringence is highlighted here by polarised light.

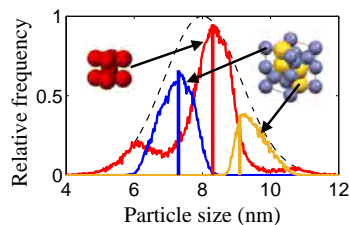


Figure 5.30: A polydisperse particle distribution (dashed line) is compressed, and two co-existing colloidal crystals form. A bcc crystal (red) collects the average-sized particles, leaving a binary distribution (blue and yellow) to build a more complex unit cell, with larger and smaller lattice sites. Vertical lines indicate experimental measurements for the mean size at each lattice site; curves are numerical simulations [3].

Colloidal dispersions are the basis of many paints, inks, coatings, ceramics and composites. When dried, these dispersions can show a surprising variety of patterning mechanisms. They may buckle or crack into spirals or parallel lines for example, while their dried shapes can vary from a coffee-ring to textured surfaces controlled by evaporation-lithography. This abundance of patterns suggests diverse means for the directed self-assembly of micro-structured materials, if the underlying dynamics can be understood and controlled.

One such pattern, which is commonly encountered, but has been hitherto unexplained, is a series of regular stripes, or bands, as in Figure 5.29. In [1] we show how these bands are the result of shears, similar to how two tectonic plates slip by each other along a very narrow fault. We further describe how the forces that give rise to these shears come about, how their spacing may be controlled by the thickness of the drying film, and how they can be eliminated, if desired.

The driving force for the shear-bands, and other mechanical instabilities, is drag. The basis of our paints are nanoscopic charged colloidal spheres. These materials are typically prepared as a suspension of particles in liquids, but then dried before being used in products. During drying the liquid must flow past the particles to get to an evaporating surface. This produces drag on the particles, which compresses them against each other. We have explored the liquid-to-solid transition of drying colloids, and have shown how this drag generically leads to permanent effects like a structural anisotropy, or birefringence [2].

Finally, for colloids and other nanomaterials it has been an empirical rule that even small particle size variations prevent the formation of regular structures, *i.e.* crystals. However, for nearly twenty years numerical modeling has repeatedly predicted that colloidal crystals should also exist in highly polydisperse suspensions, with each crystal collecting a different range of particle sizes. Experimentally, these crystals have consistently evaded observation, and kinetic effects have been blamed for this long-standing disagreement. Using industrially-produced colloidal silica, we have shown that polydisperse particles can spontaneously segregate at intermediate concentrations to build first one, then two distinct sets of colloidal crystals (see Fig. 5.30). These dispersions thus demonstrate fractional crystallization and multiple-phase coexistence, with an even richer phase diagram than predicted [3]. Their remarkable ability to build complex structures from a disordered population originates from long-range interparticle forces, and suggests routes for designing self-assembling crystals from the bottom-up.

[1] P.-C. Kiatkirakajorn and L. Goehring, *Phys. Rev. Lett.*, **115**, 088302 (2015)

[2] F. Boulogne, L. Pauchard, F. Giorgiutti-Dauphiné, R. Botet, R. Schweins, M. Sztucki, J. Li, B. Cabane, and L. Goehring, *EPL*, **105**, 38005 (2014)

[3] B. Cabane, J. Li, F. Artzner, R. Botet, C. Labbez, G. Bareigts, M. Sztucki and L. Goehring, under review

5.9 THE ROLE OF DIMENSIONAL CONFINEMENT AND HYDRODYNAMICS IN MICROSWIMMER DYNAMICS

C. C. Maaß, Ch. Bahr, S. Herminghaus
C. Krüger, G. Klös

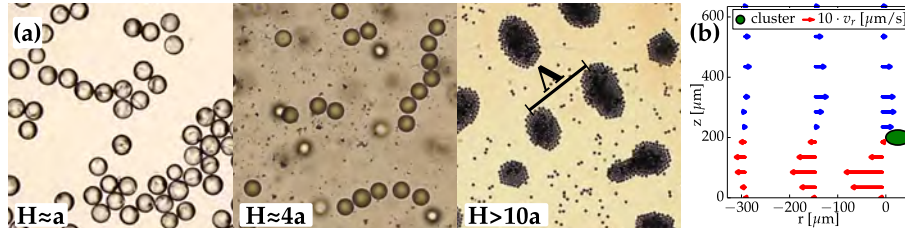


Figure 5.31: (a) transition from transient (unstable) clusters to line formation to convection mediated clustering with increasing cell height H . Λ : average cluster distance. (b) radial convection pattern around cluster as reconstructed from colloidal tracers.

Artificial experimental swimmers systems are a prime example for out of equilibrium dynamics and play an important role in the modelling of collective dynamics of biological swimmers by bridging the gap between biological complexity and the computational restrictions of large scale numerical simulations.

Our experimental system consists of an active emulsion of liquid crystal (LC) droplet swimmers in an aqueous surfactant solution [1] (see also sections 5.1 and 5.12). We present evidence that both a full 3D treatment and hydrodynamics are necessary to understand the dynamics of our system.

After injecting droplets of diameter a at comparable volume fractions into reservoirs of variable height H , we observe different aggregation regimes (Fig. 5.31 (a)): the fully confined system, $H \approx a$, shows only transient clusters, as swimmers colliding head on will inhibit each other's progress until they can escape by either rotational diffusion (cf. [3]) or might be actively pushed apart by mutual chemotaxis (see sec. 5.12). For less compressed systems, $H \approx 4a$, swimmers aggregate in line structures perpendicular to their direction of motion, since equatorial attraction is expected for pusher type swimmers as the flow field expands into 3D. For unconfined sedimenting swimmers, $H > 10a$, we observe large scale clustering driven by a convective flow pattern (Fig. 5.31 (b), see also [2]).

Within clusters, swimmers arrange hexagonally (Fig. 5.32) at a distance h from the cell bottom, with their leading edge pointing upwards. Surfactant solution is constantly pumped downward by each droplet, flows out along the cluster boundary and rises again to feed a toroidal convection roll around the cluster. Swimmers at the boundary tilt inwards at an angle α to counter the radial flow. If the flow exceeds the radial swimmer velocity, the cluster cannot grow any further, which should limit the cluster radius R to $R \approx 2.7h \sin \alpha$. We have measured a linear $R(h)$ dependence corresponding to $\alpha = 22^\circ$ (Fig. 5.33). This is consistent with observations from polarised microscopy (Fig. 5.32), which suggest $\alpha = 25 \pm 6^\circ$.



Figure 5.32: Cluster under crossed polarisers: Boundary swimmers are tilted inwards by $\alpha = 25 \pm 6^\circ$

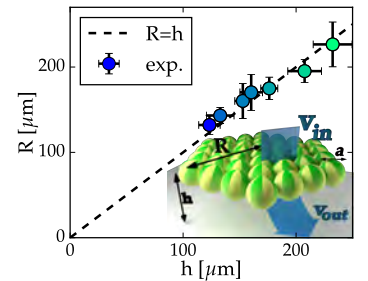


Figure 5.33: Cluster radius R vs. hovering height h , colour coded by fuel concentration. $R = h$ corresponds to $\alpha = 22^\circ$.

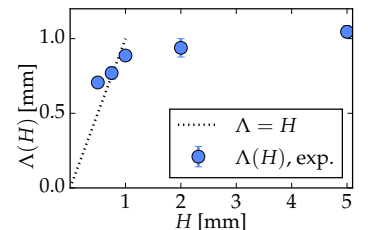
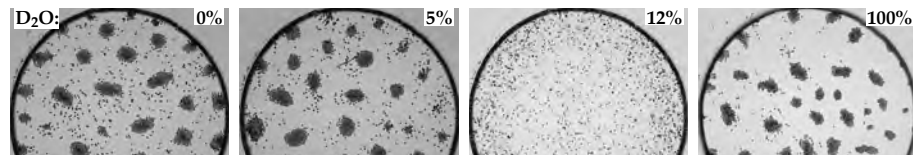


Figure 5.34: Cluster spacing Λ vs. cell height H .

Figure 5.36: Clustering is suppressed by progressive buoyancy matching via D₂O addition (far right: floating swimmers)



The hovering height h is determined by the balance of gravity, stagnation pressure, and the compression of the convection roll from the top, limited by H . In shallow cells ($H < 1\text{mm}$), the average cluster spacing Λ tends to follow $\Lambda = H$ (see dotted line in Fig. 5.34), which strongly suggests that the pattern is due to convection rolls. We have confirmed the existence of a convective flow field around the cluster using colloidal tracer particles (Fig. 5.31 (b)). For reservoir heights on a scale below $10a$ ($500\mu\text{m}$), we observe no clustering. Increasing the fuel concentration and thereby the pumping speed increases h and leads to larger clusters (colour coding in Fig. 5.33).

If the pumping exceeds the sedimentation speed of the droplets, there should be no formation of convection rolls or stable clusters. Due to the small mass density difference between droplets and water, $\Delta\rho = \rho_{\text{LC}} - \rho_{\text{H}_2\text{O}} = 0.022\text{g/cm}^3$, we are able to tune $\Delta\rho$ by addition of heavy water, D₂O ($\rho_{\text{D}_2\text{O}}=1.1\text{g/cm}^3$), from sedimenting to floating swimmers. As expected, clustering is fully suppressed even at 12 vol.% D₂O, which is still well below neutral buoyancy (Fig. 5.36) and sets in again at the top of the reservoir for swimmers floating in 100% D₂O.

Having buoyant swimmers capable of exploring environments far from interfaces (cf. sec. 5.12), our interest was raised in mapping this 3D behaviour by tracing individual droplets. For this purpose, we built a fluorescent light sheet microscope, consisting of a laser sheet and a high speed video microscope with coinciding focal planes, scanning periodically through a bulk sample containing fluorescently labelled droplets at sufficiently low number density to avoid multiple scattering (fig 5.35, top). Trajectories are reconstructed from the fluorescent signal in the video data via a Crocker-Grier type algorithm [4]. As a first result, we have been able to simultaneously track multiple nematic droplets and compared them to the helical trajectories from the 2D confined system described in section 5.1. The bottom panel of Fig. 5.35 shows a reconstruction of two such trajectories. The “telephone coil” shape suggests a precession of the defect around the droplet cap and confirms that the helical instability is not caused by interaction with an interface, but must be inherent to the swimming mechanism.

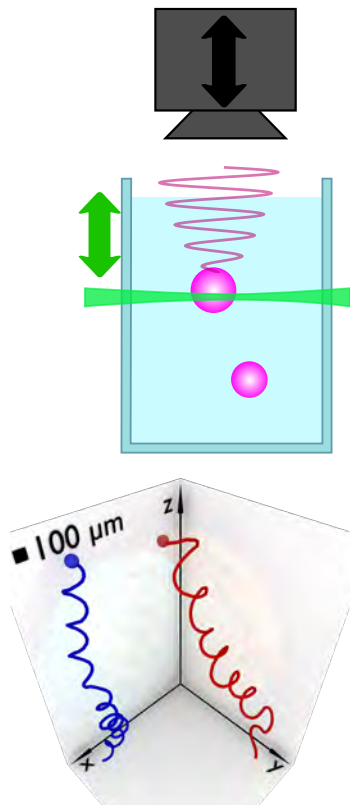


Figure 5.35: top: Light sheet schematic, bottom: Reconstructed 3D trajectories for buoyancy matched $100\mu\text{m}$ droplet swimmers.

- [1] Herminghaus et al., *Soft Matter* **10**, 7008 (2014)
- [2] Maass et al., *Annu. Rev. Cond. Mat.* **7**, in press (2016), doi: 10.1146/annurev-conmatphys-031115-011517
- [3] Buttinoni et al., *PRL* **110**, 238301 (2013)
- [4] Crocker and Grier, *J. Colloid Interface Sci.* **179**, 298–310 (1996)

5.10 BIOFLUID DYNAMICS FROM PHYSICS TO MEDICINE

Y. Wang, E. Bodenschatz

J. Christoph, G. Eichele (MPI-bpC),
J. Frahm (MPI-bpC), R. Faubel (MPI-bpC), A. Krekhov,
J. Lotz (Univ. Med. Göttingen), S. Luther, C. Westendorf (Univ. Graz),
W. Zimmermann (Univ. Med. Göttingen)

Biofluid Dynamics includes the analysis, control, and manipulation of fluid flow inside living mammals. We are investigating (i) with experiments and numerical simulation cilia driven flow of Cerebrospinal fluid (CSF) in the 3rd ventricle of the mammalian brain and (ii) with numerical experiments the flow in the human heart for a patient specific contraction profile.

Cerebrospinal fluid conveys many physiologically important signaling factors through the ventricular cavities of the brain. The walls of the ventricular cavities are covered with motile cilia that were previously thought to generate a unidirectional CSF flow. We investigated the transport of CSF in the 3rd ventricle and discovered a highly organized network of cilia modules collectively giving rise to a network of fluid flows that allow for precise transport paths within this ventricle [1]. We also discovered a cilia-based switch that reliably and periodically alters the flow pattern so as to create a dynamic subdivision that controls substance distribution within the 3rd ventricle. With numerical simulations of the natural cavity geometry we study the contribution of the ciliary network to overall CSF flow and identify target areas for site-specific delivery of CSF-constituents. Our work reveals a so far unknown capability of ciliated epithelia: the generation of a complex spatiotemporally regulated transport system.

Blood flow in the heart is 3-D, pulsating, and turbulent. Recently Zimmermann et al. [2] have shown that diseased matched heart muscle implants can be generated in vitro. These implants when attached surgically are hoped to increase ejection fraction. In collaboration with the University Medical Center Göttingen and the MPI for Biophysical Chemistry we are developing a computational model for patient specific blood flow. We are using medical imaging technologies for recovering the contraction patterns during cardiac cycle (Figure 5.38). With image segmentation and registration, we reconstruct the movement of the endocardial surface. Time dependent and patient specific dynamical heart geometry is imported into a solver with a state-of-art lattice Boltzmann method [3] and an immersed boundary method. The model will be validated against MRI velocity data measured by our collaborators. Once verified the heart wall contraction will be modified as inferred from muscle implants. The ultimate goal is to understand better ejection fraction and ultimately to give the surgeon suggestions of where to implant the in vitro grown muscle on the heart.

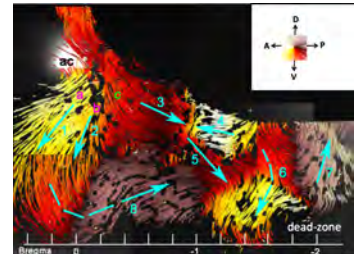


Figure 5.37: The flow map of the 3rd ventricle of a mouse shows that the near-wall flow is subdivided into multiple domains representing a transport network for signaling factors. The associated eight major flow directions are indicated with turquoise arrows.

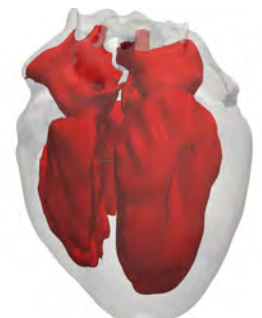


Figure 5.38: Geometry of a rabbit heart reconstructed from CT scan data. The endocardial surface is highlighted in red.

- [1] R. Faubel, C. Westendorf, E. Bodenschatz, G. Eichele, preprint.
- [2] W.H. Zimmermann et al., *Nat. Med.* **12**, 452 (2006).
- [3] Y. Wang, S. Elghobashi, *Respir. Physiol. Neurobiol.* **193**, 1 (2014).

5.11 MICROSWIMMERS IN COMPLEX GEOMETRIES I: MICROALGAE SWIMMING IN CONFINEMENT

T. Ostapenko, T. Böddeker, C. Kreis, O. Bäumchen

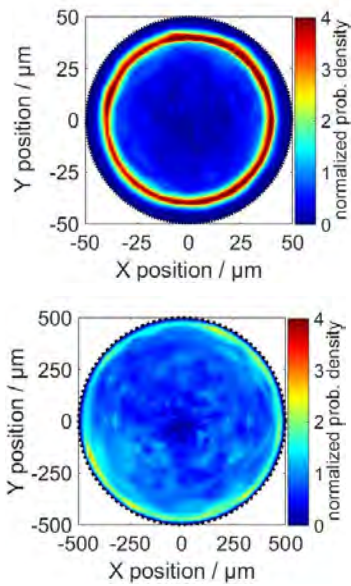


Figure 5.39: Probability distribution of a single cell trajectory for chamber diameters $d = 100 \mu\text{m}$ (upper) and $d = 1000 \mu\text{m}$ (lower).

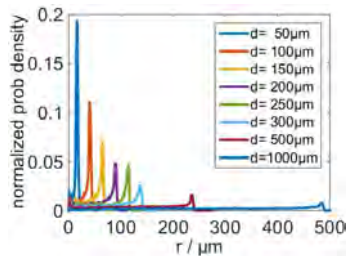


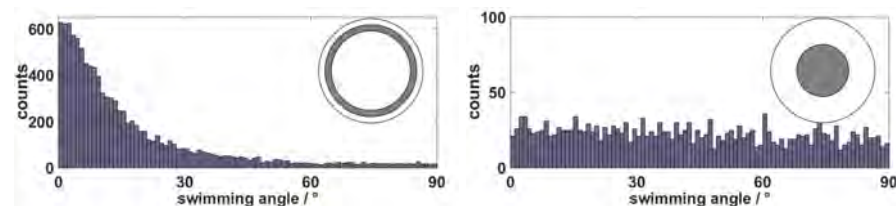
Figure 5.40: Radial probability distributions of motile cells for different chamber sizes from $d = 50 \mu\text{m}$ to $1000 \mu\text{m}$.

Figure 5.41: Distribution of local swimming angles with respect to the wall tangential for $d = 100 \mu\text{m}$ near the wall (left) as compared to cell trajectories in the chamber center (right).

The characteristics of active fluids, such as suspensions of active colloids, droplets and biological microswimmers, may not only originate from the mutual interactions between the constituents, but also from their interactions with interfaces and confining walls. Such interactions have raised interest among researchers from several perspectives: The natural habitat of many living organisms are complex geometric environments, rather than bulk situations [1]. In addition, the confinement and, in particular, the exposure to solid/liquid interfaces is expected to play an important role with regard to the adhesion of cell populations and, subsequently, the formation of biofilms.

We study the dynamics of the green algae *Chlamydomonas reinhardtii*, unicellular biflagellated puller-type swimmers, in geometrical confinement in order to determine the effect of wall curvature on the swimming dynamics: In circular 2D compartments, the radial probability distribution of trajectories for single motile cells displays a characteristic wall hugging effect (Fig. 5.39), which to date has only been experimentally reported for pusher-type motile bacteria, where hydrodynamic interactions trap the cell at the interface. In contrast, we observe that the algae are more trapped at a curved interface for decreasing compartment size. Thus, this effect is directly related to wall curvature (Fig. 5.40), rather than hydrodynamic surface interactions. A geometrical explanation arises from the interplay between the persistence length of the (short-time ballistic) cell trajectories and characteristic preferred wall scattering angles, which originate from the contact interactions between the cell's flagella and the wall [2]. For trajectories in the vicinity of the concave wall, an alignment of the local swimming direction with the local wall tangent is observed (Fig. 5.41), ultimately leading the algae to follow the boundaries. At the same time, the trajectory vectors exhibit an isotropic distribution at distances far from any cell-wall interactions. These results provide strong evidence that the trapping of motile organisms by curved interfaces is not only observed for pusher-type swimmers such as *E. coli* exclusively, but also for a puller-type swimmers at concave walls exhibiting a sufficiently long persistence length of synchronous flagellar beating, in combination with specific flagella-wall interactions.

- [1] P. Denissenko et al., PNAS **109**, 8007 (2012).
[2] V. Kantsler et al., PNAS **110**, 1187 (2013).



5.12 MICROSWIMMERS IN COMPLEX GEOMETRIES II: ARTIFICIAL DROPLET SWIMMERS

C. Jin, C. Krüger, C. C. Maaß

Guiding forces of swimmers in complex environments include gradient chemotaxis, wall interaction, wall curvature and trajectory persistence, as well as autochemotaxis, i.e. swimmers reacting to their own trail of depleted fuel. We investigate the interplay of such forces in the droplet swimmer model system described in section 5.1.

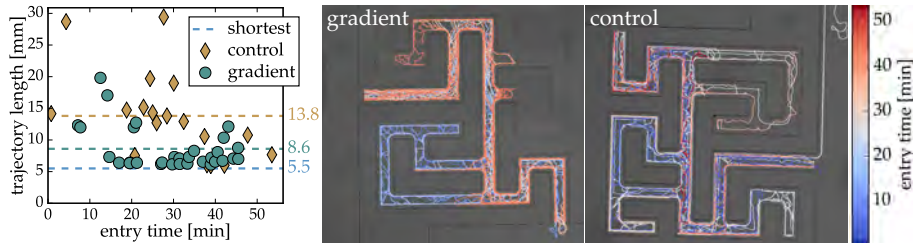


Figure 5.42: Droplets guided through a maze by a surfactant gradient: (l) Trajectory length vs. entry time. (r) Trajectories with gradient and without (control), colour coded by entry times.

Our droplets exhibit chemotaxis by swimming towards higher concentrations of empty surfactant micelles. We demonstrate this in a microfluidic maze, where a supply of solid surfactant is allowed to gradually dissolve and diffuse into the structure, which is fed by droplets from the opposite side. Trajectories colour coded by entry times are plotted on the right side of Fig. 5.42. Swimmers will closely follow the shortest path as soon as a gradient has developed along it and has not equilibrated in the side branches yet, as shown by plotting path lengths versus entry time for the same trajectories, compared to the shortest path length (Fig. 5.42 left).

To investigate the effects of wall attraction, curvature forcing and autochemotaxis, we have inserted droplet swimmers into arrays of circular pillars of variable radii (Fig. 5.43) and plotted the distribution of attachment length per pillar interaction for each radius. If the pillars are roughly less than twice as wide as the droplets, the curvature forcing will be too strong for the rather ballistic swimmers to be captured. For larger pillars, a distinct peak beyond one pillar circumference emerges: Capture is successful, but after one full circle the swimmer encounters its own trail of filled micelles and is repelled. For very large pillars, wall attraction dominates autochemotaxis and multiple orbits emerge. We will extend these preliminary results by varying trajectory persistence and swimmer size.

We have also observed the effect of mutual chemotactic interaction between swimmers following each other through a channel with pillars at regular intervals (Fig. 5.44). When given a choice on which side to pass an obstacle, the trailing swimmer will pick the side where the leading swimmer has not passed.

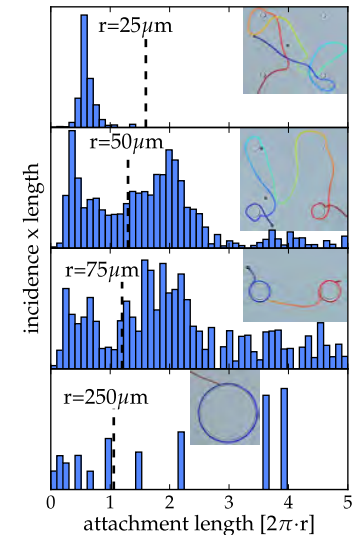
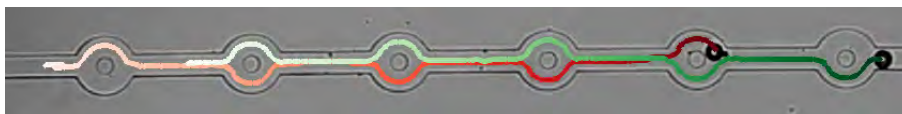


Figure 5.43: Attachment statistics for variable pillar radii r , with example trajectories, for $30\mu\text{m}$ droplet swimmers. The dashed line marks one orbit of $2\pi(r + 30\mu\text{m})$, trajectories are time-colour coded from red to blue.

Figure 5.44: Swimmers choosing alternating paths, time encoded bright to dark.

5.13 MICROSWIMMERS IN COMPLEX GEOMETRIES III: TAXIS AND BIOFILM

M. G. Mazza

R. Breier, G. Schkolnik, L. Stricker, H. Zwirnmann

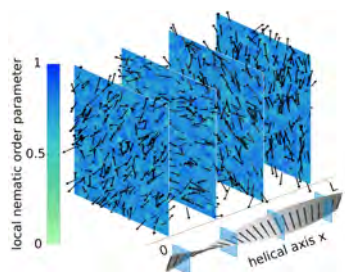


Figure 5.45: Cross-sections of a typical chiral configuration. Arrows: active swimmers; ribbon in the bottom: local director in different cross-sections.

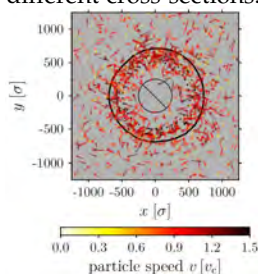


Figure 5.46: Aerotactic band next to an air bubble.

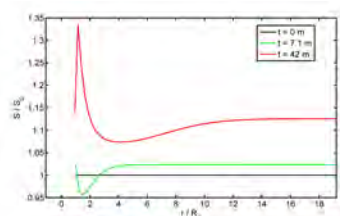


Figure 5.47: Evolution of an aerotactic band from advection-diffusion equations.

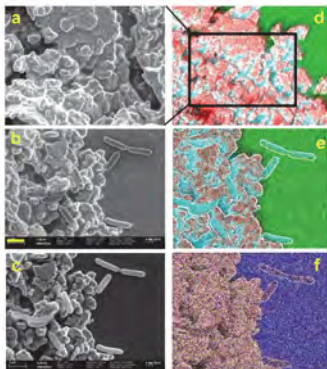


Figure 5.48: left column: SEM images; right column: overlay of SEM-EDX. Colors: ■ Ag, ■ C, ■ O, ■ P, ■ S, ■ Si. Yellow bar is 1 μm , for all images but (d); (a) and (b) were obtained at 1.5 kV, (c) to (f) at 5 kV.

We study the interplay of interaction, geometry and external fields in the behavior of active swimmers, both with computer simulations and experiments. To first order, hydrodynamics interactions between microswimmers are nematic, that is, have head-tail symmetry. However, stochasticity plays an important role, and their relative importance is currently under debate. We investigate these aspects through large-scale, 3D molecular dynamics (MD) simulations (up to 10^6 particles) of swimmers interacting nematicly. We find stable (or long-lived metastable) collective states that exhibit chiral organization although the interactions are achiral (Fig. 5.45). We elucidate under which conditions these chiral states will emerge and grow to large scales [1].

Some bacteria exhibit surprising behavior in the presence of an oxygen gradient. They perform an aerotactic motion along the gradient until they reach their optimal oxygen concentration. They often organize collectively by forming dense bands that travel towards the oxygen source. We have developed a model of swimmers with stochastic interaction rules moving next to an air bubble. Our MD simulations reproduce the aerotactic behavior of bacteria, such as *Shewanella oneidensis* (*S.o.*): If the oxygen concentration in the system sinks locally below a threshold value, an aerotactic band migrating toward the bubble can be observed. Fig. 5.46 shows the positions and velocities of the swimmers next to an air bubble (solid circle in the center). A dense aerotactic band is clearly visible. To account for more complex effects, we solve the advection-diffusion equations. Air is modeled as a mixture of oxygen and nitrogen; bacterial motility, the aerotactic current, bacterial reproduction and oxygen consumption, and the shrinking of the bubble due to diffusion are included. We reproduce quantitatively the experimental observations on the aerotactic band. Fig. 5.47 shows the dependence of the bacterial concentration profile on the distance from the air bubble at different times.

We have also conducted experiments on *S.o.* to study its biofilm, a complex protective structure. *S.o.* is an electroactive bacterium, capable of reducing extracellular insoluble electron acceptors, making it important for both nutrient cycling in nature and microbial technologies, such as microbial fuel cells and microbial electrosynthesis. We have developed a novel method that combines surface enhanced Raman spectroscopy and confocal Raman spectroscopy (Fig. 5.48), utilizing Ag nanoparticles bio-produced by the bacteria. This method allows the *in situ* spatial and temporal mapping of the biofilm. It generally applies to noble metal nanoparticle-precipitating bacteria in laboratory cultures or in their natural habitats [2].

[1] R. Breier et al., Phys. Rev. E, under review (2015)

[2] G. Schkolnik et al., PLOS One, under review (2015)

DISORDER IN SPACE AND TIME

6

Disorder and random fluctuations govern the dynamics of many complex systems in physics and biology. These systems are therefore often best described or analyzed by stochastic theories. The randomness can either be an expression of the complex intrinsic, out-of-equilibrium properties of the system itself or can be caused by extrinsic environmental fluctuations. For chaotic systems such as turbulent flows, disorder and fluctuations are defining features and in biological systems they are omnipresent. We explore experimental and theoretical paradigms, develop stochastic theories and general tools for the study of spatially and temporally disordered, complex systems as well as for extracting information from measured noisy signals.

CONTENTS

- 6.1 Processing of randomly sampled data 92
 - 6.2 Friction with your neighbors? Think locally! 93
 - 6.3 Branched flow in anisotropic media 94
 - 6.4 Space-time correlations of wall turbulence 96
 - 6.5 Characterizing multi-scale interaction in turbulence 98
 - 6.6 Anomalous dynamics in disordered systems 100
 - 6.7 Heterogeneity in models of infectious diseases 102
 - 6.8 Morphogenesis control by mechanical stresses 104
 - 6.9 Stochastic terminal dynamics in Epithelial cell intercalation 105
 - 6.10 Towards a theory of efficient stimulus encoding at auditory synapses 106
 - 6.11 Feature-based and machine-learning analyses of neural data 107
 - 6.12 Inferring dynamical states under spatial subsampling 109
 - 6.13 Field biology as a data analysis challenge 110
-

6.1 PROCESSING OF RANDOMLY SAMPLED DATA

H. Nobach

N. Damaschke, V. Kühn (Universität Rostock)

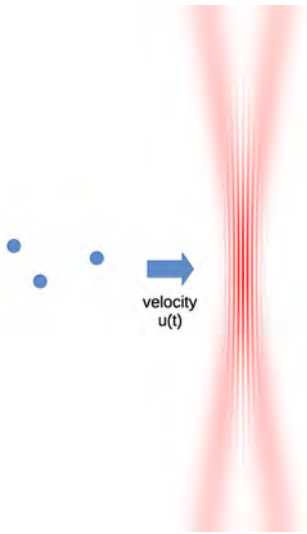


Figure 6.1: Laser Doppler measurement system

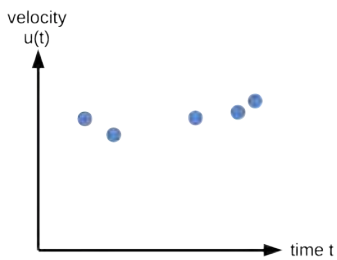


Figure 6.2: Randomly sampled data set

If the measurement system influences the statistical properties of the measured signal compared with the underlying process, classical signal processing will generate systematic errors in the statistics derived from the measured signal only. In these cases, the influence of the measurement system needs to be analysed to develop effective corrections to allow statistical estimation free of systematic errors. The laser Doppler velocity measurement system (Fig. 6.1) is known to produce biased estimates of the statistics derived from the measured velocity data due to (a) the random sampling of the velocity-time series (Fig. 6.2) due to the requirement of individual tracer particles passing the measurement volume, (b) the correlation between the instantaneous data rate and the velocity, and (c) a noise component in the measured data due to an uncertainty of the signal processing of individual velocity measurements of the measurement device. The development of bias-free statistical estimators for laser Doppler measurement systems is a key component for appropriate experimental studies of flow fields, e.g. in turbulent flows.

While significant progress in the development of various statistical estimators has already been made in the 1970's, no general agreement of the appropriateness of the processing tools has been achieved until today. Recently, a new debate has been conducted about the theoretical relation of the three known correlation and spectral estimators, namely the slot correlation, the direct spectral estimation and the interpolation method incorporating a low-pass filter correction. While for the case of equidistantly sampled data, the Wiener-Khinchin theorem proves the equivalence between the correlogram and the periodogram, the three processing methods, so far yield different results for randomly sampled data. In a series of journal publications [1, 2, 3] it has been shown, that the three methods in principal are equivalent, provided, that the methods apply equivalent processing parameters, such as block length, temporal and spectral resolution, weighting scheme or normalization. This requirement seems obvious. However, since the three methods have been developed individually and optimized in different ways, a consolidation is challenging. The above mentioned publications, therefore, discuss extensively how developments for particular methods in the past can be adapted to the other methods. As a result, the comparison of the various techniques reveals great similarities between the three processing methods.

- [1] Nobach, H.: Experiments in Fluids, vol. 56 (2015), no. 5: 109
- [2] Nobach, H.: Experiments in Fluids, vol. 56 (2015), no. 5: 100
- [3] Nobach, H.: Experiments in Fluids, vol. 56 (2015), no. 9: 182

6.2 FRICTION WITH YOUR NEIGHBORS? THINK LOCALLY!

M. Schröter, G. Schröder-Turk (Murdoch University), F. Schaller (FAU Erlangen), W. Drenckhan (Université Paris-Sud)

Scientific question: Many mechanical properties of jammed packings of particles depend on the number of contacts Z a particle forms on average with its neighbors. If the particles are soft and frictionless spheres, as in emulsions and foams, then both Z and the the global volume fraction ϕ_g are controlled by the compression of the packing and are therefore related by a simple argument.

However, in frictional granular media such as sand, salt, or sugar the control of ϕ_g and Z is not achieved by compression but by changing the geometric structure of the sample. This requires a new theoretical approach which explains Z using only locally (i.e. on a particle level) defined parameters.

Results: In the last two years we have used X-ray tomography to characterize packings of frictional, oblate ellipsoids of aspect ratio α (c.f. Fig. 6.3 and 6.4). We find that Z can be explained by an analysis [1] where the environment of each particle is described by its local volume fraction ϕ_l computed from a Voronoi tessellation (shown in Fig. 6.5).

As shown in Fig. 6.6 a), Z can then be expressed by an integral over all values of ϕ_l including two terms: a local contact number function $Z_l(\phi_l, \alpha)$ describing the relevant physics in terms of local variables only. And a conditional probability to find a specific value of ϕ_l which depends *only on* ϕ_g , and not even on α (Fig. 6.6 b).

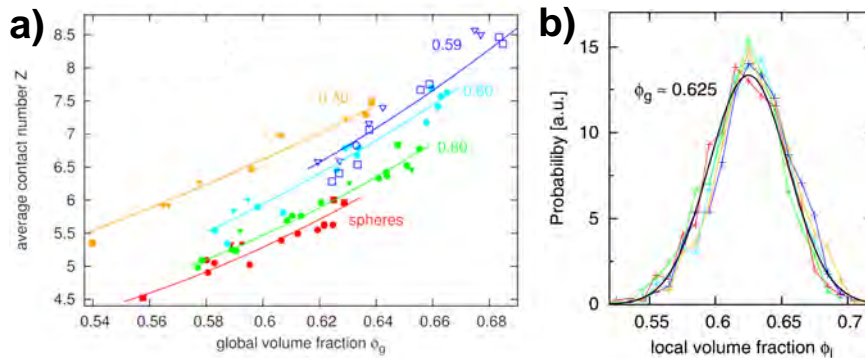


Figure 6.6: a) The contact number increases with the volume fraction in packings of oblate ellipsoids. Solid lines are our theory using only locally defined variables. Colors and numbers indicate the different aspect ratios. b) The probability distributions of local volume fractions is independent of the shape of the ellipsoids.

Ongoing work: Presently, we try to understand a) how to include a dependence on the preparation history in our theory and b) how special foams with tangential contact forces will modify our ansatz.

[1] F. Schaller, M. Neudecker, M. Saadatfar, G. Delaney, G. Schröder-Turk, and M. Schröter. Local Origin of Global Contact Numbers in Frictional Ellipsoid Packings. *Physical Review Letters*, 114:158001, 2015.

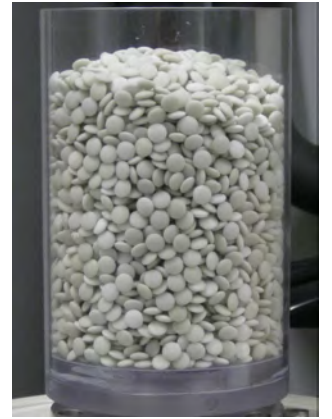


Figure 6.3: Container filled with 3D printed ellipsoids. Packings are prepared by vertical tapping.

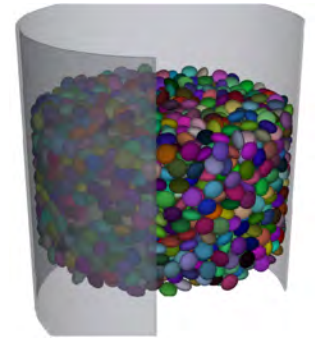


Figure 6.4: Reconstruction based on a X-ray tomogram of an ellipsoid packing similar to figure 6.3.

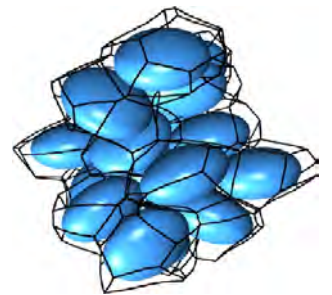


Figure 6.5: The wireframe indicates the Voronoi cells i.e. the volume which is closer to a given ellipsoid than to any other particle.

6.3 BRANCHED FLOW IN ANISOTROPIC MEDIA

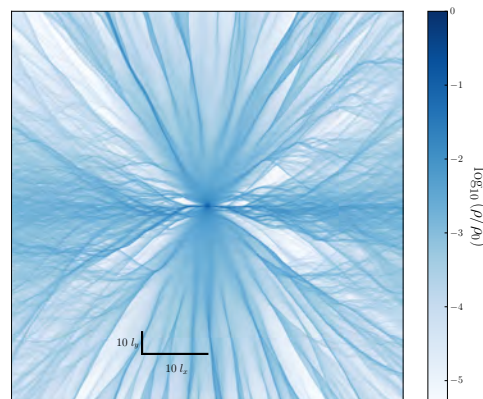
H. Degueldre, E. Schultheis, R. Fleischmann
J. J. Metzger (Rockefeller Univ., NY)

In many natural and technological systems, waves are weakly scattered by a complex medium that is often best described as random. Due to its internal structure, however, the randomness exhibits spatial correlations. If these correlations persist on scales longer or comparable to the wavelength even tiny fluctuations in the medium will focus the waves into branches, leading to strong fluctuations in the wave intensity. Examples that have been experimentally and theoretically studied in the literature range from the propagation of electrons in the correlated disorder potential of semiconductors [1], via the microwave transmission through arrays of random scatterers [2] and the sound propagation in the inhomogeneous oceans [3], to the focusing of tsunami waves by small underwater structures (see report 5.5). This very general phenomenon of *branched flow* is tightly connected to the formation of *random caustics* [4], i.e. singularities in the corresponding ray dynamics, with universal statistical properties [5]. It leads to heavy tailed intensity distributions and extreme wave events [6] and has been shown to be an important mechanism for the formation of so called *rogue* or *freak waves* in the oceans [7].

While the theory of branched flows so far can only describe homogeneous, isotropic random media, many real systems show a pronounced anisotropy in their structure. The example that initially motivated our work is the dynamics of tsunami waves (see report 5.5). The geological processes that generate the ocean floor topography that scatters tsunami waves tend to be highly anisotropic. There is a wide range of other systems, however, to which our theory is applicable, including the electron dynamics in anisotropic semiconductor crystals, the transmission of light through layered biological tissue, or the scattering of seismic waves, which is probably a prime example of anisotropic wave propagation.

We have therefore studied particle and wave flows in random media that are characterized by anisotropic, elliptic correlation functions, i.e. correlations that decay differently in two principal directions, which, for

Figure 6.7: Example of a branched flow in a Gaussian correlated anisotropic random medium with an aspect ratio of the correlation lengths of $\ell_y/\ell_x = 1/3$ (the correlation lengths in x and y direction are indicated by thick black lines). The color code shows the logarithmic relative density of Newtonian trajectories emitted from a point source in the center.



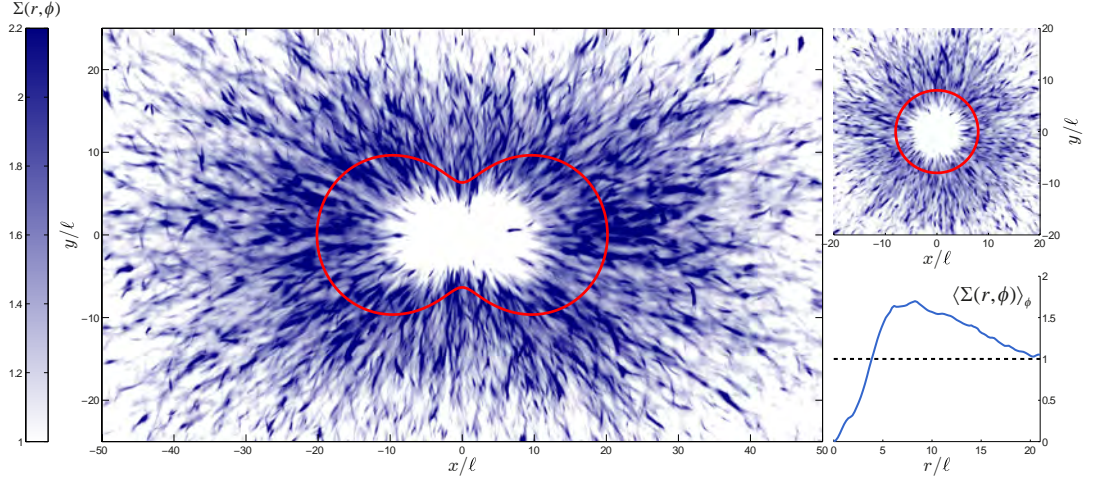


Figure 6.8: Scintillation index, $\Sigma(r, \phi) = \langle I(r, \phi)^2 \rangle / \langle I(r, \phi) \rangle^2 - 1$, of shallow water waves calculated by an ensemble average over approx. 1000 realizations of random ocean floor topographies. $I(r, \phi)$ is the intensity of the wave fields in polar coordinates. In the upper right inset the case of an isotropic correlation is shown. The red circle indicates the distance from the source to the strongest focusing, which corresponds to the peak in the angle averaged scintillation index shown in the panel below. This average illustrates that the small structure in the spatially resolved scintillation index above is due only to the finite ensemble, i.e. in an infinite ensemble a smooth annulus would be visible. The main panel shows the scintillation index for systems with an anisotropic disorder with $\ell_y/\ell_x = 2$. It shows excellent agreement with the prediction of Eq. (6.1) shown by the red curve.

simplicity, we assume in this report to coincide with the coordinate axes. Figure 6.7 shows an example of a bundle of Newtonian trajectories (or a *ray field*) emitted from a point source into such a medium. It shows a highly non-trivial angle dependence of the random focusing. For the focusing distance as a function of the angle of propagation α we derived the expression

$$d_{fc} \sim \epsilon^{-2/3} \ell (ab)^{-4/3} (a^2 \cos^2 \alpha + b^2 \sin^2 \alpha)^{5/6}, \quad (6.1)$$

where the two principal correlations lengths are $\ell_x = \ell/a$ and $\ell_y = \ell/b$ and ℓ is an appropriate length scale. Equation (6.1) not only gives a perfect prediction for ray fields but also helped us to understand the focusing of waves in anisotropic media as illustrated in Fig. 6.8 (details will be given in [8] and [9]).

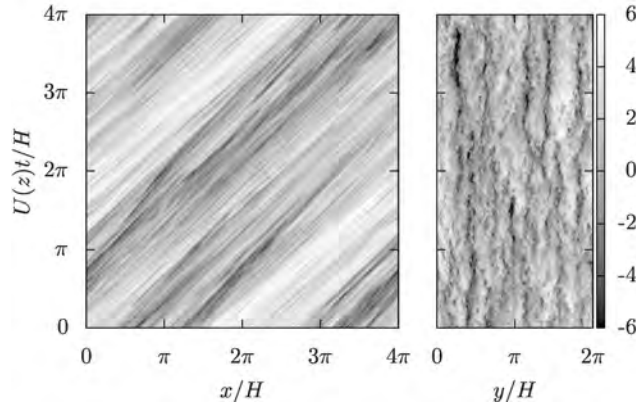
- [1] M. A. Topinka et al., Nature **410**:183 (2001); K. E. Aidala et al. Nat Phys **3**:464 (2007); D. Maryenko et al., Phys. Rev. B **85**:195329, (2012).
- [2] R. Höhmann, et al., Phys. Rev. Lett. **104**:093901 (2010); S. Barkhofen et al., Phys. Rev. Lett. **111**:183902 (2013).
- [3] M. A. Wolfson and S. Tomsovic, J. Acoust. Soc. Am. **109**:2693 (2001).
- [4] L. Kaplan, Phys. Rev. Lett. **89**:184103 (2002).
- [5] J. J. Metzger, R. Fleischmann, and T. Geisel, Phys. Rev. Lett. **105**, 020601 (2010).
- [6] J. J. Metzger, R. Fleischmann, and T. Geisel, Phys. Rev. Lett., **112**, 203903 (2014).
- [7] E. J. Heller, L. Kaplan, and A. Dahlen. J. Geophys. Res. **113**:C09023 (2008); L. H. Ying et al., Nonlinearity **24**:R67 (2011).
- [8] H. Degueldre, Dissertation, Univ. Göttingen (2015)
- [9] H. Degueldre, J. J. Metzger, E. Schultheis, and R. Fleischmann, to be published (2015)

6.4 SPACE-TIME CORRELATIONS OF WALL TURBULENCE

M. Wilczek

R.J.A.M. Stevens (University of Twente, Netherlands),
C. Meneveau (Johns Hopkins University, Baltimore, USA)

Figure 6.9: Space-time plots of the streamwise velocity fluctuations in the logarithmic layer of a turbulent wall-bounded flow ($z/H \approx 0.154$) from LES. Left: streamwise cut, right: spanwise cut. The color bar is given in units of the friction velocity. Figure adopted from [6].



Turbulent flow over a rough wall is a prototypical setup for many natural and engineering environments [1, 2]. Neutral atmospheric boundary layers may serve as one of the most prominent examples. Here we consider a flow driven by an imposed pressure gradient in x -direction, which leads to a height-dependent mean velocity $\mathbf{U} = U(z)\mathbf{e}_1$. Such flows exhibit a rich spatio-temporal structure as illustrated in Fig. 6.9, which shows a space-time plot of the streamwise velocity component. These plots reveal that turbulent fluctuations are predominantly advected with the mean velocity $U(z)$ in the streamwise direction with additional large-scale perturbations. The latter effect thereby adds a variation to the classical Taylor frozen eddy hypothesis.

In this project, which was mainly carried out while MW was postdoc at JHU, we derived a simple, physics-based model for the space-time correlation in terms of the wavenumber frequency spectrum, which represents one of the most fundamental statistical quantities to characterize turbulence. Our analytical model is benchmarked with large eddy simulations (LES), which provide high Reynolds number data with sufficient spatio-temporal resolution at a reasonable computational cost. We ran simulations on a $4\pi \times 2\pi \times 1$ domain with more than 134 million grid points and collected data over tens of thousands of time steps spanning several flow-through times.

One example of a wavenumber frequency spectrum from the logarithmic layer of the flow is shown in the left panel of Fig. 6.10. The most striking features of this projection to the k_1 - ω plane are a Doppler shift of frequencies as well as a Doppler broadening. To capture these effects, our analytical model is based on the Tennekes-Kraichnan random sweeping hypothesis with additional mean flow [3, 4], i.e. we assume that small-scale velocity fluctuations are passively advected (in planes at a fixed height z) by the mean velocity as well as the large-scale random sweeping velocity. By a number of simplifying assumptions (large-scale Gaussian velocities, scale separation etc.) we obtained a sol-

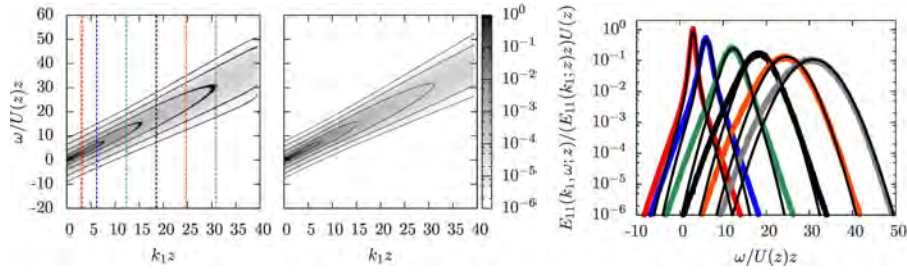


Figure 6.10: k_1 - ω spectra of the streamwise velocity component at $z/H \approx 0.154$. In the left panel the spectrum is evaluated directly from LES. The middle panel shows the spectrum obtained from the random sweeping hypothesis with mean flow, for which only the wavenumber spectrum and the mean and random-sweeping velocities evaluated from the LES data have been used. The right panel shows normalized cuts through the k_1 - ω spectrum from LES (colored lines) together with the results from the linear random advection model (black lines). The positions of the cuts are indicated in the left panel. Figure adopted from [6].

able model [5, 6], which predicts the wavenumber-frequency spectrum $E_{11}(\mathbf{k}, \omega; z)$ as a product of the wavenumber spectrum $E_{11}(\mathbf{k}; z)$ and a Gaussian frequency distribution:

$$E_{11}(\mathbf{k}, \omega; z) = \frac{E_{11}(\mathbf{k}; z)}{\sqrt{2\pi} \langle (\mathbf{v} \cdot \mathbf{k})^2 \rangle} \exp \left[-\frac{(\omega - \mathbf{k} \cdot \mathbf{U})^2}{2 \langle (\mathbf{v} \cdot \mathbf{k})^2 \rangle} \right]. \quad (6.2)$$

Here, \mathbf{k} denotes the wavevector in horizontal planes, ω is the frequency, \mathbf{U} is the mean velocity and \mathbf{v} the large-scale random sweeping velocity. Based on the idea of advection with a mean and a random velocity, the analytical result naturally contains frequency shift and broadening.

A comparison of the model spectrum given by Eq. (6.2) and the spectrum directly evaluated from LES is presented in Fig. 6.10 (middle and left panel, respectively), along with a number of representative cuts in the right panel. Given the underlying simplifying assumptions of the model, a remarkable agreement is found. Having established Eq. (6.2) as a good approximation, we furthermore motivated an analytical model for the height-dependent wavenumber spectrum $E_{11}(\mathbf{k}; z)$ as well as the Doppler shift and broadening term. This novel, fully analytical model is based on the logarithmic height dependence of the mean velocity and the velocity fluctuations as well as on the assumption of small-scale isotropy. We invite the reader to take a look at [6, 7] for further details. Together with Laura Lukassen, this work is continued at MPIDS. As part of the WINDINSPIRE collaboration, the goal is to use the model for the prediction of power output fluctuations of wind farms.

- [1] Jimenez, J. *Phys. Fluids* **25** (2013) 101302
- [2] Smits, A. J.; McKeon, B. J.; Marusic, I. *Annu. Rev. Fluid Mech.* **43** (2011) 353
- [3] Kraichnan, R. H. *Phys. Fluids* **7** (1964) 1723
- [4] Tennekes, H. *J. Fluid Mech.* **67** (1975) 561
- [5] Wilczek, M.; Narita, Y. *Phys. Rev. E* **86** (2012) 066308
- [6] Wilczek, M.; Stevens, R.; Meneveau, C. *J. Fluid Mech.* **769** (2015) 888
- [7] Wilczek, M.; Stevens, R.; Meneveau, C. *J. Turbul.* **16** (2015) 937

6.5 CHARACTERIZING MULTI-SCALE INTERACTION IN TURBULENCE

C. C. Lalescu, M. Wilczek

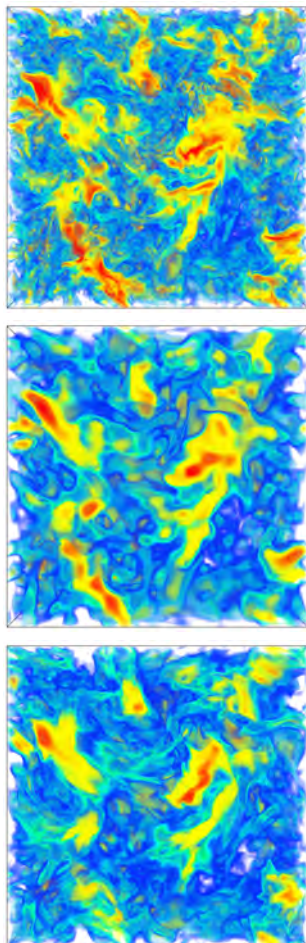


Figure 6.11: Snapshots of velocity field: original (top), spatially filtered (center) and temporally filtered (bottom). Images obtained with VAPOR (described in [2]), with the same color convention applied to all three fields (from blue for low velocity magnitude to red for high velocity magnitude).

Turbulence is a true multi-scale phenomenon with a broad range of interacting spatial and temporal scales. For example, the energy cascade has been described by L.F. Richardson in [5] as follows: “big whirls have little whirls that feed on their velocity, and little whirls have lesser whirls and so on to viscosity”. The quote describes the sweeping and stretching of small-scale vortices by large-scale vortices, a widely discussed process that is evidenced for instance in [1]. In this context, one speaks of *eddies*, which can be associated to individual Fourier modes of the full field. The energy cascade can then be viewed as the process of energy moving from larger to smaller eddies.

By definition, such eddies have a characteristic length scale. A direct application of the 1941 Kolmogorov theory predicts that eddies of scale ℓ , in the inertial range, should have a characteristic time scale $\tau \sim (\ell^2/\varepsilon)^{1/3}$, where ε is the mean energy dissipation rate. As a consequence, one would naively expect that removing length scales below a certain threshold should also eliminate the corresponding time scales. However, in turbulence interactions take place between eddies of different sizes (therefore with different time scales), so we expect that there is no simple relationship between space and time scales.

In broad terms, the current project aims to help better discriminate between large-scale and small-scale dynamical effects. Starting from kinematic considerations, it has already been argued that only eddies of similar sizes interact effectively [3], and we would like to progress towards quantifying how different time scales are associated to different length scales. The results presented here come from an initial foray into the problem, where Eulerian statistics are analyzed, with a complementing Lagrangian investigation to follow.

If eddies of size ℓ only evolve on time scales τ , we expect that $\mathbf{u}_\ell \approx \mathbf{u}_\tau$, where \mathbf{u}_ℓ contains only eddies of size at least ℓ and \mathbf{u}_τ contains only components of \mathbf{u} that evolve over time scales of at least τ . The removal of eddies smaller than ℓ is, in practice, achieved by a spatial filtering, whereas fluctuating components that are faster than some τ are removed by temporal filtering. We run direct numerical simulations (DNS) of Navier-Stokes turbulence, and we filter the solution over time or space. We use our own newly built DNS toolset, based on a standard pseudo-spectral algorithm for the vorticity formulation of the incompressible Navier-Stokes equations.

In Fig. 6.11 we show, for illustration, an unfiltered velocity field and the corresponding filtered fields. The two filtered fields are visually quite distinct, and the difference is made more clear by the energy spectra shown in the left hand plot of Fig. 6.12. It is evident that temporal filtering does decrease the amplitude of small-scale fluctuations. However, small scales are still present after temporal filtering, even though amplitudes are lowered progressively more for decreasing scales. To quantify the difference between time-filtered and space-filtered fields

we introduce the normalized difference:

$$\mathcal{M}(\tau, \ell) = \frac{1}{n} \sum_{i=1}^n \frac{\|\mathbf{u}_\ell(\cdot, t_i) - \mathbf{u}_\tau(\cdot, t_i)\|_2}{\|\mathbf{u}(\cdot, t_i)\|_2} \quad (6.3)$$

where the L^2 norms are taken over the spatial domain of the flow and the t_i are separated by large times (i.e. the temporal averaging is used as a proxy for ensemble averaging). In Fig. 6.12 we show preliminary

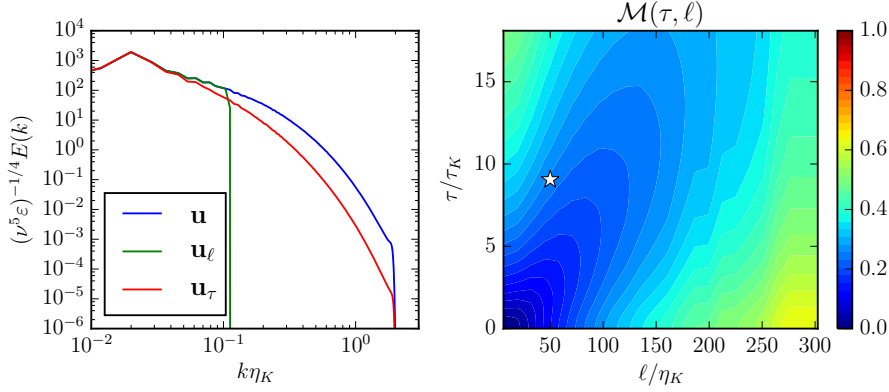


Figure 6.12: Spectra for original, spatially filtered and temporally filtered field (left) and difference between the two filtered fields, for different filter sizes (right). The white star corresponds to the parameters used for Fig. 6.11 and the spectra.

results from a DNS of a turbulent flow with $R_\lambda \approx 130$.

When studying the measure \mathcal{M} , shown in the right hand side plot of Fig. 6.12, it is immediately apparent that there is a smooth distribution of time scales τ associated with each length scale ℓ and vice versa. In other words, there is no clear mapping of a unique τ to some given ℓ , thus a naive application of Kolmogorov scaling is not enough to describe \mathcal{M} . Note that the current dataset displays only a modest inertial range, while theoretical arguments rely on a long inertial range (technically the ratio of the minimum and maximum length scales of the flow should be much larger than 1, i.e. $R_\lambda^{3/2} \gg 1$). Ongoing work therefore includes the required extension to larger values of R_λ .

It must be furthermore recognized that temporal averaging of the field at fixed positions in space samples the different small-scale structures as they are advected by large-scale structures [4, 6]. This “random sweeping” process introduces fundamental differences between Eulerian and Lagrangian statistics, constituting a major reason for a future confrontation between Eulerian and Lagrangian results. By performing a comprehensive analysis of the different length-time scale relationships extracted from our data, we hope to better distinguish between dynamic and kinematic aspects of the multi-scale character of turbulence.

- [1] Bürger, K.; Treib, M.; Westermann, R.; Werner, S.; Lalescu, C. C.; Szalay, A.; Meneveau, C.; Eyink, G. L. *arXiv:1210.3325* (2012)
- [2] Clyne, J.; Mininni, P.; Norton, A.; Rast, M. *New J. Phys.* **9** (2007) 301
- [3] Eyink, G. L. *Physica D* **207** (2005) 91
- [4] Kraichnan, R. H. *Phys. Fluids* **7** (1964) 142
- [5] Richardson, L. F. *Weather Prediction by Numerical Process*, (Cambridge University Press, 1922)
- [6] Tennekes, H. J. *Fluid Mech.* **67** (1975) 561

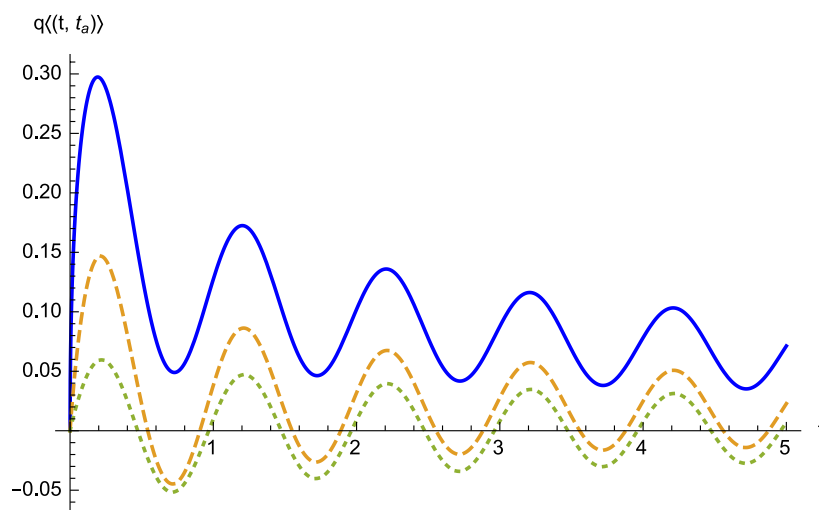
S. Eule, T. Geisel

J.J. Metzger (Rockefeller), M Wilczek

Strongly disordered complex systems frequently exhibit anomalous dynamics characterized by sudden large transitions and intermittent dynamics, where long smooth periods are interrupted by abrupt bursts of activity. In these systems the equivalence between long time averages and ensemble averages may be broken - a phenomenon referred to as weak ergodicity breaking. In such cases time averages are random quantities that cannot be reproduced and may no longer be interpreted in terms of ensemble theories. Often this behavior comes along with the appearance of aging, where observables depend on the time span between the initial preparation and the start of the measurement.

Recent single-molecule-tracking experiments have revealed that the anomalous transport of some molecules in living cells, caused by transient trapping events of random duration, is accompanied by aging as well as weak ergodicity breaking [1]. Motivated by these experiments, we study the linear response of such systems to an external perturbation. The linear response is a key observable in experimental studies because it carries substantial information about the dynamical behavior of a complex system. Our approach is based on the path integral representation of stochastic processes and includes temporal disorder by means of a process $\alpha(t)$, which is equal to zero if the process is trapped and one otherwise [2]. We obtain the analytical solution for the linear response function of a subdiffusive Continuous Time Random Walk (CTRW) in a harmonic potential - the standard model to describe aging anomalous transport of molecules confined in a biological cell - and show how the response depends on the age of the system as well as on the averaging procedure, see Fig. 6.13. Our results suggest that response measurements, e.g. by applying the recently developed techniques to track and manipulate single molecules in living cells, can be used as a tool to unravel the underlying mechanisms that give rise to anomalous kinetics and temporal disorder.

Figure 6.13: The response of the mean position $\langle q(t, t_a) \rangle$ of three CTRWs with identical parameters but different age t_a to the same periodic forcing (blue the youngest, green the oldest). The older the system gets the weaker it responds. The observation of an age-dependent response can be used to identify temporal disorder as the source of anomalous kinetics.



Furthermore, the path integral representation can be employed to obtain probability measures for entire paths of CTRWs [3]. This is particularly important because some subdiffusive processes are not uniquely characterized by their single-time statistics. In addition, our formulation generically includes the description of functionals of CTRWs.

Interestingly, weak ergodicity breaking and aging is also found in chaotic systems [4]. This observation naturally raises the question about the ergodic properties of turbulent diffusion processes in fully developed, homogeneous, isotropic turbulent flows as generated by the Navier-Stokes equation. This problem becomes even more intriguing given that several (anomalous) diffusion processes, such as the Lévy Walk, have been suggested as simple models of turbulent diffusion, where some of these models exhibit weak ergodicity breaking, while others are perfectly ergodic.

We analyze the diffusion of tracer particles in turbulent flows by means of extensive computer simulations and focus on the deviations of the time-averaged mean squared displacement (TAMSD) $\overline{\delta x^2(\tau)}$ around the ensemble average given by $P(\xi|\tau) = \langle \delta \left(\frac{\overline{\delta x^2(\tau)}}{\langle \overline{\delta x^2(\tau)} \rangle} - \xi \right) \rangle$. We observe that these deviations go to zero for increasing measurement time T and are a scaling function of the ratio of the lag time and the measurement time, see Fig. 6.14. We thus can conclude that turbulent diffusion is an ergodic process.

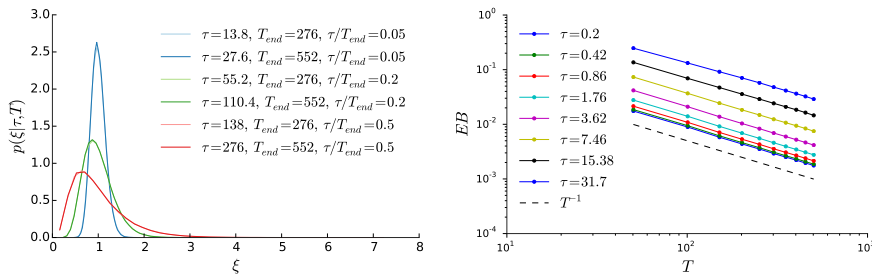


Figure 6.14: Deviations of the TAMSD around the ensemble average vanish for decreasing τ/T . For fixed τ , the ergodicity breaking parameter $EB = \frac{\langle \overline{\delta x^2(\tau)}^2 \rangle - \langle \overline{\delta x^2(\tau)} \rangle^2}{\langle \overline{\delta x^2(\tau)} \rangle^2}$ decays as T^{-1} .

- [1] A.V. Weigel, B. Simon, M.M. Tamkun and D. Krapf, PNAS **108**, 6438 (2011), S.M.A. Tabei, S. Burov, H.Y. Kim, A. Kutznesov, T. Huynh, J. Jureller, L.H. Phillipson, A.D. Dinner and N.F. Scherrer, PNAS **110**, 4911 (2013).
- [2] S. Eule, (*in preparation*) (2015).
- [3] S. Eule and R. Friedrich, J. Stat. Mech. P(12005) (2014).
- [4] T. Geisel and S. Thomaes, Phys. Rev. Lett. **52**, 1936 (1984), E. Barkai, Phys. Rev. Lett. **90**, 104101 (2003).
- [5] J.J. Metzger, M. Wilczek, and S. Eule, (*in preparation*) (2015).

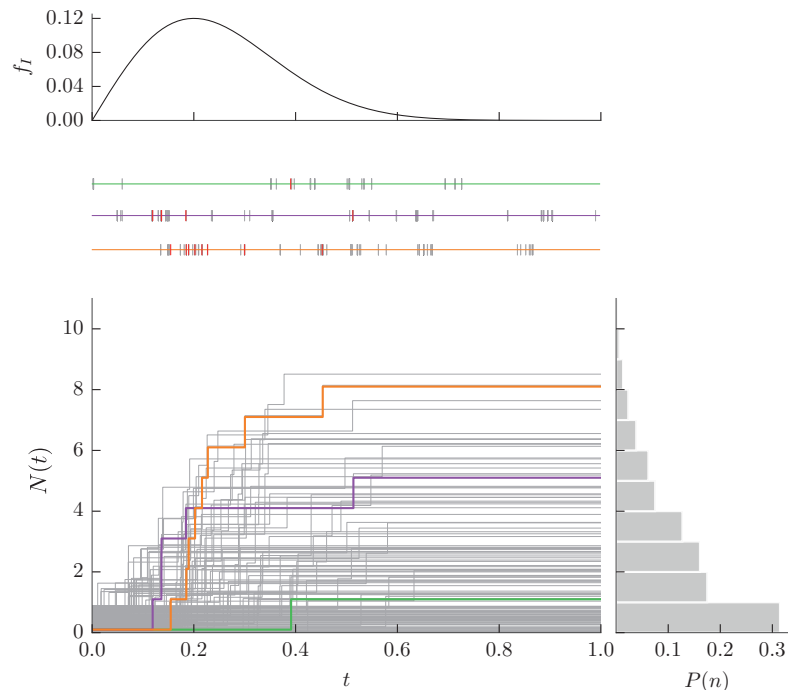
6.7 HETEROGENEITY IN MODELS OF INFECTIOUS DISEASES

S. Eule, T. Geisel

J.J. Metzger (Rockefeller), D. Lamouroux, J. Nagler (ETH Zurich)

The sudden appearance and rapid spread of an infectious disease can pose a serious threat to human or animal populations that calls for immediate actions by national and international health agencies. Their response is guided by epidemiological models whose primary use is to project the transmission routes of an outbreak and to provide means of comparing the effectiveness of different containment strategies. The focus of every control policy is to minimize transmission, i.e. to reduce the basic reproduction ratio R_0 , which is defined by the average number of secondary infections being caused by a primary case in a completely susceptible population. This can be achieved by either reducing the behavioral infectiousness through social distancing measures, by reducing the biological infectiousness through treatment (e.g. with drugs or masks), or by reducing the susceptibility of the uninfected individuals through vaccination. Our research focusses on control strategies for emerging diseases, such as SARS, MERS or Ebola, where vaccines are not available in the early stage of an outbreak. This leaves the reduction of the behavioral and biological infectiousness as the only feasible policies. To differentiate between behavioral and biological control measures, we analyze a model, which disentangles the respective contributions in the disease transmission process, see Fig. 6.15.

Figure 6.15: Sketch of the transmission model. Behavioral infectiousness is modeled as a renewal sequence of successive contacts, here plotted for three different examples in green, violet and orange. Biological infectiousness is modeled as a Bernoulli-process with a time-dependent success rate f_I (infectious events are marked in red). The number of secondary infections $N(t)$ after the time t elapsed since the own infection is a random quantity. The distribution of secondary cases $P(n)$ can be broad, reflecting a significant individual variation of disease transmission. Understanding this heterogeneity is crucial for the design of containment strategies.



An epidemic outbreak is modeled as a branching process with new branches emerging at the instance of an infection. The extinction

probability of this branching process depends not only on the mean offspring number $\langle n \rangle = R_0$ of an individual but is also crucially influenced by the shape of the offspring distribution $P(n)$. The broader the offspring distribution, the higher the probability that the introduction of an infected individual into a susceptible population does not lead to a fatal outbreak, compared on the basis of the same R_0 . We therefore investigate the effects of the respective control measures on the heterogeneity of $P(n)$, as measured by its coefficient of variation. We find that a reduction of the behavioral infectiousness results in a higher heterogeneity compared to the same decrease of the biological infectiousness [1]. Thus we can conclude that behavioral control is advantageous for outbreak prevention. This finding is confirmed by extensive numerical simulations of branching processes for a variety of contact patterns.

Another important source of variation in epidemic models is spatial heterogeneity, which is known to have a significant impact on vaccination strategies and the persistence of diseases. Especially for endemic livestock diseases, understanding the effect of spatial heterogeneity is essential for the design of containment strategies, such as transport restrictions. We study the effect of spatial heterogeneity in a simple metapopulation model, see Fig. 6.16. For the disease dynamics we use the standard *SIR* model, where susceptible individuals (*S*) can become infectious (*I*) and then recover (*R*). Surprisingly, we find that the prevalence of an infectious livestock disease in a community of animals can paradoxically decrease owing to transport connections to other communities in which the risk of infection is higher and vice versa. This result has important consequences for the design of transport restrictions. Using our model, we establish exact criteria to discriminate those connections that increase the level of infection in the community from those that decrease it. Imposing transportation restrictions to communities with higher infection rates commonly has the opposite of the intended effect and increases the fraction of infectious animals. This paradoxical effect can intuitively be understood by recalling that a disease flourishes when many potential hosts are susceptible. A higher endemic level of infectious hosts can only be sustained when there is an additional source of susceptible hosts. Coupling to a community with a lower risk of infection results in exactly such a steady import of susceptible hosts, and it is this additional source of susceptible hosts that increases the fraction of infectious animals. Our results stand in contrast to the widespread belief that transportation restrictions are unconditionally suitable to reduce the level of infection as they stop the import of the pathogen.

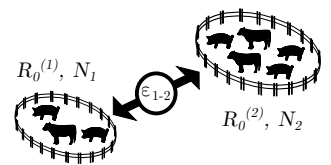


Figure 6.16: Two-community model. Two spatially separated populations are coupled by a symmetric transportation rate ϵ_{1-2} and have different values of R_0 as well as different population sizes. In any other respect the populations are identical.

- [1] S. Eule and J.J. Metzger, (*in preparation*) (2015).
- [2] D. Lamouroux, J. Nagler, T. Geisel, and S. Eule, *Proc. Roy. Soc. B*, **282**, 20142085 (2015).

6.8 MORPHOGENESIS CONTROL BY MECHANICAL STRESSES

K. Alim, J. Khadka

Adherence between cells couples the growth dynamics of individual cells into collective behaviour of the entire cell arrangement. The simple interaction of adherence counteracts fluctuations of individual cells and enforces coordinated behaviour that gives rise to the spatio-temporal patterns of cells within a tissue. Here, an exciting challenge is how cells coordinate the reproducible morphing of tissue into a desired shape.

The challenge in addressing the dynamics of cells within a tissue is their enormous number of mechanical degrees of freedom arising from each cell's cytoskeleton. By reducing cells to their bulk mechanical properties and their position within the cell arrangement in a so-called vertex model we overcome this obstacle, see Fig. 6.17. The vertex model allows one to address how mechanical stresses arising within a tissue control the spatio-temporal dynamics of tissue growth. Employing such a framework we aim to answer how mechanical stresses build up and regulate cell mechanics, cell divisions and biological messengers for reproducible, three-dimensional morphogenesis of tissues.

In plants, the cell walls shared by adjacent cells form a rigid connection between cells. A cell grows as its adjacent cell walls are yielding in response to the osmotic pressure build up within the cell. This entirely mechanical process makes plants an ideal model system to study the role of mechanical forces during the morphogenesis of a tissue.

We are developing tissue model simulations that are compared to existing imaging data of plant growth to identify step-by-step principles of the robust morphogenesis of three-dimensional tissue shapes. In previous work we built a tissue model that successfully captures the dynamics of two-dimensional, isotropically growing plant tissue [1, 2]. This model is advanced to describe anisotropically growing tissues in three dimensions including the dynamics of cell divisions. Subsequently we aim to address and answer the following questions. How do mechanical stresses control the reproducibility of an anisotropically growing tissue shape? Do mechanical stresses exert an additional level of control over stochasticity by determining the cell division orientation? How does cross talk between mechanical stresses and messenger molecule dynamics give rise to three-dimensional morphing of tissue?

The theoretical framework devised to answer these questions will give us insight into how mechanical stresses, stochasticity, and biological signals control the collective behaviour of cells. Identified principles can be readily tested in other cell systems by altering the mechanical properties of cells in the simulation.

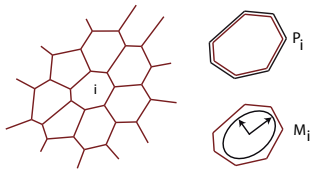


Figure 6.17: In a vertex model a tissue is abstracted to a two-dimensional tiling of space by cells. At each time-point the tissue is in mechanical equilibrium, balancing the forces arising from differential growth. Mechanical forces within plants are captured by a mechanical energy encompassing the perimeter P_i of each individual cell i and an anisotropic form tensor M_i .

- [1] M. Uyttewaal*, A. Burian*, K. Alim*, B. Landrein, D. Borowska-Wysket, A. Dedieu, M. Ludynia, J. Traas, A. Boudaoud, D. Kwiatkowska, and O. Hamant, *Cell* **149**, 439-451 (2012), * authors contributed equally
- [2] K. Alim, O. Hamant, and A. Boudaoud, *Front. Plant Sci.* **3**, 00174 (2012)

6.9 STOCHASTIC TERMINAL DYNAMICS IN EPITHELIAL CELL INTERCALATION

S. Eule, N. Lenner, F. Wolf

L. Reichl, J. Metzger (Rockefeller), J. Grosshans (UMG)

Epithelial cell rearrangement is important for many processes in morphogenesis [1]. During germband extension in early gastrulation of *Drosophila* embryos, exchange of neighbors is achieved by junction remodeling that follows a topological T1 process [2, 3]. Its first step is the constriction of dorsal-ventral junctions and fusion of two $3\times$ vertices into a $4\times$ vertex, a process believed to be junction autonomous. We established a high throughput imaging pipeline, by which we recorded, segmented and analysed more than 1000 neighbor exchanges in *Drosophila* embryos. Characterizing the dynamics of junction lengths we find that the constriction of cell contacts follows intriguingly simple quantitative laws. (1) The mean contact length $\langle L \rangle$ follows $\langle L \rangle(t) \sim (T - t)^\alpha$, where T is the finite collapse time. (2) The time dependent variance of contact lengths is proportional to the square of the mean. (3) The time dependent probability density of the contact lengths remains close to Gaussian during the entire process. These observations are sufficient to derive a stochastic differential equation for contact length analytically tractable in small noise approximation. To find the universal laws of the constriction dynamics the data is analyzed by aligning the stochastic trajectories of the junction length to their collapse point. To account for this alignment, we model the collapse by a stochastic process with a well-defined final condition that evolves backwards in time. For this we use the theory of time-reversed stochastic differential equations. The model provides an effective description of the non-equilibrium statistical mechanics of contact collapse. All model parameters are fixed by measurements of time dependent mean and variance of contact lengths. The model predicts the contact length covariance function that we obtain in closed form. The contact length covariance function closely matches experimental observations suggesting that the model well captures the dynamics of contact collapse on a time scale of minutes.

- [1] C.-P. Heisenberg, Y. Bellaiche, *Cell* 153, 948 (2013).
- [2] K. D. Irvine, E. Wieschaus, *Development* 120, 827 (1994).
- [3] Y. Zhang, D. Kong, L. Reichl, N. Vogt, F. Wolf, J. Grosshans, *Developmental Biology* 390, 208 (2014).

6.10 TOWARDS A THEORY OF EFFICIENT STIMULUS ENCODING AT AUDITORY SYNAPSES

M. Gabrielaitis, F. Wolf

N. Chapochnikov, A. Neef, T. Moser (UMG)

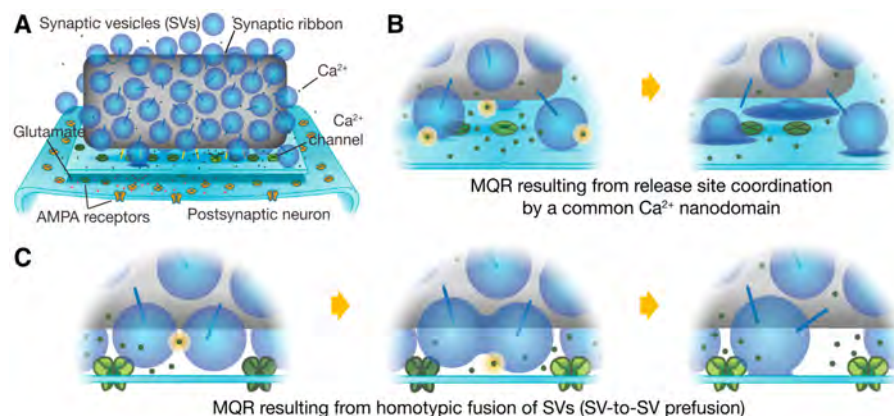


Figure 6.18: Competing hypotheses for the molecular organization of vesicle release at inner hair cell ribbon synapses. (A) A schematic of an inner hair cell ribbon synapse. (B) Scenario of Ca²⁺-synchronized multiquantal vesicle release. (C) Scenario of the homotypic-fusion based multiquantal vesicle release. Modified from [1].

All information from the auditory world is conveyed to the brain by axonal fibers of the auditory nerve. In mammals, each of these fibers is exclusively driven by single presynaptic active zones of inner hair cell ribbon synapses (Fig. A). The molecular mechanisms of functioning of these synapses are still poorly understood. Combining detailed biophysical models with experimental approaches, including electrophysiology, electron and super-resolution light microscopy, we showed that exocytosis of single synaptic vesicles at these synapses is sufficient to trigger action potentials in auditory nerve fibers [1]. This study also ruled out different hypothetical vesicle release types (Fig. B,C) that had been proposed over the past decade. In further studies, we found that the coupling of the presynaptic Ca²⁺ channels and sensors of exocytosis is very tight due to the molecular organization of the active zone [2, 3] and high concentrations of Ca²⁺ buffering proteins [3]. Based on this advanced characterization, we developed analytically tractable but molecularly accurate models of auditory sound encoding and used them to predict optimized molecular designs of the inner hair cell ribbon synapses from efficient coding principles.

- [1] N.M. Chapochnikov, H. Takago, C.-H. Huang, T. Pangrsic, D. Khimich, J. Neef, E. Auge, F. Goettfert, S.W. Hell, C. Wichmann, F. Wolf, T. Moser. *Neuron* 83, 1389 (2014).
- [2] A.B. Wong, M.A. Rutherford, M. Gabrielaitis, T. Pangrsic, F. Goettfert, T. Frank, S. Michanski, S. Hell, F. Wolf, C. Wichmann, T. Moser. *The EMBO Journal* 33, 247 (2014).
- [3] T. Pangrsic, M. Gabrielaitis, S. Michanski, B. Schwaller, F. Wolf, N. Strenzke, T. Moser. *Proceedings of the National Academy of Sciences* 112, E1028 (2015).

6.11 FEATURE-BASED AND MACHINE-LEARNING ANALYSES OF NEURAL DATA

M. Helmer, D. Hofmann, D. Lyzwa, D. Battaglia, T. Geisel, F. Wolf
D. Farina, S. Treue, F. Wörgötter, H. Gutch (Munich), J. M. Herrmann
(Edinburgh)

We have applied machine learning, unsupervised clustering and other algorithmic techniques to the analysis of different neural data types.

In a first sub-project, we have focused on the control of myo-electric prostheses. Such prostheses use neural signals recorded near the innervation sites of muscles in order to control a robotic device that replaces a missing function. Obtaining a reliable prosthetic function is however difficult because the delay between the arrival of the signal and the motor effect is to be minimal while the noisy and non-stationary signal may require a substantial sampling time [1]. To overcome this difficulty we have focused on the stochastic modelling of the signals from an electrode, representing them as a mixture of two stochastic components and providing guidance to the selection of informative features for classification or regression. The combined effect of a preprocessing filter and a learning classifier leads to good classification rates well at delay times which near the perceptual thresholds, based on a scheme of realistic complexity for practical applications.

In a second sub-project, we have focused on the decoding of natural sounds from auditory system recordings, a question important for the design of neuroprosthetic hearing aids. Based on a set of natural vocalisations obtained from guinea pigs and central inferior colliculus (IC) responses in animals of the same species, we applied a neural discrimination scheme which aims at a classification of stimuli based on the recorded activity. We assume that if classification is possible based on certain data features, then these features will be relevant for stimulus encoding. The results suggest a broadly distributed code for behaviourally relevant vocalisations in the mammalian IC with little direct interaction among parallel units.

Other sub-projects have introduced important methodological advancements. We have for instance applied fuzzy clustering methods to the unsupervised classification of neuronal data types [2]. Cortical neurons and, particularly, inhibitory interneurons display a large diversity of morphological, synaptic, electrophysiological, and molecular properties. Various classification schemes that rely on the concomitant observation of these multimodal features have been proposed. However, the attribution of specific neurons to a single defined class is often difficult, because individual properties vary in a highly graded fashion, suggestive of continua of features between types. Going beyond the description of representative traits of distinct classes, we introduced a novel paradigm for neuronal type classification, assuming explicitly the existence of a structured continuum of diversity. Our approach, grounded on the theory of fuzzy sets, identifies a small optimal number of model archetypes. At the same time, it quantifies the degree

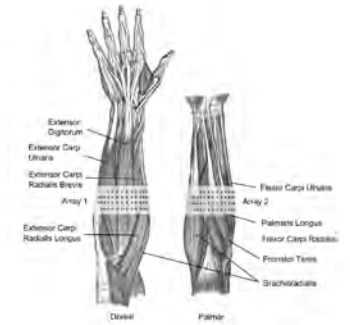


Figure 6.19: Myo-electric signals from a high density electrode array on the upper forearm are decoded for control of a prosthesis.

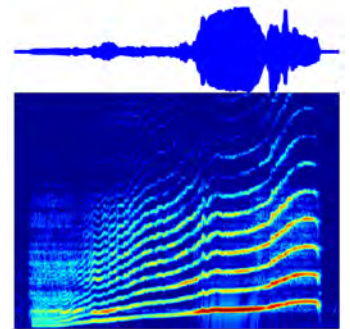


Figure 6.20: Spectrogram of a guinea pig vocalisation. Vocalizations are classified based on neural recordings from the central inferior colliculus.

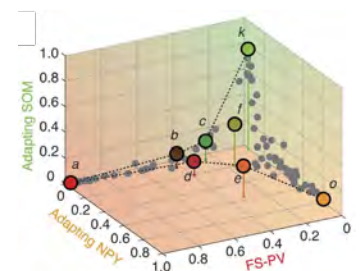


Figure 6.21: Fuzzy clustering is used not only to identify neuronal types in an unsupervised manner but also to characterize atypical transitional phenotypes, in a space spanned by fuzzy memberships, used as a non-linear dimensional reduction device

of similarity between these archetypes and each considered neuron. This allows highlighting archetypal cells, which bear a clear similarity to a single model archetype, and edge cells, which manifest a convergence of traits from multiple archetypes. Remarkably, we could adopt virtually the same approach to the analysis of a very different dataset, namely vocalizations from different species of primates [3], thus proving the versatility of our methodological framework.

We have also organized a crowdsourcing challenge, aiming at improving on our own Transfer Entropy-based methods for the reconstruction of neuronal connectivity from calcium imaging [4]. Our challenge has attracted 150 participants, many of which dramatically out-performed our benchmark, using e.g. deep learning [5].

In a last research line, we have introduced a novel framework for the characterization of heterogeneous neuronal tuning curves and of their modulation patterns. Selective responses of neurons to stimulus features are commonly determined by fitting a model e.g. a Gaussian, to the measured responses. As neuronal responses are irregular, however, and experimental measurements noisy, it is often difficult to reliably determine the appropriate model from the data. However, we could prove, by analyzing representative recordings from monkey area MT during multiple attentional tasks, that specific model choices affect both quantitatively and qualitatively statistical comparisons across different experimental conditions [6]. As a robust alternative to an often arbitrary model selection, we introduced a model-free approach, in which features of interest are extracted directly from the measured response data without the need of fitting any model. In our attentional datasets, we demonstrated that data-driven methods provide descriptions of tuning curve features such as preferred stimulus direction or attentional gain modulations which are in agreement with fit-based approaches when a good fit exists. Furthermore, these methods extended naturally to the frequent cases in which the cells have a highly atypical response. Our model-free approaches could identify attentional modulation patterns, such as general alterations of the irregular shape of tuning curves—change of skewness, peak merging or asymmetric expansions, etc.—, which cannot be captured by fitting stereotyped conventional models. Thus, our data-driven methods can reliably extract relevant tuning information from neuronal recordings, including cells whose seemingly haphazard response curves defy conventional fitting approaches.

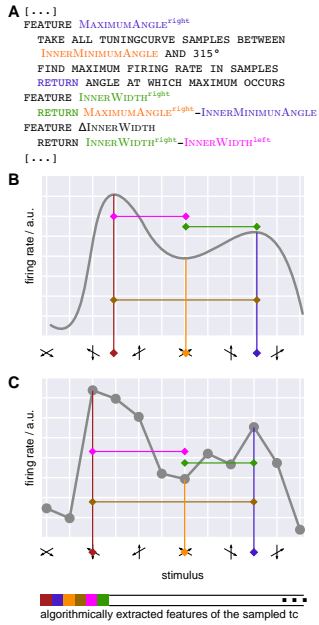


Figure 6.22: Tuning curve shapes are extracted based on features operationally defined via specific algorithmic procedures (A) rather than in terms of the parameters of some fitted model. Such features can be extracted from fitted profiles (B), in order to compare different models defined in terms of incompatible parameter sets, but can also directly from the measured data themselves (C), which avoids ambiguous model selection.

[1] N. Jiang, S. Dosen, K. Müller, D. Farina. *IEEE Signal Process. Mag.* **29**(5):152 (2012)
[2] D. Battaglia, A. Karagiannis, T. Gallopin, H. W. Gutch, and B. Cauli, *Front. Neural Circuits* **7**, 13 (2013).
[3] P. Wadewitz, K. Hammerschmidt, D. Battaglia, A. Witt, F. Wolf, and J. Fischer, *PLoS ONE* **10**, e0125785 (2015).
[4] J. G. Orlandi, O. Stetter, J. Soriano, T. Geisel, and D. Battaglia, *PLoS ONE* **9**, e98842 (2014).
[5] J. G. Orlandi, B. Ray, D. Battaglia, I. Guyon, V. Lemaire, et al., *The Journal of Machine Learning Research: W&CP* **46**, 1 (2015).
[6] M. Helmer, V. Kozyrev, V. Stephan, S. Treue, T. Geisel, and D. Battaglia, *bioRxiv* (2015).

6.12 INFERRING DYNAMICAL STATES UNDER SPATIAL SUBSAMPLING

V. Priesemann, J. Wilting

When studying complex systems in nature or society, we can rarely sample the activity or state of all components. This spatial subsampling poses severe constraints on inferences about a system's dynamical properties [1, 2]. A correct inference, however, is of particular importance when estimating the system's stability, e.g. its distance (ϵ) to a critical transition, because if it is close or even beyond that transition, its behavior changes dramatically. Such a transition will for example turn a disease outbreak into an epidemic or brain activity into epilepsy.

We discovered that under subsampling established methods [3] strongly underestimate the risk of instability. Therefore, we derived a novel estimator, which is unbiased even under strong spatial subsampling, using multiple regressions (MR) [4]. The MR estimator was derived for processes with a first order autoregressive representation, but we validated that it also returns unbiased results when estimating the stability of more detailed models (e.g. neural networks). We applied this estimator to *in vivo* spike recordings from rat, cat and monkey, to address the long standing question of whether the brain operates in a critical state [5, 6]. Criticality in models maximizes processing capacity and would therefore be an ideal target state for neural network dynamics. Contrary to this hypothesis, we found that spiking activity was not critical, but slightly subcritical ($\epsilon > 0.01$). This points at a universal organizational principle: Brains sacrifice a part of their processing capacity to gain stability and avoid epilepsy [1, 4].

Our results may merge two current contradictory theories, namely that brain dynamics either reflects a critical, or an "asynchronous-irregular" (AI) state. We showed that subsampling strongly overestimates ϵ , thereby neural activity appears AI-like, even if it is very close to critical. With not being in a critical state either, the slightly sub-critical state avoids the disadvantages of criticality for brain activity (critical slowing down, divergent susceptibility or epilepsy).

Our novel estimator provides for the first time an unbiased inference of ϵ under subsampling. Importantly, it neither requires knowledge about the system size, or the number of sampled sites. It only requires the subsampled activity. Thereby it promises novel insights not only when studying the properties of brain dynamics, but for many other dynamical systems, such as financial markets, infectious diseases, or cancer mutations.

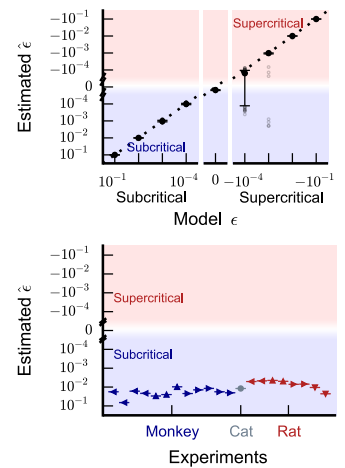


Figure 6.23: The MR estimator returned an unbiased estimate of the distance to criticality ϵ for all subsampled simulated processes (subcritical to supercritical), as expected from analytical derivation. By applying the MR estimator to spiking activity *in vivo* from rat, cat, and monkey, we showed that cortical dynamics is slightly sub-critical ($0.01 < \hat{\epsilon} < 0.06$).

- [1] V Priesemann, M Munk, M Wibral, BMC Neurosci. **10**(1):40 (2009).
- [2] V Priesemann et al., Front. Syst. Neurosci. **8**(108) (2014).
- [3] CC Heyde, E Seneta, J. Appl. Probab. **9**, 235 (1972).
- [4] J Wilting & V Priesemann, *in prep.*
- [5] S Dunkelmann, G Radons, in ICANN '94 (Proceedings of the International Conference on Artificial Neural Networks), M. Marinaro, P. G. Morasso, Eds. (Springer-Verlag, 1994), p. 867.
- [6] J M Beggs & D Plenz, J. Neurosci. **23**, 11167–11177 (2003).

6.13 FIELD BIOLOGY AS A DATA ANALYSIS CHALLENGE

S. Hallerberg, F. Noriega, F. Meigel, M. Dahlkemper, M. Timme
 H. Vester (Ocean Sounds, Norway), K. Hammerschmidt (German Primate Center), F. Wörgötter (University of Göttingen)

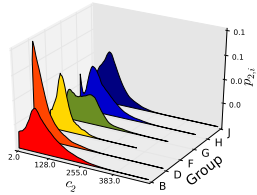


Figure 6.24: Distributions of sound features allow to infer group-specificity of animal vocalizations, e.g. here based on vocalizations of six different groups of long-finned pilot whales

Data analysis and machine learning methods are widely applied to gain information about our own species, in terms of individual behavior and social dynamics. Imagine, however, the amount of new knowledge we can discover by applying these methods to gain insight into the life of the vast variety of species on earth.

Digitalized observations of animals, automated recording of environmental sounds [1, 2], as well as GPS tracking of animals, creates huge amounts of data waiting for further exploration. We are interested in inferring social networks of animals and in understanding how acoustic communication is used among and within groups of animals.

Having developed a new method of automated sound processing, the bags-of-calls-and-coefficients approach (BOCCA) [3] we can quantify group- and context specificity of ensembles of animal vocalizations in a statistically significant way. Additionally, we study the temporal organization of classified vocalizations using approaches from human language analysis.

To facilitate the estimation of social networks of animals, we currently develop and test an algorithm for the identification of individual killer whales based on photographs of their dorsal fins [4]. The al-

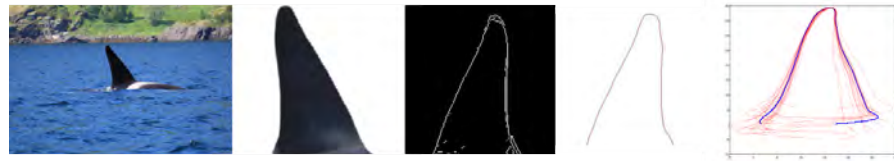


Figure 6.25: Four stages of processing pictures of killer-whales before relevant features for the classification can be extracted.

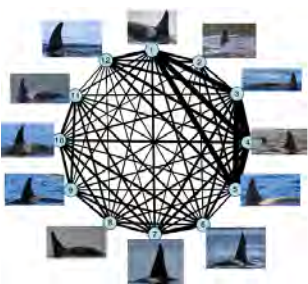


Figure 6.26: Social Network of a group of killer whales, inferred using a data-base of 11000 photographs of their dorsal fins

gorithm automatically classifies pictures of individuals with higher accuracy than the average (untrained) human observer and is capable of reproducing the accuracy of a trained human observer. Automated identification of individual animals allows to gain further insight into the social structure and social dynamics of groups of animals, see e.g. Fig. 6.26.

- [1] O. Boebel, H. Klinck and L. Kindermann, *Bioacoustics*, **17**, 19-21, (2008).
- [2] National Ecological Observatory Network, Boulder, CO, USA, <http://data.neoninc.org>.
- [3] H. Vester, K. Hammerschmidt, M. Timme and S. Hallerberg submitted to *Phys. Rev. E* (2015).
- [4] B. Ghani, F. Wörgötter, H. Vester, M. Timme and S. Hallerberg, in prep.

PATTERNS AND INSTABILITIES

7

Many spatially extended non-linear systems show spontaneous formation of spatio-temporal patterns. Underlying these self-organizing phenomena is the complex interaction of systems or subsystems that are kept out of energetic equilibrium. Similar patterns occur in systems that are different in detail, but share the underlying fundamental mathematical description. In this section we present experimental and theoretical research results on the formation of patterns in different systems of various complexity. Examples include simple inanimate systems, such as crack formation in drying and solidifying matter or electroconvection, but also more complex living systems such as biochemical oscillations in single cells, cell colonies, and even organs like the heart or the visual cortex of the brain. In the later cases the pattern forming processes are essential for the vital functions of the organism. The strong interaction between novel experimental approaches, analytical, and numerical tools is not only aimed at a better understanding of the pattern forming mechanisms, but also at controlling pattern formation, like for examples in the defibrillation of a human heart.

CONTENTS

- 7.1 Curvotaxis and pattern formation in the actin cortex of motile cells 113
- 7.2 Mechanics and dynamics of biological adhesion 114
- 7.3 The combinatorics underlying simplex equations, and “polygon equations” 115
- 7.4 Spatiotemporal complexity of electroconvection patterns in nematics 116
- 7.5 Evolving crack networks: from craquelure to crocodiles 117
- 7.6 Patterns and parameter inference of populations of *Dictyostelium discoideum* 118
- 7.7 Pseudo obstacles: a novel concept for rotor initiation in excitable media 119
- 7.8 Flow-driven waves in *Dictyostelium discoideum* 120
- 7.9 Electrotaxis: The migration of amoeba cells in an electric field 121
- 7.10 Gas-particle interaction: instabilities in protoplanetary disks 122
- 7.11 Genetic assimilation of visual cortical architecture 123
- 7.12 A synthetic neurobiology approach to orientation selectivity 124
- 7.13 Precision measurement and dynamical switching of visual cortical architecture 125

- 7.14 Music: A Dynamical Systems Perspective 126
 - 7.15 Control of Spatial-temporal Complexity of the Heart 127
 - 7.16 Modelling and Data Analysis in Biomedical Physics 131
 - 7.17 Oscillatory actin instabilities and motility statistics of amoeboid cells 134
-

7.1 CURVOTAXIS AND PATTERN FORMATION IN THE ACTIN CORTEX OF MOTILE CELLS

M. Tarantola, C. Blum, E. Bodenschatz

M. Rivetti, O. Bäumchen, S. Herminghaus, J. Thiart, M. Priebe, T. Salditt, J. Enderlein (University of Göttingen), O. Steinbock (Florida State University) A. Kortholt, P. van Haastert (University of Groningen)

We investigate cytoskeletal actin dynamics in the cortex of migrating eukaryotic cells with a particular focus on pattern formation and contact guidance. Experiments and modeling are conducted for *Dictyostelium discoideum* (*D.d.*), which is an eukaryotic model organism for chemotaxis. Our approach includes microfluidic devices, advanced high-speed high-resolution optical microscopy, x-ray imaging with nano-diffraction techniques, and single particle tracking.

Pseudopod formation is fundamental to amoeboid cell migration in which the central chemotactic signaling protein, RasG, forms activated membrane patches to guide actin polymerization [1]. Using a custom high-speed scanning confocal microscope, we find that RasG precedes actin activity in splitting pseudopodia of chemotactic competent cells in cAMP gradients. However, heterogeneity of these temporal patterns is found for non-competent cells without a gradient. Qualitatively our results agree with ongoing modelling of excitability of motile cells.

Which signal relays and networks are involved in pseudopod nucleation? To answer this question, we combine ultra-fast TIRFM with label-density controlled *D.d.* cell lines to track RasG activity in the plasma membrane on the single molecule level. State transition analysis reveals the existence of three distinct diffusing species, one fast, presumably cytosolic, and two membrane bound states.

In addition to local dynamics of actin-network activation at the membrane the acto-myosin cortex is essential for cell motility. We observe persistent elongated anisotropic diffraction signals at the cell cortex using coherent x-ray imaging and nano-diffraction. These “nematic” structures correspond to cortex areas with oriented acto-myosin fiber bundles (Fig. 7.1)[2].

Amoeboid cell migration is linked to the complex environment of motile cells: We detect preferential pseudopod extension and migration along paths of the highest curvature by imposing external curvature to *D.d.* via glass fibers. Furthermore, we are able to quantify cellular migratory behavior on positively and negatively curved areas using wrinkled polystyrene films as substrates. We thereby detect a curvotactic contact guidance dependence, which increases for geometries of higher curvature (Fig. 7.2)[3].

- [1] A. Kortholt, I. Keizer-Gunnink, R. Kataria and P.J.M. Van Haastert, *Journal of Cell Science* **19**, 4502, (2013).
- [2] M. Priebe, M. Bernhardt, C. Blum, M. Tarantola, E. Bodenschatz and T. Salditt, *Biophysical Journal* **11**, 2662, (2014).
- [3] C. Blum, M. Tarantola, M. Rivetti, O. Bäumchen, S. Herminghaus, O. Steinbock and E. Bodenschatz, Preprint

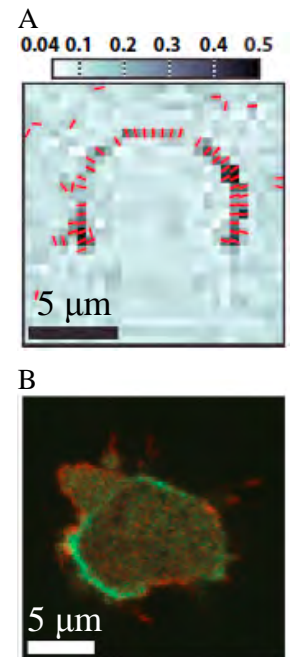


Figure 7.1: A: The red lines correspond to high diffractive anisotropy parameter of frozen hydrated *D.d.* cell. Strong anisotropy found at the cell membrane. B: Micrograph of a *D.d.* cell tagged with Myosin-II-GFP and LimE-mRFP. [2]

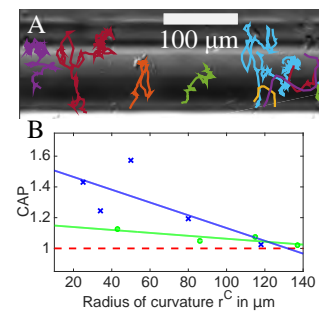


Figure 7.2: A: Overlay of DIC micrograph of *D.d.* cells migrating on an optical fiber and corresponding cell trajectories. B: Curvotactic Anisotropy Parameter $CAP = \frac{|v_{curved}|}{|v_{plane}|}$ dependence on the fiber radius (blue) or maximal radius of curvature of wrinkle (green), respectively [3].



7.2 MECHANICS AND DYNAMICS OF BIOLOGICAL ADHESION

L. Turco, N. Höppner, M. Tarantola

J. Rother, H. Leonhardt, A. Bae, T. Lampert, P. Devreotes (Johns Hopkins University), C. Beta (University of Potsdam), B. Geil, A. Janshoff (University of Göttingen), S. Luther, E. Bodenschatz

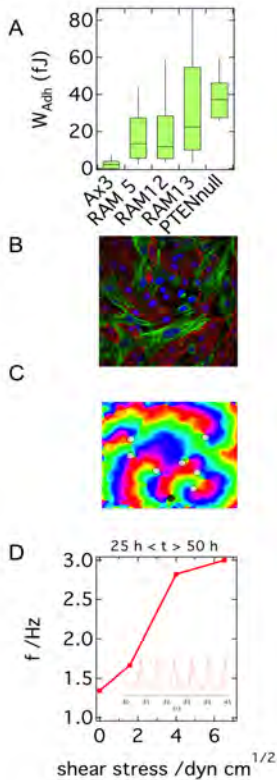


Figure 7.4: Three PTEN-like RAM mutants and PTEN null *D.d.* cells compared to the Ax3 wildtype in terms of adhesion work (A). Co-culture of cardiomyocytes (green) and fibroblasts (red) of equal cell density, the length of one side corresponding to $200 \mu\text{m}$ (B), and a phase map of the corresponding mixture (C). Beating frequency of co-cultures under flow stimulation (D).



Complex dynamics and pattern formation underlie eukaryotic cell adhesion, which guides motility, polarity, and tissue development on the single cell as well as on the cell population scale. To understand these biomechanical processes we focus on the model organism *Dicystelium discoideum* (*D.d.*) and cardiomyocyte-fibroblast co-cultures. With microfluidics, advanced light microscopy, electrical impedance spectroscopy, AFM and theoretical modeling, we investigate the dynamics and mechanics underlying biological adhesion.

While the stress fibers and myosin motors of the cytoskeleton generate protrusive and contractile forces, the interaction of the ventral cell surface with the subjacent support is necessary to transmit forces. *D.d.* cells neither show stress fibers nor express integrins, rendering the amoeba an excellent model system to study the evolutionary biophysics of the adhesome. Using single cell force spectroscopy (SCFS) we find a decrease in substratum adhesion upon development [1] and relate this behaviour to minimal synthetic model systems. When comparing SCFS, single-cell impedance spectroscopy and contact area imaging with a detachment assay, we find a good quantitative agreement for cells with adhesion depletion [2]. We also use TIRF microscopy in conjunction with SCFS revealing a strong correlation between actin foci density and tether-like rupture events.

This set of techniques allows us to determine regulators of adhesion and motility (RAM, Fig. 1A): Within this experiment series, we identify and compare PTEN null and PTEN null-like phenotypes, which show an unexpected strong adhesion increase. We also perform a theoretical study focused on excitable waves of PTEN and PIP3 to describe pattern formation of cell polarity related to substrate attachment [3].

In addition to cell-substrate adhesion, we also monitor cell-cell adhesion in small heterocellular groups of cardiomyocytes and fibroblast (Fig. 1 B and C). We find a nonlinear beating frequency decrease to accompany an increase in connectivity [4]. We furthermore use flow stimulation to increase cell-cell contact density and contractility in this model system for fibrotic conditions [5] (Fig. 1 D).

- [1] M. Tarantola, A. Bae, D. Fuller, E. Bodenschatz, W. Rappel, W.F. Loomis, PLOS ONE 9, e106574, (2014)
- [2] H. Leonhardt, M. Gerhardt, N. Hoepfner, K. Krueger, M. Tarantola, C. Beta, *Phys Rev E* (2015) under review
- [3] F. Knoch, M. Tarantola, E. Bodenschatz, W.-J. Rappel, *Phys Biol* 11 046002 (2014)
- [4] J. Rother, C. Richter, L. Turco, F. Knoch, I. Mey, S. Luther, A. Janshoff, E. Bodenschatz, M. Tarantola, *Open Biology* 5 150038 (2015)
- [5] L. Turco, M. Tarantola, paper in preparation (2016)

7.3 THE COMBINATORICS UNDERLYING SIMPLEX EQUATIONS, AND “POLYGON EQUATIONS”

F. Müller-Hoissen
A. Dimakis (Greece)

The *Bruhat order* $B(3, 1)$ is a partial order on the set of permutations of the natural numbers 1, 2, 3. It consists of the two maximal chains

$$(1, 2, 3) \xrightarrow{12} (2, 1, 3) \xrightarrow{13} (2, 3, 1) \xrightarrow{23} (3, 2, 1)$$

$$(1, 2, 3) \xrightarrow{23} (1, 3, 2) \xrightarrow{13} (3, 1, 2) \xrightarrow{12} (3, 2, 1)$$

where ij stands for $\{i, j\}$ and here indicates an inversion $(i, j) \mapsto (j, i)$. A set-theoretical realization

$i \mapsto \mathcal{U}_i, (i, j, k) \mapsto \mathcal{U}_i \times \mathcal{U}_j \times \mathcal{U}_k, ij \mapsto \mathcal{R}_{ij} : \mathcal{U}_i \times \mathcal{U}_j \rightarrow \mathcal{U}_j \times \mathcal{U}_i$ (or a realization using vector spaces and tensor products) leads to the (quantum) *Yang-Baxter equation* $\mathcal{R}_{23,12} \mathcal{R}_{13,23} \mathcal{R}_{12,12} = \mathcal{R}_{12,23} \mathcal{R}_{13,12} \mathcal{R}_{23,23}$. The boldface *position indices* are read off from the above chains. They specify on which pair of sets in the threefold direct product the map \mathcal{R}_{ij} acts. In terms of $\hat{\mathcal{R}}_{ij} := \mathcal{R}_{ij} \mathcal{P}$, where \mathcal{P} is the transposition, the Yang-Baxter equation attains the form $\hat{\mathcal{R}}_{23,12} \hat{\mathcal{R}}_{13,13} \hat{\mathcal{R}}_{12,23} = \hat{\mathcal{R}}_{12,23} \hat{\mathcal{R}}_{13,13} \hat{\mathcal{R}}_{23,12}$. If all maps are the same, the latter reduces to $\hat{\mathcal{R}}_{12} \hat{\mathcal{R}}_{13} \hat{\mathcal{R}}_{23} = \hat{\mathcal{R}}_{23} \hat{\mathcal{R}}_{13} \hat{\mathcal{R}}_{12}$. The Yang-Baxter equation is crucial for the understanding of two-dimensional exactly solvable models of statistical mechanics, or integrable (quantum) field theories. It belongs to the infinite family of *simplex equations*, which originated from the search for higher-dimensional solvable models. The underlying combinatorics of simplex equations is governed by *higher Bruhat orders* $B(N, n)$ (Manin and Schechtman 1986, see [1] for a precise definition and references). The definition of $B(N, n)$ is much more involved than in the special case of $B(3, 1)$. For any integer $N > 1$, $B(N + 1, N - 1)$ consists of two maximal chains, so that it determines an equation in the same way as in the above example, where $N = 2$. This is the *N-simplex equation*.

A central result of our recent work [1, 2] is a decomposition of any higher Bruhat order $B(N, n)$ into a corresponding Tamari order $T(N, n)$, its dual, and a “mixed order”. Furthermore, the Tamari order $T(N, N - 2)$ consists of two maximal chains and thus defines an equation as a realization of it, which we call *N-gon equation*, now with maps denoted by $\mathcal{T}_{i_1 \dots i_{N-1}}$ [1]. For $N = 5$, this is the ubiquitous *pentagon equation* (some keywords are “multiplicative unitary”, “Drinfeld associator”, “quantum dilogarithm”, see [1] for references).

Neighboring polygon equations are related by the same kind of “integrability” that connects neighboring simplex equations, and this is what makes them special and promising. The pentagon and hexagon equations appeared in realizations of Pachner moves of triangulations of a 3-, respectively 4-manifold (Korepanov, Kashaev, see references in [1]). Apart from this, polygon equations are new terrain.

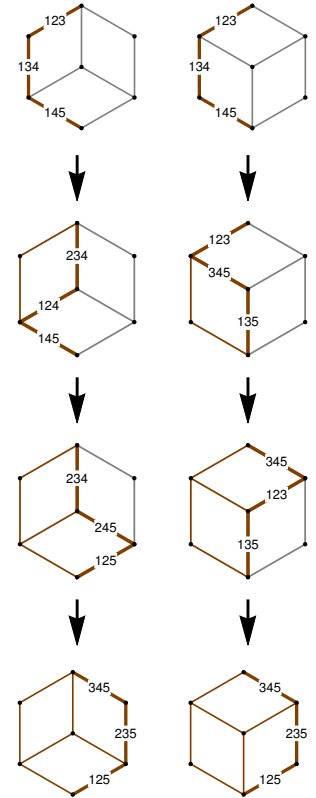


Figure 7.6: The two vertical chains correspond to the two sides of the pentagon equation, visualized on two complementary sides of a cube, formed by $T(5, 2)$. With the first step in the left chain we associate an application of $\mathcal{T}_{1234,12}$. The second step in the right chain is of a different nature. The transposition map \mathcal{P}_{12} is associated with it. In a similar way, the hexagon equation is visualized on the *associahedron*, a polyhedron with a 1-skeleton built from pentagons and squares. All simplex and polygon equations have a corresponding visualization on a polyhedron.

- [1] A. Dimakis and F. Müller-Hoissen, SIGMA 11 042 (2015).
- [2] A. Dimakis and F. Müller-Hoissen, J.Gen.Lie Theory Appl. 9, e103 (2015).

7.4 SPATIOTEMPORAL COMPLEXITY OF ELECTROCONVECTION PATTERNS IN NEMATICS

A. Krekhov

W. Pesch (Bayreuth), Á. Buka (Budapest), N. Éber (Budapest)
E. S. Batyrshin (Ufa), V. A. Delev (Ufa)

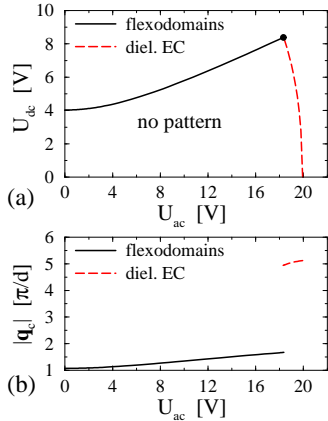


Figure 7.7: Phase diagram for flexodomains and dielectric EC rolls in nematic Phase 5 in the $U_{dc} - U_{ac}$ plane under combined dc and ac voltage with $\omega\tau_q = 6$ in the dielectric regime: (a) boundary curve for the pattern-free region; (b) the critical wave number $|q_c|$ along the boundary curve. The transition between flexodomains and dielectric EC rolls is marked by the filled circle in (a).

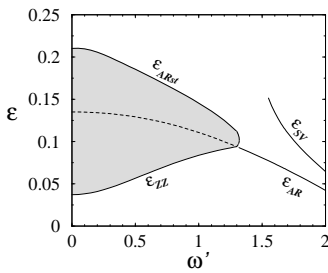


Figure 7.8: Stability diagram for normal EC rolls in nematic MBBA in the ac frequency (ω') – control parameter (ϵ) plane in the framework of the coupled amplitude equations. $\omega' = \omega\tau_q$, $\epsilon = (U/U_c)^2 - 1$, ϵ_{ZZ} denotes the zig-zag instability, ϵ_{AR} is the transition line to abnormal rolls with its restabilization at ϵ_{ARst} , and ϵ_{SV} stands for skewed varicose instability.

Electroconvection (EC) in nematics is a prime paradigm for pattern forming instabilities in anisotropic systems (see, e.g., [1, 2]). Typically, a nematic layer is sandwiched between two electrically conducting plates parallel to the x - y plane to apply a voltage. The confining plates are also used to ensure a homogeneous director orientation $n \parallel \hat{x}$, where n describes the locally preferred orientation of the nonspherical molecules of the nematic. Above a certain critical applied voltage U_c the homogeneous basic state is destabilized against the EC instability and one observes a common convection roll pattern whose periodicity in the x - y plane is characterized by the critical wave vector q_c .

A full theoretical description of EC based on the well accepted nemato-hydrodynamic equations (NHE), which describe the intricate coupling of the electric field E , of the director n and of the flow field v , is highly demanding. In some nematic materials one finds in addition to EC also flexodomains (FD), which represent equilibrium patterns. We have shown by linear stability analysis that a transition between FD and EC patterns can exist under combined ac and dc driving and verified it in experiments [3]. Further, we found that an interplay between different pattern forming mechanisms is responsible for the spatiotemporal ordering of zig-zag EC patterns and synchronization of their oscillations in the nonlinear regime [4].

To describe complex spatiotemporal patterns and their stability above the EC onset, the NHE have been substantially simplified by reducing them to a system of partial differential (amplitude) equations in the horizontal coordinates; a general discussion of this procedure is for instance found in [5]. A complete description of EC in the weakly nonlinear regime needs three coupled amplitude equations for the roll amplitude, a vorticity potential and a quantity associated with in-plane rotations of the director field [6]. Their direct numerical simulations match surprisingly well new experiments, which serves as a convincing test of our theoretical approach.

- [1] E. Bodenschatz, W. Zimmermann, L. Kramer, *J. Phys. (France)* **49**, 1875 (1988)
- [2] *Pattern Formation in Liquid Crystals*, edited by Á. Buka and L. Kramer (Springer, New York, 1996)
- [3] A. Krekhov, W. Decker, W. Pesch, N. Éber, P. Salamon, B. Fekete, Á. Buka, *Phys. Rev. E* **89**, 052507 (2014)
- [4] E. S. Batyrshin, A. P. Krekhov, O. A. Scaldin, V. A. Delev, *JETP* **114**, 1052 (2012); *Tech. Phys. Lett.* **40**, 1095 (2014)
- [5] P. C. Hohenberg, A. P. Krekhov, *Phys. Rep.* **572**, 1 (2015)
- [6] A. Krekhov, B. Dressel, W. Pesch, V. A. Delev, E. S. Batyrshin, *Phys. Rev. E* (to be published) (arXiv:1510.04125 [cond-mat.soft])

7.5 EVOLVING CRACK NETWORKS: FROM CRAQUELURE TO CROCODILES

L. Goehring, P. Nandakishore

What do the Giant's Causeway, a broken-up mud puddle, patterned ground, and the scales on a Nile crocodile have in common? They are all examples of similarly ordered patterns of cracks [1, 2], as demonstrated in Fig. 7.9. Understanding how such patterns form can impact many fields, such as plant biology (leaf vein development may be initiated by a crack-like instability), forensics (cracks in dried blood splatter), or art conservation (craquelure in paint). We study contraction cracks in thin layers in an attempt to understand the different patterns that can emerge – such as spirals, waves, self-replicating crescents, or regular polygons – from the interactions of cracks with their environment.

Drying mud occupies a central place in this work. Why watch mud dry? This is not simply whimsy, but rather reflects the value of desiccation fracture as a simple reliable model for investigating fracture in general. Contraction may result from many distinct processes: drying, cooling, syneresis, stretching of a substrate, or differential growth of biological tissue, to give a few examples. However, once the geometry and stress state of a system is set, a crack does not need to know which of these was its driving force. Moisture is often easier to work with, especially when extreme environments would otherwise be involved.

Consider a lacquer or painted coating on an old wooden table, for example. It is cracked, and the cracks curiously follow the grain of the wood. We have explored this phenomenon in clays dried over rippled substrates, and quantified when such thin film cracks will be influenced by what lies beneath them. The substrate and the cracking film can couple to give rise to wavy, ladder-like, or isotropic crack patterns [3]. Indeed, the most ordered patterns occur when the thickness of the cracking layer and the characteristic length of the substrate relief are about the same. We are currently exploring how to adapt this physics to interpret buried craters on Mars and Mercury, and how to design or template micro-scale patterns of cracks in thin coatings.

Cracks advance to release as much strain energy as possible, while spending as little energy as they can on creating new fracture surfaces. This concept can be used to accurately model the transitions in crack patterns described above [3], but can also explain the similarity in the patterns displayed in Fig. 7.9. Here, each case involves a planar network of cracks that *nearly* repeats itself, either by carving out a columnar shape as it advances through space (like in lava), or recurring in the same plane at different times (permafrost cracks opening in different winters). If each crack, at all times, grows in a way to release as much strain energy as possible, we showed in [1] how the *network* of cracks will gradually evolve towards such well-ordered hexagonal cells.

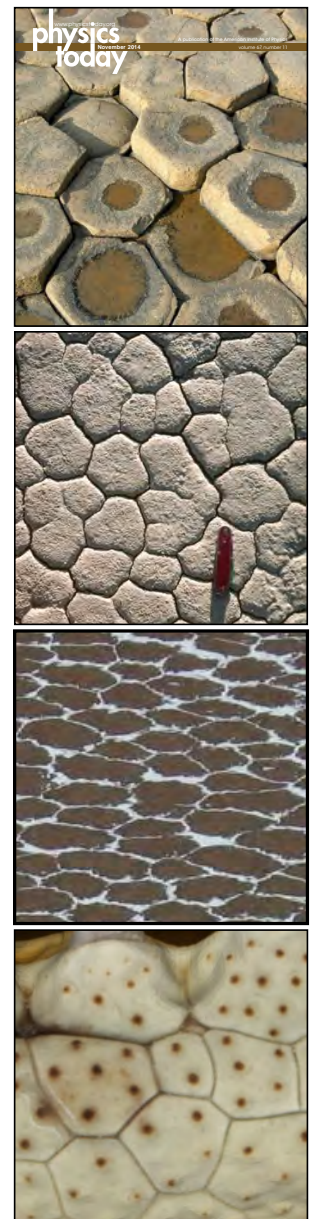


Figure 7.9: The polygonal stones of the Giant's Causeway have captivated visitors for centuries. Their spectacular cracks (top panel, from [2]) share the same physics as those of mud puddles (2nd panel, courtesy B. Hallet), polygonal cracks in permafrost (3rd panel) and crocodile skin (lower panel, courtesy M. Milinkovitch). In [1], we demonstrated how initially disordered cracks evolve into hexagons, by repeatedly wetting and drying clay films.

- [1] L. Goehring, *Phil. Trans. R. Soc. A* **371**, 20120353 (2013)
- [2] L. Goehring, S. W. Morris, *Phys. Today* **67**(11), 39 (2014)
- [3] P. Nandakishore and L. Goehring, *Soft Matter*, in press (2015)

7.6 PATTERNS AND PARAMETER INFERENCE OF POPULATIONS OF *Dictyostelium discoideum*

K. H. Prabhakara, A. Gholami, V. S. Zykov, E. Bodenschatz
T. Hohage (University of Göttingen)

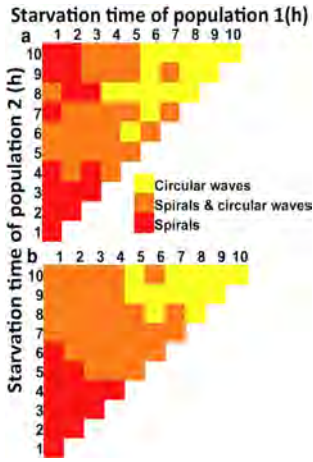


Figure 7.10: Starvation time of population 1 on the horizontal and of population 2 on the vertical axis. Summary of the patterns (a) experiments and (b) numerical simulations.

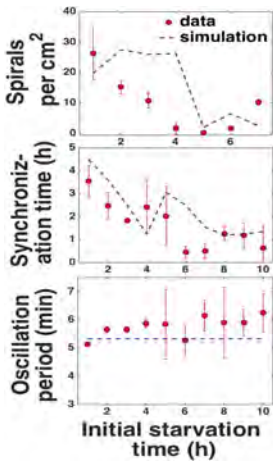


Figure 7.11: Quantitative analysis of the patterns. Red dots correspond to experimentally obtained values and the dashed blue lines are obtained from numerical simulations.

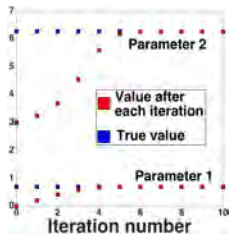


Figure 7.12: Two parameters of the Colpitts oscillator rapidly converge to the true value in an implementation of the Gauss-Newton algorithm.

One of the prime examples of pattern formation in living systems is displayed by starved populations of *Dictyostelium discoideum* (*D. d.*). This system belongs to the general category of reaction-diffusion systems, where spirals and targets are commonly observed patterns. While it is generally easy to observe patterns in these systems, inferring their dynamics is more complex. In *D. d.*, not only is it unclear whether the dynamics is oscillatory or excitable, but it also changes with time due to the varying expression levels of enzymes. To resolve this issue, we observe the effect of heterogeneity on patterns by mixing equal cell populations starved for different durations. The results of 55 experiments are summarized in Fig. 7.10a. We observe a transition in the patterns as initial starvation time increases: from numerous small spirals, to few large spirals and to targets. To interpret these patterns in terms of the dynamics of the system, we simulate the model proposed in [1]. We can qualitatively reproduce the experimental results only by permitting the parameters of the model to vary with starvation time (Fig. 7.10b). The quantitative measures match approximately (Fig. 7.11).

Although we can conclude that the dynamics changes from excitable to oscillatory around an initial starvation time of 5 h and predict the time variation of the parameters of the system, a systematic approach to recover the parameters of the model from the copious experimental data is needed. This is the domain of inverse problems, which is extensively applied to models of weather prediction [2]. The model T , acts on the space of the model variables ϕ to produce data g : $T\phi = g$. Experimental data are noisy: g^δ (δ is the noise-amplitude). To obtain a ϕ that approximately produces g^δ , the functional $\|T\phi - g^\delta\|^2$ is minimized. This is a non-trivial task because the parameter space potentially spans large dimensions, and the existence, uniqueness and the stability of the solution is uncertain. A technique to overcome these problems is to add a penalty term to the functional to be minimized. However, when the operator T is non-linear, as is common, more advanced techniques are required. In collaboration with Prof. Hohage (Dept. of Mathematics), who has developed a regularization toolbox to deal with ill-posed inverse problems [3], we attempt to incorporate our data into the models for pattern formation in *D. d.* to extract parameters. As a prelude, we implemented a three parameter model for a Colpitts oscillator. The data was a noisy time series of the first component. The regularization algorithm rapidly converged to yield the unknown parameters (Fig. 7.12). Now, we are implementing models of *D. d.* If successful, this would not only verify the assumptions of the models, but also enable us to efficiently distinguish between the models.

- [1] D. Kessler, H. Levine, Phys. Rev. E, **48**, 4801 (1993)
- [2] F. Sorrentino, E. Ott, Chaos **19**, 033108 (2009)
- [3] T. Hohage, K. Giewekemeyer, T. Salditt, Phys. Rev. E, **77**, 051604 (2008)

7.7 PSEUDO OBSTACLES: A NOVEL CONCEPT FOR ROTOR INITIATION IN EXCITABLE MEDIA

V.S. Zykov, A. Krekhov, E. Bodenschatz

An excitable medium represents a population of active elements locally connected to each other through a diffusion like coupling, which can be characterized by a coupling strength D . The resting steady state can be excited by a suprathreshold external stimulus that initiate an excitation wave, which is propagating through the medium. Such a wave includes a rapid transition from a stable resting state to an excited state (wave front) followed by a plateau and finally by a recovery transition (wave back) toward to the resting state. Under normal conditions the wave back is following the wave front and they never touch each other. However, in the presence of an obstacle, the wave front can be broken and connected to the wave back at so called phase change points. That is the necessary condition for the initiation of spiral waves, which have been observed in a broad spectrum of excitable media in chemistry, biology and medicine [1].

One long standing challenge is to identify mechanisms of rotor formation that, for example, can help to predict and/or to prevent the appearance of this life-threatening self-sustained electrical activity in cardiac muscle.

We have shown that, under quite natural conditions, permanently rotating spiral waves can be created after application of one stimulus only (see, e.g., Fig. 8.15). Note that the modern paradigm for spiral wave initiation requires at least two excitation stimuli [2-4].

The newfound simple scenario of spiral wave generation is based on a counterintuitive fact that in an inhomogeneous excitable medium a sharp spatial increase in wave propagation velocity can result in a propagation block, i.e. in a pseudo obstacle [5,6]. We present quantitative conditions for the propagation block and demonstrate many possibilities to initiate spiral waves. Our simulations based on the modified Barkley model show that this mechanism is valid for trigger-phase waves as well as for trigger-trigger waves [7].

The discovered mechanism involving the concept of pseudo obstacles gives new insights into spiral wave generation and has to be further studied especially in context of cardiac arrhythmias and epileptic seizure. For instance, it can explain the high efficiency of a recently introduced ablation procedure to prevent atrial fibrillation.

- [1] A.T. Winfree, *The Geometry of Biological Time* (Springer, 2001)
- [2] V.S. Zykov, *Simulation of Wave Processes in Excitable Media*, (Manchester Univ. Press, Manchester, 1987)
- [3] J.J. Fox, R.F. Gilmour, Jr. and E. Bodenschatz, *Phys. Rev. Lett.* **89**, 198101 (2002)
- [4] T. Quail, A. Shrier, and L. Glass, *Phys. Rev. Lett.*, **113**, 158101 (2014)
- [5] X. Gao, H. Zhang, V. Zykov, and E. Bodenschatz, *New J. Phys.* **16**, 033012 (2014)
- [6] V.S. Zykov, A. Krekhov and E. Bodenschatz, preprint
- [7] V.S. Zykov and E. Bodenschatz, *Phys. Rev. Lett.* **112**, 054101 (2014)

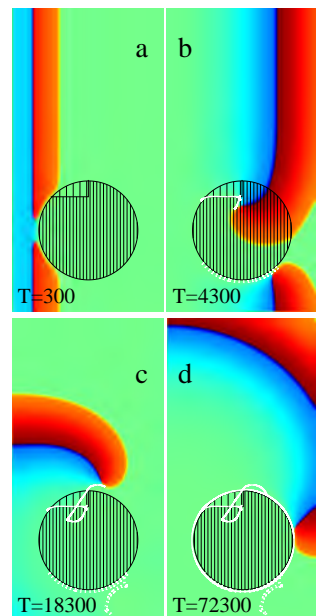


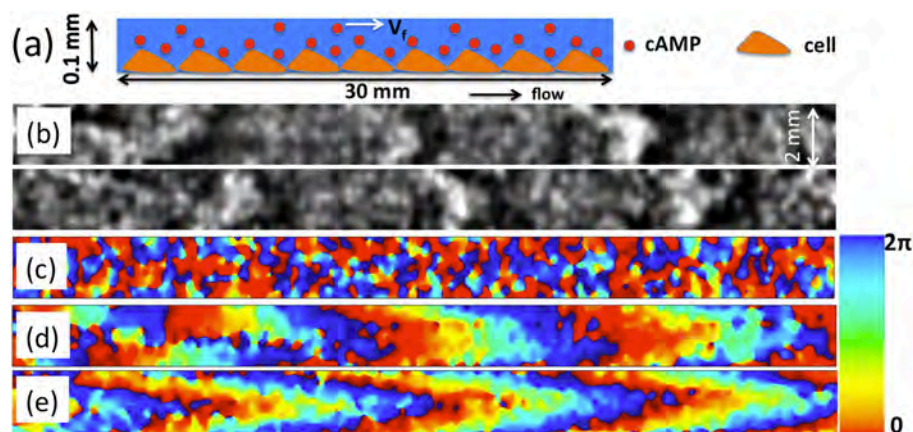
Figure 7.13: Rotor initiation in an excitable medium containing a pseudo obstacle. The coupling strength D is fixed to $D = 1$ everywhere except in a circular region where $D = 2$ (dense filling) and $D = 1.5$ (rare filling). The trajectories of the two phase change points created due to a break up of a planar wave propagating from the left side are shown by white solid and dotted lines correspondingly. (a) Two phase change points were created. (b) The bottom point is following the pseudo obstacle boundary. In contrast to this, since at a part of the boundary the jump of the parameter D is smaller than a critical one, the top wave was able to penetrate inside and is rotating faster. (c) After collision of two waves the bottom one is pushed toward the medium boundary and disappeared. (d) The remaining spiral wave continues to rotate. The ablation of the pseudo obstacle strongly reduces a probability of the undesirable rotor initiation.

7.8 FLOW-DRIVEN WAVES IN *Dictyostelium discoideum*

A. Gholami, V. Zykov, E. Bodenschatz
O. Steinbock (Florida)

Transport-coupled nonlinear dynamics is fundamental to most types of spatiotemporal self-organization [1]. Here we show that reaction-diffusion-advection has important consequences for biological systems that use solutes as signaling agents [2, 3, 4]. We present experimental

Figure 7.14: (a) A schematic side view of the experimental setup. (b) Top view of flow-driven waves at flow velocity of $V_f = 2$ mm/min. The wave trains, developed spontaneously, propagated with the flow velocity and had a period of ~ 7 min. (c) Phase maps of the observed spatiotemporal oscillations before and (d) during flow-driven wave propagation. (e) At $V_f = 5$ mm/min, deformations of the wave fronts are increased.



results on flow-driven waves in the signaling of the amoebae *Dictyostelium discoideum* (*D.d.*). In the natural environment, populations of starving *D.d.* may experience fluid flows that will profoundly alter the wave generation processes. We investigate spatiotemporal dynamics of a uniformly distributed population of *D.d.* cells in a flow-through narrow microfluidic channel. The starved amoebae are attached to the surface of the channel and exposed to an external fluid flow that advects the signaling cAMP molecules downstream (Fig. 7.14). This transport anisotropy in the extracellular medium induces macroscopic wave trains that differ profoundly from conventional excitation waves in this system. In the absence of flow, spiral or target patterns of cAMP emerge at different locations along the channel. This is in contrast to flow-driven waves, where waves originate at the inlet region of the device and propagate in flow direction, as shown in Fig. 7.14. The image contrast reflects the shape changes of the cells. The light bands correspond to high concentrations of cAMP and consist of elongated chemotactic cells while in the dark bands the cAMP concentrations is small and cells remain round. To investigate the dynamical selection of flow-driven waves, we perturbed the system by periodically injecting of the signaling agent (cAMP) at the upstream end of the channel (Fig. 7.15). These perturbations of flow-driven waves induced 1:1, 2:1 and 3:1 frequency responses, reminiscent of Arnold tongues in forced oscillatory systems.

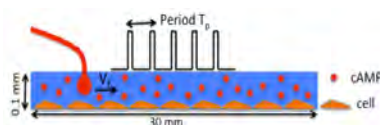


Figure 7.15: The modified experimental set up with periodic cAMP injections.

- [1] M. J. Scheffer J. Plankton Res. **13** 1291 (1991).
- [2] A. Gholami, O. Steinbock, V. Zykov, E. Bodenschatz Phys. Rev. Lett. **114** 018103 (2015).
- [3] A. Gholami, O. Steinbock, V. Zykov, E. Bodenschatz NJP **17** 063007 (2015).
- [4] A. Gholami, V. Zykov, O. Steinbock, E. Bodenschatz NJP **17** 093040 (2015).

7.9 ELECTROTAXIS: THE MIGRATION OF AMOEBA CELLS IN AN ELECTRIC FIELD

I. Guido, E. Bodenschatz

Cells have the ability to detect DC electric fields (EFs) and respond to them with a directed migratory movement either parallel or antiparallel to the field vector according to the cell type. *Dictyostelium discoideum* (*D.d.*) cells, a key model organism for the study of eukaryotic chemotaxis, orient and migrate toward the cathode under the influence of an electric field [1, 2]. The underlying sensing mechanism and whether it is shared by the chemotactic response pathway remains unknown. Whereas genes and proteins that mediate the electric sensing as well as that define the migration direction have been previously investigated in *D.d.* cells [3], a deeper knowledge about the cellular kinematic effects caused by the electric field is still lacking. Here we show that besides triggering a directional bias the electric field influences the cellular kinematics by accelerating the movement of cells along their paths (Fig. 7.18). We found that the migratory velocity of the cells in an electric field increases linearly with the exposure time (see Fig. 7.17) [4]. This phenomenon is independent of the cellular developmental stage and it has not been observed in chemotaxis. Electrophoretic effects on the cell membrane or in the intracellular space suggested by other studies cannot explain our observation, as the drift velocity caused by electrophoresis is constant for an invariant electric field.

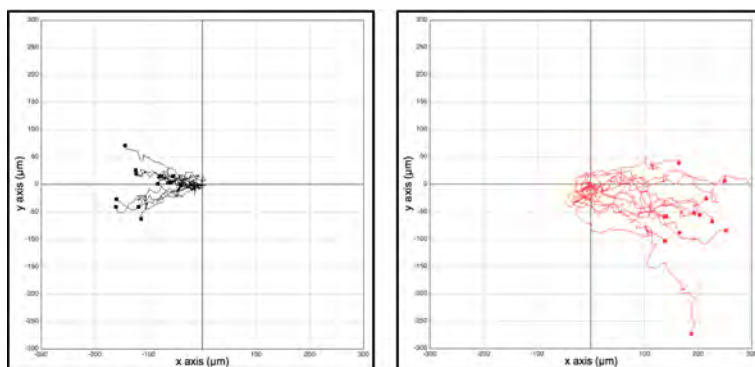


Figure 7.18: Cell tracking of *D.d.* cells migrating toward the cathode under the effect of an EF. By reversing the EF polarity, the cells respond by inverting their trajectory.

We believe that the acceleration could be more likely attributed to the single dominant anterior pseudopod morphology that the cells develop in the electric field. Our work poses new mechanistic questions about how electric fields interact with biological matter and shed a new light about its application in processes such as wound healing.

- [1] M. Zhao et al., *J. Cell Biol.*, **157**, 921 (2002)
- [2] J.M. Sato et al., *BioSystems* **88**, 261 (2007)
- [3] R. Gao et al., *Sci.Signal.* **8**, 378 (2015)
- [4] I. Guido, E. Bodenschatz, (Submitted)

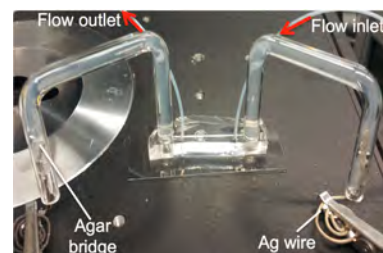


Figure 7.16: Experimental setup. We apply the electric field to cells seeded into microfluidic devices equipped with agar bridges to avoid any harmful effects of the electric field on the cells (ions formation, pH changes, etc.) and a constant flow to prevent the build-up of chemical gradient that elicits chemotaxis.

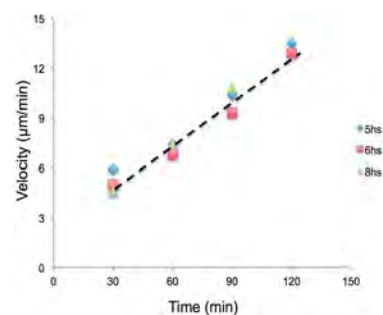


Figure 7.17: Linear speeding up effect of the EF on the directional migration of the cells.

7.10 GAS-PARTICLE INTERACTION: INSTABILITIES IN PROTOPLANETARY DISKS

E. Bodenschatz, H.L. Capelo, H. Xu

J. Blum (TU Braunschweig, DE)

A. Johansen, M. Lambrechts (Lund Observatory, SE)

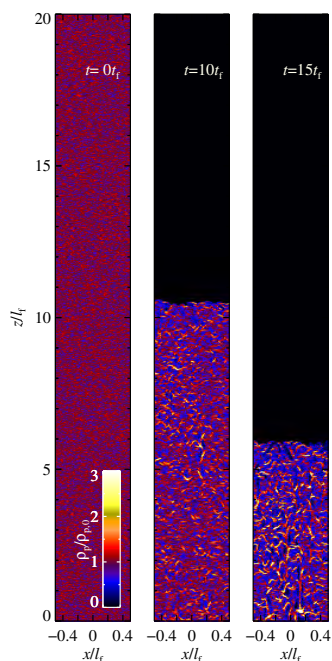


Figure 7.19: Growing particle-density inhomogeneities in a sedimenting suspension with overall particle mass loading 1 and large Kn , i.e., free-molecular gas flows around individual particles [4].

As we know now, most of stars are surrounded by planets, which grow out from the gas-dominated dusty protoplanetary disks (PPDs) around the stars. It is generally accepted that the planets finally emerge from the gravitational interactions among km-sized planetesimals that the PPDs evolve to. On the other hand, how km-sized planetesimals form from micrometer to mm-sized dust particles in the PPDs remains unclear. The observed lifetimes of PPDs are about 10^6 years, which are too short for planetesimals to form by gradual growth mechanisms alone. Moreover, particles experience a gas drag when they orbit in PPDs. Hence they lose kinetic energy and drift radially towards the central star. For m-sized particles, even if they could form by collisional growth, this radial drift is very fast, leading them to spiral into the central star in 10^3 years [1], which would prevent planetesimals to form at all from the gradual growth of dust particles.

Flow instabilities and turbulence, however, may quickly enhance local dust concentration and lead to gravitational collapse, thus providing an alternative way to planetesimal formation. Therefore, in the study of planetesimal formation, it is crucial to treat correctly the hydrodynamical interaction between the gas and the dusty components of the PPD. Among the instability mechanisms, streaming instability (SI) [2], which results from the variation of gas drag with particle concentration, is the most promising and has been observed to lead to rapid planetesimal formation in numerical simulations [3].

Whereas earlier studies only considered SI in a rotational frame around the center star, recent simulations [4] show that the instability is more general as spontaneous concentration of solids also occurs in a vertically settling stream of particles under constant gravity (Figure 7.20).

To study SI experimentally, we developed a new facility to produce dilute particle-gas flows under reduced pressure (Figure 7.19). This allows us to mimic the conditions of PPDs by independently varying (i) particle mass loading, which determines the overall momentum dominance between the gas and the particles, and (ii) the Knudsen number $Kn = \lambda/d$, the ratio of the mean free path of the gas λ to particle size d , which characterizes the local interaction between individual particles and the gas molecules and hence determines the gas drag on the particles. Using Lagrangian particle tracking, we investigate the effect of particle-gas-particle interaction, which is not considered in current astrophysical flow instability theories and simulations.

[1] P. J. Armitage, *Astrophysics of Planet Formation*, Camb. Univ. Press. (2010).

[2] A. Youdin & J. Goodman, *Astrophys. J.*, **620**,459 (2005).

[3] A. Johansen, et al., *Nature*, **448**,1022 (2007).

[4] M. Lambrechts, A. Johansen, H. L. Capelo, J. Blum, & E. Bodenschatz, (under review).

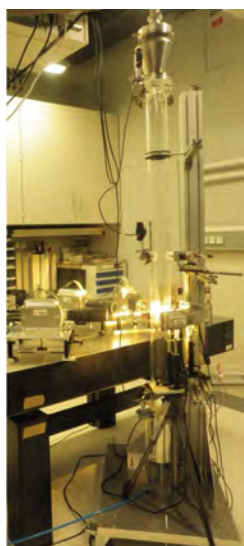


Figure 7.20: Vertical sedimenting chamber to study SI under reduced pressure conditions.

7.11 GENETIC ASSIMILATION OF VISUAL CORTICAL ARCHITECTURE

J. Liedtke, F. Wolf

Although genetic information is critically important for brain development and structure, it is widely believed that neocortical functional architecture is largely shaped by activity dependent mechanisms. The information capacity of the genome, however, appears too small to contain a blueprint for hardwiring the cortex. Here we show theoretically that genetic mechanisms can circumvent this apparent information bottleneck.

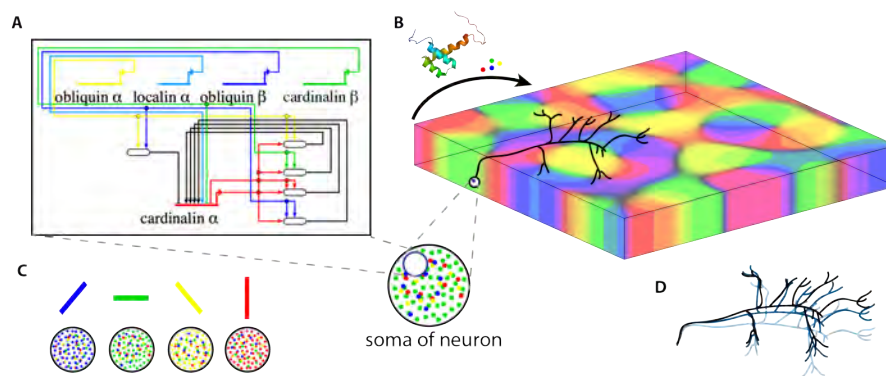


Figure 7.21: Scheme of genetic networks specifying layout of orientation domains in V1. **a)** Shown is an example genetic subnetwork illustrating how morphogens regulate their expression rates mutually in neuronal nuclei. **b)** Morphogens are actively transported over dynamic long-range connections as indicated by the arrow. The transport of morphogens induces a signaling cascade, which exerts a regulation of morphogen expression. **c)** The concentration of morphogens in a neuron is illustrated by the colored dots. The difference of morphogen concentrations encodes orientation selectivity. **d)** Long-range connections are dynamic and target specific morphogen concentration profiles.

Using our prior research on universality classes of circuit self-organization in the visual cortex [1], we devised mathematical models of genetic networks of neurons interacting by long-range axonal morphogen transport. Neurons dynamically generate morphogen patterns that prescribe the layout of orientation domains as experimentally observed in the primary visual cortex (V1) of primates and carnivores[2, 3, 4]. We use analytical methods from weakly non-linear analysis[5] complemented by numerical simulations to obtain solutions of example genetic networks. The hypothesis of genetic circuits shaping the complex architecture of V1 is in line with several recent biological findings. For instance, (1) transcription factors have been found to be transported via axons and to translocate into the nucleus of target neurons[6], (2) a molecular correlate was recently found for ocular dominance columns in V1[7], (3) V1's architecture is intriguingly robust against radically abnormal developmental conditions such as dark rearing[2, 4, 8]. Our theory provides for the first time a scheme that shows how a complex cortical processing architecture can be specified using a genetic mechanism of small bandwidth.

- [1] F. Wolf, Phys. Rev. Lett. **95**, 20 (2005)
- [2] M. Kaschube, et al., Science **330**, 6007 (2010)
- [3] W. Keil, et al., Science **336**, 6080 (2012)
- [4] M. Schottdorf, W. Keil, et al., PLoS CB **11**, 11 (2015)
- [5] M. Cross, P. Hohenberg, Rev. of Mod. Phys. **65**, 3 (1993)
- [6] S. Sugiyama, et al., Cell **134**, 3 (2008)
- [7] K. Tomita, et al., Cerebral Cortex **23**, 11 (2012)
- [8] L.E. White, et al., Nature **411**, 6841 (2001)

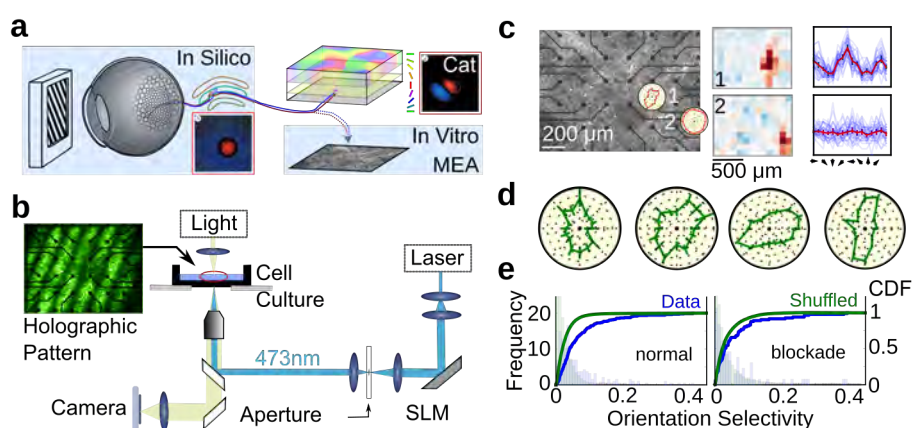
7.12 A SYNTHETIC NEUROBIOLOGY APPROACH TO ORIENTATION SELECTIVITY

M. Schottdorf, F. Wolf

T. Keith, R. Merino, A. Neef, G. Rapp (Rapp OptoElectronic GmbH), H. Schrobsdorff, S. Shoham (Technion), W. Stühmer (MPI-EM)

One of the most prominent features of primary visual cortical neurons is their orientation preference [1, 2]. Many competing models for the emergence of orientation preference have been proposed, from cortical self-organization [1] and retinally imposed tuning [2, 3] to pinning by disorder [4] and randomness of neuronal circuits [5]. In the brain, feedforward and cortical circuits, which are contributing to selectivity, cannot be selectively manipulated. Having developed methods for optogenetic stimulation [6] and structuring [7] of cultured neurons, we established a synthetic biology approach for reconstituting this emergent property in a surrogate visual cortex.

Figure 7.22: **a** The retinohalamic pathway of the cat provides input into V1. Here, we simulate the retinohalamic pathway to provide input for a cell culture. **b** A schematic drawing of the holographic photostimulation setup [8]. **c** Fluorescence image of rat cortical neurons expressing YFP on a MEA. Overlays show polar plots of tuning curves for two example electrodes (left). Right: their receptive fields and tuning curves (blue: single trials, red: average + 95% C.I.). **d** Polarplots for the tuning curves of four example neurons. **e** Histogram and cumulative distribution function (CDF) of observed orientation selectivities (blue) together with the shuffled control (green) for neurons with intact (left) and pharmacologically severed synaptic connections (right).



We constructed a model of the early visual pathway *in-silico* (**a**) that controls a holographic photostimulation setup providing *retinohalamic input* to a culture of optogenetically-modified neurons (**b**). We monitor neural responses with a multielectrode array (MEA) [6, 7]. Stimulating the cell culture with moving gratings revealed a substantial degree of orientation tuning even in the absence of orientation tuned afferent input (**c,d**). We probe this orientation tuning and its origin pharmacologically and by various stimulation conditions (**e**). Our approach can open up a new way to experimentally dissect the influence of recurrent connections and their connectomic parameters *in-vitro*.

- [1] M. Kaschube, et al., *Science* **330**, 6007 (2010)
- [2] M. Schottdorf, W. Keil, et al., *PLoS CB* **11**, 11 (2015)
- [3] M. Schottdorf, et al., *PLoS ONE* **9**, 1 (2014)
- [4] U. A. Ernst, et al., *Nat Neurosc* **4**, 4 (2001)
- [5] F. Wolf, et al., *Curr Op Neurobiol* **25**, 228 (2014)
- [6] A. El Hady, G. Afshar, et al., *Frontiers Neur Circ* **7**, 167 (2013)
- [7] R. Samhaber, M. Schottdorf, et al., *J Neur Meth* **257**, 194 (2016)
- [8] I. Reutsky-Gefen, et al., *Nat Comm* **4**, 1509 (2013)

7.13 PRECISION MEASUREMENT AND DYNAMICAL SWITCHING OF VISUAL CORTICAL ARCHITECTURE

J. D. Flórez Weidinger, F. Wolf

D. E. Whitney (MPI Florida), J. Crowley (Carnegie Mellon U.)

Neurons in the primary visual cortex are selective for the orientation of light/dark edges in their receptive fields [1]. In primates and carnivores the preferred orientation of the neurons changes systematically across the cortical surface forming iso-orientation domains ordered around point-like topological defects called pinwheel centers [2]. It is a long standing theoretical prediction that visual cortical circuits are in a state of flux, such that the preferred orientation of the neurons represents a non-equilibrium steady state of circuit turnover [3]. If this prediction is true and multiple steady states coexist, then signatures of the underlying dynamical process should be observable as a rearrangement of the domains over time.

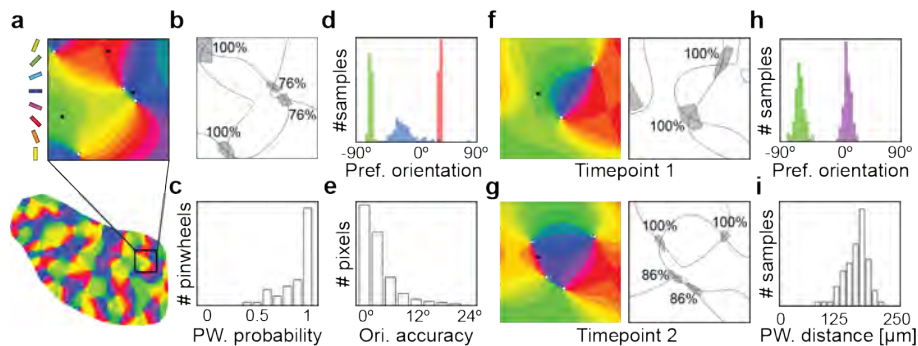


Figure 7.23: **a-e)** Precision measurement of orientation domains: **a)** Color coded orientation preference layout recorded in ferret V1. Inset size 640 micrometers. White dots mark the position of the pinwheels. **b)** Percentage of bootstrap samples in which corresponding pinwheels are found. Black lines mark the zero contours of the layout. Gray areas mark the confidence range of the pinwheel position. **c)** Pinwheel probabilities for the complete layout. **d)** Distribution of orientation preferences in the bootstrap samples for the three example pixels marked with black dots in **a)**. **e)** Accuracy of the orientation preference estimation for each pixel in the layout. **f-i)** Pinwheel generation event: **f-g)** Layout and pinwheel probabilities for the same region in two consecutive imaging sessions. **h)** Orientation preference distribution of the pixel marked with a black dot in **f)** and **g)**. **i)** Distance between the generated pinwheel pair in the different bootstrap samples.

We tested this hypothesis by investigating the occurrence of the largest topological change conceivable in the layout: the generation and annihilation of pinwheel pairs. We conducted acute high accuracy large scale intrinsic signal imaging experiments in 32 ferrets. In 24 of the ferrets we further employed an adapted pairing protocol [4] between imaging sessions to drive the cortical circuits out of a potential stationary state. To harvest significant topological changes we quantified the certainty of the measurements using re-sampling methods. The probability of pinwheel existence was calculated by tracking their position between bootstrap samples. The accuracy of the estimated orientation preference of individual pixels was computed from their inter-sample tuning distribution. We analyzed the dynamics of 2620 pinwheels by comparing the measured layouts in subsequent imaging sessions of 42 minutes each. Using this extensive data set and precise analysis methods we found rare but conclusive examples of pinwheel rearrangement. The rate of these events was increased when the pairing paradigm was used. These results demonstrate for the first time dynamical changes of visual cortical architecture driven by neuronal activity.

- [1] D. Hubel, T. Wiesel, Proc. R. Soc. Lond. [Biol]. **198**, 1130 (1977)
- [2] T. Bonhoeffer, A. Grinvald, Nature **353**, 6343 (1991)
- [3] F. Wolf, T. Geisel, Nature **395**, 6697 (1998); F. Wolf, Phys. Rev. Lett. **95**, 208701 (2005); M. Kaschube, et al. Science **330**, 1113 (2010)
- [4] S. Schuett, T. Bonhoeffer, M. Hubener, Neuron **32**, 2 (2001)

7.14 MUSIC: A DYNAMICAL SYSTEMS PERSPECTIVE

T. Geisel, H. Hennig, V. Priesemann, M. Sogorski, A. Witt

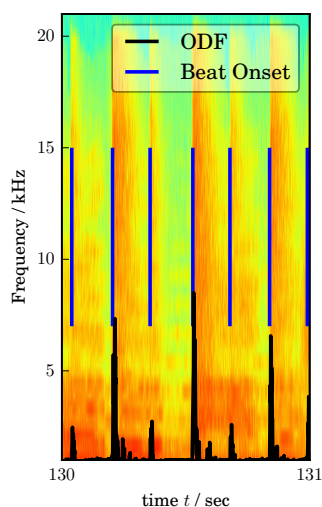


Figure 7.24: Spectrogram of an excerpt from “I Keep Forgettin” with the calculated onset detection function and the corresponding hi-hat onset times.

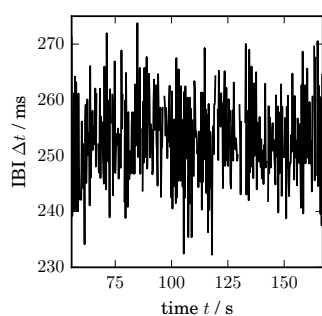


Figure 7.25: Interbeat interval time series of Benny Carter’s “Crazy Rhythm”.

Long range temporal correlations (LRC) characterize both, human behavior and brain dynamics. We study LRC using a characteristic human skill – making music. We have previously shown that individuals exhibit fractal LRC in their timing deviations when following a metronome, and that artificial music becomes more enjoyable when introducing these humano-typic LRC [1]. Before moving back to Göttingen, Holger Hennig demonstrated the same LRC when skilled piano players perform a complex music piece, and that the LRC are independent of auditory feedback [2]. He further showed that the interbeat intervals between individuals exhibited scale-free cross-correlations, i.e. the next beat played by an individual is dependent on the entire history (up to several minutes) of her partner’s interbeat intervals [3].

While LRC have been widely studied in the behavior of isolated individuals under laboratory conditions, the ultimate goal is to study music from real concerts. We tested whether the results from the laboratory translated to the real world, by analyzing the LRCs of Jeff Porcaro’s one-handed hi-hat pattern in “I Keep Forgettin”. This piece is known for its sustained 16^{th} note patterns, which also match the patterns we studied earlier. Indeed, the fluctuations of hi-hat amplitudes and interbeat intervals showed clear LRC, thereby confirming that our previous results translate from the laboratory to live music [4].

Currently, we investigate whether LRC are characteristic for musical genres. To this end we developed a semi-automated method to determine the onsets of the beat from the hi-hat in standard Rock and Jazz recordings. We chose the hi-hat because it frequently coincides with the beat, and because its sharp onset allows a millisecond precise onset detection. With this method we already extracted the beat of ≈ 100 recordings, providing a very rich data base [5]. For music pieces as complex self-paced timing tasks the fluctuations are expected to be LRC on long time scales (clock component) and uncorrelated on short time scales (motor component) [6]. However, in contrast to the results by Gilden and colleagues, we clearly found the motor component to show LRC, as predicted from our earlier work [1]. Interestingly, the motor LRC did not differ between genres, indicating that they are generic signatures of motor dynamics. In the future, we will assess LRCs of the clock component, i.e. the temporal structure of the piece, because these may elucidate the characteristics of different genres. Taken together, our work showed that LRC characterize the temporal structure of music from laboratory to live music performance.

- [1] H Hennig, et al., PLoS ONE 7(4):10.1371, (2011).
- [2] M Herrojo Ruiz, et al., Frontiers in Psychology 5:1030, (2014).
- [3] H Hennig, Proc. Natl. Acad. Sci. USA 111(36), 12960, (2015).
- [4] E Räsänen, O Pulkkinen, T Virtanen, M Zollner, H Hennig, PLoS ONE 10(6): e0127902, (2015).
- [5] M Sogorski, V Priesemann, A Witt, T Geisel, *in prep.*
- [6] D Gilden, T Thornton, M Mallon, Science, 267(5205):1837 (1995).

7.15 CONTROL OF SPATIAL-TEMPORAL COMPLEXITY OF THE HEART

S. Luther, U. Parlitz, J. Christoph, C. Richter, D. Hornung, T. Baig, M. Chebbok, A. Schlemmer, T. Lilienkamp, S. Berg, H. tom Würden, E. Boccia, J. Schröder-Schetelig, A. Witt, V. Krinsky F.H. Fenton (Atlanta), G. Hasenfuss, S.E. Lehnart, M. Zabel, W.-H. Zimmermann (Göttingen), R. Hinkel, C. Kupatt (München), O. Steinbock (Tallahassee), K.-H. Kuck (Hamburg)

During cardiac fibrillation, coherent mechanical contraction of the heart is disrupted by unstable vortex-like rotating waves that interact with each other and the complex anisotropic and heterogeneous anatomical substrate. Due to a loss of pumping function, ventricular fibrillation (VF) is immediately life threatening, resulting in approximately 300.000 sudden cardiac deaths per year in the U.S. alone. For a lack of a better strategy, high-energy electric shocks are applied to terminate cardiac fibrillation. Standard defibrillation aims at depolarizing all cardiac cells, thereby terminating all electrical activity at once. Brute-force high-energy shocks, however, may have severe side effects including traumatic pain and tissue damage indicating a significant medical need. Low-Energy Anti-Fibrillation Pacing (LEAP) addresses this need. By selectively targeting phase singularities associated with vortices that drive cardiac fibrillation, LEAP requires 80-90% less energy than conventional defibrillation [1, 2, 3]. Therefore, LEAP technology may open the path towards a new generation of medical devices, which will permit for the first time painless and non-damaging termination of cardiac arrhythmias. The Biomedical Physics group conducts fundamental research that will enable the translation of LEAP into clinical application. This research includes the development of novel imaging modalities, such as electro-mechanic imaging and optogenetic tools, and the disease specific optimization and validation of LEAP in pre-clinical large animal models of myocardial infarction and heart failure.

Visualization of 3D Vortices inside the Heart. The visualization of wave dynamics inside cardiac tissue has evaded experimental realization. Using high-resolution ultrasound, we have measured for the first time rotating mechanical waves inside the ventricular wall [4, 5, 6, 8]. Advancing state of the art ultrasound imaging technology and model based data analysis, our research aims at fully time resolved 3D visualization of vortex dynamics inside the heart. The experimental visualization of transient wave phenomena during cardiac fibrillation and defibrillation will significantly enhance our understanding of the mechanisms underlying arrhythmia onset and control and will open the path towards novel diagnostic and therapeutics. The Biomedical Physics Group develops multimodal fluorescence imaging techniques for simultaneous measurement of membrane voltage, intracellular calcium, and mechanical deformation on the epi- and endocardial surfaces of intact, Langendorff-perfused hearts (rabbit, dog, pig). This unique technique permits for the first time multimodal fluorescence imaging of

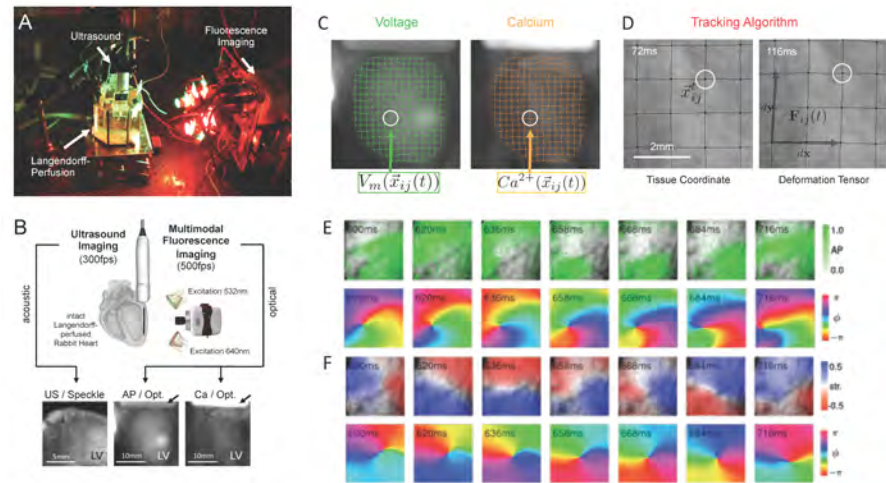


Figure 7.26: **A** Photograph of the experimental setup for simultaneous optical mapping and ultrasound imaging of intact Langendorff-perfused rabbit hearts. Optical mapping permits the simultaneous measurement of membrane voltage, intracellular calcium (following [7]), and mechanical contraction on the surface of the heart [8]. Ultrasound imaging allows for imaging of mechanical deformation inside cardiac tissue. **B** Schematic of the imaging modalities indicating the relative orientation of the ultrasound imaging plane. **C** Illustration of the voltage and calcium signals in the reference frame. **D** Tracking of contractile tissue motion reveals deformation tensor. **E** Propagation of action potential (AP, green) and corresponding phase indicate a rotor and the corresponding phase singularity. **F** Strain rate obtained from motion tracking (compressible strain red, tensile strain blue) shows rotating wave pattern. Corresponding phase analysis reveals phase singularity obtained from mechanical motion [6].

the beating heart and the investigation of electromechanical instabilities underlying the onset of cardiac arrhythmias *ex vivo*.

Optogenetic Control of Cardiac Arrhythmias. We are developing optical methods and optogenetic tools to access and control cardiac excitation on a cellular level. In intact Langendorff-perfused optogenetic α -MHC-ChR2 mouse hearts, we could demonstrate the optical induction of ventricular fibrillation and subsequent optical defibrillation [9]. The development of structured illumination using digital light processors will permit optical stimulation and optical mapping of cardiac dynamics in real-time [10, 11]. For *in vivo* applications, we have developed a fiber-optical FRET imaging system for genetically encoded voltage sensors (e.g. VSFP2.3) [12]. To elucidate mechanisms underlying the onset, perpetuation, and control of cardiac arrhythmias in models of patient mutations, we combine optogenetic control methods and tools with specific genetic disease models (atrial and ventricular arrhythmias and diastolic dysfunction caused by RyR2 or Nav1.5 patient mutations). In collaboration with S.E. Lehnart (University Medical Center) optogenetic tools are employed to develop, optimize, and conceptualize tissue-specific therapeutic approaches including pacing strategies and low-energy defibrillation in knock-in models of RyR2 and Nav1.5 patient mutations towards the clinical development of tissue-based endogenous control of cardiac dysfunction.

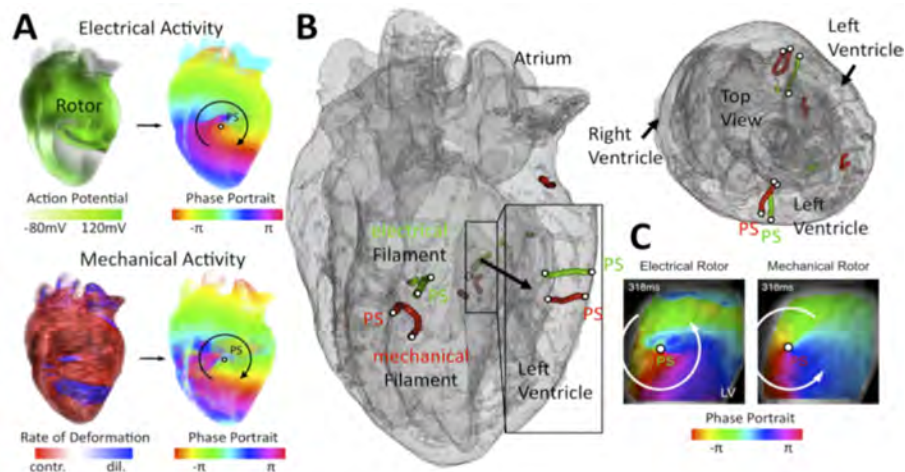


Figure 7.27: **A** Electro-elasto-mechanical rotor patterns in a computer simulation of a rabbit heart (geometry obtained from micro-computed tomography scan). Phase maps of electrical scroll wave rotor and induced elastic deformation pattern shows rotor topology. **B** Simulation of electro-mechanical filaments (green: electrical vortex filament, red: mechanical topological defect line). **C** Rotating electrical and mechanical rotor patterns and phase singularities on epicardial surface imaged with fluorescence imaging during ventricular fibrillation [6, 8].

The Role of Disease Specific Heterogeneity. In contrast to conventional defibrillation, low-energy control strategies aim at selectively controlling vortex-like rotating waves that drive cardiac fibrillation. The interaction of rotating waves with anatomical obstacles or heterogeneities in electrical conduction (e.g. fibrotic tissue, scars, vessels etc.) known as vortex pinning remains a major scientific challenge. It has been shown previously, that a pulsed electric field may be used to remove a single vortex from an anatomical pinning center [13, 14, 15]. Si-

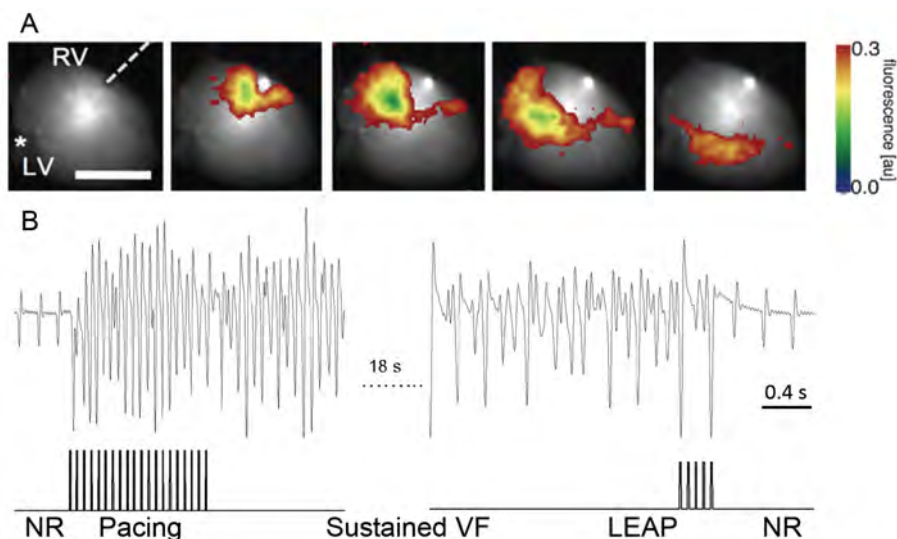


Figure 7.28: Optogenetic tools are employed to elucidate genetic/molecular and dynamic arrhythmia triggers and control mechanisms. **A** Optical mapping (V_m) of one light pulse (RV = right ventricle, LV = left ventricle). The fiber position is represented in the first snapshot by the gray dashed line. The snapshots are separated in time by 2 ms. (Scale bar, 0.5 cm.) The asterisk shows the MAP electrode position [10]. **B** Induction of sustained ventricular fibrillation (VF) from normal rhythm (NR) in a Langendorff-perfused α -MHC-ChR2 mouse heart [9] using periodic optical pacing and subsequent optical LEAP-based termination (unpublished data).

multaneous control of multiple vortices was proposed theoretically [16]. We have demonstrated control of AF and VF through simultaneous and direct access to multiple vortex cores resulting in rapid synchronization of cardiac tissue and therefore, efficient termination of fibrillation in healthy cardiac tissue [1]. However, the mechanisms underlying the onset, perpetuation, and control of cardiac arrhythmia are expected to be disease-dependent. Heart failure is associated with structural and functional remodeling of the multi-cellular substrate [17, 18]. On one hand, increased heterogeneity in electrical conductance may result in an increased likelihood of spatio-temporal instabilities and therefore in general an increased risk of arrhythmia. However, stabilization of wave pattern due to heterogeneity could also be observed [19]. The increased number of heterogeneities in electrical conductance, on the other hand, increases the density of wave sources (virtual electrodes) that may be recruited using weak pulsed electric fields and therefore potentially improve LEAP-induced control of arrhythmias. Chronic myocardial infarction is associated with macroscopic scar regions and an increased risk of cardiac arrhythmias. Supported through the GO-Bio programme and the DZHK e.V. we are studying LEAP-based termination in myocardial infarction (40 days post MI, LVEF < 35%) and heart failure in large animal models under conditions similar to human pathology.

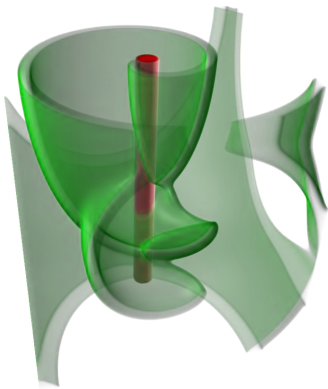


Figure 7.29: Scroll waves in a three-dimensional medium with negative filament tension may break up and display spatio-temporal chaos. The presence of heterogeneities can influence the evolution of the medium, in particular scroll waves may pin to such heterogeneities. We show that as a result the medium may be stabilized by heterogeneities of a suitably chosen geometry. Thin rodlike heterogeneities suppress otherwise developing spatio-temporal chaos and additionally clear out already existing chaotic excitation patterns [19].

- [1] S. Luther, F.H. Fenton et al., *Nature* **475**, 235-239 (2011)
- [2] S. Luther et al., U.S. Patent No. 8,886,309
- [3] S. Luther et al., U.S. Patent No. US20090062877 A1
- [4] N.F. Otani et al., *Annals of Biomedical Engineering* **38**, 3112-3123 (2010)
- [5] N.F. Otani et al., U.S. Patent No. US8666138 B2
- [6] J. Christoph, S. Luther, European Patent Application No. EP15150588.0
- [7] P. Lee et al., *Heart Rhythm* **8** 1482-91 (2011)
- [8] J. Christoph, Dissertation, Georg-August-Universität Göttingen (2014)
- [9] C. Richter et al., In: Kianianmomeni A (ed) *Optogenetics - Methods and Protocols*. Springer New York (in press)
- [10] T. Zaglia et al., *PNAS* **112**, E4495-E4504 (2015)
- [11] M. Dura et al., *Frontiers in Physiology* **5**, 337 (2014)
- [12] M.-L. Chang Liao et al., *Circ. Res.* **117**, 401-412 (2015)
- [13] A. Pumir and V. Krinsky, *J. Theor. Biol.* (99), 311 (1999)
- [14] P. Bittihn, M. Hoerning, and S. Luther, *Phys. Rev. Lett.* **109**, 118106 (2012)
- [15] S. Takagi et al., *Phys. Rev. Lett.* **93**, 058101 (2004)
- [16] A. Pumir et al., *Phys. Rev. Lett.* **99**, 208101 (2007)
- [17] J. Rother et al., *Open Biol.* **5**, 150038 (2015)
- [18] S. Filippi et al., *Europace* **16**, 424-34 (2014)
- [19] F. Spreckelsen et al., *Phys. Rev. E* **92**, 042920 (2015)

7.16 MODELLING AND DATA ANALYSIS IN BIOMEDICAL PHYSICS

S. Luther, U. Parlitz

A. Schlemmer, J. Schumann-Bischoff, S. Stein, F. Koeth

Observability and Parameter Estimation

For many physical processes, dynamical models are available but often not all their state variables and parameters are known or easily accessible. In quantitative biology, for example, mathematical models of single neural or cardiac cells or networks may contain many state variables and parameters, whose values are not easy to measure (without destroying the system). In such cases, data based estimation methods can be used to determine these unknown states and parameters by adapting a suitable model to reproduce and predict the measured time series. This approach can be successful only if two conditions are fulfilled: (i) the available data have to provide sufficient information, i.e., the unknown state variables and parameters have to be observable and (ii) the estimation algorithm (like the synchronization based method proposed in Ref. [1, 2]) has to be properly initialized with initial guesses sufficiently close to the true solution (as we analyzed in detail for the Lorenz-96 model in Ref. [3]). To address the observability problem of state variables and parameters we introduced a measure of uncertainty that is based on the Jacobian matrix of the delay coordinates map [4, 5]. This measure allows to identify regions in state and parameter space where the specific unknown quantity can (or cannot) be estimated from a given time series as illustrated for the Ikeda map [4] in Fig. 7.16.

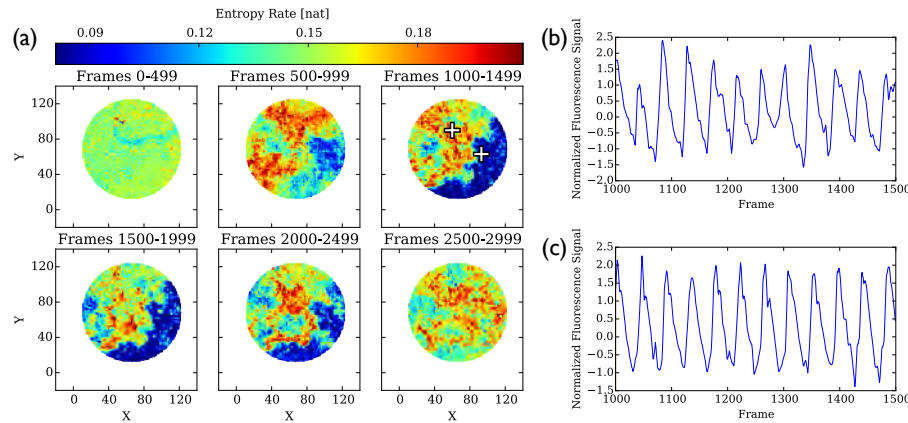


Figure 7.31: a) Entropy rate maps for six different windows of a length of 500 frames without overlap from a cell culture video. Two time series extracted from the third window at positions (60, 90) (b) and (93, 63) (c) (highlighted as white crosses).

Entropy Rate Maps of Experimental Video Data

Fluorescence imaging (optical mapping) is an important tool for experimentally investigating cardiac dynamics, because it provides video data of membrane potential and intracellular calcium concentration with high spatial and temporal resolution. However, the characterization of the spatiotemporal complexity occurring in these data sets

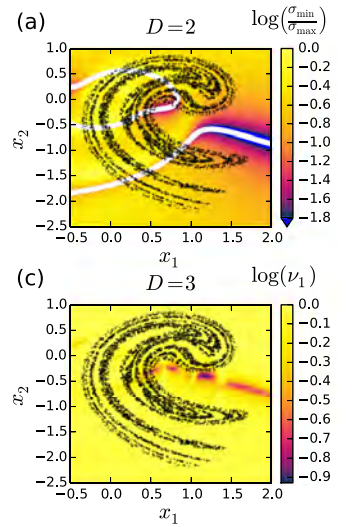


Figure 7.30: Observability of the state variables x_1 and x_2 of the Ikeda map from a x_1 time series. (a) Color-coded ratio of singular values $\sigma_{min}/\sigma_{max}$ of the Jacobian matrix of the delay embedding map vs. x_1 and x_2 for reconstruction dimension $D = 2$. White curves indicate the location of singularities. (c) Uncertainty ν_1 of x_1 estimates with $D = 3$.

remains a challenging task. In addition to common analysis methods like dominant frequency maps or the detection of phase singularities we employed entropy rates for quantifying spatiotemporal complexity patterns of excitable media [6]. Entropy rate maps provide information about local complexity, the origins of wave breakup and the development of patterns governing unstable wave propagation. As an example, Fig. 7.31 shows entropy rate maps and representative time series of local activity for video data from an embryonic chicken cell culture.

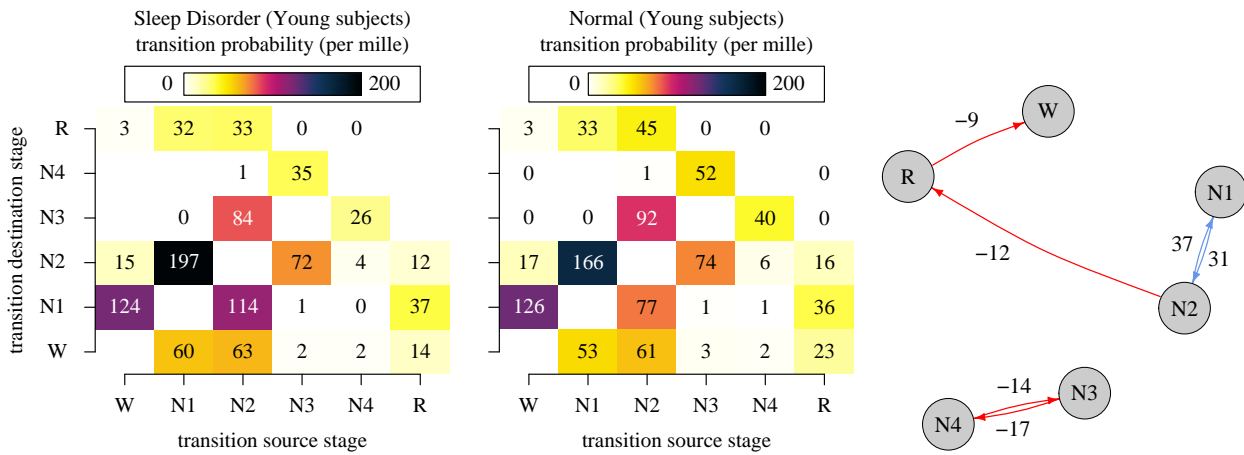
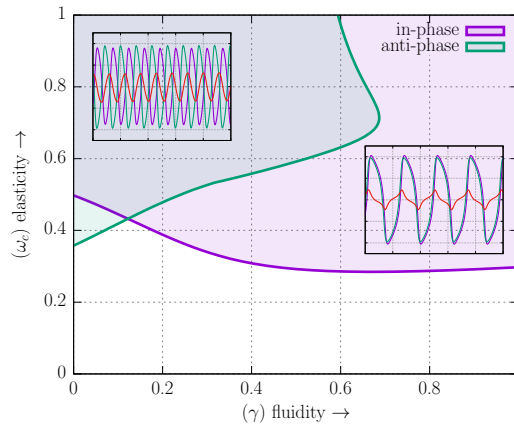


Figure 7.32: Difference of sleep-stage transition probabilities of normal young subjects and young subjects suffering from sleep disorder displayed as a transition graph obtained from both transition matrices. The numbers at the links in the transition graph equal the difference of the transition probabilities (in per mille). Only significant links ($p < 0.01$) are plotted in the graph.

Sleep Transition Graphs

In collaboration with T. Penzel and N. Wessel (both Charité, Berlin) typical patterns of sleep-stage transitions of 196 healthy subjects and 98 patients suffering from different sleep disorders have been identified and quantified in terms of transition probabilities [7]. Transition patterns between sleep stages awake (W), non-REM1 (N1), non-REM2 (N2), non-REM3 (N3), non-REM4 (N4) and REM (R) are analysed in terms of probability distributions of symbolic sequences for young and old subjects with and without sleep disorder. Changes of these patterns due to ageing are compared with variations of transition probabilities due to sleep disorder. To characterize the corresponding transition matrices (see, for example, Fig. 7.32), we computed statistics like (normalized) joint entropy and spectral entropy distributions (WSE and HSE), and we performed a Markov order tests which revealed that considering two-step transitions (Markov order of 2) is suitable for sleep-stage transition analysis. Furthermore, changes of one-step transition patterns due to ageing and sleep disorders are discussed using (pruned) transition graphs as given in Fig. 7.32 showing a comparison of young subjects with and without sleep disorders. Patients suffering from sleep disorders exhibit a higher probability of transitions within light sleep N1-N2, less transitions within slow wave sleep N3-N4 and no significant change in N2-N3 transitions. Also transitions from N2 to REM sleep are reduced.

Figure 7.33: Phase diagram of visco-elastically coupled van der Pol oscillators (??) showing stability regions of (slow) in-phase and (fast) anti-phase oscillations for $\omega_1 = 0.57$ and $\omega_2 = 0.63$.



Synchronization of Visco-elastically Coupled van der Pol Oscillators

Synchronization and bifurcations of a pair of visco-elastically coupled van der Pol oscillators

$$\begin{aligned}
 \dot{x}_1 &= \overbrace{(1 - x_1^2)}^{\text{van der Pol oscillator}} \dot{x}_1 - \omega_1^2 x_1 + \overbrace{\omega_c^2 (\Delta x - d)}^{\text{elastic coupling}} \\
 \dot{x}_2 &= \overbrace{(1 - x_2^2)}^{\text{van der Pol oscillator}} \dot{x}_2 - \omega_2^2 x_2 - \omega_c^2 (\Delta x - d) \\
 \dot{d} &= \overbrace{\gamma (\Delta x - d)}^{\text{creep}}
 \end{aligned} \tag{7.1}$$

are investigated as a qualitative model of mechanical coupling of oscillating cardiomyocytes embedded in the extra cellular matrix. Figure 7.33 shows stability regions of in-phase and anti-phase oscillations in parameter plane given by the linear coupling parameter ω_c and the fluidity coefficient γ . Above a critical value of $\gamma \approx 0.76$ only orbits synchronized in-phase are stable.

Complex dynamics, coexisting attractors, and chaos has also been studied in different ionic cell models of cardiomyocytes, including a model for the Brugada syndrome, an electro-physiological disease which primarily affects the dynamics of the sodium ion channel and can lead to sudden cardiac death. Furthermore, the hierarchical structure of periodic windows in the bifurcation set of periodically driven oscillators has been studied in detail [8] as well as chances and challenges when estimating Lyapunov exponents from time series [9].

- [1] D. Rey, M. Eldridge, U. Morone, H.D.I. Abarbanel, U. Parlitz, J. Schumann-Bischoff, Phys. Rev. E **90**, 062916 (2014).
- [2] D. Rey, M. Eldridge, M. Kostuk, H. Abarbanel, J. Schumann-Bischoff, U. Parlitz, Physics Letters A **378**, 869-873 (2014).
- [3] J. Schumann-Bischoff et al., Chaos **25**, 053108 (2015).
- [4] U. Parlitz, J. Schumann-Bischoff, and S. Luther Phys. Rev. E **89**, 050902(R) (2014).
- [5] U. Parlitz, J. Schumann-Bischoff, and S. Luther Chaos **24**, 024411 (2014).
- [6] A. Schlemmer, S. Berg, T. K. Shajahan, S. Luther, and U. Parlitz, Entropy **17**, 950-967 (2015).
- [7] A. Schlemmer, U. Parlitz, S. Luther, N. Wessel, T. Penzel, Phil. Trans. R. Soc. A **373** (2034), 20140093 (2015).
- [8] V. Englisch, U. Parlitz and W. Lauterborn, Phys. Rev. E **92**, 022907 (2015).
- [9] U. Parlitz, Lecture Notes in Physics, accepted (2015).

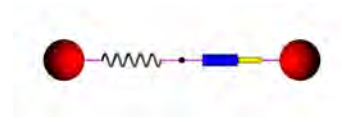


Figure 7.34: Visco-elastically coupled oscillators.

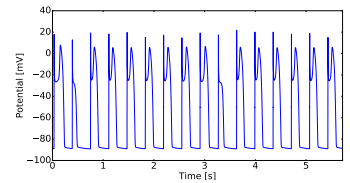


Figure 7.35: Chaotic action potentials of an ionic cell model of the Brugada syndrome.

7.17 OSCILLATORY ACTIN INSTABILITIES AND MOTILITY STATISTICS OF AMOEBOID CELLS

H. Hsu, J. Negrete Jr., N. Scholand, A. Pumir, C. Beta, M. Tarantola, E. Bodenschatz, C. Westendorf, A. Gholami, C. Blum, A. Bae, V. Zykov

Actin-driven membrane protrusions are a key component underlying the locomotion of eukaryotic cells. Noise intrinsic to the biochemical networks affects their extension and with it the efficacy of directional cell migration. We investigate how this noise impacts the dynamics of cell migration and how it couples to the intracellular actomyosin cytoskeleton that drives the spatio-temporal pseudopod dynamics. We examine these phenomena exemplarily for *D. discoideum* cells, for which many of the biochemical networks carry over to mammalian cells. We expect results from our fundamental investigations to contribute to the understanding of immune system cells and cancer metastasis.

We develop a model based on Langevin equations (Fig 7.36A) to quantify the deterministic and noisy (additive and multiplicative) parts of cell migration [1, 2]. We measure these parameters for wild-type cells and cells where regulators of de-/ polymerization (Coronin, Aip1) and contractility (Myosin II) are knocked out. We find that only the lack of Coronin evokes a reduction of deterministic migration components. All knock-out cells, however, show a modified additive noise, while the multiplicative noise remains unaffected. We find cells to be close to the onset of oscillations of the intra cellular actin network [3]. By applying controlled chemical stimuli to individual cells in microfluidic devices (arrow in Fig. 7.36B) we prove that chemotacting cells have highest sensitivity at low metabolic costs. We also observe that the recovery after chemical stimulation reflects slow time scales associated with cell polarization [4]. We quantitatively assess the dynamics of these regulators and discover that cells show robustness in the actin-polymerization phase, enabling a reliable formation of pseudopods irrespective of large variations in receptor inputs (Fig. 7.36C). We detect a monotonous increase between the depolymerization time of the actin network and the amplitude of activity (Fig. 7.36D) [5]. Surprisingly cells in the oscillatory phase do almost not incorporate Arp2/3, suggesting mainly linear loose cytoskeletal matrix. The lack of myosin II has no effect on this behavior; it is however essential for regulating actomyosin cortex dynamics [6].

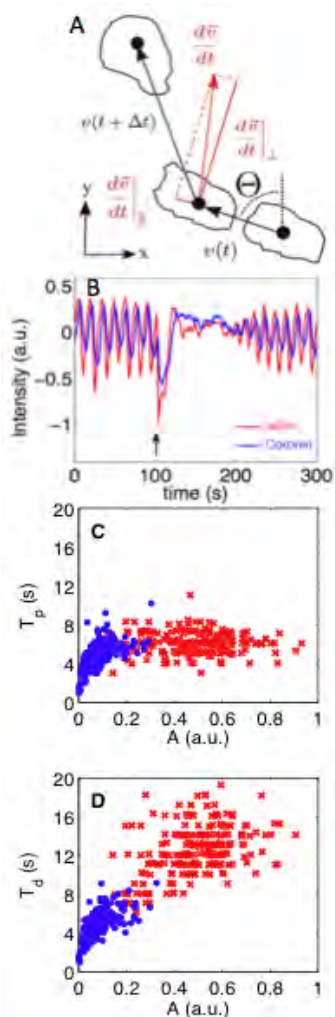


Figure 7.36: (A) Stochastic description of chemotaxis. (B) Oscillatory cell responding to chemical perturbation (arrow). (C) & (D) Relation between oscillatory cells (blue) and chemical-stimulating cells (red). (C) Actin-polymerization time (T_p) v.s. response amplitude (A). (D) Actin-depolymerization time (T_d) v.s. A .

- [1] G. Amselem, M. Theves, A. Bae, C. Beta, E. Bodenschatz, Phys. Rev. Lett. **109**, 108103 (2012).
- [2] G. Amselem, M. Theves, A. Bae, E. Bodenschatz, C. Beta, PLoS ONE **7**, e37213 (2012).
- [3] C. Westendorf, J. Negrete, A. Bae, Rabea Sandmann, E. Bodenschatz, C. Beta, Proc. Natl. Acad. Sci. USA, **110**, 3853 (2013)
- [4] J. Negrete, A. Pumir, H. Hsu, C. Westendorf, M. Tarantola, C. Beta, E. Bodenschatz, preprint
- [5] H. Hsu, E. Bodenschatz, C. Westendorf, A. Gholami, V. Zykov, M. Tarantola, C. Beta, preprint
- [6] H. Hsu, M. Tarantola, C. Beta, E. Bodenschatz, preprint



NETWORKS



From vascular networks in animals and plants to route networks in public transport, from neural circuits in the brain to power grids spanning entire continents – systems with fascinating complex webs of interactions permeate every aspect of our lives. Understanding how these networks are organized and how they behave dynamically constitutes a challenging endeavor of current cross-disciplinary research and bears a growing potential for applications. Complex webs constitute a major thrust at the MPIDS and are represented by a wide variety of projects, ranging from the applied, such as novel approaches to distributed public transportation, the biological transport or neural network function, to the more abstract, such as the study of limits to network inference.

CONTENTS

- 8.1 Pruning to increase particle spread in transport networks 136
 - 8.2 The form and function of biological flow networks 137
 - 8.3 The encoding bandwidth of the cortical gateway 139
 - 8.4 Neuronal sodium channels: surface density and kinetics 140
 - 8.5 Nano-physiology of the action potential generator 141
 - 8.6 Modelling the role of neural oscillations in information routing 142
 - 8.7 Attractor basins of stable state sequences in balanced circuits of spiking neurons 143
 - 8.8 Selective processing in neuronal circuits 144
 - 8.9 Information processing in neural networks 146
 - 8.10 Dynamics and self-organization in brain networks 147
 - 8.11 Connectomics through dynamics: Revealing synaptic connectivity from spikes 149
 - 8.12 *EcoBus* – flexible public mobility 150
 - 8.13 Characterization and Reconstruction of Complex Networked Systems 152
 - 8.14 Model-free inference of networks from dynamics 153
 - 8.15 Dynamically smart power grids: Collective stability, economy and control 154
 - 8.16 Signal propagation and integration in adapting tubular networks 155
 - 8.17 Biodiversity and extinction 157
-

8.1 PRUNING TO INCREASE PARTICLE SPREAD IN TRANSPORT NETWORKS

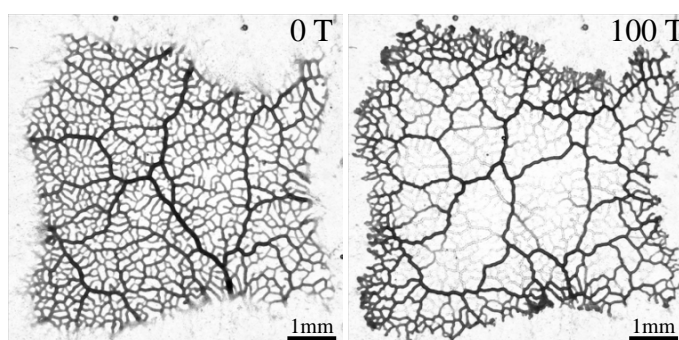
K. Alim, N. Andrew

M. P. Brenner (Harvard, USA), S. Marbach (ENS Paris, France)

A. Pringle (University of Wisconsin, USA)

Transport via fluid flowing through a tubular network is of widespread interest for a variety of technological application and biological transport networks. Often we have a measure of flows in a network but predicting the spread of particles even when the flow is stationary is a theoretical challenge. We study one of nature's tubular transport networks the slime mold *Physarum polycephalum* to measure how the topology of the network and the hierarchy of tube radii affect the transport of particles [1]. We developed a method to efficiently map out the

Figure 8.1: Pruning as observed in bright-field images of a *P. polycephalum* individual cut-off from a larger network (*left*) and same pruned individual 100 contraction periods later (*right*).



effective dispersion from any particle initiation site throughout a network with non-stationary but periodic fluid flows. We use this method to study the change in dispersion patterns as the network adjusts its morphology over time (see Fig. 8.1). We find that the pruned state presents in average higher transport capabilities than the initial state. Central tubes concentrate the flow in the pruned state, allowing higher flow velocities in the overall network. Finally we study the influence of hierarchy of tube radii by comparing the un-pruned and pruned states to their counterparts with all tube radii equal. We find that the hierarchy of radii influences the dispersion patterns at the local scale, whilst the change in the average transport capabilities is small.

We believe that the effective dispersion introduced by us is a universal measure for transport in stationary and non-stationary but periodic flows that can elucidate the dynamics of particle spread in technologically relevant as well as biological networks. By observing *P. polycephalum* we learned that pruning increases transport properties tremendously - a fact that is also relevant for technological applications. It is fascinating to speculate that also pruning in other biological systems as for example during vessel development in zebrafish brain [2] serves a similar objective of enhanced effective dispersion.

[1] S. Marbach, K. Alim, N. Andrew, A. Pringle, M. P. Brenner, under review

[2] Q. Chen, L. Jiang, C. Li, D. Hu, J.-w. Bu, D. Cai, J.-l. Du, PLoS Biol. **10(8)**, e1001374 (2012)

8.2 THE FORM AND FUNCTION OF BIOLOGICAL FLOW NETWORKS

E. Katifori

Henrik Ronellenfitch, Jana Lasser, Desislava Todorova, Carl Modes (Rockefeller)

Both plants and animals have developed circulatory systems of striking complexity to solve the problem of nutrient delivery and waste removal. Despite their complexity and variability, their vascular networks obey some basic universal design principles, such as large vessels primarily serving long distance transport and small vessels primarily occurring at exchange sites. Typically, circulatory systems have to satisfy competing demands that have resulted in topologically complex and heterogeneous, hierarchical vascular structures. Hierarchical reticulate vascular structures in particular are ubiquitous in biological systems but their theoretical underpinnings are rather sparse.

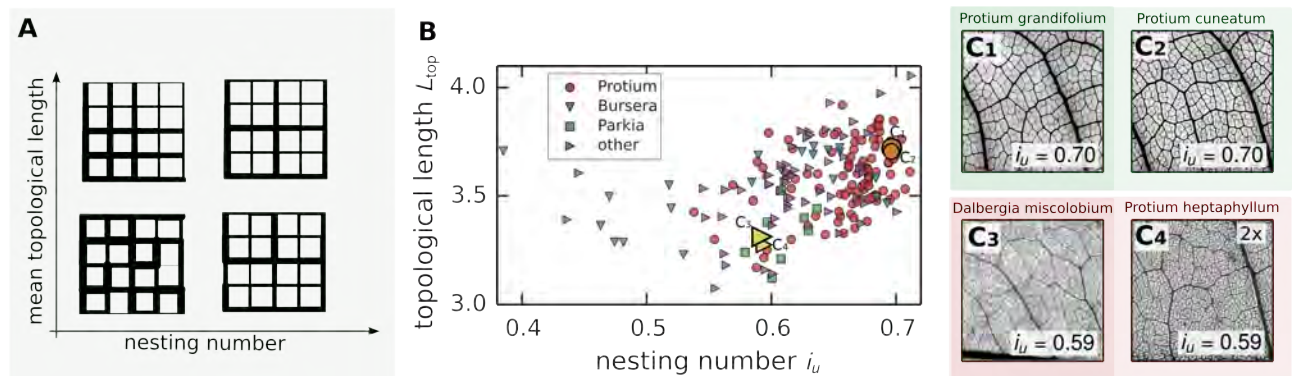


Figure 8.2: (A) Typical networks exhibiting various combinations of vein tapering and loop nestedness. (B) Plot of the whole dataset consisting of 186 leaf networks depending on the nesting number and mean topological length. One leaf of *Protium grandifolium* (*Dalbergia miscalobium*) is marked by a circle (triangle) with black border as well as shown in C₁ (C₃). The smaller circles (triangles) in the same color show the nearest neighbor according to the topological metrics. (C) Images of the same leaves as those specially marked in (B), together with their nearest neighbors C₂ and C₄. All images except for C₄ show a 1cm × 1cm crop of the original scan. Image C₄ was zoomed in by a factor of 2.

We have built theoretical and computational models and investigated the design principles in the vascular architecture of plants. We developed nuanced topological metrics to characterize and quantify these principles. We used ideas inspired by computational topology to define two new metrics, the topological nestedness and the mean topological length, suitable to quantify the architecture of higher order venation of leaves. We have found that the topological nestedness, the way in which higher order loops nest into lower order ones (quantified by the nesting number), is a metric that is robust to noise and can provide information about the leaf vein architecture that is not captured by traditional geometrical information metrics, such as edge weight or junction angle distributions. The mean topological length quantifies the average length of tapered veins and like the topological nestedness, its value depends not on exact measurements of vein diameters but only on relative order. Fig. 8.2A shows a qualitative representation of

various example network topologies using mean topological length and nesting number.

We applied our topological metrics to a dataset of 186 leaves and leaflets representing 137 species, digitized at high resolution (6400 dpi) and vectorized it using a general computational framework we developed in house [2]. We have shown the topological nestedness, along with the average tapered vein length can be used as a classification tool that groups together leaves with similar phenotypes and thus can aid in species identification in cases where the whole leaf is not available, as is frequently the case in fossils (Fig. 8.2B). We demonstrated that our characterization constitutes a new phenotypic trait in plant leaves and carries information orthogonal to previously used, mostly geometric quantities [3] (vein density σ , mean distance between veins a , mean areole area A , areole density ρ_A , and average vein diameter weighted by length of venation between junctions d , see Fig. 8.3A). We showed that adding topological information to geometrical one significantly improves identification of leaves from fragments by calculating a leaf venation fingerprint from topology and geometry (Fig. 8.3B).

This work opens the path to new quantitative identification techniques for leaves which go beyond simple geometric traits such as vein density and is directly applicable to other planar or sub-planar networks such as blood vessels in the brain. However, as originally formulated it is only applicable to planar graphs. Keeping in mind potential applications in reticulate animal vascular networks, we generalized our classification algorithm to 3D networks [4].

The function of the plant vascular system is not determined only by the topology of the network, but also by the properties of the individual network “links”, the plant xylem vessel elements. The vessels are frequently ornamented with ring-like, helical or striated corrugations. Several groups have speculated on the function of those corrugations, which has typically considered to be reduction of hydrodynamic resistance and structural reinforcement of the vessel elements. We investigated the potential biological role of the fluid recirculation in the corrugations (see Fig. 8.4). In particular, we found that, contrary to what was generally believed, building secondary cell wall and corrugations actually increase the hydrodynamic resistance compared to smooth vessels of equal diameter. We investigated the relative decrease in hydrodynamic efficiency because of the corrugations as compared to the increase in structural stability. We developed a model that predicts the relative importance of flow and mechanics for each design and are now testing it against published data for xylem anatomy of different species.

- [1] E. Katifori, M. O. Magnasco PloS one 7 e37994 (2012).
- [2] Jana Lasser, *Computational Analysis Framework for Vascular Network Images*, Univ. Goettingen, Bachelor thesis, (2013).
- [3] H. Ronellenfitch, J. Lasser, D. Daly, E. Katifori, *Topological phenotypes of leaf vascular networks*, submitted (2015).
- [4] C. M. Modes, M. O. Magnasco, E. Katifori *Extracting Hidden Hierarchies in 3D Distribution Networks*, arXiv:1410.3951v1, submitted (2015).

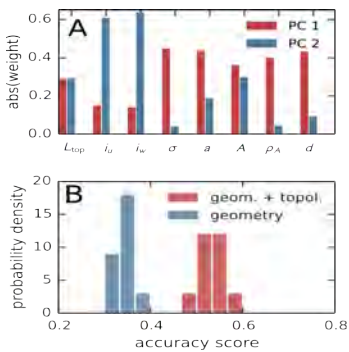


Figure 8.3: (A) Weights of geometrical and topological 8 metrics, in the first two principal components of the dataset. Component 1 contains mostly geometry, Component 2 mostly topology ((un)weighted nesting number $i_{(u)w}$ and topological length L_{top}). (B) Results of leaf identification from fragments using Linear Discriminant Analysis (LDA). The plot shows histograms of the resulting accuracy scores. [?].

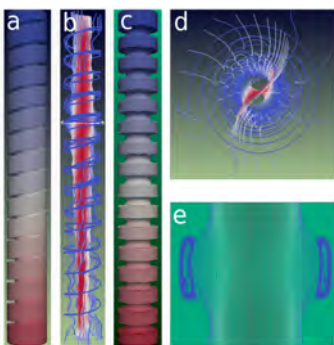


Figure 8.4: Flow streamlines in helical and annular pipes. Shown is the pressure drop along a helical (a) and an annular pipe (c). In (b) and (d) are shown flow streamlines (side and top view) corresponding to case (a). In (e) we plot the streamlines of the flow in the annular geometry from (c). The red color-coding corresponds to higher values of the pressure and velocity magnitude.

8.3 THE ENCODING BANDWIDTH OF THE CORTICAL GATEWAY

Andreas Neef, Fred Wolf

Mike Gutnick (Hebrew University), Omer Revah (Hebrew University)

Somatosensory information enters the primary sensory cortex through thalamic axons that innervate spiny stellate (SpSt) cells in cortical layer 4. We showed earlier [1], that the population of layer 2/3 pyramidal cells (Pyr), the main target of SpSt cells output, can encode input changes in less than a millisecond. Their large dendritic tree might significantly contribute to this ability [2]. It is intuitively clear that the entry site for thalamic information, i.e. SpSt cells, should have an encoding bandwidth at least as wide as those of later processing stages, i.e. layer 2/3 and layer 5 Pyr cells. However, SpSt cells feature the smallest dendritic compartment of all excitatory cortical neurons, which leads to the expectation that they have a severely limited bandwidth. This discrepancy between a required wide bandwidth at the entry level and an expected severely limited bandwidth prompted us to explore whether SpSt cells employ compensatory mechanisms to retain a high bandwidth of information encoding in the absence of large dendrites.

We find that SpSt cells employ two compensatory mechanisms to obtain a superior bandwidth for information encoding. Firstly, the sub-threshold synaptic input fluctuates much slower in SpSt cells¹ than in Pyr cells and that leads to an enhanced encoding (Figure 8.6 B, C). This is the first report of such a mechanism employed in neural encoding. Secondly, the detrimental effects of small dendritic tree are reduced by a reduction in soma size.

With a combination of experimental and theoretical approaches, we revealed how different biophysical principles are at play to allow for ultra-fast processing of somato-sensory input during cortical processing.

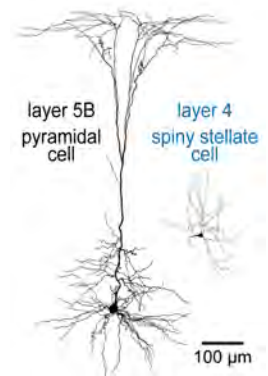


Figure 8.5: Spiny stellate cells are the smallest excitatory cells in the cortex

1. Due to the presence of an unconventional NMDA receptor, operating already at subthreshold voltages [3]

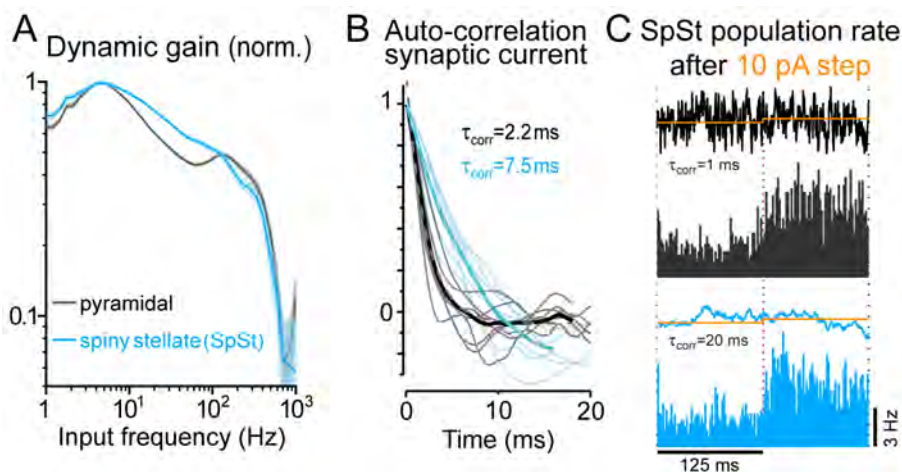


Figure 8.6: **A** SpSt cells' encoding bandwidth is only marginally smaller than those of Pyr cells. **B** Synaptic currents change much slower in SpSt cells. **C** SpSt population rate rapidly encodes input changes embedded in fluctuations. An ideal observer was faster to detect a step in the input (not shown) when the background fluctuations had a longer correlation time (blue).

- [1] T. Tchumatchenko, F. Wolf et al. *J. Neurosci.* **31**, 34 12171 (2011)
- [2] G. Eyal, et al. *J. Neurosci.* **34**, 24 8063(2014)
- [3] I.A. Fleidervish A.M. Binshtok, M.J. Gutnick *Neuron* **21** 1055 (1998)

8.4 NEURONAL SODIUM CHANNELS: SURFACE DENSITY AND KINETICS

Andreas Neef, Fred Wolf

Mike Gutnick (Rehovot), Ilya Fleidervis (Be'er Sheva)

2. Hodgkin and Huxley [1] pioneered the combination of quantitative analysis of unclamped action potential plus voltage-clamp characterization of selective conductances. Intricate morphology and diverse ion channel populations vastly complicate equivalent studies in mammalian cortical neurons.

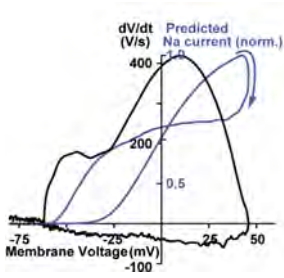
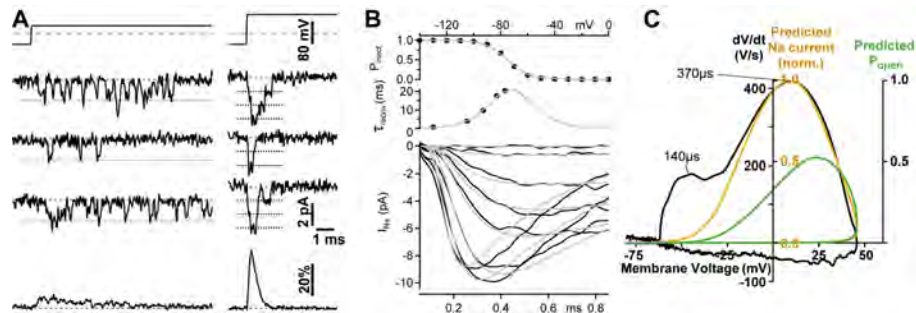


Figure 8.7: The Na^+ -channel model [2] used in the Blue-BrainProject is driven with a recorded AP (phaseplot in black). The predicted somatic Na^+ -current (blue) is inconsistent with the AP waveform, indicating a faulty model.

Models of Na^+ -channels form the basis of our biophysical understanding of action potential (AP) initiation and hence of information encoding. Due to this important role, Na^+ -channels have been studied for decades². However, even widely accepted and used Na^+ -channel models do not pass a fundamental test of consistency (Figure 8.7): the current, which a model generates in response to a recorded somatic AP waveform, should be compatible with the notion that the AP upstroke is mainly shaped by the somatic Na^+ -current: $\dot{V}_{mem} \cdot C = -I_{Na} - I_{leak} - I_{lateral} \dots$ Any large discrepancy between $\dot{V}_{mem}(V_{mem})$ and $I_{Na}(V_{mem})$ during the upstroke suggests a faulty model (Figure 8.7). This prompted us to develop a new model, derived from our own high-resolution measurements, the first measurements to combine minimally invasive cell-attached recordings at single channel resolution with appropriate time resolution necessary to resolve the kinetics of Na^+ -channel activation (Figure 8.8A). We obtained a Markov model for Na^+ -channel gating that reliably describes the currents evoked by voltage steps (8.8B). Importantly, the model also passes the consistency test (Figure 8.8C), although it has not been optimized for this task at all.

The accurate description of somatic Na^+ -channels (Figure 8.8C) even allows for a quantitative interpretation of the dynamics of action potential waveform. Having directly measured most of the parameters in this equation: $\dot{V}_{mem} \cdot C = -N_{chan} \cdot P^{open} \cdot i_{Na}(V_{mem}) - I_{leak} - I_{lateral}$, a strict lower bound for the Na^+ -channel density N_{chan}/A of 10 channels per μm^2 can be derived; about *twice as much* as previously thought. A more elaborate estimate yields even 30 Na^+ -channels per μm^2 . We currently use the accurate model and these somatic channel density to obtain a mechanistic understanding of information encoding capabilities of neurons.

Figure 8.8: **A** Single channel resolution yields single channel current amplitudes $i_{Na}(V)$ and open probability p^{open} **B** Modelled waveforms (gray) closely match measured (black) activation kinetics (bottom) and inactivation properties (top) **C** The new model passes the consistency test (see Figure 8.7).



[1] A. L. Hodgkin and A. F. Huxley, J Physiol **117**, 4 500 (1952)
 [2] C. M. Colbert and E. Pan, Nat Neurosci **5**, 6 533 (2002)

8.5 NANO-PHYSIOLOGY OF THE ACTION POTENTIAL GENERATOR

Andreas Neef, Fred Wolf

Mike Gutnick (Rehovot), Elinor Lazarov (Rehovot), Melanie Dannemeyer

A few tens of micrometers into the axon, special cytoskeletal proteins organize those ion channels that generate the action potential (AP) output of a neuron. This organelle, the axon initial segment (AIS), features a corset-like cytoskeleton with parallel rings of actin, regularly spaced by spectrin fibres [1]. The ion channels are tethered there through an adaptor protein, AnkyrinG. Whether this recently discovered near-crystalline spatial arrangement has any impact on the function of the axon initial segment was unclear, especially as the space constant is only 190 nm, a negligible distance for cellular electrodynamics (Figures 8.9 and 8.10B). We succeeded, for the first time, in altering the encoding properties of neurons by means of specific changes to the regular cytoskeleton. We found that the *qv3J* mutation of β IV-spectrin leads to a complete loss of this spectrin isoform. Only β II-spectrin remains to recruit some Na^+ -channels to the AIS. While the somatic and dendritic Na^+ -channel densities developed normally, the density in the AIS of mutants remained low over the course of cell maturation. Control cells, on the other hand, incorporated more and more Na^+ -channels into the AIS during maturation. Mature mutant cells showed a significantly higher AP voltage threshold and their AP waveform lost the rapid initial increase in voltage rate of rise, reflecting a loss of current from the initial segment. As a result, the ability of mutant neurons to encode rapid changes in the input was impaired (Figures 8.10C). In contrast, peak rate of rise, peak potential, and AP duration appeared virtually unaffected. We conclude that in order to ensure that APs are always initiated in the AIS, the number of axonal Na^+ -channels must

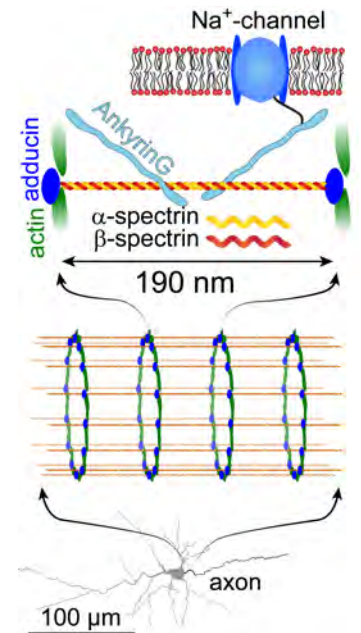


Figure 8.9: Schematic of AIS cytoskeleton.

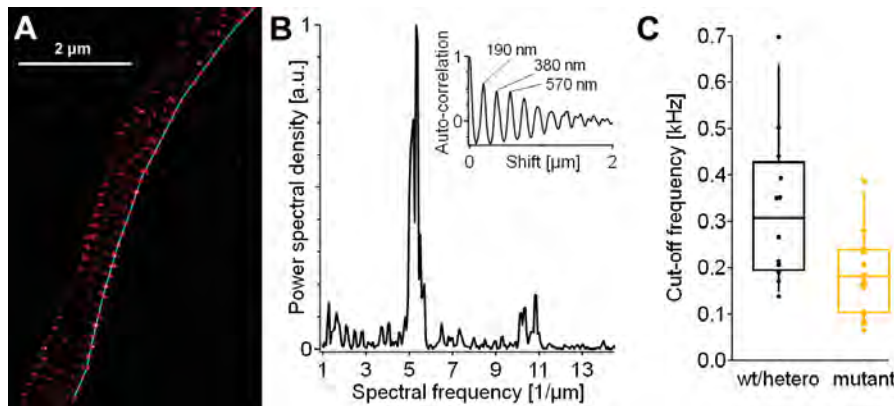


Figure 8.10: **A** Single fluorophore localization microscopy from antibodies against β IV-spectrin reveals the regularity of the cytoskeleton. **B** The power spectrum of the localization probability along the line indicated in **A** reveal strong regularity, the typical distance is 190 nm (auto-correlation as inset). **C** Neurons with mutated β IV-spectrin perform worse at encoding high input frequencies.

increase as the cells mature, since more and more current is required to depolarize the growing somato-dendritic compartment. A functional C-terminus of β IV-spectrin is essential to provide sufficient numbers of Na^+ -channel binding sites and thereby maintains the AIS as the AP initiation site and the ability to encode fast changes in the input.

[1] K. Xu, G. Zhong, X. Zhuang, *Science*, **339**, 6118-6122 (2013)

8.6 MODELLING THE ROLE OF NEURAL OSCILLATIONS IN INFORMATION ROUTING

M. Helmer, A. Palmigiano, D. Battaglia, T. Geisel, F. Wolf

It has been hypothesized that dynamic patterns of oscillatory coherence modulate the direction and the efficiency of communication between different brain regions. We have directly confirmed this hypothesis, studying information routing in simple multi-areal circuits and verifying that changes of phase-locking induce rerouting of information transfer [1]. However, in this early study, the simulated oscillations were unrealistically persistent. In contrast, oscillations *in vivo* are transient and their frequency varies stochastically [2]. We have recently generalized our model of inter-areal information routing to operate in a regime, which we call the “edge of synchrony”. In such a regime, collective oscillations are meta-stable, but self-organize to give rise to transient episodes of phase-locking, which still regulate information transfer. We thus prove that stochasticity of oscillations *in vivo* is not incompatible with their use for flexible routing [3].

Figure 8.11: State-resolved Transfer Entropy analyses reveal that the direction and efficiency of information transfer is still regulated by oscillatory phase coherence, even at the edge of synchrony where it is highly transient.

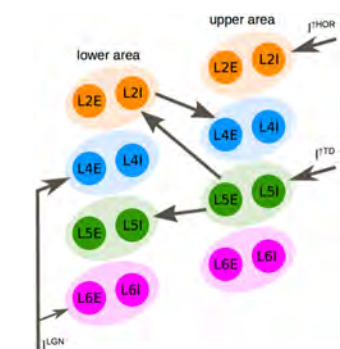
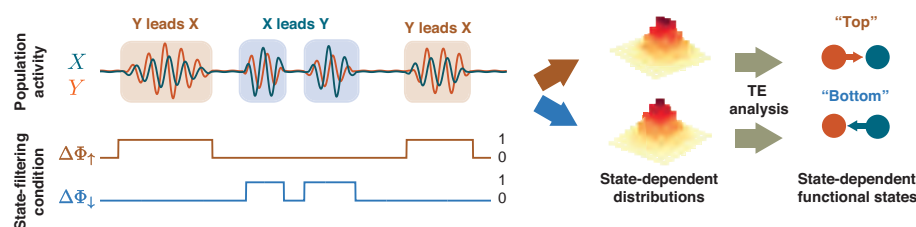


Figure 8.12: When multiple brain regions are wired according to canonic cortical connectivity, our model reproduces the experimental finding that top-down and bottom-up inter-areal communication operate in different frequency bands.

Recent massively parallel electrophysiological recordings suggest that communication-through-coherence in different directions exploits different frequency bands. Fast oscillations would mediate bottom-up communication, while beta or even slower oscillations top-down influences from higher order cortical areas [4]. We have studied a mean field model of two model regions wired according to the so called canonic local and long-range cortical connectivity [5]. Such a model automatically causes different cortical layers to oscillate at different frequencies as an effect of chaotic inter-layer entrainment. As a result, the emergent frequency-dependent patterns of inter-areal phase-locking naturally reproduce experimental findings. We show that this effect would not occur in random circuit, thus proving that the experimentally observed connectivity affects dynamics in a highly specific manner. However we also predict that other functionally-equivalent connectomes may exist, by constructing suitable examples.

- [1] D. Battaglia, A. Witt, F. Wolf, and T. Geisel, PLoS Comp Biol 8, e1002438 (2012).
- [2] D. Xing, Y. Shen, S. Burns, C.-I. Yeh, R. Shapley, and W. Li, Journal of Neuroscience 32, 13873 (2012).
- [3] A. Palmigiano, T. Geisel, F. Wolf, D. Battaglia, under review
- [4] A. M. Bastos, J. Vezoli, C. A. Bosman, J.-M. Schoffelen, R. Oostenveld, J. R. Dowdall, P. De Weerd, H. Kennedy, and P. Fries, Neuron 85, 390 (2015).
- [5] M. Helmer, X. J. Chen, W. Wei, F. Wolf, and D. Battaglia, bioRxiv (2015).

8.7 ATTRACTOR BASINS OF STABLE STATE SEQUENCES IN BALANCED CIRCUITS OF SPIKING NEURONS

M. Puelma Touzel, M. Monteforte, R. Engelken, F. Wolf

In the brain, information is processed by dynamically generated sequences of circuit activity states encompassing thousands of neurons. Although fundamental to information processing, the phase space structure of circuits of spiking neurons remains poorly understood. Recently, a collective phase of cortex-like circuit activity was discovered [1] that naturally partitions the phase space into a rich set of diverging attractor basins of complex stable network state trajectories. We have developed a theory for the geometry and scaling properties of their attractor basins. We find they are structured by the preimages of future spike crossing events involving particular network connectivity motifs. We examine the statistical mechanics of their random geometry by introducing and averaging a function dependent on the microstate with zeros at the basin boundaries. This theory provides a foundation for the rational design of spiking circuits that use intrinsic stable spiking patterns for neuronal computation.

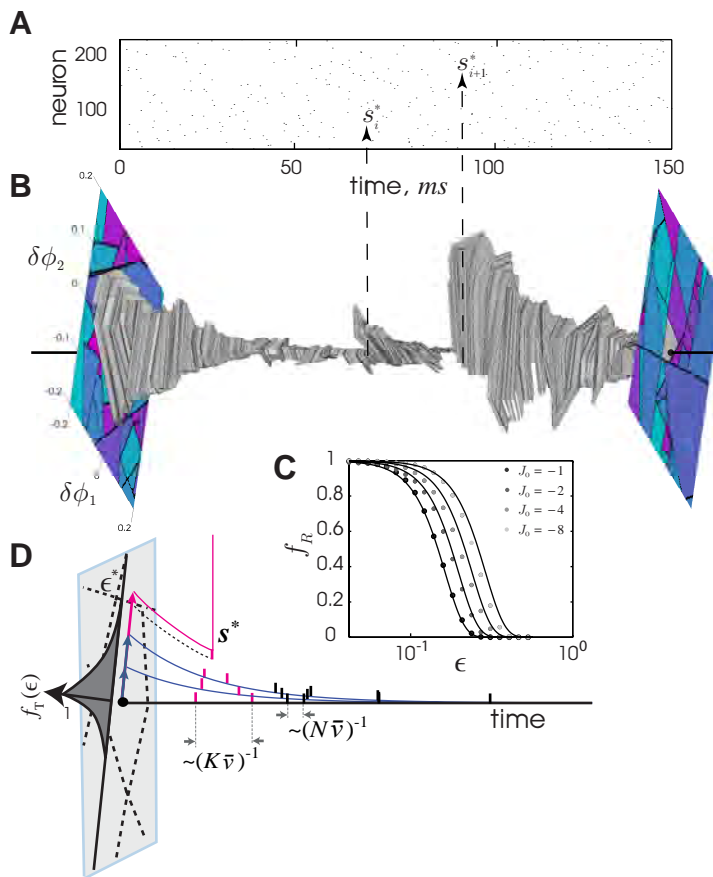


Figure 8.13: (A) Neuron index versus time showing spike times from all neurons of the given attracting trajectory, $\phi(t)$, in a 150 ms window ($N = 200$, $K = 50$). (B) 2+1D folded phase space volume, $(\delta\phi_1, \delta\phi_2, t)$, centered around $\phi(t)$ located at $(0, 0, t)$ (black line). The center basin is filled grey, and the two cross-sections, $(\delta\phi_1, \delta\phi_2, 0)$ and $(\delta\phi_1, \delta\phi_2, 150)$ are shown. The basin size decays exponentially but can undergo abrupt jumps at spikes, e.g. s_i^* and s_{i+1}^* , corresponding to crossings of spikes from neurons that share a connection. (C) The fraction of restored perturbations, f_R , as a function of the perturbation strength, ϵ , for different values of the coupling strength, J_0 , with the expression for ϵ_{ft} . (D) A schematic illustration of the boundary contracting with the phase space until the crossing event and the boundary flagging function, f_T .

- [1] Monteforte, M., Wolf, F. (2012). Dynamic Flux Tubes Form Reservoirs of Stability in Neuronal Circuits. *Physical Review X*, 2(4), 112. doi:10.1103/PhysRevX.2.041007
- [2] M.Puelma Touzel, F. Wolf (in preparation) (2015)

8.8 SELECTIVE PROCESSING IN NEURONAL CIRCUITS

S. Jahnke, W.-C. Chou, M. Timme

D. Breuer (Potsdam), A. Fiala (Göttingen), C. Kirst (Rockefeller), R.-M. Memmesheimer (Nijmegen and New York)

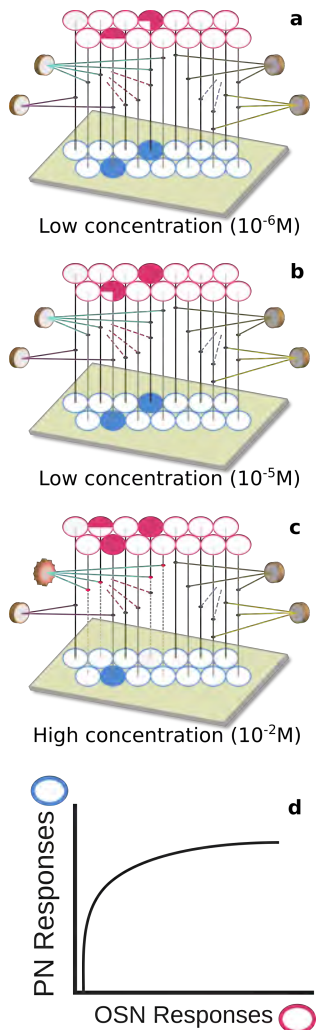


Figure 8.14: **Selective inhibition induces concentration-invariant and nonlinear circuit response.** Increasing odor concentration increases the activity of sensory neurons (red circles, filling indicates activity) in primary olfactory circuits. (a,b)

Output representations are invariant to moderate concentration changes due to (d) the nonlinearity of signal transformation from the input layer to the output layer (blue circles).

(c) Once selected, inhibitory local interneurons (lateral red circles) become activated at high concentrations; such feedback inhibition blocking partial pathways between layers changes the representations at the output, differentiating patterns of different concentrations for the same odor.

Spatially and temporally coordinated patterns of neural activity are key to information processing in the brain. Yet, their dynamical origin and the mechanisms underlying pattern-based processing is far from being understood. In two project areas, we study how heterogeneous network structure and non-additive coupling may induce selective processing at the circuit level: (A) in the primary circuits of olfactory sensory processing and (B) specifically coordinated activity patterns in cortical networks.

(A) Multiple olfactory functions via selective inhibition?

The first olfactory processing circuits of both insects and vertebrates exhibit a number of astonishing collective nonlinear functions. These include generating concentration-invariant input encodings [1], classifying odor mixtures into discrete states [2], and modulating the separation between representations of odor pairs [3]. For instance, it was long believed that the antennal lobe basically separates representations of inputs resulting from two different odor signals, such that their representations on the sensory neuron level have substantially larger overlap than on the level of projection neurons. Our complementary joint work with the Molecular Neurobiology group of Andre Fiala (University of Göttingen) now suggests that the same antennal lobe may also join representations of other pairs of odors [3].

How the wide range of collective olfactory functions dynamically emerges from the neuronal units and their wiring into a circuit, however, is not known. We propose a conceptual model of first olfactory processing circuits demonstrating that selective heterogeneous [4] rather than average (mean field) inhibitory circuit connectivity, combined with saturating input-output characteristics of individual local units contributes to explaining all of these computational functions simultaneously (Fig. 8.14). In particular, such selective inhibition may play a central role in reshaping odor representations between sensory and projection (output) neurons by inhibiting activities of specific subsets of output neurons, thereby offering a combinatorial number of functional options. These results indicate that selective lateral wiring of first olfactory processing circuits, together with the nonlinear response properties of their local units jointly create their complex collective functions.

Intriguingly, besides a common nonlinear local filter, such connection selectivity alone may explain all of the above unexplained collective functions at once [5].

(B) Selective information transmission via non-additive coupling?

Recent neurophysiological experiments [6] found that under certain conditions the neuronal dendrites – branched projections of the neuron that transmit inputs from other neurons to the cell body (soma) – process input signals in a non-additive way: If two or more input spikes

(action potentials) arrive in sufficiently close temporal and spatial proximity, the dendrite can actively generate a fast nonlinear electric voltage excitation, a 'fast dendritic spike'. Such an excitation then propagates to the neuronal soma, inducing a somatic response that is nonlinearly amplified. This response is temporally highly precise and supports the detection of synchronous inputs by a neuron. Our results suggest that such nonlinear dynamic features of local neurons contribute a key mechanism for information transmission in neural circuits to be robust and reliable.

Fundamental analytical studies of single neurons and neural circuits with non-additive dendritic interactions [7, 8, 9, 10] reveal how non-additive dendritic interactions enable guided signal propagation and information transmission even in entirely random cortical circuits. Simulational studies further support that neuronal non-additivities specifically and dynamically change processing with input synchrony. As such, non-additive coupling dynamically enhances circuit function, as relevant, e.g., in hippocampal and other neocortical circuits. Our study thus adds a novel view on the dynamics of networks with nonlinear interactions in general and offers a viable route for the occurrence of patterns of precisely timed spikes in recurrent networks under physiologically plausible conditions.

In fact, our findings may severely change our perspective on how various neural circuits compute: For example, neuronal oscillations induce resonances between propagating signals and oscillations emerge, and they thus, besides supporting signal transmission in general, provide a mechanism to selectively activate different pathways (Fig. 8.15) [11]. Such oscillations might naturally emerge in networks with broad degree distribution of synaptic connections [12]. Further, our results provide an explanation of how hippocampal activity patterns, where previously learned spike sequences are replayed in conjunction with global high-frequency oscillations, are dynamically generated [13].

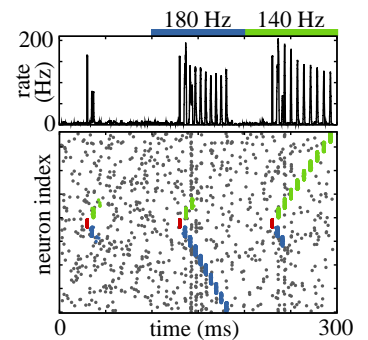


Figure 8.15: **Selective activation of signal transmission pathways by (background) oscillations.** A synchronous signal (red) extinguishes in the absence of oscillations (left), but might be selectively guided along weak feed-forward structures of a random network by oscillations of different frequencies (blue: 180Hz, green: 140Hz) [11].

- [1] M. Stopfer, V. Jayaraman, G. Laurent, *Neuron* **39**, 991 (2003).
- [2] J. Niessing, R. Friedrich, *Nature* **465**, 47 (2010).
- [3] T. Niewalda et al., *PLoS One* **6**, e24300 (2011).
- [4] Y.-H. Chou et al., *Nature Neurosci.* **13**, 439 (2010).
- [5] W.-C. Chou, A. Fiala, M. Timme, in prep. (2015).
- [6] G. Ariav, A. Polsky, J. Schiller, *J. Neurosci.* **23**, 7750 (2003).
- [7] R.-M. Memmesheimer, M. Timme, *PLoS Comput. Biol.* **8**, e1002384 (2012).
- [8] S. Jahnke, M. Timme, R.-M. Memmesheimer, *Phys. Rev. X* **2**, 041016 (2012).
- [9] S. Jahnke, R.-M. Memmesheimer, M. Timme, *Front. Comput. Neurosci.* **7**, 153 (2013).
- [10] D. Breuer, M. Timme, R.-M. Memmesheimer, *Phys. Rev. X* **4**, 011053 (2014).
- [11] S. Jahnke, R.-M. Memmesheimer, M. Timme, *PLoS Comput. Biol.* **10**, 1003940 (2014).
- [12] S. Jahnke, R.-M. Memmesheimer, M. Timme, *Phys. Rev. E* **89**, 030701 (2014).
- [13] S. Jahnke, M. Timme, R.-M. Memmesheimer, *J. Neurosci.*, in press (2015).

8.9 INFORMATION PROCESSING IN NEURAL NETWORKS

T. Geisel, A. Levina, V. Priesemann

E. Bullmore, O. Paulsen, M. Schroeter (U Cambridge), T. Deller, A. Vlachos, M. Wibral (U Frankfurt), J. Lizier (U Sydney)

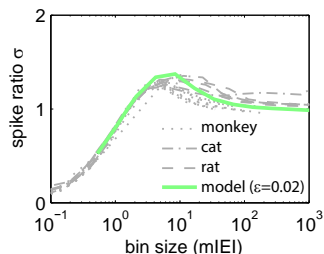


Figure 8.16: Spiking activity from monkey, cat and rat reflected a slightly sub-critical state (distance to criticality $\epsilon = 0.02$ (see [3])).

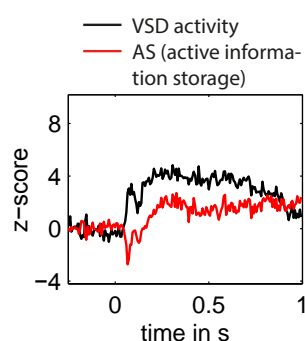


Figure 8.17: This figure shows the dynamics of active information storage (AS). With stimulus onset, AS transiently turned negative (“surprise”). During the stimulus, AS was positive, reflecting the maintenance of stimulus information in the neural activity of the cat visual system (area 17/18). The VSD activity, at the same time was positive and slowly decayed (see [5]).

How do neural networks provide the basis for reliable, yet flexible information processing *in vivo*? Theoretical predictions suggest that neural networks should self-organize to a critical state, because this dynamical state maximizes information processing capacity in models. We investigated this relation in developing neural networks *in vitro*. We showed that with maturation the networks approached criticality, and at the same time showed a more than 100 fold increase in processing capacity (quantified by transfer entropy and active information storage [1]). Importantly, the processing capacity diverged at criticality, thereby providing first evidence for the theoretically predicted link between dynamical state and computational capacity [2].

Criticality maximizes processing capacity. For brains, however, criticality also comes with the risk of instability (epilepsy). We showed that spiking activity *in vivo* approached a critical state - thereby increasing processing capacity - , but remained in a slightly sub-critical regime - thereby keeping a safety margin from instability. These results were consistent from human to monkey, cat, and rat recordings, pointing at sub-criticality as a universal dynamical state of neural networks *in vivo* [3, 4].

Information is stored on long time scales in the strengths of synapses. On short time scales, however, information can be stored in the activity of a neural network. We for the first time quantified this “active storage” (AS) locally in space and time [1]. We demonstrated *in vivo* that unpredicted onsets of stimuli induced negative storage (“surprise”), followed by significant positive storage during the predictable progression of the stimulus movie. This method now allows us to follow AS at each step in space and time [5].

In two related projects about information transfer, we demonstrated that (transcranial) magnetic stimulation altered spike propagation *in vitro* by specifically inducing plasticity in proximal, but not in distal synapses [6]. We also revisited “cross frequency coupling” (CFC), a popular hypothesis about communication between brain areas. CFC suggests that a brain area oscillating at a low frequency (A1) sends information to one oscillating at a high frequency (A2) if the phase in A1 modulates the amplitude in A2. We showed that current measures to assess this “coupling” are at best ambiguous, and suggested novel, more rigorous analyses [7].

- [1] M Wibral, J T Lizier, V Priesemann, *Front. Robotics and AI* 2(5), (2015)
- [2] V Priesemann, et al., *in prep.*
- [3] V Priesemann, et al., *Front. Syst. Neurosci.* 8(108) (2014).
- [4] V Priesemann, et al., *PLoS Comp Biol.* 9(3), e1002985 (2013).
- [5] M Wibral, et al., *Front Neuroinform.* 8(1) (2014).
- [6] M Lenz*, S Platschek*, V Priesemann*, et al., *Brain Struct Funct* 220(6), (2014).
- [7] J Aru, et al., *Curr Op Neurobiol.* 31:51-61, (2015).

8.10 DYNAMICS AND SELF-ORGANIZATION IN BRAIN NETWORKS

T. Geisel, A. Levina, J. Pineiro Neto, V. Priesemann, J. Wiltig
 X. Denker (U Gottingen), F. Effenberger & J. Jost (MPI Leipzig),
 M. Herrmann (U Edinburgh), O. Shriki (Ben Gurion U),
 H. Cuntz & M. Wibral (U Frankfurt)

Self-organization of network structure. It is widely believed that the connectivity structure of neuronal circuits plays a major role in brain function. Although the full synaptic connectivity for larger populations is not yet assessable by state of the art experimental techniques, available data show that neither synaptic strengths nor the number of synapses per neuron are homogeneously distributed. Several studies have found long-tailed distributions of synaptic weights with many weak and a few exceptionally strong synaptic connections, as well as strongly connected cells and subnetworks that may play a decisive role for data processing in neural circuits. Little is known about how this structure arises in developing brains, and we hypothesize that there is a self-organizing principle behind their appearance. We studied how structural inhomogeneities can emerge by simple synaptic plasticity mechanisms from an initially homogeneous network [1].

The key component of the model is inhibitory spike-timing-dependent plasticity (STDP) that allows the network to keep its activity balanced without the necessity to fine tune parameters. Combined with excitatory STDP and synaptic scaling it led to a development of highly connected subnetwork of *driver neurons* with predominantly strong outgoing synapses. Coincident spiking activity of several driver neurons can evoke population bursts, and driver neurons have similar dynamical properties as leader neurons found experimentally. We performed numerical simulations and demonstrated analytically how a small imbalance in the initial structure is amplified by the synaptic plasticity rules and their interplay. The plasticity rules in our network could account for the emergence of all empirically observed structural network features. We thereby identified a set of plasticity rules as a unifying candidate explanation for the emergence of empirically observed synaptic connectivity structure.

Assessing network dynamics. Small changes in the network's dynamics can dramatically alter its function. This effect is particularly strong in the vicinity of an instability or phase transition. We investigated networks in the vicinity of a critical state, a 2nd order phase transition. Criticality is an important topic in neuroscience, because at criticality information processing capacity is maximized in models, rendering criticality a candidate state for optimal neural processing *in vivo*. To test this hypothesis, an unbiased estimate of the network's dynamical state from experimental data is essential. However, when studying complex systems, such as the brain, we are often limited by (i) the degree to which we can assess the activity or state of each component, (ii) the degree of control we can exert on the system, and (iii) potential non-stationarity. This poses severe constraints on our

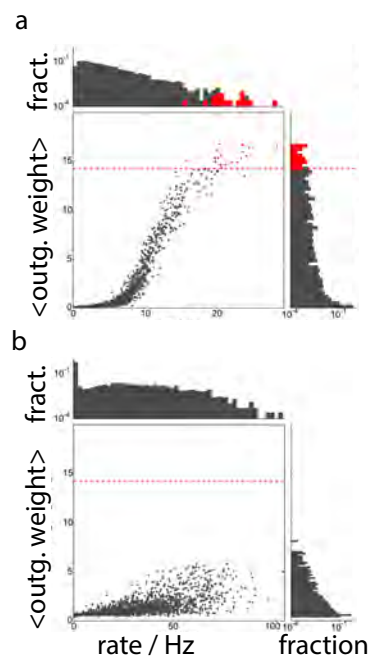


Figure 8.18: **The emergence of driver neurons (marked red) requires inhibitory spike-timing-dependent plasticity.** **a:** network including inhibitory STDP, **b:** Network without inhibitory STDP. Each dot represents one excitatory neuron. Dashed red lines mark threshold on the mean outgoing weight for the driver neuron definition. Histograms (top, right) show the firing rates and mean outgoing excitatory weights, respectively.

ability to gain insights about a system's dynamical properties. In the following, we outline our recent results on tackling these challenges when assessing the distance to criticality ϵ from experimental data.

(i) When assessing spiking dynamics *in vivo*, one can sample only a small fraction of all neurons (subsampling), or alternatively one has to resort to a coarse sampling, i.e. an averaged indirect measure of the spiking activity (e.g. EEG or local field potential (LFP)). Both, subsampling and coarse sampling hinder inference about the dynamical state of a neural network if one relies on the commonly used avalanche distribution [6]. In this case, critical as well as sub-critical neural networks can show apparent critical, sub-critical, or super-critical distributions, depending on the distance of the electrodes (fig. 8.10). We currently work on harnessing systematic changes in the electrode distance to develop a reliable estimator of the distance to criticality ϵ under these LFP-like measures.

(ii) When assessing criticality, it is essential to disentangle deviations from the scaling relations that are caused by the finite size (FS) of the system, from those caused by subsampling. We showed that FS scaling differs from the behavior under subsampling. Importantly, power law scaling is not conserved under subsampling, but under FS scaling. This allows us to differentiate FS effects from subsampling effects [7]. In a parallel study, we derived mathematical properties of the avalanche size distributions that in the future will enable a better characterization of FS critical systems [8]. To translate avalanche size distributions from neural networks into a mathematically rigorous form we introduced an avalanche transformation that defines a group action on the subset of an N -dimensional unit cube. We showed that the skew product of the dynamical system generated by the avalanche transformation and the shift on the input sequence is topologically transitive [9].

(iii) Is the frequently observed power law scaling of avalanches in experiments indeed a signature of criticality, or do they arise from inhomogeneous Poisson processes instead? We showed that specific non-stationarities (inhomogeneous rates) can indeed mimic some of the signatures of critical systems, e.g. power-laws for avalanche distributions, but not all of them. We showed how to distinguish these apparent critical systems from truly critical systems by evaluating the full set of scaling relations [10]. Thereby we expect to settle the long standing debate on whether power laws in the size distributions reflect criticality or simple non-stationarity in the firing rate.

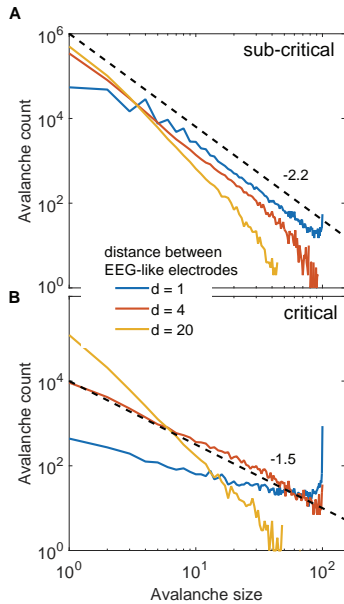


Figure 8.19: **Avalanche size distributions from EEG-like signals** of (A) a sub-critical, and (B) a critical neural network model. In both models, the avalanche size distribution depended more strongly on the distance d between electrodes than on the dynamical state of the network proper. [4].

[1] F Effenberger, J Jost, A Levina, PLoS Comput Biol **11**(9) (2015).
 [2] V Priesemann, et al., Front Syst Neurosci. **8**(108) (2014).
 [3] V Priesemann, et al., PLOS Comp. Biol. **9**(3), e1002985 (2013).
 [4] J Pinheiro, H Bluhm, H Cuntz & V Priesemann, *in prep*.
 [5] J Wilting & V Priesemann, *in prep*.
 [6] J Beggs & D Plenz, J Neurosci. **23**(35) (2003).
 [7] A Levina & V Priesemann, *in prep*.
 [8] A Levina & M Herrmann, Stochastics and Dynamics **14**(3), (2014).
 [9] M Denker & A Levina, *under revision* (2015).
 [10] V Priesemann & O Shriki, *in prep*.

8.11 CONNECTOMICS THROUGH DYNAMICS: REVEALING SYNAPTIC CONNECTIVITY FROM SPIKES

J. Casadiego, D. Maoutsa, M. Timme

Brain function emerges through billions of neurons interacting across circuits established through a vast number of synaptic connections. Dynamical recordings in neuroscience experiments such as EEG or fMRI recordings typically yield connectivity measures that evaluate the statistical correlations of the activities at various scales, from local neural populations to brain areas. As a consequence, these experiments yield effective or functional connectivity measures that offer information about the overall collective dynamics of the relevant circuits. Such statistical measures do not reveal which units directly act on which other units – and thus the system’s structural connectivity.

Generally, structural connectivity of networks reflects the direct physical interactions between pairs of dynamical units. How to uncover interaction structure from measured time series of networked systems remains an open question. In ongoing research, we work towards a theory of inferring synaptic connectivity between neurons based on observations of the circuits’ spike trains only.

We express the observed network dynamics in terms of discrete events (Fig. 8.20a), specifically the times and neural identity of action potentials (spikes). We take each given *inter-spike* interval ΔT_i of one neuron i as a (hidden) function h_i of the *cross-spike intervals* w_j^i – time differences between the previous spike of neuron i and the most recent spike of other neurons j in the circuit. We propose to infer the structural connectivity from local samplings in the *event spaces* made up of inter-spike intervals ΔT_i and the w_j^i via the relation

$$\Delta T_i = h_i(\Lambda^i \mathbf{w}^i). \quad (8.1)$$

Here, we proposed *explicit dependency matrices* Λ^i , each a diagonal matrix whose j th diagonal entry is non-zero if and only if unit j directly acts on i . For differentiable h_i , local samplings in the event spaces yield conditions identifying connectivity from discrete events (Fig. 8.20b).

Thereby we propose an approach to reveal network structural connectivity from recorded spike time series only. Our work thus bridges the gap between hard-to-obtain (e.g. intracellular) signals from real state space (e.g. membrane potential dynamics) so far required to reveal networks [1, 2, 3, 4] to typical neural circuit dynamics where the observables are spike timing data, i.e. only discrete, state-dependent outputs of the neurons [5]. In general, these results advance our knowledge about revealing network structure for systems where direct access to output dynamics is simpler than access to connectivity.

- [1] V.A. Makarov et al., J. Neurosci. Meth. **144**, 265 (2004).
- [2] F. v. Bussel et al., Frontiers Comput. Neurosci. **5**, 3 (2011).
- [3] M. Timme, Phys. Rev. Lett. **98**, 224101 (2007).
- [4] M. Timme and J. Casadiego, J. Phys. A **47**, 343001 (2014).
- [5] D. Maoutsa, J. Casadiego and M. Timme, in prep. (2016).

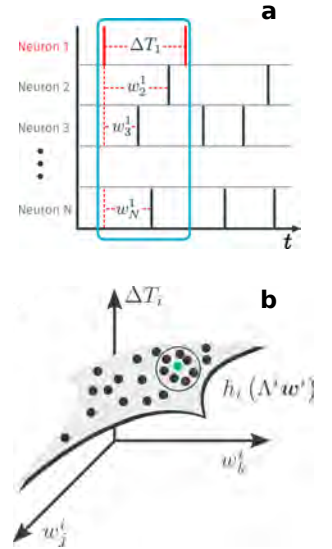


Figure 8.20: **Inferring structural connectivity from spike timing data.** (a) Instead of the continuous dynamics in state space of the neurons, discrete outputs in terms of spike times of the neurons are commonly recorded. For each inter-spike interval ΔT_i of a given neuron $i = 1$, the second spike is controlled by inputs from spikes potentially generated by arbitrary other neurons j . Their spike times define *cross-spike intervals* w_j^i . (b) In the event space of cross- and inter-spike intervals, each inter-spike interval of one neuron defines a point assumed to lie on a smooth manifold generated by a (hidden) function $\Delta T_i = h_i(\Lambda^i \mathbf{w}^i)$.

8.12 *EcoBus* – FLEXIBLE PUBLIC MOBILITY

M. Timme, A. Sorge, S. Herminghaus

D. Manik, N. Molkenhain, J. Kassel, M. Wendland, L.-J. Deutsch, C. Hoffrogge, F. Fix, X. Zhang, J. Schlüter (IST Austria), J. Nagler (ETH Zurich)

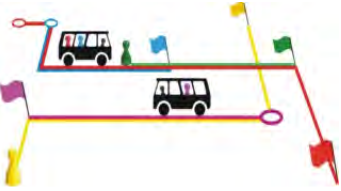


Figure 8.21: **Principle of the *EcoBus* system.** Two buses serving five passenger requests (open circles: starting points, flags: destinations). One bus with passengers Lord Red and Madame Blue picks up Dr. Green before it delivers Blue, Green and then Red at their respective destinations. A second bus, with Miss Violet on board, delivers her before taking Prof. Yellow. Other routing would also be possible (e.g., Red, Blue and Yellow served by bus 1 and Violet and Green by bus 2). The tours are organized such that routes of different passengers strongly overlap in time *and* space, minimizing waiting times.

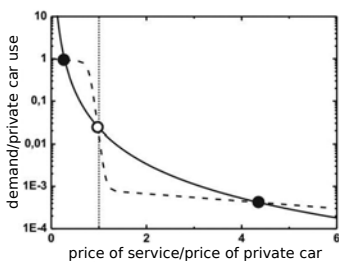


Figure 8.22: **Market dynamics in demand-driven public transport.** Solid curve: demand necessary for break-even at given price. Dashed curve: estimated price-demand relation. The sign of the relative slope of the curves at the intersections (fixed points of the dynamics) determines their stability (filled circles: stable; open circle: unstable). Note the logarithmic vertical scale.

One of the most important complex fluids we encounter in everyday life is traffic. It mainly consists of individual active ‘particles’ collectively forming a flowing matter of strongly variable consistency. The sometimes poor transport efficiency, e.g., of motorized individual traffic mainly owes to the ill-adjusted parameters of the self-organization processes at work. It appears possible, through modern means of (digital) communication, to organize these processes such that a much more efficient system emerges. Potentially, this would lead to less pollution, less consumption of precious resources, and a more relaxed experience for the participants.

Current standards of publicly available local and intra-regional transport focus on buses (and trams, subways etc.) for multi-passenger transport as well as on taxis and rental cars for individual transport. Multi-passenger transport is typically organized via a number of lines with fixed stopping times and stations. At high demand along lines, it is relatively inexpensive. Publicly available (or privately organized) individual transport by cars is more flexible in time and in space but more expensive. It also contributes substantially to carbon dioxide emissions, environmental pollution, congestion, and problems with limited space in cities.

***EcoBus* Idea.** We propose a public, decentralized and demand-driven mobility system *EcoBus* that shall simultaneously be economically and ecologically efficient and reduce total traffic load (Fig. 8.21). By means of suitable network algorithms and statistical physics analyses, *EcoBus* shall efficiently combine the benefits of taxis and buses: Minibuses pick up passengers at their departure points and transport them to their desired destinations. The simultaneous service of many minibuses traveling in various directions ensures that passengers can be economically served in a timely manner.

***EcoBus* Economy.** Similar mobility concepts already exist, but have not been economically sustainable. The reason for this failure can be appreciated on the basis of a Mean Field Theory of flexible, demand-driven public transport [1]. We computed the price to be paid by each passenger (per distance travelled) which is necessary to operate the system at operational costs (‘break-even’, solid curve in Fig. 8.22). A rough estimate of the price-demand relation is shown as the dashed curve. The intersections of the curves represent the fixed points of market dynamics. The latter is driven away from the unstable (open circle) and towards one of the stable (closed circles) fixed points. Current systems have only explored the region to the right of the unstable fixed point, and thus gathered in the region around the stable fixed point to the right (approximately four to five times larger than costs of individual car traffic). If the price is lower than at the

unstable fixed point, demand increases and prices reduce further until a second fixed point is reached at substantially lower price. This is where an *EcoBus* system may operate [1] sustainably.

Challenges for Statistical Physics and Network Dynamics. Designing and operating an *EcoBus* system requires to answer a number of questions (cf., e.g., [2, 3, 4]) about static network analysis of street maps, coupled processing of requests, dynamic networked assignments of passengers to buses, distributed multiple-bus routing, monitoring of stochastic loads as well as their intelligent control.

One key question in service systems with stochastic loads is how to detect whether the system is overloaded. For the *EcoBus* system, longer-term loads above some threshold would indicate that additional buses must be added to the existing service. For instance, such overload problems are intrinsically hard to detect from data using standard queuing theory. Using a statistical physics approach, we uncovered a mapping between stochastic fluctuations of loads and a one-dimensional percolation problem in time (Fig. 8.23). The resulting theory of *temporal percolation* we are currently finalizing [5] indicates that known results from scaling theory and an analysis of the percolation transition yield useful measures to predict whether a system is only currently highly loaded or more permanently overloaded – only based on observed load time series. Prospectively, such measures may help estimating when to increase or decrease the number of buses in an operating *EcoBus* system.

The *EcoBus* initiative started at our MPIDS in 2010/2011 as a joint venture between the Department of Complex Fluids and the Max Planck Research Group on Network Dynamics. Meanwhile, the public sector, in particular in the Göttingen district and the State of Lower Saxony, got highly interested. In 2015, many counties and municipalities, the Southern Lower Saxony Office for Regional Development (headed by Dr. Ulrike Witt) as well as research institutions and companies in the region agreed on supporting our *EcoBus* initiative at the MPIDS (Fig. 8.24). A grant proposal has been submitted in collaboration with the local public transport agencies of Göttingen (GöVB GmbH) and Southern Lower Saxony (VSN), for supporting basic research at the MPIDS, with a practical pilot phase starting 2016/2017.

- [1] S. Herminghaus et al., in prep. (2015).
- [2] M. Schmidt and A. Schöbel, *Networks* 65, 228 (2015).
- [3] P. Santi et al., *Proc. Natl. Acad. Sci.* 111, 13290 (2014).
- [4] O. Sagarra et al, arxiv.org: 1504:01939 (2015).
- [5] A. Sorge, J. Nagler, S. Herminghaus and M. Timme, in prep. (2015).

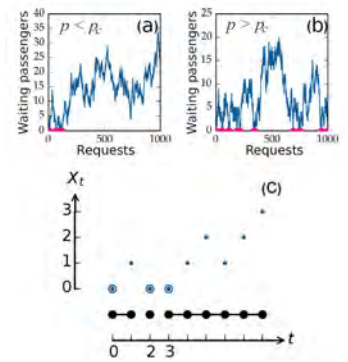


Figure 8.23: **Statistical Physics of request dynamics.** (a),(b): Discrete time request dynamics for random queuing processes. New requests are added with probability p , and processed with probability $(1 - p)$. The critical load above which the system jams is $p_c = 0.5$. (a): transiently high loads, despite being below the jamming transition ($p = 0.48$). (b): seemingly sustainable load dynamics, but in fact above the jamming transition ($p = 0.52$). (c) *Temporal percolation* as an equivalent representation of the request dynamics. Scaling analyses from percolation theory help separating subcritical (a) from supercritical (b) load dynamics.



Figure 8.24: **Southern Lower Saxony Cooperation Agreement in support of *EcoBus* Research.**

8.13 CHARACTERIZATION AND RECONSTRUCTION OF COMPLEX NETWORKED SYSTEMS

Annette Witt, Jan Nagler, Theo Geisel

Complex networked systems such as traffic, the internet, or our brain are composed of many interacting units where the details of the interactions are often hidden or unknown [1]. Crucial for the understanding of how a complex network operates are thus methods that allow the characterization and reconstruction of hidden interactions by analyzing recorded time series of the different network components. In the past, noisy but correlated interactions have been quantified by correlation measures that are based on the correlation matrix.

We have investigated three different kinds of correlation networks [2]: The *correlation network of the recorded time series* is defined in the following way: Every single time series represents a network node, the links between these nodes are given by a measure for the sequential cross correlations of the two involved time series. More specifically, we have considered correlation networks where the i -th node is associated with the temporal development of an observable $x_i(t)$ and the non-directed link between nodes i and j is defined by the cross power spectrum $S_{ij}(f)$ which depends on the frequency f . We have described the complete set of *backbones* of these correlation networks (an example is given in Fig. 8.13), i.e., sub-networks which are sufficient for the reconstruction of the complete correlation network. These backbones are characterized by a specific topology.

The *correlation network of a stochastic process* is defined equivalently [3]: nodes represent the dynamics of observed quantities, and the non-directed links between each pair of nodes are defined by the linear cross-correlation functions. We have described the relation between correlation networks on the process level and the time series level and have provided an algorithm that generates time series and their correlation networks from the correlation network of a process.

Causal networks on the other hand have directed links. We have analyzed networks whose links are based on spectrally decomposed Granger causality (SDGC) [4]. We have found that pairs of causal and correlation networks have identical nodes but a contradicting link structure, as peaks of SDGC may show up for frequencies with negligible spectral power. We showed that this non-correspondence is typical rather than exceptional and introduced a causality measure that avoids these flaws and accurately captures directed causal influences. Our framework is consistent with both, artificial and real data. We have applied it to electro-physiological recordings of the brain activity in behaving monkeys and to recordings of the human cardio-respiratory system.

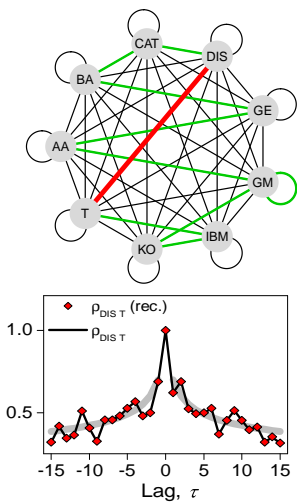


Figure 8.25: Correlation networks of log-returns (i.e., logarithm of relative price changes) of New York Stock Exchange daily closing prices. Top: complete correlation network (black), a backbone (green) and the reconstructed correlation function (red). Bottom: original (lines) and reconstructed (symbols) correlation function of the time series and of a model (gray lines).

- [1] S. Boccaletti et al., Phys. Rep. **424**, 175 (2006); L. Costa et al., Adv. Phys. **56**, 167 (2007)
- [2] A. Witt, M. Kersting, T. Geisel, J. Nagler, under review.
- [3] J. Geweke, Journal of the American Statistical Society **77**, 304 (1982)
- [4] C.W.J. Granger, Econometrica **37**, 424 (1969)

8.14 MODEL-FREE INFERENCE OF NETWORKS FROM DYNAMICS

J. Casadiego, H. Hähne, M. Timme
M. Nitzan (Hebrew University, Israel)

Networks often self-organize collectively resulting from the dynamics of individual units and their physical interactions. Complex collective phenomena in such systems emerge across fields, from biology to physics to engineering. They include, for instance, synchronization in power grids, congestion in traffic networks, regulation of gene and protein interaction networks and distributed computation in neural circuits.

In many current experimental systems such as genetic networks, unit activity becomes more and more easily accessible whereas structural and anatomical techniques still lack behind. Yet, most theoretical studies so far have focused on the forward problem of studying the dynamics of a system under variation of one or a few of its parameters. Our aim is to push the theoretical frontier on network *inverse* problems, specifically on inferring network interaction topologies given observations of the units' dynamics [1].

Recent work demonstrated, first computationally [2] and then theoretically [3], that a given collective dynamics is not unique to a specific network. Instead, identical dynamics may be generated by an entire (high-dimensional) family of networks [4]. It thus appears curious to ask 'How can a network's collective dynamics alone reveal its interaction topology?'

We are currently developing a theory of inferring physical interaction networks. From a dynamical system's perspective, we aim at understanding how, why and under which conditions one may recover physical connections of a network from its collective dynamics. We take different inverse perspectives that solely rely on measured dynamics of the individual units [1]. Specifically, combining concepts of nonlinear dynamics, linear algebra, numerical analysis, and optimization theory, we are currently characterizing two main approaches for revealing connections from network dynamics. The first, *local sampling*, is based on linearizations around reference states or trajectories in the state space. The second, a *distributed sampling*, requires the sampling of different regions of the state space and amends that space by additional observables such as the rate of change of a variable (Fig. 8.26).

The concept of a *dynamics space*, we developed makes the novel type of reconstruction option model-free. First tests indicate that topologies may be derived (i) from highly chaotic dynamics, (ii) for interactions that are of different types or (iii) for systems with units hidden (Fig. 8.27).

- [1] M. Timme and J. Casadiego, J. Phys. A **47**, 343001 (2014).
- [2] A. Prinz et al., Nature Neurosci. **7**, 1287 - 1288 (2004).
- [3] R. Memmesheimer and M. Timme, Phys. Rev. Lett. **97**, 188101 (2006).
- [4] J. Casadiego and M. Timme, Network Dynamics as an Inverse Problem, in Mathematical Technology of Networks, Springer (2015).

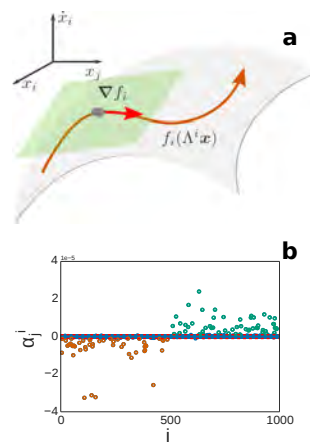


Figure 8.26: **Network reconstruction from observed time series.** (a) Dynamics space of states and their temporal derivatives locally offers information about the network topology. (b) Activating and inhibiting interactions can be identified separately.

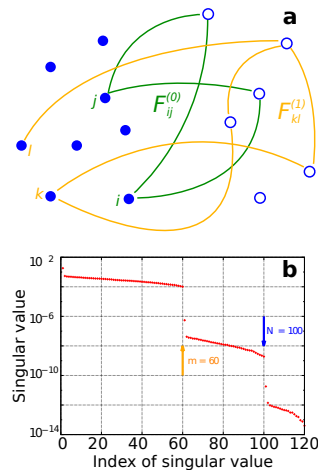


Figure 8.27: **Inferring structure of networks with hidden units.** (a) Feedback paths from measurable units (disks) to non-measurable units (open circles) and back and their length in the hidden part of the network may be inferred. (b) Gap in spectrum of singular values of inference matrix indicates number of hidden units.

8.15 DYNAMICALLY SMART POWER GRIDS: COLLECTIVE STABILITY, ECONOMY AND CONTROL

M. Timme, D. Manik, B. Schäfer, X. Zhang, M. Schröder,
S. Hallerberg, D. Witthaut (FZ Jülich)

J. Casadiego, L.-J. Deutsch, N. Molkenhain, B. Ghani, M. Rohden (JU Bremen), C. Grabow, S. Auer, J. Kurths (all PIK Potsdam), M. Matthiae (U Aarhus, Denmark), T. Sollacher (Siemens, Munich), T. Walter (EasySmartGrid GmbH Karlsruhe)

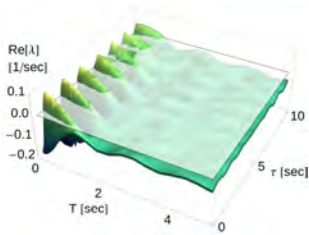


Figure 8.28: **Decentral Smart Grid Control.** Responses after certain delays cause instabilities (eigenvalues $Re(\lambda) > 0$). Temporal averaging of the frequency measurements over sufficiently large periods T stabilize network dynamics across delays τ .

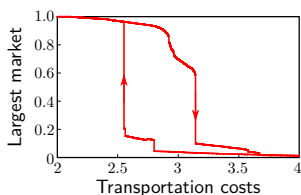


Figure 8.29: **Explosive Globalization?** Transition of largest market size with lowering transportation costs maps to percolation transition that may be explosive [7].

Robust energy supply and distribution fundamentally underly our economy, industry and virtually all aspects of daily life. The ongoing transition from fossil to renewable energy sources creates a multitude of challenges for operating modern power grids and energy systems in general. Renewable-source generation is intrinsically smaller, more distributed, more heterogeneous, weather-dependent, more fluctuating, less predictable and more correlated. It thus requires system-wide planning, balancing collective dynamics and network control as prerequisites for a sustainable future energy system. The research group on *Network Dynamics* at the MPIDS focuses on challenges from the perspective of network dynamical systems. Its 2012 publication in *Physical Review Letters* [1, 2] constitutes the first study addressing the influence of multiple nonlinear feedback on the self-organized dynamics of power distribution networks. More generally, it initiated a novel branch of research on collective dynamical phenomena in energy science.

Our projects in particular address the question how collective aspects of network dynamics emerge through a multitude of co-acting nonlinearities, cf. [3, 4, 5]. For instance, recent work in collaboration with EasySmartGrid GmbH (Karlsruhe) revealed that decentral instead of centralized control of smart grid operations may be feasible if the local deviation of the AC frequency is used as an incentive (price signal) to increase or decrease user demand. Intriguingly, as technical reaction times to adapt consumption are non-zero and not the same for all consumers, decentralized feedback may lead to collective instabilities due to reaction delays. We proposed a local averaging scheme (Fig. 8.28) that removes this problem [6].

Current research focuses on the impact of fluctuations and economic factors on the collective dynamics of power grid networks. We recently managed to analytically predict the speed of spreading of local influences through arbitrary network topologies. Furthermore, we discovered an economically driven percolation transition in consumer buying behavior, where the transition might be ‘explosive’ [7], depending on local energy pricing and transportation costs, Fig. 8.29.

- [1] M. Rohden et al., *Phys. Rev. Lett.* **109**, 064101 (Editorial Suggestion, 2012)
- [2] M. Rohden et al., *Chaos* **24**, 013123 (2014)
- [3] D. Witthaut and M. Timme, *New J. Phys.* **14**, 083036 (2012).
- [4] D. Witthaut and M. Timme, *Phys. Rev. E* **92**, 032809 (2015).
- [5] D. Manik et al., *Eur. J. ST* 02274-y-1:1 (2014).
- [6] B. Schäfer et al., *New J. Phys.* **17**, 015002 (2015).
- [7] J. Nagler, A. Levina, M. Timme, *Nature Phys.* **7**, 265 (2011).

8.16 SIGNAL PROPAGATION AND INTEGRATION IN ADAPTING TUBULAR NETWORKS

K. Alim, N. Andrew

M. P. Brenner (Harvard, USA)

A. Pringle (University of Wisconsin, USA)

Tubular networks are essential to transport both signals and resources in an extended organism. Well-known examples are the vertebrate circulatory system or the plant vascular system. In fact, such transport networks self-organize their network geometry utilizing the dynamics of fluid flow. Tubes are dilated or deflated in response to signals propagated with the fluid flow. The network-forming slime mold *Physarum polycephalum* is an easily manageable prototype to study the dynamics of fluid flows in tubular networks and how they serve to self-organize the dynamics of flow and transport throughout the network. Understanding the principles of self-organized fluid dynamics in this organism will serve to identify general principles of tubular transport networks and pave the way for engineering applications such as autonomous micro/nanofluidics and predict for example drug delivery in biomedical applications.

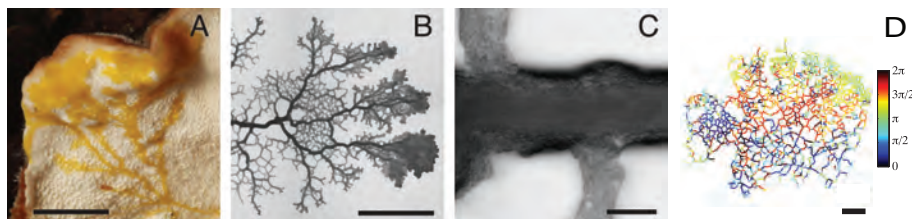


Figure 8.30: *Physarum polycephalum*. (A) The slime mold in its natural habitat. Scale bar ~ 0.5 cm. (B) Bright field microscopy image showing the tubular network of the organism with more fan-like structures at the growing front (to the right). Scale bar 0.5 cm. (C) The cytoplasm streams within the network's tubes. Scale bar $100 \mu\text{m}$. (D) Phases of contraction are patterned in a peristaltic wave. Scale bar 2mm.

Physarum polycephalum is an acellular slime mold that grows as a connected network of tubes sharing the same cytoplasmic fluid throughout its extend of up to tens of centimeters [1], see Fig. 8.30. As the organism grows and moves the network is reshaped and adapted to stimuli the tubes encounter. Networks formed are found to be efficient for transport but also sufficiently robust against destruction of tubes [2]. The cytoplasmic fluid streams through the network and changes direction periodically about every 100 seconds. Cross-sectional, acto-myosin based contractions of the tubes drive the fluid flows. We showed, that the contractions are organized into a peristaltic wave to create coordinated flows optimal for transport [3]. The length of the peristaltic wave is self-organized to match to the organism's size. With these flows signaling molecules are rapidly distributed throughout the organism. In fact, recent data of us shows that the contractions driving the fluid flows are changing in response to signaling molecules transported by the flows themselves. This establishes the basis of a complex feedback

between flows in an extended network and the contractile forces driving the fluid flows. Uncovering the rules of this feedback will enable us to learn how a tubular transport network can self-organize its fluid flow and transport properties.

We will test hypothesis on rules of self-organized fluid dynamics in well-controlled experiments on *Physarum polycephalum* allowing for a one-to-one comparison with theory and numerical calculations. At first we will uncover the signal that couples the contractions driving the fluid flow to the flow transporting signaling molecules. The rules of self-organized fluid dynamics identified and tested in scenarios with a single signal will then be tested and expanded to understand how multiple signals at different locations in the network are 'added up'. Finally, we will investigate if there are general principles of how fluid flows can self-organize tubular transport network, by testing our theoretical models on data of fungal networks [4] and the rat cortical circulatory network [5].

Understanding how fluid dynamics can self-organize in biological organism is an interdisciplinary effort requiring skills for biological and chemical experiments, theoretical models of soft matter and numerical simulations of fluid flows. Results have application potential in engineering and biomedicine. Furthermore, slime molds are charismatic. Their improbable appearance and unlikely behaviors attract attention and generate questions beyond the scientific world; we are often approached by the public and journalists to explain why slime molds are discussed as intelligent. *Physarum polycephalum* is a class-room appropriate organism to introduce the next generation of researchers to the puzzles of complex fluid dynamics.

- [1] N. Kamiya, Annu. Rev. Plant. Physiol. **32**, 205 (1981)
- [2] A. Tero, S. Takagi, T. Saigusa, K. Ito, D. P. Bebbler, M. D. Fricker, K. Yumiki, R. Kobayashi, T. Nakagaki, Science **327**, 439 (2010)
- [3] K. Alim, G. Amselem, F. Peaudecerf, M. P. Brenner, A. Pringle, Proc. Natl. Acad. Sci. U.S.A. **110**, 13306 (2013)
- [4] L. Heaton, B. Obara, V. Grau, N. Jones, T. Nakagaki, L. Boddy, M. D. Fricker, Fungal Biol. Rev. **26**, 12 (2012)
- [5] P. Blinder, P.S. Tsai, J. P. Kaufhold, P. M. Knutsen, H. Suhl, D. Kleinfeld, Nat. Neurosci. **16**, 889 (2013)

8.17 BIODIVERSITY AND EXTINCTION

F. Stollmeier, T. Geisel, J. Nagler

More than 30 percent of the known species living on Earth are listed as being threatened by extinction [1]. These species constitute a complex ecosystem, i.e. most of them depend highly on the existence of other species. Consequently the extinction of one species can result in subsequent extinctions. However, little is known about how many species that are not listed are indirectly endangered.

We regard the global ecosystem as a network in which species are the nodes and dependencies are the links. We ask what are the properties of this network and how does it develop, if species are continuously added and removed. In particular, can the removal of a single species result in large extinction cascades?

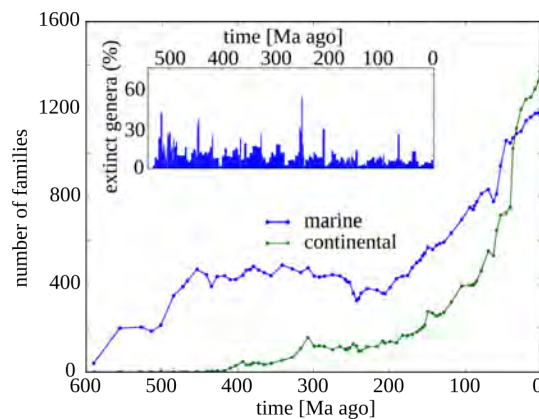


Figure 8.31: Evolution of the global biodiversity on land and in the sea during the Phanerozoic at the taxonomic level of families according to Fossil Record 2 [2]. The inset shows the extinctions of marine animals at the level of genera according to Sepkoski's Compendium [3].

The majority of living species have not been discovered as yet and even less is known about the dependencies between living species. We therefore use fossil databases [2, 3] to infer characteristics about the aforementioned dependency network. These databases provide a low resolution but long time series (nearly 600 million years) of the biodiversity and the extinctions on Earth (see Fig. 8.31).

We developed a simple model of a stochastic network process [4] with statistical properties similar to the fossil databases. The model can explain the circumstances in which it is likely that the extinction of a single species initiates a mass extinction. Furthermore, the model can explain why the growth of the biodiversity on land seems to follow an exponential increase while the growth of the biodiversity in the sea was interrupted by a stagnation of almost 300 million years.

- [1] IUCN. Red List of Threatened Species (2012)
- [2] M.J. Benton. Chapman & Hall, London (1993)
- [3] J.J. Sepkoski. Bull. of American Paleontology **363** (2002)
- [4] F. Stollmeier, T. Geisel and J. Nagler. Phys Rev Lett **112**, 228101 (2015)

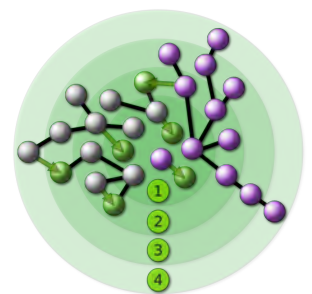


Figure 8.32: Cartoon of the biodiversity model. In this example the species in purple become extinct by exogenous causes at level 1 and at higher levels due to their dependence on species at lower levels. The species in green originate from existing species.

PART II

INFRASTRUCTURE

At the MPIDS an efficient infrastructure supports both scientists and non-scientific staff in their work, creates an excellent research environment, and ensures smooth workflows behind the scenes. These service units are headed by the delegate manager relieving the board of directors and the managing director of many tasks.

The infrastructure is organized in three service units: administration, technical services, and information technology. Outreach activities and media relations are coordinated by a separate staff unit.

ADMINISTRATION

While the institute's administration covers a wide range of responsibilities and tasks, its main focus is on the divisions human resources, financial affairs, and grant administration.

All tasks of personnel management and advisory services are at the heart of the human resources division. The team not only attends to all workflows dealing with employment contracts, stipends, and the promotion of young researchers, but also offers help and advice in questions dealing with health insurance, tax and collective bargaining law. As a first contact point for all new employees taking up their duties, the human resources division helps with all necessary formalities – both those at the institute and those at the local administration. To facilitate the first steps in the new environment, the institute has issued a visitor's guide containing information and helpful hints for all aspects of every-day life – from opening a bank account to finding suitable day care. Visitors and new employees often spend their first weeks in one of three institute's guest houses. These are located at the institute's old site in the Bunsenstrasse and provide accommodation for up to thirty persons. The administration oversees the management of these houses.

The division for financial affairs oversees and manages all of the institute's financial affairs and processes. The team takes care of book-keeping, procurement, and travels costs. Since the MPIDS is very successful at applying for third-party funded research projects, grant administration is another important task of the administration. Experienced personnel offers the scientists advice and support when applying for third-party funds and handles all financial issues connected with the grants.

Since a few research groups are still located at the institute's old site in the Bunsenstrasse, transportation between the old and the new building is an important service organized by the administration. This helps scientists and non-scientific staff to commute between both sites in a time-saving manner. The administration also deals with the transportation of scientific goods and transportation within Göttingen and to more distant destinations.

In 2014, the MPIDS took an organizationally important step. Based on a comprehensive exchange between scientists and administration, the introduction of a cooperative style of leadership was agreed upon. The goal being to promote a good work environment in every form,

such that the identity, motivation, satisfaction and loyalty of each team member is constantly reinforced.

An important milestone has already been implemented: the joint development, formulation and conception of a vision for the institute. It represents a basis for all actions required to reach the aforementioned goal.

On this basis, important measures were taken, including the introduction of dialogue-oriented management standards and team building based on the seminar series "Wissenschaft vorm Wochenende" ("Science before the weekend"), conceived for a general audience. Closely linked with the development step described above, the MPIDS introduced sustainable quality management in 2015. Based on a process-oriented approach, the goal is to continually question infrastructure processes, their adequacy and effectiveness and to adapt them if necessary. For the MPIDS this is a continuous task, working constantly to bring us another step closer to our vision of a completely compliant, efficient and sustainable organisation.

TECHNICAL SERVICES

The service unit "technical services" encompasses, on the one hand, the facility management and maintenance, and, on the other, the precision machining and electronics workshops. The facility management is responsible for the upkeep and maintenance of all of the institute's technical infrastructure including heating, air condition, plumbing and ventilation, fire detection technology, telecommunications, and emergency call systems. While small and mid-sized repairs are performed by team members, larger tasks are outsourced and coordinated by the facility management.

Many of the experimental setups and scientific apparatuses used at the MPIDS are one of a kind specifically designed, built, and continuously modified for the required research tasks. Many of these tasks are performed by the precision mechanics and electronics workshop. The staff closely collaborates with the scientists providing valuable advice and expertise in all stages of the construction process from the first idea to the finished component.

The precision mechanics workshop is responsible for the development and construction of mechanical apparatuses and components. Based on the request from the scientific departments, the mechanical design group designs and builds custom tailored solutions. The group uses the most advanced software tools that allow to design complex parts in three dimensions. This includes the simulation of the components as well as their three-dimensional assembly. Once the technical design is finished, technical drawings are generated or the design is directly entered into the CAD engines that generate instruction sets understood by the CNC-machines. The workshop is equipped with conventional as well as computer controlled lathes, milling and EDM machines. In 2015 we have acquired a 5-axis milling machine that basically is a mill combined with a lath. The associated metal shop



A look into the workshop for precision mechanics.

manufactures frames and other large metal parts and has state of the art welding equipment for handling steel and aluminum. From the very beginning, the training of apprentices has been an important part of the work of the mechanical precision workshop. On average, the workshop educates two mechanical technicians specializing in precision tool-making every two years. An impressive confirmation of the excellent training the young technicians receive at the MPIDS is the number of all-state winners of the examinations for mechanical technicians of the State of Lower Saxony coming from the MPIDS: In the past ten years six apprentices passed these examinations as winners. In addition, several apprentices have been honored by the Commercial and Industrial Chamber and by the Max Planck Society.

The staff of the scientific electronics workshop develops and builds the electronic interfaces between computer and measurement technology for scientific apparatuses that cannot be commercially obtained. The circuits are designed with CAD engines and then built in house. We are in the process of acquiring modern machines for surface mounting of modern electronics.

For more than two decades the electronics workshop has been training apprentices to become electronic technicians for devices and systems. All of these young people have successfully passed their exams. Many go on to university to become electrical engineers, others found jobs in renowned industrial enterprises.

INFORMATION TECHNOLOGY

Central IT Services

The IT service (ITS) group is tasked with operating the computer network and the servers needed for running central infrastructure applications of the MPIDS at the two sites at Bunsenstraße and on Faßberg. The ITS group also provides desktop support for the infrastructure departments and consulting services for the scientists. In addition to maintaining and developing the existing IT infrastructure the ITS group has to deal with Big Data issues resulting from the needs of scientific users. Since there are usually no off-the-shelf solutions which meet the requirements of the scientific users the ITS group has to participate actively in the development of customized solutions geared towards contributing to a versatile and useful IT ecosystem for the MPIDS and its scientific users. This includes topics like searchable web access for Terabytes of data, providing data for the scientific community following Open Access strategies and long term archival. In close cooperation with the local data center (GWDG) and the University of Applied Science in Göttingen, masters theses on those topics are offered and supervised by the ITS group.

High-Performance Computing

Ongoing advances in computer technology enable the collection of enormous amounts of experimental data, running more complex simu-



Apprentices receive the 2015 "Azubi"-award of the Max Planck Society.

lations and fine grained data analysis. This trend is accompanied by a higher demand for direct access to powerful computing resources in most groups at the MPIDS. The necessary infrastructure scales well over single workstations but below traditional large computing centers, but has to allow interactive use, e.g. for developing large-scale parallel applications or directed parameter space exploration.



Cooling cabinets with HPC clusters in the main server room of the department of Nonlinear Dynamics. Open racks for infrastructure servers in the front. The cabinets have a dedicated control and monitoring unit, are built in a modular fashion so that they can easily be moved, and can be customized to cool up to 36 kW.

Despite the diverging requirements for computing power of the various research groups in the MPIDS, a strong goal of the HPC group is to keep the landscape of HPC clusters as homogenous as possible minimizing maintenance workload and maximizing interoperability. Based on only a few different server platforms, some clusters provide an Infiniband network for fast parallel applications, some have many cores in each node and large memory, harddisk raids for the handling of huge amounts of data, or powerful GPGPU accelerators. Scientists at the MPIDS have direct access to HPC clusters with a total of about 1000 HPC systems with 12,500 CPU cores, approximately 50 TB RAM, and 4 PB of storage capacity.

Hosting computing facilities of that scale in a single institute requires a very dense packing of servers which is provided by multicore machines and efficient designs like blade server enclosures. Power densities of 24kW per square meter cannot be cooled by traditional open air flow cooling via a double flooring. An efficient cooling system is required from an environmental perspective, but also is mandatory from a financial point of view as in traditional cooling systems electricity costs of the cooling can be as high as 30% of the electricity costs for the computers themselves. The MPIDS was among the first institutes to solve this issue by using optimized water cooled cabinets with a heat exchange and redundant fans each to cool only the necessary parts of the server rooms, as shown in the above photo.

Due to space limitations at the MPIDS, and to improve service reliability as well as data security, the institute teamed up with the GWDG to set up a new facility in the former 'Fernmeldezentrale' of the university, which will accommodate about 250kW of the institute's compute servers.

In order to manage such a complex facility a monitoring system based on open source software was set up, which collects important

health data of both the HPC hardware and the cooling facilities on a frequent basis. This data is summarized on a comprehensive overview, its history can be assessed for diagnostics and the system is able to perform emergency shutdowns autonomously in case of cooling failure to prevent machine damage by high temperatures.

THE GÖTTINGEN TURBULENCE FACILITY

To understand turbulence in a fundamental sense and to make predictions useful in real-world applications, one needs not only to observe turbulence at high Reynolds numbers, but also to realize flows with various spatial and temporal large scale properties. These well defined flows must go hand in hand with precise measurements. In addition one must have the ability to adjust the conditions in various ways, so that dependencies can be uncovered. The facilities at the MPIDS make it possible not only to generate turbulence with the highest Reynolds numbers yet possible under laboratory conditions, but to do so with unprecedented control. To match our achievements in controlling turbulent flows, we have advanced measurement technologies, and have even adapted these to field experiments of natural flows.

The Variable Density Turbulence Tunnel (VDTT) [1] is a recirculating pressurized wind tunnel that consists of two measurement sections with cross-sectional areas of 1.9 m^2 and lengths of 9 m and 7 m. The chief merits of the VDTT are that it produces high Reynolds number flows and stable operating conditions. Furthermore, the Reynolds number is finely adjustable by changing the pressure of the gas in the tunnel, usually sulfur hexafluoride (SF_6) up to a pressure of 15 bar. In its current configuration, a grid of crossed bars generates Reynolds numbers (R_λ) up to 1700, much higher than in any comparable facility. Yet higher Reynolds numbers and increased control will be possible in the VDTT once we install a novel “active grid” with position-controlled flaps that agitate the flow. Uniquely, our active grid has a large number of degrees of freedom (129). Among other attributes, the homogeneity, isotropy, and intensity of the turbulent fluctuations can be set by programming the motions of the flaps appropriately. Once in the VDTT, we predict that we will reach Reynolds numbers up to 7000. This grid is presently operating in the Prandtl tunnel, an open-circuit wind tunnel dating to the 1930’s. The wind tunnel can be equipped with hot-wire anemometers or with high-speed cameras for Lagrangian particle tracking. A sled driven by linear motors will be installed in the upper measurement section, which allows measurement devices (e.g. cameras and optics) to be moved with the mean velocity of the circulating gas (up to 5 m/s).

The High Pressure Convection Facility (HPCF) [2] utilizes a general-purpose pressure vessel called the “U-Boot”, which is 5.3 m long and has a diameter of 2.5 m and can be filled with SF_6 up to a pressure of 19 bar. We precisely control both the temperature and the pressure in the vessel. Within the vessel are two cylindrical Rayleigh–Bénard (RB) experiments (diameter 1.1 m, heights 2.2 m and 1.1 m) that reach



The Variable Density Turbulence Tunnel (VDTT)



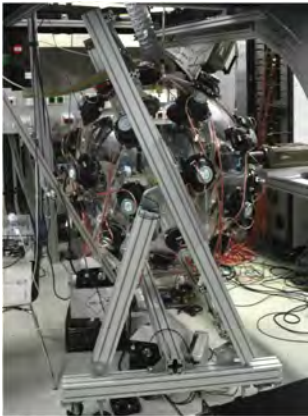
The “U-Boot”, a general-purpose pressure vessel, housing the High-Pressure Convection Facility (HPCF)



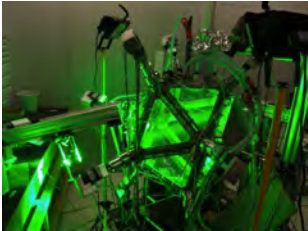
The “Cigar”, a general-purpose pressure vessel



The von Kármán mixer



A "soccer ball"



The Lagrangian Exploration Module



¹The European Commission supports the project European High-Performance Infrastructures in Turbulence (EuHIT, Grant Agreement Number 312778)

Rayleigh numbers as high as 10^{15} . Recently, we installed a rotating table for the RB cells inside the U-Boot, which allows for the study of turbulent heat convection under the influence of rotation.

The "Cigar" is a general-purpose pressure vessel with a length of 4 m and an inner diameter of 1.5 m. It can be filled with SF_6 up to a pressure of 19 bar to perform smaller convection or turbulence experiments or to test equipment for the other pressurized facilities.

Two von Kármán mixers generate high Reynolds number turbulent water flows between two counter-rotating baffled disks. Because the average displacement of fluid particles near the middle of the mixers is close to zero, their motions can be followed for a long time. The mixers are about a half-meter in diameter, and R_λ can be as high as 1200. Large glass windows provide optical access for imaging techniques. The apparatus can be pumped down to reduced-pressure for the study of bubble dynamics. A frequency doubled high-power (50 W), high-repetition-rate Nd:YAG laser is devoted to measurements in this apparatus.

Theoretical knowledge is most developed for turbulence that is stationary and isotropic. But real flows are neither. Three novel apparatuses [3, 4], make it possible for the first time to control the degree to which a turbulent flow is anisotropic both, in gases and in water. We produce cloud-like conditions in one soccer ball.

The facilities make use of state-of-the-art three-dimensional Lagrangian particle tracking (LPT) technologies that we have developed in-house. The technology relies on multiple ultra high-speed cameras viewing the same particles from different angles, with megapixel resolution and kilohertz frame rates. Recently we have developed a techniques that enables us to measure the 3D vorticity in water flow. We also employ a Dantec hot-wire system in conjunction with nano-fabricated hot-wires from Princeton University, a LaVision tomographic particle image velocimetry system, and a TSI laser Doppler velocimetry and particle sizing system. All of this equipment is compatible with pressures up to 15 bar. Some of these techniques require substantial light, which is typically produced by Nd:YAG lasers or argon-ion lasers. The systems produce data at rates that necessitate high-performance computing and storage clusters.

The Göttingen Turbulence Facilities (GTF) are open to visiting researchers for example in the European High-Performance Infrastructures in Turbulence (EuHIT) project³. It aims to integrate cutting-edge European facilities for turbulence research across national boundaries [5, 6].

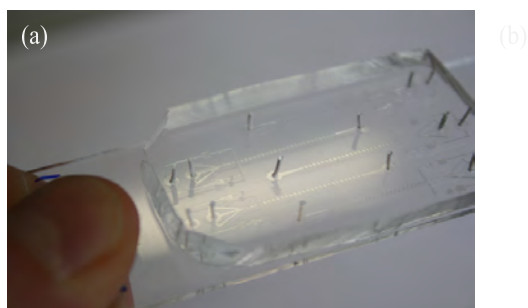
- [1] E Bodenschatz, G P Bewley, H Nobach, H., M Sinhuber, H Xu: Rev. Sci. Instrum., vol. 85 (2014), 093908
- [2] G Ahlers, D Fünfschilling, E Bodenschatz: New J. Phys., vol. 11 (1009), 123001
- [3] K Chang, G P Bewley, E Bodenschatz: Journal of Fluid Mechanics 692 (2012), 464?481
- [4] R Zimmermann, H Xu, Y Gasteuil, M Bourgoin, R Volk, J-F Pinton, E Bodenschatz: Rev. Sci. Instrum., vol. 81 (2010), 055112
- [5] <http://www.euhit.org>

MICROFABRICATION FACILITY

The Microfabrication Facility generates devices for the various groups within the institute. In addition, the facilities play a central role in the Max Planck Network on Synthetic Biology (*MaxSynBio*), a joint Max Planck - BMBF initiative whose goal is to create cell-like functions from modules. The facility here is involved in developing microfluidic platforms for generating the compartmentalization between the inside of a synthetic cell and its external environment. The fabrication facility is open to all members of the network, and provides assistance and training at all levels, from the design to the use of microfluidic devices.



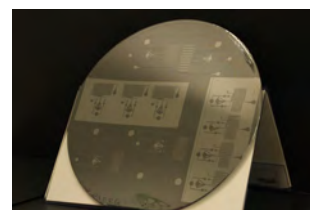
Class 1000, 35 m², clean room



Microfluidic devices fabricated by (a) replica molding of PDMS and by (b) micromachining of PMMA.

Microfluidic devices are generated by the replica molding of PDMS or by the micromachining of PMMA. The replica molds, with feature sizes between 5 and 200 microns, are generated in a 35 m², class 1000 clean room. Within the clean room is a spin-coater for depositing well-defined uniform layers of photoresist (SU-8 or AZ), hotplates for baking the resist, and a mask aligner (EVG-620) for exposing patterns on the layers of photoresist. A white light interferometer (Wyko NT1100) is used to accurately measure the heights of the structures. Once the replica mold is generated, the steps of soft lithography, i.e. molding the PDMS and assembling the microfluidic devices, are conducted outside the clean room environment.

Besides soft lithography, the institute is equipped with a high-precision milling machine (DMU 50, DMG Mori Seiki) which is used to pattern microchannels in hard plastics like PMMA and metals with feature sizes ranging between 150 microns and 10 cm. By heating the PMMA above the glass transition temperature, microfluidic channels can be assembled.



SU-8 wafer used for replica molding of PDMS

GÖTTINGEN FOCUS ON COMPLEX FLUID DYNAMICS

The summer of 2015 marked the beginning of a new phase for the MPIDS: the beginning of construction work for the new Göttingen Focus on Complex Fluid Dynamics. By middle 2016 this Focus will be home to up to 63 scientists working together on topics such as the physically correct description of turbulent flows, the prediction of multiphase flows in complex geometries, and the behavior of active fluids in living matter. The Focus will be built with two stories in timber construction – the first construction of this sort within the Max Planck Society. While the two upper stories will house offices for 60 scientists and three group leaders as well as a seminar room, the lower part will make room for roofed bike -parking spaces. The architecture of the building is simple and straightforward allowing the Focus to harmoniously complement the older building and the experimental hall. A covered walkway will connect the second floor of the current building with the first floor of the new.

The concrete foundation and ground floor of new building is almost finished and the wood construction is to be delivered at the beginning of 2016.



The scope of the new Focus is to significantly strengthen the research on complex fluid dynamics and to create an internationally unique and distinguished competence center in this field. Hopefully, this will lead to the deeper understanding of many basic questions necessary to tackle some of the most urgent and intriguing problems of today's society, such as the prediction of the global climate as well as atmospheric and marine transport, the development of efficient wind and tidal power stations, and the use of sedimentary reservoirs for oil production or the storage of carbon dioxide.

PART III

PUBLIC RELATIONS, EQUAL OPPORTUNITIES, AND SUPPORT FOR YOUNG SCIENTISTS

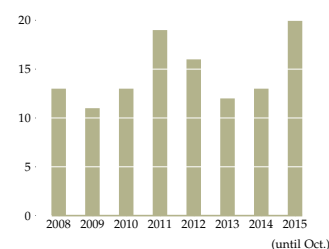
PUBLIC RELATIONS

Public outreach and media relations are recognized as an important part of the institute's responsibility. This is shown not only in the increasing number of press releases, but also by the institute's ongoing participation in public events and exhibitions. All outreach and media activities are coordinated in the Institute's press office.

Press releases

Press releases continue to be an important means of communicating with the local, national, and international media. These releases deal with scientific results from all departments and Max Planck Research Groups, inform the media about important prizes awarded to MPIDS scientists, and advertise special events the institute organizes or takes part in.

Most press releases are published in German and English. In recent years, the number of press releases issued per year has continued to be high but could even be increased. In addition, frequently these press releases spark the interest of industrial partners or direct other colleagues from science and research to our work.



Number of press releases.

Homepage

Since 2013 the homepage of the MPIDS has a new design, which is in accordance with the design used by the Max Planck Society and several other Max Planck institutes. The most important change from an outreach point of view is that now the front page offers the possibility to promote current news such as press releases, prizes or announcements.

Guided Tours

The MPIDS offers school and student groups regular tours of the institute. Young participants learn about science, either in the institute's own experimental hall, in the computer cluster or in laboratories: the public relations office and the scientists involve explain the scientific content in a clear and attractive manner.

Poetry of the Clouds

The film "The Poetry of the Clouds" at the MPIDS exemplifies innovative fundamental research into the microphysics of clouds and is now available on the institute's homepage. In the film, Professor Eberhard Bodenschatz and his team of scientists from MPIDS explain how a 5.5-ton steel seesaw was taken from the lab in Göttingen to the Environmental Research Station at the Schneefernerhaus atop Germany's highest mountain, the Zugspitze. The physicists and engineers of the MPIDS designed and built the seesaw's steel structure over several years. The seesaw serves as a multifunctional foundation and supports up to four high-speed cameras. The cameras capture the dynamics of individual droplets, all in 3D. This research provides insights into the



Address of Welcome to the new Göttingen University students of Physics in front of the Göttingen Turbulence Facility at the MPIDS, October 23, 2015

mechanism of rain formation and could improve, in highly turbulent clouds, the ability to predict rain.

BCCN-Visit by the Governor of Lower Saxony

On the 8th December 2014 the Governor of Lower Saxony, Stephan Weil, visited the Bernstein Center for Computational Neuroscience (BCCN), to inspect the collaboration of the MPIDS with the Universitätsmedizin Göttingen and the German Primate Center. The Governor found the

The Governor of Lower Saxony visiting the Göttingen Bernstein Center of Computational Neuroscience (BCCN), December 8, 2014



connection between theoretical neuroscience in connection with applied prosthetic technology most impressive.

Symposium on the occasion of 10th anniversary of the foundation of MPIDS

The Max Planck Institute for Dynamics and Self-Organization was founded in the fall of 2004. With a new name and an innovative scientific concept, it originated from the previous Max Planck Institute for Fluid Dynamics. The institute devotes itself to elucidating dynamic and self-organizing phenomena in nature, from nanomachines in living cells and the cooperative activity of heart and nerve cells, to cloud formation and turbulence on a planetary scale. Over the past ten years numerous fruitful collaborations have emerged with other scientists and research groups in Göttingen. On the 12th of December 2014 the MPIDS celebrated the occasion with a historical lecture and a symposium exhibiting the breadth of our research program through lectures from our collaborators.



Director Theo Geisel and his Jazz Band performing on the occasion of the 10th anniversary of the foundation of MPIDS

Symposium to initiate the CoNDyNet project

On December 12, 2014 the collaborative research project CoNDyNet, initiated by Marc Timme and Dirk Witthaut from the MPIDS, started off

with a symposium. About 70 scientists of the five academic institutions (the MPIDS, the Potsdam Institute for Climate Impact Research (PIK), the Forschungszentrum Jülich (FZJ), the Jacobs University Bremen (JUB) and the Frankfurt Institute for Advanced Studies) and five additional application partners are collaborating to push their conceptual studies on the collective nonlinear dynamics of future-compliant power grid networks, including the grid's ecological and economic efficiency and potential risks. During the next 3 years, the Federal Ministry of Education and Research (BMBF) is funding CoNDyNet with 2.7 million Euros.



Researchers of the BMBF-funded collaboration CoNDyNet (Collective nonlinear dynamics of power grid networks) meet for their Kick-Off Symposium in the Paulinerkirche in Göttingen, December 11, 2014

Night of Science in 2015

For the second time Göttingen hosted a major science festival, to which the MPIDS contributed: the “Night of Science” (January 17, 2015) organized by the University of Göttingen and the Max-Planck-Institutes. At the festival the MPIDS presented with lectures dealing, for example, with the Smart grids and the beat of the heart. In addition, MPIDS scientists offered hands-on activities and information stands introducing the guests to the world of turbulent flows and complex fluids. A highlight of the “Night of Science” was a spectacular laser experiment demonstrating the turbulent flows in clouds.



Light Sheet shown in front of the Max Planck Institute for Solar System Research in Göttingen on the occasion of the Night of Science, January 17, 2015

Cultural Committee of the Göttingen town council

On April 30, 2015 the Cultural Committee of the Göttingen town council held their official meeting at the MPIDS. The meeting was open to the public and lasted 3 hours. One of the topics discussed was the new “Kunstquartier” in the town center of Göttingen.

Science Tunnel

The Max Planck Science Tunnel 3.0 is an exhibition devoted to basic research presenting various scientific topics with the help of impressive multimedia displays. The Science Tunnel was set up (July 4-12, 2015) in the Expo-area in Hanover. Young members of the Institute acted as guides and science communicators through the exhibition. The MPIDS contributed to the exhibition on the topic "complexity" with information and material on turbulence and network analysis.



Science Communicator Manuel Schottdorf explains complexity on turbulence and network analysis to visitors of the Max Planck Science Tunnel 3.0 in Hanover, July 4, 2015



Irish Artist exhibits "Wow-Brows", brows of prominent scientists on two sailclothes hanging in the entrance hall of the MPIDS, July 16, 2015

WowBrows

On July 16, 2015 the managing director Theo Geisel inaugurated the exhibition „Wow brows“ by the Irish artist Fintan Whelan. Two large, impressing sailclothes hung from the ceiling of the entrance hall of our institute. Each showed brows of prominent scientists, e.g. Max Planck and Marie Curie.

Summer festival

On July 23, 2015 we celebrated the annual summer festival together with our neighboring institute MPIBPC. Pleasant discussions, sporting activities and musical highlights turned the summer day into a happy event. For the first time, this year the regular summer festival was celebrated on two days. The series „stage free for science“ opened the first day. This part was organized by the MPIBPC. Next year we (the MPIDS) will stage this event with talks and other content.

Impulses for the Future – Science meets economy

Professor Timme was invited as a speaker by the Max Planck Society and the Technologiestiftung Berlin for their series "Impulses for the Future - Science meets Economy". The topic of the evening on October

14, 2015 was "Rethinking Smart Grids". A public debate with Dr. Oliver Weinmann (CEO of Vattenfall Innovation Europe), Members of the German Parliament, representatives of several embassies as well as experts and representatives from engineering industry and the economy followed the talk of Professor Timme. The event took place in the historic building of the former "Schaltwerk" in Berlin Mitte, a former power layover station.



Invited by the Max Planck Society Timme talks about "Rethinking Smart Grids".

Göttinger Literaturherbst

As in previous years, the MPIDS took part in the annual literary festival in Göttingen, the "Göttinger Literaturherbst". This festival features a scientific lecture series where internationally renowned scientists present their latest books in the unique atmosphere of the historic Paulinerkirche in Göttingen. These lectures are introduced and chaired by scientists from the local Max Planck Institutes, with the aim of stimulating an interesting and vivid exchange of ideas. In 2015 a highlight was the lecture presented by Colin Crouch. In his lecture „The Knowledge Corrupters. Hidden Consequences of the Financial Takeover of Public Life". Crouch described, how strongly schools, hospitals and the police are dependent on financial markets and how students and passengers become customers, acting like machines. On this path to an information-driven society, for the social critic Crouch one central resource is lost; knowledge itself. For his major contribution in explaining on television complex scientific themes to the general public, Harald Lesch was awarded this year's Science Communication Medal. The prize is awarded as part of the scientific series of talks during the Göttinger Literaturherbst and distinguishes individuals who have shown strong commitment to communicate current scientific results to the general public. The award winner last year was the British physicist David McKay.

Ask the Scientist

In recent years the series „Ask the Scientist“ has been successfully established. In this series, appearing every other Sunday in the Göttingen newspaper ExtraTip, scientists from the MPIDS and other scientific institutions answer questions asked by readers. These questions cover all scientific areas and often deal with topics related to the institute's research.

EcoBus – from basic research to the streets

The research project EcoBus on flexible shared mobility run by the Network Dynamics team and the Department Dynamics of Complex Fluids now is on its way to the streets. Its aim is becoming a sustainable, integrated and publicly backed mobility system for urban and rural areas. EcoBus will implement a door-to-door transport system with travel times matching customer requests and at affordable prices. Therefore it will complement the already existing, highly-frequented public



Flyer EcoBus

transport corridors, and will thus reinforce classical transit and cab services. EcoBus seeks to team up with regional transport companies to operate the vehicles (small and medium buses as well as taxis). To promote EcoBus, the EcoBus team at the MPIDS, together with Southern Lower Saxony Programme (SNiP) Headquarter, has been developing a network of heads of municipal authorities, further regional public transport managers and Göttingen University researchers over the past year. Already 33 public institutions have signed up as Ambassadors for EcoBus! In addition, the EcoBus research project is proceeding. The team around Prof. Timme and Prof. Herminghaus submitted a grant proposal to the ministry of Lower Saxony for science and culture, applying for funding from to the European Regional Development Fund (EFRE). The proposal entitled 'Physics of the integrated public transportation system – decentralized – on request – cross-linked' shall support research and pilot phases in 2016 and 2017 with a total or more than 2 million Euros. The team has publicized the idea and practical options of EcoBus at regional exhibitions, with local governments, citizen groups and meetings of transport committees.



Ambassadors for EcoBus: Max Planck Researchers with the group of initial signees of the Cooperation Agreement for flexible regional mobility, July 13, 2015

Science before the weekend

Since February 2015 we have restarted the series „Science before the weekend“. In understandable, attractive and entertaining lectures scientists of MPIDS explain their work. This greatly contributes to internal communication within the Institute and is regularly attended by up to 70 listeners.

Internal Newsletter MPI Aktuell

For an efficient, quick, and uncomplicated internal communication an email newsletter has been initiated. It is distributed to all employees once a month and contains brief information about news items, new

appointments, important dates, and publications. In addition, each month a special topic (such as new research co-operations, public events or scientific results) is highlighted in more detail. In this way, the newsletter offers both quick and in depth information.

The Göttingen Campus

The Göttingen Research Council (GRC) was established by the university in 2006 in order to coordinate campus wide activities with the non-university institutes. The main task of the GRC is the consultation of the executive committees of the University (Presidential Board, University Medical Centre Board, Senate) and of the non-university institutes. Our institute is one of the eight non-university members of the GRC. Topics range from joint teaching and research activities towards the identification of research foci for the development of the Göttingen Campus. Since 2013 the GRC is supported by a Campus Network Group with collaborators from the member institutes. Current projects to strengthen the Göttingen Campus are the launch of a Campus Webpage (www.goettingen-campus.de), the preparation of a common event calendar and a leaflet advertising the Campus. All GRC and Campus activities will strongly support the candidature of the university in the next Excellence Program of the German government in 2016/17.

Max Planck Campus

Together with the neighboring Max Planck Institute for Biophysical Chemistry (MPIBPC) and the Gesellschaft für wissenschaftliche Datenverarbeitung mbH Göttingen (GWDG) the MPIDS forms the Göttingen Max Planck Campus. The GWDG is a corporate facility of the Georg-August University of Göttingen and the Max Planck Society. It serves the purpose of data processing and is an IT competence center for the Max Planck Institutes in Göttingen and a data processing service center for the University of Göttingen. Several infrastructures such as the Otto-Hahn-Library and the canteen are available to all partners of the Max Planck Campus and help cultivate an atmosphere of exchange and participation. In the past years, further efforts have been made to increase the cooperation of both Max Planck Institutes and create synergy effects.

Board of Trustees

Since January 2013 the MPIDS and the MPIBPC have a joint Board of Trustees. The board supports the exchange between the institutes and the general public and advises the institutes on social and scientific policy. Members of the Board of Trustees include representatives from politics, economy, science, and media. The Board of Trustees convened on May 8, 2015 for its constituent meeting, electing Gerd Litfin as chair and Gerhard Scharner as co-chair. Additional meetings take place annually.

Board of Trustees of the MPIDS and MPI bpc led by Gerd Litfin joining for their annual meeting, May 8, 2015



Meetings of the Scientific Members of MPIDS and MPIbpc

The meetings of the scientific Members of the MPIDS and the MPIbpc consolidate the close collaboration of both institutes on a scientific level. In these meetings the directors of both institutes convene regularly to discuss not only scientific issues, but also organizational and infrastructural topics concerning the Max Planck Campus as a whole.

Further Max Planck Campus Activities

In recent years, several tools have been established to foster the scientific exchange between researchers from both Max Planck Institutes. Most prominently, this is the Campus Seminar, a regular series of lectures held two to three times per month. In these lectures, scientists from both institutes present their projects and results to their colleagues thus allowing for a preliminary exchange of ideas with the aim of triggering scientific cooperation. A more informal framework for getting to know colleagues from the MPIbpc and their research is offered by mutual activities such as the summer festival.

EQUAL OPPORTUNITIES / RECONCILIATION OF WORK AND FAMILY LIFE

Creating equal opportunities for both female and male employees and reconciling work and family life is an important part of the institute's organizational culture and identity. Every four years, an equal opportunities commissioner as well as a deputy commissioner are elected to help promote these goals and act as a contact point for employees with questions regarding career support for female employees, work-life-balance, day care options, legal and work-related aspects of pregnancy, and sexual harassment or mobbing at the workplace.

For parents taking care of children the institute offers several services to facilitate a reconciliation of work and family life. For example,

these employees may take advantage of the services of the pme Familienservice GmbH, a family service specialized in finding day care solutions. In addition, all information regarding day care is displayed in the intranet.

pme Familienservice GmbH offers the following services: Locating of daycare services including child minders, emergency daycare for sick children, care for children or teenagers, au pair personnel, private kindergartens, parent initiatives, daycare, holiday programs, emergency childcare, hotlines, home care and elderly care.

Since 2010 the institute offers a small playroom for children where employees nursing babies find privacy and parents bringing their children to work find helpful toys and a play area. Since 2006 the quality audit "Beruf und Familie" (engl.: "Work and Family") regularly evaluates the measures taken at the Max Planck Society to improve the compatibility of work and family life for women and men. In 2012 the MPIDS was awarded the according certificate for the third time. The MPIDS sees to a timely implementation of the objectives with regard to the audit. For example, all employees are now regularly informed about new and existing day care options and employees who had taken advantage of the services of the pme Familienservice GmbH were given the possibility to evaluate this service.

In order to promote equal opportunities for both female and male employees the equal opportunities commissioner is involved in all job offers and application procedures. All employees are regularly informed about networking possibilities for female scientists and training measures such as self-assertion for women. The equal opportunities commissioner took part in compiling the operating agreement dealing with performance-oriented payment for all employees.

Every year - excluding 2011 when the institute moved from the Bunsenstraße to Faßberg - the MPIDS hosts the "Zukunftstag" (engl.: "Future Day"). On this day young girls and boys throughout Germany explore different career options. The MPIDS regularly invites approximately 20 girls and boys to take part in different activities in the laboratories and the workshops. The day is an excellent opportunity to interest young people (especially young girls) for science and engineering. In order to offer positive role models, this day is organized chiefly by the institute's female scientists. Both the participating children and their parents are very enthusiastic about the activities offered by the MPIDS and give very positive feedback.

YOUNG SCIENTISTS

The approximately 80 PhD students at the MPIDS do not only carry out a substantial part of the scientific research, but are also active in the Max Planck Society-wide PhDnet, represent their interest in the committees of the International Max Planck Research School for Physics of Biological and Complex Systems (IMPRS PBCS) and work together with the institute administration. They organize events to support the advancement of young researchers and the interaction within the



Girls are visiting one of the labs of the MPIDS



Boys exploring a Stirlingmotor constructed in the Apprentices' workshop of the MPIDS

institute and between the research institutes and faculties of the Georg-August University School of Science (GAUSS). The representatives' goal is to ensure that the best possible working conditions are provided for the students at the institute, to offer a point of contact for any issues that arise and to give students a broader perspective outside their specific field of research.

A range of events were organized by students of the institute. One notable example was the the second realization of the international conference "Third Infinity" which took place from October 14 - 16, 2015 in Göttingen. The conference was organized jointly by a group of PhD candidates belonging to IMPRS PBCS, affiliated to the University of Göttingen and the MPIDS.

Third Infinity covered a broad range of topics from the field of physics of complex systems and biophysics. Fourteen excellent speakers came from literally all over the world to give talks on strain-controlled criticality, quantum optics, epidemiology, explosive percolation and data science, among other topics. In addition, the conference included a lively panel discussions about the new challenges being faced by scientists today; as well as a public talk on insights about scientific publishing.

Another student-run event organized by graduate students of the Institute is the "Göttingen Fall Course on Computational Neuroscience". Supported by the Bernstein Center for Computational Neuroscience it has been held annually in the Institute since 2003 as a fall school of the NWG, the German Neurowissenschaftliche Gesellschaft. With lectures given by international experts it attracts students from Germany and other European countries. Also with financial and other support from the BCCN a group of female PhD-students has been organizing a series of "Seminars in Biophysics by Outstanding Female Scientists". With outstanding international invitees, frequently from the US, it is intended to promote young women's scientific careers by lectures, tutorials, and networking.

Within the framework of IMPRS-PBCS graduate school, PhD candidates have the opportunity to offer method courses to their peers: thereby disseminating the knowledge and expertise they gain during the course of their doctoral work. Each year numerous method courses were given by the young scientists of MPIDS, with wide variety of topics ranging from Electric Cell-substrate Impedance Sensing to network analysis and visualization.

Locally, PhD students serve as representatives on the selection panels and organization committees of the IMPRS PBCS. On the scale of the Max Planck Society, students from the institute are active in different groups of the PhDnet, which addresses the working conditions and opportunities for the students in cooperation with the general administration. Alexander Schlemmer is currently working within the Web Group of PhDnet. The 14th PhDnet general meeting took place between November 22 - 24, 2015 in Göttingen, with active participation from many young scientists of MPIDS.

Florencia Noriega of the network dynamics group has been organizing a Career seminar since fall 2014: which gives the young researchers

an opportunity learn about the post PhD professional life of various alumni from the institute. Invited talks so far touched upon career in a broad range of fields including logistics startups, Volkswagen foundation and computer simulation solution providers.

Of course the activities of the PhD students are not solely focused on scientific advancement and career perspectives. To maintain a work-life balance, social events are organized for the students, both on the level of the institute and through the IMPRS. Especially the dinners with the speakers of invited talks provide a valuable opportunity for students as they provide a very informal environment to discuss both current research and life in science in general. Also, the students attempted to convert some square meters of the greenland behind the institute into a vegetable garden.

HOW TO REACH US AT THE MAX PLANCK INSTITUTE FOR DYNAMICS AND SELF-ORGANIZATION

Fassberg site (new building)



Address:
Am Fassberg 17
D-37077 Göttingen

Departments:	Nonlinear Dynamics (Prof. Geisel) Dynamics of Complex Fluids (Prof. Herminghaus) Fluid Dynamics, Pattern Formation, and Biocomplexity (Prof. Bodenschatz)
Research Groups:	Biomedical Physics (Honorarprofessor Luther) Theoretical Neurophysics (Honorarprofessor Wolf)
Max Planck Research Groups:	Biological Physics and Morphogenesis (Dr. Karen Alim) Theory of Turbulent Flows (Dr. Michael Wilczek)
Services:	Institute Management, Administration, Facility Management, Electronics and Mechanics Workshops, IT-Services, Library, Outreach Office, Stock Rooms, Lecture Hall, Göttingen Turbulence Facility, Clean Room, and Cell Biology Laboratories

By plane

From Frankfurt am Main Airport (FRA): Use one of the railway stations at the airport. Trains to Göttingen (direct or via Frankfurt main station) leave twice an hour during daytime (travel time: 2 hours). From Hanover Airport (HAJ): Take the suburban railway (S-Bahn) to the Central Station (»Hannover Hauptbahnhof«). From here direct ICE trains to Göttingen depart every 1/2 hour.

By train

Göttingen Station is served by the following ICE routes: Hamburg-Göttingen-Munich, Hamburg-Göttingen-Frankfurt am Main, and Berlin-Göttingen-Frankfurt. From Göttingen railway station: On arrival at Göttingen station take a taxi (15 minutes) or the bus (20 minutes). At platform D take the bus No. 21 (direction: »Nikolausberg«) or No. 23 (direction: »Faßberg«). After about 20 minutes get off at the »Faßberg« stop, which is directly in front of the entrance of the Max Planck Campus (MPIDS and MPI for Biophysical Chemistry). Ask at the gate to get directions.

By car

Leave the freeway A7 (Hanover-Kassel) at the exit »Göttingen-Nord«, which is the northern of two exits. Follow the direction for Braunlage (B 27). Leave town – after about 1.5 km at the traffic light (Chinese restaurant on your right) turn left and follow the sign »Nikolausberg«. The third junction on the left is the entrance to the Max Planck Campus (MPIDS and MPI for Biophysical Chemistry). Ask at the gate to get directions.

Bunsenstraße site (old building)

Research Groups: Network Dynamics (apl. Prof. Timme)
Emeritus Group: Molecular Interactions (Prof. Toennies)
Services: Guest Houses



Address:
Bunsenstraße 10
D-37073 Göttingen

By plane

From Frankfurt am Main Airport (FRA): Use one of the railway stations at the airport. Trains to Göttingen (direct or via Frankfurt main station) leave twice an hour during daytime (travel time: 2 hours). From Hanover Airport (HAJ): Take the suburban railway (S-Bahn) to the Central Station (»Hannover Hauptbahnhof«). From here direct ICE trains to Göttingen depart every 1/2 hour.

By train

Göttingen Station is served by the following ICE routes: Hamburg-Göttingen-Munich, Hamburg-Göttingen-Frankfurt, and Berlin-Göttingen-Frankfurt. From Göttingen railway station: From the Göttingen station you can take a taxi (5 minutes) or walk (20 minutes). If you walk, you need to leave the main exit of the station and turn to the right. Follow the main street, which after the traffic lights turns into Bürgerstraße. Keep walking until you come to the Bunsenstraße. Turn right – you will reach the entrance gate of the MPIDS after about 300 m.

By car

Leave the freeway A7 (Hanover–Kassel) at the exit »Göttingen«, which is the southern exit. Follow the direction »Göttingen Zentrum« (B3). After about 4 km you will pass through a tunnel. At the next traffic light, turn right (direction »Eschwege« B27) and follow the »Bürgerstraße« for about 600 m. The fourth junction to the right is the »Bunsenstraße«. You will reach the institute's gate after about 300 m.